Premier Reference Source

AI Applications for Disease Diagnosis and Treatment

Rajae El Ouazzani, Mohammed Fattah, and Nabil Benamar

IGI Global
PUBLISHER of TIMELY KNOWLEDGE

AI Applications for Disease Diagnosis and Treatment

Rajae El Ouazzani
Moulay Ismail University of Meknes, Morocco

Mohammed Fattah
Moulay Ismail University of Meknes, Morocco

Nabil Benamar
Moulay Ismail University of Meknes, Morocco

IGI Global
PUBLISHER of TIMELY KNOWLEDGE

A volume in the Advances in
Medical Diagnosis, Treatment, and
Care (AMDTC) Book Series

Advances in Medical Diagnosis, Treatment, and Care (AMDTC) Book Series

MISSION

Advancements in medicine have prolonged the life expectancy of individuals all over the world. Once life-threatening conditions have become significantly easier to treat and even cure in many cases. Continued research in the medical field will further improve the quality of life, longevity, and wellbeing of individuals.

The **Advances in Medical Diagnosis, Treatment, and Care (AMDTC)** book series seeks to highlight publications on innovative treatment methodologies, diagnosis tools and techniques, and best practices for patient care. Comprised of comprehensive resources aimed to assist professionals in the medical field apply the latest innovations in the identification and management of medical conditions as well as patient care and interaction, the books within the AMDTC series are relevant to the research and practical needs of medical practitioners, researchers, students, and hospital administrators.

COVERAGE

- Chronic Conditions
- Disease Prevention
- Diagnostic Medicine
- Experimental Medicine
- Alternative Medicine
- Patient Interaction
- Cancer Treatment
- Internal Medicine
- Emergency Medicine
- Medical Testing

IGI Global is currently accepting manuscripts for publication within this series. To submit a proposal for a volume in this series, please contact our Acquisition Editors at Acquisitions@igi-global.com or visit: http://www.igi-global.com/publish/.

Titles in this Series

For a list of additional titles in this series, please visit:
http://www.igi-global.com/book-series/advances-medical-diagnosis-treatment-care/129618

Historical and Epidemiological Analyses on the Impact of Infectious Disease on Society
Edward Greenberg (Cigna, USA)
Medical Information Science Reference ● © 2022 ● 261pp ● H/C (ISBN: 9781799886891)
● US $295.00

Handbook of Research on Natural Products and Their Bioactive Compounds as Cancer Therapeutics
Ashok Kumar Pandurangan (B.S. Abdur Rahman Crescent Institute of Science and Technology, India) Suresh Kumar Anandasadagopan (Central Leather Research Institute, India) and Fahad A. Alhumaydhi (Department of Medical Laboratories, College of Applied Medical Sciences, Qassim University, Buraydah, Saudi Arabia)
Medical Information Science Reference ● © 2022 ● 643pp ● H/C (ISBN: 9781799892588)
● US $495.00

Exploring the Efficacy and Beneficence of Complementary and Alternative Medicinal Products in Disease Therapy
Etetor Roland Eshiet (Sustainable Energy Environmental and Educational Development (SEEED), USA)
Medical Information Science Reference ● © 2022 ● 315pp ● H/C (ISBN: 9781799841203)
● US $295.00

The Pediatric Eye Exam Quick Reference Guide Office and Emergency Room Procedures
Lily Zhu-Tam (Citywide Eye Care Optometry, USA) and Ida Chung (College of Optometry, Western University of Health Sciences, USA)
Medical Information Science Reference ● © 2022 ● 409pp ● H/C (ISBN: 9781799880448)
● US $295.00

Medical Atlas of Cornea and External Diseases in Middle Eastern Populations
Anna Hovakimyan (Malayan Ophthalmologic Centre, Armenia)
Medical Information Science Reference ● © 2022 ● 384pp ● H/C (ISBN: 9781799869375)
● US $265.00

For an entire list of titles in this series, please visit:
http://www.igi-global.com/book-series/advances-medical-diagnosis-treatment-care/129618

Editorial Advisory Board

Table of Contents

Section 1
AI Opportunities and Challenges in Healthcare

Chapter 1
Lana I. S. Hamad, Yildiz Technical University, Turkey
Elmustafa Sayed Ali Ahmed, Red Sea University, Sudan
Rashid A. Saeed, Taif University, Saudi Arabia

Section 2
Diagnosis and Treatment of Some Common Diseases Using AI

Chapter 2
Masud Rabbani, Ubicomp Lab, Department of Computer Science,
Marquette University, USA
Munirul M. Haque, University of Indianapolis, USA
Dipranjan Das Dipal, Marquette University, USA
Md Ishrak Islam Zarif, Marquette University, USA
Anik Iqbal, Marquette University, USA
Shaheen Akhter, Bangabandhu Sheikh Mujib Medical University,
Bangladesh
Shahana Parveen, National Institute of Mental Health, Dhaka,
Bangladesh
Mohammad Rasel, Bangabandhu Sheikh Mujib Medical University,
Bangladesh
Tanjir Rashid Soron, Telepsychiatry Research and Innovation Network

Section 3
COVID-19 Diagnosis and Treatment Using AI

Detailed Table of Contents

Section 1
AI Opportunities and Challenges in Healthcare

Lana I. S. Hamad, Yildiz Technical University, Turkey
Elmustafa Sayed Ali Ahmed, Red Sea University, Sudan
Rashid A. Saeed, Taif University, Saudi Arabia

Due to the increase in healthcare data provided by IoT, there is a need to use new methods for data analysis. Machine learning (ML) techniques promise solutions for many challenges facing the IoT-based healthcare services. MLs provide significant improvement in different IoT aspects related to storage size, computational power, and data transfer speeds. In addition, MLs provide a number of solutions for medical imaging, resources, medical data processing, detection, diagnosis, and prediction. Recently, many applications have appeared in the field of medicine and healthcare, which are closely related to the IoT. This chapter presents basic concepts related to the use of ML techniques, in addition to some algorithms used in the medical field and healthcare technology based on IoT devices and systems. Moreover, the chapter will discuss the ML opportunities and challenges in healthcare and future trends as well. The chapter gives the reader full perception of the possibility of using ML techniques in the medical and healthcare fields, with a systematic description of their applications.

Section 2
Diagnosis and Treatment of Some Common Diseases Using AI

Chapter 2

*Masud Rabbani, Ubicomp Lab, Department of Computer Science,
Marquette University, USA*

Munirul M. Haque, University of Indianapolis, USA

Dipranjan Das Dipal, Marquette University, USA

Md Ishrak Islam Zarif, Marquette University, USA

Anik Iqbal, Marquette University, USA

*Shaheen Akhter, Bangabandhu Sheikh Mujib Medical University,
Bangladesh*

*Shahana Parveen, National Institute of Mental Health, Dhaka,
Bangladesh*

*Mohammad Rasel, Bangabandhu Sheikh Mujib Medical University,
Bangladesh*

*Tanjir Rashid Soron, Telepsychiatry Research and Innovation Network
Ltd., Bangladesh*

Naveen Bansal, Marquette University, USA

Amy Schwichtenberg, Purdue University, USA

Syed Ishtiaque Ahmed, University of Toronto, Canada

Sheikh Iqbal Ahamed, Marquette University, USA

Currently, one out of 160 children have autism spectrum disorder (ASD) in the world. This problem is observed in both developed and low-middle-income countries (LMICs) around the globe. Usually, in developed countries, the number can be estimated, but in LMICs, this number is largely unknown, and in some cases, many children with ASD are not treated after identification of the problem. In these cases, both for the developed and LMICs, mobile technology can continuously monitor children with ASD. In this chapter, the authors describe the techniques of remote monitoring of the behavioral and milestone parameters development for children with ASD that care practitioners can use as an evidence-based tool to make the decision in the treatment process. Lastly, the authors describe the advantages and challenges of using the mHealth tools in the ASD treatment based on the NIH-funded successful completion project "mCARE" in Bangladesh.

Sakshi Juneja, Panjab University, Chandigarh, India
Alka Bali, Panjab University, Chandigarh, India
Nishu Bali, Chitkara University, Punjab, India

Artificial intelligence (AI) is a set of technologies that allows robots to detect, understand, act, and learn at human-like levels. The vast bulk of the AI that surrounds us now is powered by ineffective AI. This sort of AI is demonstrated by IBM Watson, self-driving cars, and Apple's Siri. Machine learning includes deep learning as a subset which is commonly utilised in predictive modelling. It functions in the same manner that neurons do in our brains. Its structure and networking are also influenced by neural networks found in our brains. Since the 1950s, artificial intelligence (AI) has been applied in medicine. The use of artificial intelligence in ophthalmology is mostly focused on high-incidence illnesses such as diabetic retinopathy, glaucoma, age-related macular degeneration, and cataract. The chapter reviews research demonstrating AI enhancing medical diagnosis with a focus on diabetic retinopathy.

Mateo Gende, CITIC, INIBIC, Universidade da Coruña, Spain
Joaquim de Moura, CITIC, INIBIC, Universidade da Coruña, Spain
Jorge Novo, CITIC, INIBIC, Universidade da Coruña, Spain
Marcos Ortega, CITIC, INIBIC, Universidade da Coruña, Spain

The epiretinal membrane (ERM) is an ocular pathology that can cause visual distortions. To prevent a loss of vision, symptomatic ERM needs to be removed before it can cause irreversible damage. In order to do this, the ERM needs to be located early, so that it can be peeled from the retina. This chapter explores an automatic methodology for ERM segmentation, as well as its intuitive visualization in the form of colour maps. To do this, visual features that are compatible with ERM presence are extracted from ophthalmologic images by using computer vision algorithms and deep learning models. This methodology achieved satisfactory results, reaching a dice coefficient of 0.826 and a Jaccard index of 0.714, contributing to highlight the applicability of deep learning models for the detection of pathological signs in medical images.

Chapter 5

Sara El Omary, IMAGE Laboratory, Higher School of Technology,
Moulay Ismail University of Meknes, Morocco
Souad Lahrache, Faculty of Sciences, Ibn Zohr University, Morocco
Rajae El Ouazzani, IMAGE Laboratory, Higher School of Technology,
Moulay Ismail University of Meknes, Morocco

Worldwide, cardiac arrhythmia disease has become one of the most frequent heart problems, leading to death in most cases. In fact, cardiologists use the electrocardiogram (ECG) to diagnose arrhythmia by analyzing the heartbeat signals and utilizing electrodes to detect variations in the heart rhythm if they show certain abnormalities. Indeed, heart attacks depend on the treatment speed received, and since its risk is increased by arrhythmias, in this chapter the authors create an automatic system that can detect cardiac arrhythmia by using deep learning algorithms. They propose a deep convolutional neural network (CNN) to automatically classify five types of arrhythmias then evaluate and test it on the MIT-BIH database. The authors obtained interesting results by creating five CNN models, testing, and comparing them to choose the best performing one, and then comparing it to some state-of-the-art models. The authors use significant performance metrics to evaluate the models, including precision, recall, sensitivity, and F1 score.

<div align="center">

Section 3
COVID-19 Diagnosis and Treatment Using AI

</div>

Chapter 6

Hamlili Ali, Mohammed V University of Rabat, Morocco

Survival analysis is one of the most important research topics in probability and statistics applications to health and medical data. Its implementation has caught the attention of a large community of researchers from several skills including data analysis, statistical modeling, data mining, data science, and artificial intelligence. Survivor function and death intensity allow the analyst to assess the dynamics of the proportion of deaths and the risk of death over time. This chapter proposes an approach to the analysis of interval-censored survival data based on plug-in estimation as well as tools to assess the predictive quality of these estimators. Graphical tests are provided to support the choice between health security policies with the objective of leading to low mortality. The intertwining of this method with artificial intelligence tools paves the way for both personalized, precise, and efficient medicine and automated, informed, and rapid decision-making in health security.

Chapter 7

Harold Brayan Arteaga-Arteaga, Universidad Autónoma de Manizales, Colombia

Melissa delaPava, Universidad Nacional de Colombia, Colombia

Alejandro Mora-Rubio, Universidad Autónoma de Manizales, Colombia

Mario Alejandro Bravo-Ortíz, Universidad Autónoma de Manizales, Colombia

Jesus Alejandro Alzate-Grisales, Universidad Autónoma de Manizales, Colombia

Daniel Arias-Garzón, Universidad Autónoma de Manizales, Colombia

Luis Humberto López-Murillo, Universidad Nacional de Colombia, Colombia

Felipe Buitrago-Carmona, Universidad Autónoma de Manizales, Colombia

Juan Pablo Villa-Pulgarín, Universidad Autónoma de Manizales, Colombia

Esteban Mercado-Ruiz, Universidad Autónoma de Manizales, Colombia

Fernanda Martínez Rodríguez, Universidad de Guadalajara, Mexico

Maria Jose Palancares Sosa, Instituto Politécnico Nacional, Mexico

Sonia H. Contreras-Ortiz, Universidad Tecnológica de Bolívar, Colombia

Simon Orozco-Arias, Universidad Autónoma de Manizales, Colombia

Mahmoud Hassaballah, South Valley University, Egypt

María de la Iglesia Vayá, Fundación para el Fomento de la Investigación Sanitario y Biomédica de la Comunidad Valenciana, Spain

Oscar Cardona-Morales, Universidad Autónoma de Manizales, Colombia

Reinel Tabares-Soto, Universidad Autonóma de Manizales, Colombia

COVID-19 caused by the SARS-CoV-2 virus has affected healthcare and people's lifestyles worldwide since 2019. Among the available diagnostic tools, reverse transcription-polymerase chain reaction has proven highly accurate. However, the need for a specialized laboratory makes these tests expensive and time-consuming between sample collection and results. Currently, there are initial steps for the diagnosis of COVID-19 through chest x-ray images. Additionally, artificial intelligence techniques like deep learning (DL) help identify abnormalities. Inspired by the reported success of DL, this chapter presents an introduction to state-of-the-art DL-based approaches applied to the detection of COVID-19 in chest x-ray images, which currently allows assessing disease severity. The results presented are obtained using well-known models and some novel networks designed for this task. In addition, the models were evaluated using the most used public datasets, applying preprocessing

techniques to improve detection results. Finally, this chapter shows some possible future research directions.

Chapter 8
Daniel Iglesias Morís, Grupo VARPA, CITIC, INIBIC, Universidade da Coruña, Spain

Joaquim de Moura, Grupo VARPA, CITIC, INIBIC, Universidade da Coruña, Spain

Jorge Novo, Grupo VARPA, CITIC, INIBIC, Universidade da Coruña, Spain

Marcos Ortega, Grupo VARPA, CITIC, INIBIC, Universidade da Coruña, Spain

The diagnosis and the study of the evolution of COVID-19 is crucial to tackle the challenge that this disease represents for healthcare services. Chest x-ray imaging allows us to visualize the pulmonary regions, where COVID-19 causes its main affectation. In order to reduce the risk of cross-contamination, a crucial aspect in the pandemic, portable chest x-ray devices are advantageous being easier to decontaminate in comparison with the fixed machinery, despite offering a lower image quality. Furthermore, the recent emergence of COVID-19 implies a data scarcity that must be tackled. In this chapter, the authors present the analysis of a strategy that generates novel synthetic portable chest x-ray images using the CycleGAN, an architecture for image translation that is trained with unpaired data. The novel set of images is then added to the original dataset, improving the performance of the classification model.

Preface

Artificial intelligence (AI) has recently gained an unprecedent success in various fields, such as healthcare, aeronautics, autonomous driving, finance, agriculture, advertising, etc. AI is a revolutionary technology that has a direct impact on various aspects of our daily life ranging from human wellbeing management to economic development and healthcare. Today, technology is playing a critical role in introducing smart solutions in healthcare ecosystem. AI is one of the main techniques that are bringing new approaches and solutions to a variety of existing issues in healthcare. This book chapter is an attempt to present new advances in AI applications in healthcare especially disease diagnosis and treatment.

AI advances allow a rapid analysis of a big amount of patients' data; therefore, many AI systems were implemented to detect, classify, and predict healthcare activities with good accuracy. Various medical data sources may be used to diagnose diseases, especially Magnetic Resonance Imaging (MRI), Ultrasound scans, mammography, Computed Tomography (CT) scan, etc. The analysis of these data using AI algorithms allows to reduce the scans analysis duration, decrease the human errors, and save lives. Machine Learning (ML) algorithms permit diagnosing diseases such as Autism Spectrum Disorder (ASD), Diabetic Retinopathy (DR), cardiac arrhythmia, COVID-19, tuberculosis, cancer, Alzheimer, hypertension, skin diseases, diabetes, stroke and cerebrovascular, and liver disease, etc. (Chen et al., 2019a; Kohlberger et al., 2019; Luo et al., 2019). Deep Learning (DL) algorithms have been extensively used to identify different cancerous tumors. AI with both machine and deep learning algorithms have proved their effectiveness in making earlier and correct diagnosis in ambiguous situations and giving treatment to patients and remarkable guidance to pharmaceutical companies in many diseases (Keenan et al., 2020).

In the following, we present some studies on disease diagnosis and treatment using machine and deep learning algorithms. Soundarya et al. (2020) proposed a method to diagnose the Alzheimer's disease. They have implemented many ML and DL algorithms and their results show that DL algorithms give better accuracy. Aggarwal et al. (2020) analyzed the heart rate variability to predict diabetes disease. The authors used Artificial Neural Network (ANN) and Support Vector Machine

(SVM) for their models using 526 datasets for experiments; the testing phase shows a good accuracy. In an attempt to diagnose cardiac diseases, Haq et al. (2018) developed a machine learning model and they got promising results. Sathitratanacheewin et al. (Sathitratanacheewin et al., 2020) implemented a Convolutional Neural Network (CNN) model to diagnose tuberculosis. They used a chest X-ray dataset taken from many hospitals. Their CNN based approach showed good results in terms of the area under the curve, specificity, and sensitivity metrics. Rodrigues et al. (2020) proposed an IoT framework to diagnose melanoma, skin sores, and average nevi. They joined two models; a DenseNet201 and a k-Nearest Neighbors (KNN) classifier and made their experiments on the International Society for Bioluminescence and Chemiluminescence - International Standard Industrial Classification dataset. Koshimizu et al. (2020) implemented an ANN to measure the blood pressure. Khaled et al. (2018) implemented an ANN to diagnose the hepatitis virus. The authors utilized the information about histology and protein to feed their network. Zaar et al. (2020) carried out many AI algorithms to classify images of skin disease. The images were collected from the department of Dermatology at the Sahlgrenska University. All the proposed models were evaluated using various metrics such as accuracy, precision, sensitivity, specificity, recall, F1-score, and area under the curve.

The use of AI in healthcare is facing various challenges that need to be overcome such as the unavailability of data for some diseases, the high data dimensionality requiring an efficient algorithm for dimensionality reduction and features selection (Koshimizu et al., 2020), the generalization of AI models on multiple sites (Fukuda et al., 2019), and the validation of the proposed models in clinics in order to be approved by doctors (Huang et al., 2020).

This book is organized in eight chapters divided into three sections. The first section discusses some AI opportunities and challenges in healthcare. The second section provides some interesting research papers dealing with diagnosis and treatment of some common and widespread diseases using AI. Finally, the third section presents AI based techniques for COVID-19 diagnosis and treatment. A brief description of each chapter is given below:

Chapter 1 discusses ML opportunities, challenges in healthcare, and future trends. The chapter sheds light on the critical role that IoT plays in healthcare management. Healthcare Internet of Things (H-IoT) integrates devices such as GPS systems, heart rate tracking sensors, and communication systems into medical applications to make both clinical diagnosis and health monitoring.

Chapter 2 presents a mobile health application for monitoring the children with an ASD. The proposed mHealth application will help both doctors and nurses to assist patients with ASD by managing the behavioral development data, taking the optimal decisions and giving the appropriate treatment in complex situations, etc.

Chapter 3 proposes an AI aiding medical diagnosis focusing on DR disease. The chapter makes an overview of the current foundation and the potential of AI for DR diagnosis. An AI based DR will help doctors and practitioners in this field to quickly interpret retina images and thus, decide about the following steps of treatment.

Chapter 4 presents a fully automatic framework using CNN to segment Epiretinal Membrane (ERM) in OCT scans. This framework takes the advantages of the power of computer vision techniques and DL algorithms especially CNN in making accurate objective detection of the visual features that characterize this disease.

Chapter 5 proposes a lightweight CNN to identify cardiac arrhythmia using 2D ECG images. The authors have transformed signals into images and used a 2D CNN to classify various types of heart arrhythmias. Detecting cardiac arrhythmias is a task that needs much time and careful analysis of ECG recordings by clinical experts. Automating this task will improve the performance of cardiologists' diagnosis.

Chapter 6 provides an intelligibility of nonparametric survival analysis of health security policies evaluation for the analysis of COVID-19 pandemic data. This chapter explores a medical data application in probability and statistics to assess the dynamic death's proportion and the risk of death over time. The author made experiments to support the choice of health security policies with a low mortality rate. The proposed application aims to make personalized, precise, efficient, and automated medicine for rapid decision-making in health security.

Chapter 7 proposes a deep learning algorithm to detect COVID-19 in X-Ray images. This chapter examines distinctive methods of AI and IoT to produce a healthcare application that detects COVID-19 in X-Ray images. This application will determine the risk factors for infection in order to make an early prediction of the following infected people.

Chapter 8 makes a generation of synthetic portable chest X-ray images for an automatic COVID-19 Screening. The authors developed a new methodology for the automatic COVID-19 screening using chest X-ray images captured with portable devices. This new methodology is expected to provide the expert clinicians with an automatic and efficient tool to reduce their workload during the worldwide pandemic.

The book *AI Applications for Disease Diagnosis and Treatment* is a reference in AI applications on healthcare, especially ML, DL, implementation of healthcare solutions, and soft computing. This book takes you on a journey into various healthcare applications using AI such as disease diagnosis and treatment, physical assistance, and trucking.

Rajae El Ouazzani
Moulay Ismail University of Meknes, Morocco

Mohammed Fattah

Preface

Moulay Ismail University of Meknes, Morocco

Nabil Benamar
Moulay Ismail University of Meknes, Morocco

REFERENCES

Aggarwal, Y., Das, J., Mazumder, P.M., Kumar, R., & Sinha, R.K. (2020). Heart rate variability features from nonlinear cardiac dynamics in identification of diabetes using artificial neural network and support vector machine. *Integr Med Res*. .2020.05.001 doi:10.1016/j.bbe

Chen, J., Remulla, D., Nguyen, J., Aastha, D., Liu, Y., Dasgupta, P., & Hung, A. J. (2019a). Current status of artificial intelligence applications in urol- ogy and their potential to influence clinical practice. *BJU International*, *124*(4), 567–577. doi:10.1111/bju.14852 PMID:31219658

Fukuda, M., Inamoto, K., Shibata, N., Ariji, Y., & Kutsana, S. (2019). Evaluation of an artificial system for detecting vertical root fracture on panoramic radiography. *Oral Radiology*, *36*, 1–7.

Haq, A. U., Li, J. P., Memon, M. H., Nazir, S., & Sun, R. (2018). A hybrid intelligent system framework for the prediction of heart disease using machine learning algorithms. *Mob Inf Syst*, *8*, 1–21. doi:10.1155/2018/3860146

Huang, S., Yang, J., Fong, S., & Zhao, F. (2020). Artificial intelligence in can- cer diagnosis and prognosis. *Cancer Letters*, *471*, 61–71. doi:10.1016/j.canlet.2019.12.007 PMID:31830558

Keenan, T., Clemons, T., Domalpally, A., Elman, M., Havilio, M., Agron, E., Chew, E., & Benyamini, G. (2020). Intelligence detection versus artificial intelligence detection of retinal fluid from OCT: age- related eye disease study 2: 10 year follow on study. *Ophthalmology*. Advance online publication. doi:10.1016/j.ophtha.2020.06.038 PMID:32598950

Khaled, E., Naseer, S., & Metwally, N. (2018). Diagnosis of hepatitis virus using artificial neural network. *J Acad Pedagog Res*, *2*, 1–7.

Kohlberger, T., Norouzi, M., Smith, J., Peng, L., & Hipp, J. (2019). Artificial intelligence based breast cancer nodal metastasis detection. *Archives of Pathology & Laboratory Medicine*, *143*(7), 859–868. doi:10.5858/arpa.2018-0147-OA PMID:30295070

Koshimizu, H., Kojima, H., & Okuno, Y. (2020). Future possibilities for artificial intelligence in the practical management of hypertension. *Hypertension Research*, *43*(12), 1327–1337. doi:10.103841440-020-0498-x PMID:32655135

Luo, H., Xu, G., Li, C., & Wu, Q. (2019). Real time artificial intelligence for detection of upper gastrointestinal cancer by endoscopy: A multicentre, case control, diagnostic study. *The Lancet. Oncology*, *20*(12), 1645–1654. doi:10.1016/S1470-2045(19)30637-0 PMID:31591062

Rodrigues, D. A., Ivo, R. F., Satapathy, S. C., Wang, S., Hemanth, J., & Filho, P. P. R. (2020). A new approach for classification skin lesion based on transfer learning, deep learning, and IoT system. *Pattern Recognition Letters*, *136*, 8–15. doi:10.1016/j.patrec.2020.05.019

Sathitratanacheewin, S., Sunanta, P., & Pongpirul, K. (2020). Heliyon deep learning for automated classification of Alzheimer-related chest X-ray: dataset distribution shift limits diagnostic performance generalizability. *Heliyon, 6*. .heliyon.2020.e04614 doi:10.1016/j

Soundarya, S., Sruthi, M.S., Sathya, B.S., Kiruthika, S., & Dhiyaneswaran, J. (2020). Early detection of Alzheimer disease using gadolinium material. *Mater Today Proc*. .2020.03.189 doi:10.1016/j.matpr

Zaar, O., Larson, A., Polesie, S., Saleh, K., & Olives, A. (2020). Evaluation of the diagnositic accuracy of an online artificial intelligence application for skin disease diagnosis. *Acta Dermato-Venereologica*, *100*(16), 1–6. doi:10.2340/00015555-3624 PMID:32852557

xx

Acknowledgment

Editing the book *AI Applications for Disease Diagnosis and Treatment* with the IGI Global Publisher was an amazing trip. We enjoyed every step in the editing process.

First, we thank each one of the authors for their valuable contributions. The good quality of their chapters, according to the reviewers' appreciations, gave a great scientific value to this book.

Our sincere gratitude goes to the Editorial Advisory Board (EAB) members and reviewers who contributed their time and expertise for the improvement of the quality, coherence, content, and presentation of the chapters. Thank you so much for letting this book see the light of day.

We are deeply thankful to everyone in the IGI Global publisher team for their professionalism, guidance, availability, help, and kindness.

Finally, we would like to acknowledge the help of all the people involved in this project. Without their contribution and support, this book would not have become a reality.

Rajae El Ouazzani
Moulay Ismail University of Meknes, Morocco

Mohammed Fattah
Moulay Ismail University of Meknes, Morocco

Nabil Benamar
Moulay Ismail University of Meknes, Morocco

Section 1
AI Opportunities and Challenges in Healthcare

Chapter 1
Machine Learning in Healthcare:
Theory, Applications, and Future Trends

Lana I. S. Hamad
Yildiz Technical University, Turkey

Elmustafa Sayed Ali Ahmed
https://orcid.org/0000-0003-4738-3216
Red Sea University, Sudan

Rashid A. Saeed
https://orcid.org/0000-0002-9872-081X
Taif University, Saudi Arabia

ABSTRACT

Due to the increase in healthcare data provided by IoT, there is a need to use new methods for data analysis. Machine learning (ML) techniques promise solutions for many challenges facing the IoT-based healthcare services. MLs provide significant improvement in different IoT aspects related to storage size, computational power, and data transfer speeds. In addition, MLs provide a number of solutions for medical imaging, resources, medical data processing, detection, diagnosis, and prediction. Recently, many applications have appeared in the field of medicine and healthcare, which are closely related to the IoT. This chapter presents basic concepts related to the use of ML techniques, in addition to some algorithms used in the medical field and healthcare technology based on IoT devices and systems. Moreover, the chapter will discuss the ML opportunities and challenges in healthcare and future trends as well. The chapter gives the reader full perception of the possibility of using ML techniques in the medical and healthcare fields, with a systematic description of their applications.

INTRODUCTION

IoT aims to allow objects/things to connect with each other at any place and time, with any network to do any service for anyone (Alnazir et al. 2021) and (elmustafa el at. 2021). IoT can be defined as a group of connected manageable sensors or actuators representing a part of infrastructure with the ability to connect with the other network devices and exchange collected data to achieve a specific function (Bruno et al. 2015). With the development of the IoT and entry in many areas, its use area has expanded to include many applications. IoT applications include; supply chain management, transportation, disaster alerting & recovery, and healthcare applications.

Nowadays, healthcare represents the most important aspect of people's lives, so most countries strive to provide a strong and effective health care system. Technologies such as AI, and IoT, have entered the healthcare field, turning traditional healthcare into intelligent healthcare (Zeinab et al. 2017). IoT-based healthcare systems provide a promising solution for the inefficiencies in health infrastructure by generating a global network of smart connected devices (Stephanie et al. 2017). These devices enable the remote monitoring of the patients and continuously process the data and store it in the cloud to be ready when it is needed in additional processes

The world is witnessing an increase in the number of births on the one hand and the aging populations on the other hand, which has led to an increase in the number of patients with chronic diseases (Australian et al. 2014). This increasing causing a huge pressure on healthcare system. Moreover, population healthcare occupies large amount of the countries budgets. Effective solutions must be obtained to reduce pressure on health facilities and staff as well as increasing the quality of provided health services (Stephanie et al, 2017). Due to being, an important solution IoT interred into a number of healthcare applications domains. The IoT based Healthcare Network as shown in figure 1, enables healthcare devices to communicate with the IoT through gateways in the communication network and to send and exchange the healthcare information to the health smart decisions and cloud and data platforms for analytics and applications services. In general, IoT healthcare applications can be categorized into three scenarios as reviewed in the next subsections.

Figure 1. IoT based healthcare network
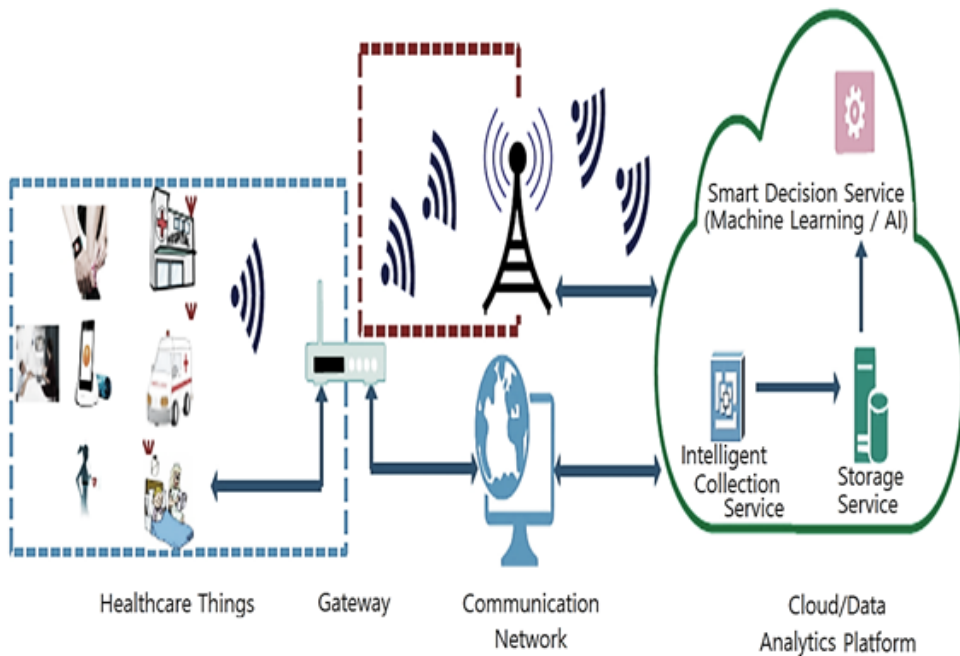
Acute Disease Care

Acute diseases are defined as diseases that require intensive care, as three applications related to the IoT fall under them, namely, the detection and control of infectious diseases, telemedicine, and then the vital sign monitoring. IoT shows very promising results in making positive effect with cases that requires immediate actions such as in acute disease. Acute diseases can include broken bone, a heart attack, a respiratory infection, etc. In the cases that require emergency department inters, the blood pressure, body temperature, respiratory rate, heart rate and other measurements depending on the clinical settings, are monitored to determine the appropriate treatment and avoid deterioration of the patient's condition such as in vital sign monitoring for the emergency department (Qi Lin et al. 2021).

Acute care telemedicine provides a remote medical intervention for patients who need urgent and emergency care (Qi Lin et al. 2021). IoT technology enables improved detection of infectious diseases and effective assistance in combating them, in addition helps to detect the disease's sources and causes to facilitate controlling its infections. In general, the detection process is the first stage in the diagnosis to find out infectious diseases. Recently, IoT have entered strongly in the processes of early identification of infectious diseases and help in developing the possibilities of

isolation and treatment for patients, especially as was the case when the emerging coronavirus appeared. The IoT realizes the concept of building smart health systems, but it requires a large range of monitoring systems that are deployed in several regions around the world, which constitutes a great challenge. Mobile Health (mHealth) devices are used with connected diagnostic devices, adding effective capabilities that help in the optimal diagnosis, tracking and limiting of infectious diseases. However, these devices face a challenge in how to deploy them in to clinical care levels and infectious disease surveillance systems (Wood et al. 2019).

Chronic Disease Care

Chronic disease care include arthritis, Alzheimer's disease high blood pressure, chronic kidney disease, diabetes, and heart failure. Chronic diseases are the medical conditions that require continuous medical attention and lasts at least a year. To continuously tracking chronic diseases patients' health, the IoT healthcare system using wearables and other home equipment, which enable the physicians to apply the treatment process by analyzing the patient's data. These wearables are known as remote health monitoring (RHM), which enables the electronic exchange of the health information between patients and therapist outside the boundaries of the ordinary health system.

The remote health monitoring system (RHMS) monitor the desired passion's health parameter by the sensors, send the collected health data remotely and analyze it and based on the output the treatment will be offered. The system also can detect the sudden health conditions and send an alert for immediate intervention. RHMS works to provide health care using information technology and helps in monitoring and verifying patient's health outside the traditional clinical environment (Qi Lin et al. 2021).

Self-Health Management

Self-health management that requires data sensing, data processing, and the use of wearable devices such as wrist-mounted, head-mounted, or wearable devices that allow information to be displayed. The most popular device for self-health management is the smartwatches that widely used for functions such as, exercise monitoring, sleep monitoring, step tracker, and workout reminder (Qi Lin et al. 2021).

The typical IoT- based healthcare system which represented by figure 2, mainly consist of the things that will be monitored, the communication network and cloud data platform. In Healthcare, medical things are the most important application area in IoT technology. The importance of using IoT technology in our daily lives becomes real due to the fact that today world became dynamic. The concept of IoT

4

is a technology that combines a number of tools with the exchange of information between them to provide convenient and advanced services to solving many human problems. One of the most important IoT technologies considered to be of great benefit is the Internet of medical things (IoMT) (Dragorad et al. 2017).

Figure 2. IoT based healthcare system architecture
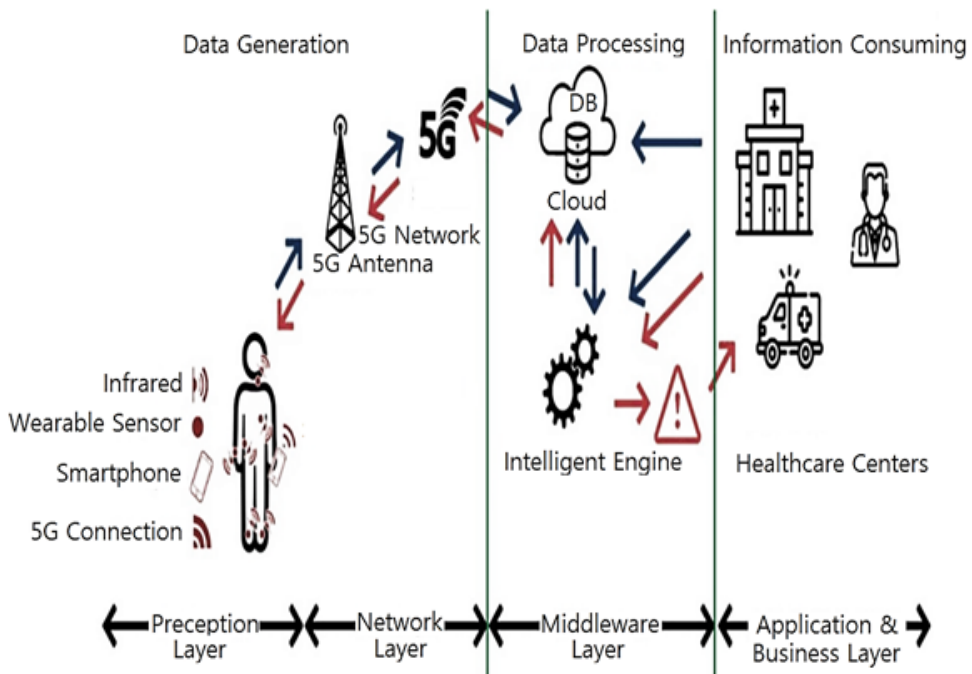
INTERNET OF MEDICAL THINGS (IOMT)

The IoMT is radically changes the way people communicate with each other and with the world around them (Minhee et al. 2018). The IoT concept utilizes the integration of digital communications with medical things in order to enable high healthcare quality outside the hospitals as shown in figure 3. Electronic systems have an important role to play in meeting the concept of IoT in healthcare. Recently, a number of modern electronic devices have been introduced that have helped improve the quality of people's treatment in health institutions and increase their chances of survival from chronic and serious diseases (Assefa et al. 2018). Another benefit of IoT technology is to help assisting doctors in detecting and diagnosing health problems in patients in order to reach effective treatments.

5

Mobile health technology enables people to track their activities and assists in making medical measurements that help promote health safety and decision-making in chronic inflammatory conditions. The concept of this technology has become widely spread in homes, which helps to prepare medical reports and analyze health statistics for users (Rameswari et al. 2018). Remote access technology in health care helps to provide care to patients in accordance with their health status in their places. Such technology uses a number of programs and applications, such as the recently used like FaceTime and Skype, which play a major role in providing close follow-up of doctors to their patients. There is also the possibility to use screens or a camera at home or any other devices that enable remote monitoring of patients who are enrolled in a medical rehabilitation program (Minhee et al. 2018).

Electronic health records (HER) technologies provides many benefits to patients, and for doctors as well to review the patient's information with intelligent record systems. Electronic health records enable physicians to share lab reports, thus enhancing the delivery of superior care with less frequent medical tests and examinations (Adeniyi et al. 2018). In addition, electronic records allow clinicians to log into their patients' medical records easily to make decision about who patients are need to be assisted first and according to the responses in a long day by day.

Figure 3. Integration of medical things and internet

6
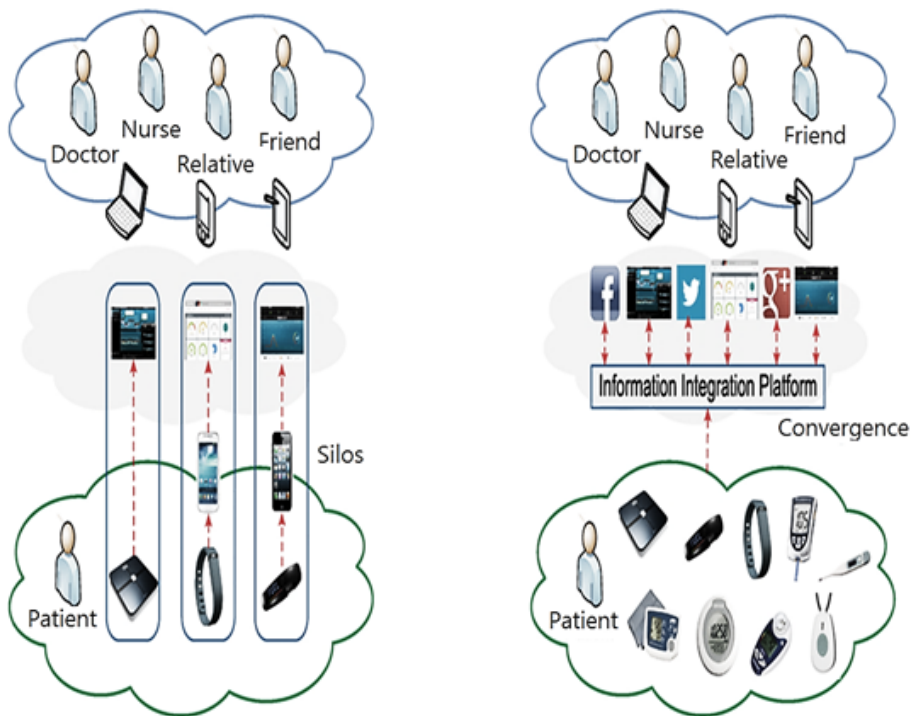
Wearable systems help monitor the human body and measure vital signs such as heart rate and body temperature using monitors that are attached to the patient. The data is more robust and valuable due to continuous monitoring by these wearable systems rather than periodic sampling (Assefa et al. 2018). In addition, Many IoMT systems and products are changing businesses in many industries. Both patients and service providers can benefit from the IoMT, which is bringing a greater presence in healthcare. Hospitals use IoT to monitor the location of medical devices, personnel and patients (Hemantha et al. 2021).

The use of remote IoMT management system, managing a lifestyle related diseases and conditions, fitness programs, care at home, chronic diseases and care for the elderly are some of the important use cases (Rameswari et al. 2018). Other cases that include improving a patient's compliance to treatment and medication in hospitals, clinics or in other care facilities. All these cases require that the IoMT systems must handle some issues such as data aggregation, storage, analytics, and visualization in addition to host user centric services (Hemantha et al. 2021). These issues require main features to operate and manage the IoMT systems; such features are intelligence using electronics and embedded systems, environmental sensing a complex environment, connectivity, complexity, and energy efficiency, security, and cloud solutions (Rameswari et al. 2018.

Intelligence

Software's and hardware's together add some kind of intelligence to makes a product experience smart. Algorithms with embedded computers should work together under one-operation concepts to achieve a degree of flexibility and compatibility with highly intellectual operational efficiency for internet of healthcare system. Such example is to distribute tasks computations between a smartphone and the cloud (Adeniyi et al. 2018).

Connectivity

The connectivity in IoMT defines the path to connecting a patients' medical things information to their care team. Its focus is identifying the sources of electronics healthcare information then making it sharable with other healthcare devices through integration with healthcare assets and delivering it to the people who need it (Padmavathi et al. 2016). In addition, it describes how health care information will be connected to create integrated medical things one that provides a lifetime record of an individual's health history. The connectivity should enables network accessibility and compatibility (Adeniyi et al. 2018).

Environmental

Sensing technologies offer new paradigms that reflect a true awareness of the physical world and people as well. In other words, they are acts as inputs that represent the physical world and provide a realistic understanding of our complex world (Ali et al. 2021) and (Hemantha et al. 2021). It is possible to connect a number of devices such as smart phones and sensor systems, which work to build a healthcare core that provides access to health services and medical sciences. These devices help improve lives by enabling the convergence of wireless communication systems, sensor networks, and computing technologies with the medical field and health care (Redowan et al. 2018).

Energy and Power Efficiency

The most effective medical things in IoT for healthcare application, it is so difficult to create billions of medical things that all run on batteries (Hemantha et al. 2021). Energy harvesting, power efficiency, and charging infrastructure are necessary parts a power intelligent ecosystem that must be designed. Of course, many medical devices in IoT must be always on which need for greater energy efficiency (ali et al. 2021). If the IoMT devices unable to operate with low power, which supplied by batteries, then the idea of being always working is not be possible.

Security Issues

With more benefits gained by IoMT, there are important issues that will affect the IoT medical systems, which they are safety and security. As both the creators and recipients of the IoT, it must design for security and safety. This includes the safety access to personal data and the security in storing or in processing of data. Securing the endpoints, the networks, and the data moving across all of it means creating a security paradigm that will scale (Redowan et al. 2018). The need for security today covered entities is pervasive and as health information transfers between consumer and enterprise devices, message level data encryption will become essential. When a communication established between a device system, the healthcare institutions' agreements with vendors and cloud services providers to ensure that data traffic of the device and its software application is encrypted when communicating the institution's private network and those of its outsourcing providers and any cloud systems (Padmavathi et al. 2016).

Cloud Solutions

In IoMT, cloud solutions have three distinct issues; storage, analytics, and visualization. Cloud based medical data storage is a very important parameter in IoMT. Analytics that use the sensor data along with E-Health records that are becoming prevalent can help with diagnoses and prognoses for a number of health conditions and diseases (Lee et al. 2015). The visualization process is very important in such systems as it enables doctors to examine a huge number of data and information collected by wearable sensors. When designing such systems, long-term storage mechanisms must be upgraded to preserve medical information related to patients in order to assist physicians in diagnostic processes (Moeen et al. 2015) and (Adeniyi et al. 2018). Clouds systems should provide many solutions in managing the dynamic nature of the health data, keeping the data of all patients secure and applying the right analytic technique to use the information most effectively (Adeniyi et al. 2018).

ARTIFICIAL INTELLIGENCE IN HEALTHCARE

In Medicine field, AI and IoT applications provides an intelligent platform to analyses symptoms and diseases treatment. Medical devices enable to transmit the data in adopted measures, and doing processing by mobile applications (Mohan et al. 2018). Prioritizes sensing data are preprocessed in intelligence manner by using the AI algorithms (Papadokostaki et al. 2016). ML with data mining are both plays a vital role to extract the signature of data and provides medical interpretation.

The use of AI enables to assessment the condition of patient's health, and provides an intelligent remote diagnosis in addition to best medication through the IoT based edge-computing network. Moreover, AI algorithms such as ML provide smart decision making in data analyzing for diagnoses and extracting treatment choices (Machorro-Cano et al. 2019). In addition, AI able to recognize the patient's behavior and intends in reaction with healthcare decisions in case of critical situation.

Machine Learning Classifications in Healthcare

ML is the study of tools and methods through computer algorithms for identifying patterns, which can then be used to either increase our understanding of the current world or make predictions about the future in data (Chen et al. 2014). Now a day ML used with the current covide-19 pandemic to identify the risk factors for infection and predict who will become infected. In general ML goals to find the best model to explain the data.

9

Figure 4. Machine learning approaches
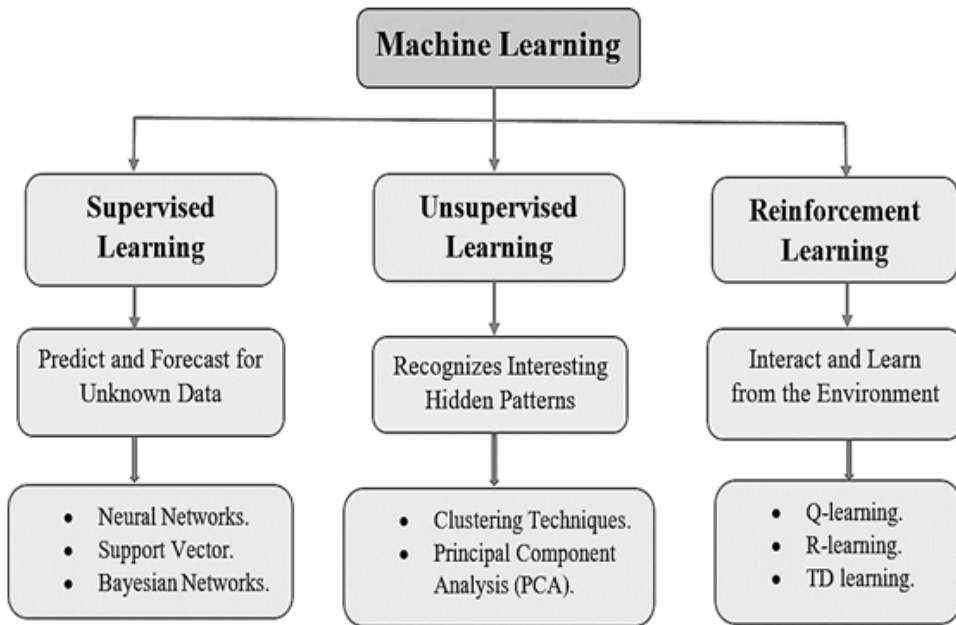
Recently by learning from row, data ML techniques is successes in achieving complicated tasks. ML algorithms are classified into the following three categories considering the nature of the experience in learning: supervised, unsupervised, and reinforcement learning (Carrio et al. 2017) and (Raeesi et al. 2021). Figure 4 represent the classification of ML algorithms.

Supervised Learning Algorithms

In supervised ML algorithms the data are divided into labeled training set and testing set and use the labeled data on a training model (Arwinder et al. 2019). The trained model then can be used with another new data either for identification or prediction tasks. In supervised ML algorithms, there is a specific interested outcome related to the patient is infected or not. For example the supervised ML algorithms is used in healthcare for cancer diagnosis by analyzing the input tested data, identifying strange patterns in human organs and finally determining wither the patient is infected or not. Deep neural networks, logistic regression, ensemble approaches, and decision trees are from the most used supervised ML algorithms in healthcare domain.

10

Figure 5. Supervised learning process
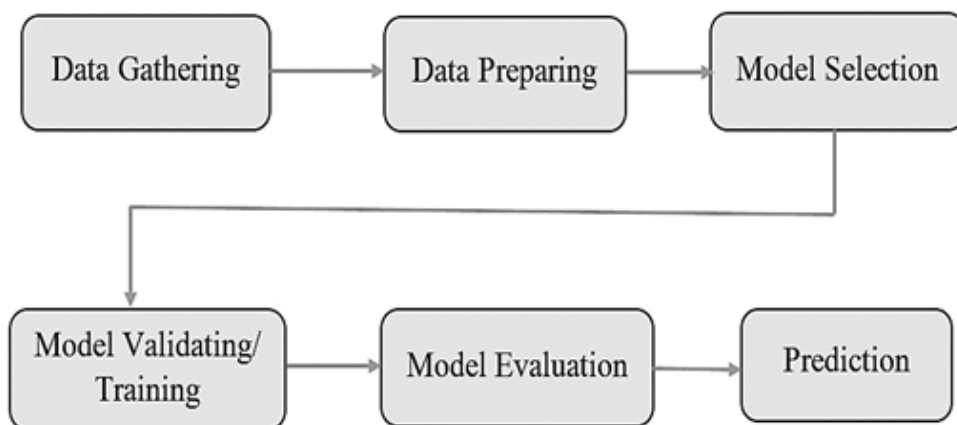
The supervised ML algorithms includes Neural Network and Ensemble methods, K Nearest neighbor, Decision trees, Naïve Bays Classifier, Support Vector Machines. To solve a given problem using supervised learning first the type of training example should be determined and gathered by an expert or measurements. Figure 5 shows how to solve a given problem using supervised learning. There are usually particular steps that need to be followed. First, the type of training example should be determined. To complete the design the used learning algorithm is selected followed by running the learning algorithm on the gathered training data. The accuracy of the learned function should be evaluated before the parameter adjustment and learning-using test set which separate from the training set (Amani et al. 2021).

In general, the supervised ML algorithms enable to analyze large and complex health data for clinical implementation and ethics in health care delivery. It also helps categorize risk, prognosis, and survival outlook. It can also be combined with laboratory results and medical images to predict risks and identify diagnostic trends.

Unsupervised Learning Algorithms

Unsupervised learning is an ML technique, which also trains the machine, but with unlabeled data and the target value is unknown (Arwinder et al. 2019). It is also referred as self-organizing maps. By find hidden patterns, the algorithms under this method try to cluster the similar type of data like attributes, trend, patterns, etc. The main target of the unsupervised learning is to find patterns rather than prediction as the supervised learning. The input of the unsupervised learning could be any type of data however; due to the unknown of the labeled value, the outcome is cannot be predicted (Neha et al. 2021). Clustering techniques, which is used for

heart disease prediction, and principal component analysis (PCA) which is used in hepatitis prediction is two important unsupervised learning techniques that is used in healthcare (Singh et al. 2019).

In healthcare, unsupervised learning algorithms analyze unsupervised data and develop methods such as deep learning to improve the efficiency and accuracy of health-based application systems. Unsupervised learning technologies offer the potential to automate health monitoring, disease diagnosis, health index monitoring, drug discovery, and medical imaging diagnosis (Salih et al. 2021). It also helps improve the efficiency of various healthcare applications such as smart health monitoring and management, medical robotics, imaging diagnostics, epidemiological prediction and other applications.

Reinforcement Learning Algorithms

The working system with reinforcement learning (RL) is developing its work with an iterative process by taking feedback from the actins take place within the environment instead of expecting the output giving a set of input (Neha et al. 2021). Without any human interference and by the aid of the testing and error learning the machine could learn from its experience, taking instantaneous decisions; so it is an iterative process (Arwinder et al. 2019). In healthcare, the reinforcement learning is used for developing the expert systems. Reinforcement learning working process can be seen in Figure 6.

Figure 6. Reinforcement learning process
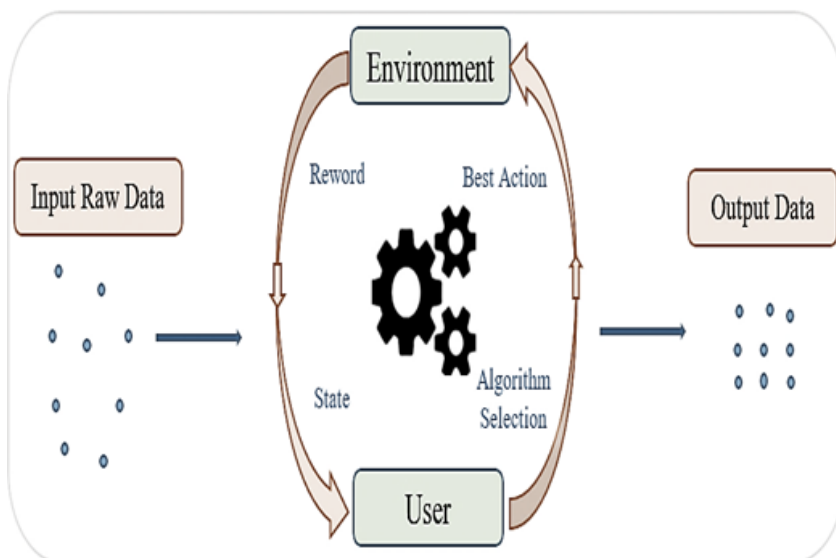
The RL algorithms empowers an individual's behavioral decision-making abilities using experience of interaction with the world and evaluative feedback, whereby diagnostic decisions or treatment regimens are typically characterized by a lengthy, sequential procedure. In the healthcare, RL offers effective solutions to the healthcare system by endowing the individual with behavioral decision-making skills by using the experience of interacting with the surrounding environment and creating feedback related to diagnosing medical decisions.

Machine Learning Models in Healthcare

Since the healthcare domain is the regarded as a vital part in the human's life, it handles with many data about patients and diseases daily. The heath data needs to be analysis and the hidden patterns in disease's recognition, treatment, and prediction need to be found. Instead of found these patterns by the humans, ML helps to automate the healthcare system. With the presence of ML, the machine instead of the humans will make accurate decision (Rohan et al. 2017). The accuracy of the decisions taken helps to save time and decrease the cost when treating the patients and controlling diseases. The ML techniques used in Healthcare includes; ML-based Prediction System, ML-based Data Aggregation, and ML-based Secured Analysis.

ML-Based Prediction System

In most of the ML-based IoT disease prediction systems the data flow from the source like sensors, actuators, and wearable devices to the destination goes through three stages; gathering the data and transmit it to the cloud, processing the data and storage and mining. First, the monitoring devices will monitor the phenomenon and send to local processing devices such as smart phones, and laptop in which could be preprocessed and deduced some emergency decisions. The data then will be send to the cloud or to a host server to be stored. The last stage is the data mining stage in which the data will be processed, analyzed via different ML algorithms and the outcome is extracted.

Based on ML algorithms many of diseases prediction systems are proposed. A smart tele-health monitoring system for identifying and predicting the concurrency of Parkinson's disease using K-mean algorithm is proposed in (Borthakur et al. 2017). In study by (Khan F et al. 2019), authors using ML techniques the stress prediction is evaluated by gathering the data at different time intervals.

ML-Based Data Aggregation

The aggregation data of the healthcare can be processed either on the gathered data at the sensing devices levels, before sending it to the cluster head or the local server, or it at the cloud before sending it to the physicians. Several ML algorithms are used to aggregate the data and reduce the number of data sending, hence the network lifetime. In study (F Khan et al. 2019), authors using big data techniques to extract the critical information from sensors the authors eliminate the redundancy before send the data to the distention (clinic). To extract useful patterns from the gathered data known as health informatics processing pipeline proposed in (Alsheikh et al. 2016). The proposed work is a novel framework for big data analytics in IoT and it includes data capturing, storage, analysis, and searching.

ML-Based Secured Analysis

The data security in IoT-based healthcare system during all stages that the data passing until the outcome is critical due to its sensitive nature. Therefore several of future trends toward using ML techniques for secured gathering, classification, testing and sharing of the patient data. To the big data analytics a framework for novel mobile cloud computing using various ML and DL techniques for classifying and testing the data, is proposed in (Essa et al. 2018). In (Gope et al. 2015), various ML techniques are used to enhance wireless body sensor network (WBSN) security and protect the network from intruders and various attacks.

ML BASED IOT ARCHITECTURE AND FRAMEWORK FOR HEALTHCARE SYSTEMS

Due to the expansion in IoT devices deployment and the increasing desire of healthcare cost-effective, the technology of IoT is play a powerful role in all aspects of health management. The healthcare-related Internet of Things is known as Healthcare Internet of Things (H-IoT), which is defined within two application domains: clinical diagnosis and health monitoring. The H-IoT technology integrated devices such as heart rate tracking devices or sensors, communication technologies, positioning systems in addition to medical applications as shown in figure 7.

The IoT and ML-based applications have a major role in enhancing the quality of everyday human's life. The H-IoT system network consist of three common operation layers (Almotiri et al. 2016) and (Hemantha et al. 2021). The data collection layer is responsible for collecting the medical monitoring data from many sensor wearable by patients. The data storage layer, which stores the sensor, has collected data before

sending it over internet. In addition, data processing layer, which enables to analyzes and generate the required response by applying several of computer programing algorithms after collecting and store the data in the server. The following enabling technologies aid to implement the previous mentioned layers (Song et al. 2015) and (Hemantha et al. 2021).

Figure 7. Healthcare internet of things (H-IoT) technology
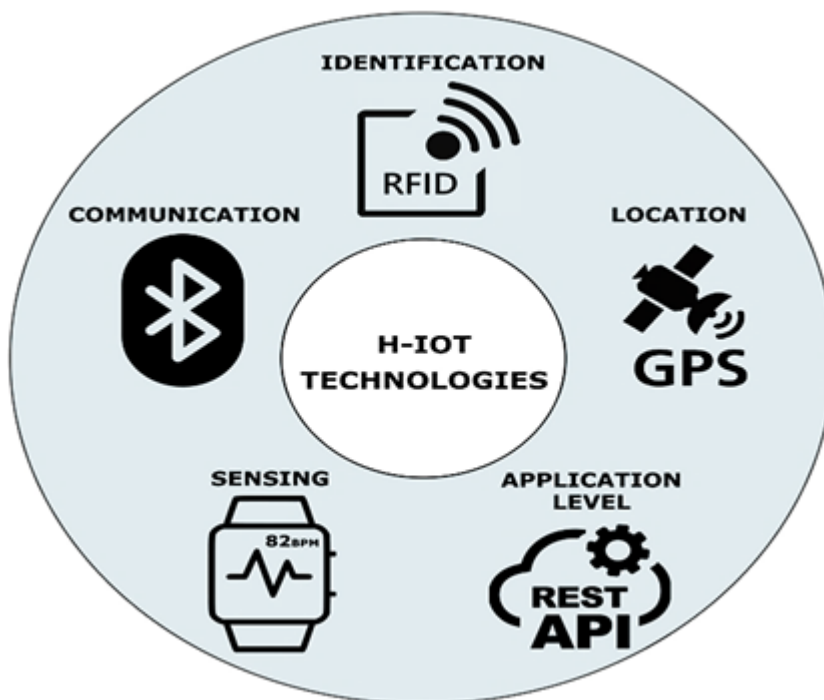
Identification Technology

In unique identifier (UID) technology each node of the H-IoT framework is uniquely identified to have secured inter-connection and information access.

Communication Technology

H-IoT devices can communicate via short or long distances. If the network is implemented in relatively short distances then technologies such as local area network, which could be Wi-Fi, or Bluetooth Zigbee, RFID, etc. compared to 4G, 5G, and LTE-A technologies used to connect long area distance.

15

Location Technology

In sum applications and use cases of H-IoT the location determination of the nodes is extremely important to tracking each other. Various location-tracking systems are used beside GPS, which authorizes many nodes to accurately determine the geographical locations.

Sensing Technology

The primary source of the analyzed date on which the decision is based in H-IoT system is the sensors. Therefore, evolution in sensing technologies reflects positively on the H-IoT framework development; thus leads to more accuracy in the prediction and diagnosis process, which also leads to reducing the costs .Based on the importance of the sensing data, sensor mechanisms that monitor patient's body physiological changes in real time have an espial importance too (Song et al. 2015). To collect the patient monitoring data a number of sensors with different functions are used, for example electrocardiogram (ECG) sensors is used to measure electrical activity in the heart (Sethi et al. 2017).

In H-IoT application level architecture, the representational state transfer (REST) and service-oriented architecture (SOA) are from the application level architecture used to allow the H-IoT various devices to perform independently. Each device operation's is fully defined and could be changed as required without effecting on the other system's devices functions (Hemantha et al. 2021).Beside previous enabling technologies and to implement H-IoT framework common building elements are used (Lee et al. 2020).

Sensors that collect data like medical sensors attached with the patient to measure vital parameters, and the environmental sensors, which monitor the surroundings of the patient (Moeen et al. 2015). The sensors that could be medical or environmental. The attached sensors with the patient, which measure vital parameters, are the medical sensors; while the environmental sensors monitors the surroundings environment of the patient. Microcontrollers, which process, analyze and communicate the data wirelessly (Ali et al. 2021). Microprocessors that enable rich graphical user interfaces; and Healthcare-specific gateways through which sensor data is further analyzed and sent to the cloud.

ML ALGORITHMS IN IOT BASED HEALTHCARE (H-IOT)

In H-IoT system, the primary source of the medical data are including physical objects and detection devices which could be in form of RFID, bar code, or different types

of sensors. The temperature sensor monitoring the patient temperature, ECG sensor monitoring the heart rate, blood pressure sensor etc. the monitored data is collected, processed and transmitted via a wireless or wire network to the user. This health related data is extracted, stored, and analyzed by cloud-based devices embedded with ML techniques to be used in further analysis and prediction processes (Sadhukhan et al. 2018). The most widely used ML applications in the healthcare domain including different algorithms, where the most popular ML algorithms in medical filed are shown in the figure 8. These ML algorithms mainly work on summarizing data features, extracting patient-related features and clinical outcomes of interest.

Figure 8. Machine learning algorithms in healthcare applications
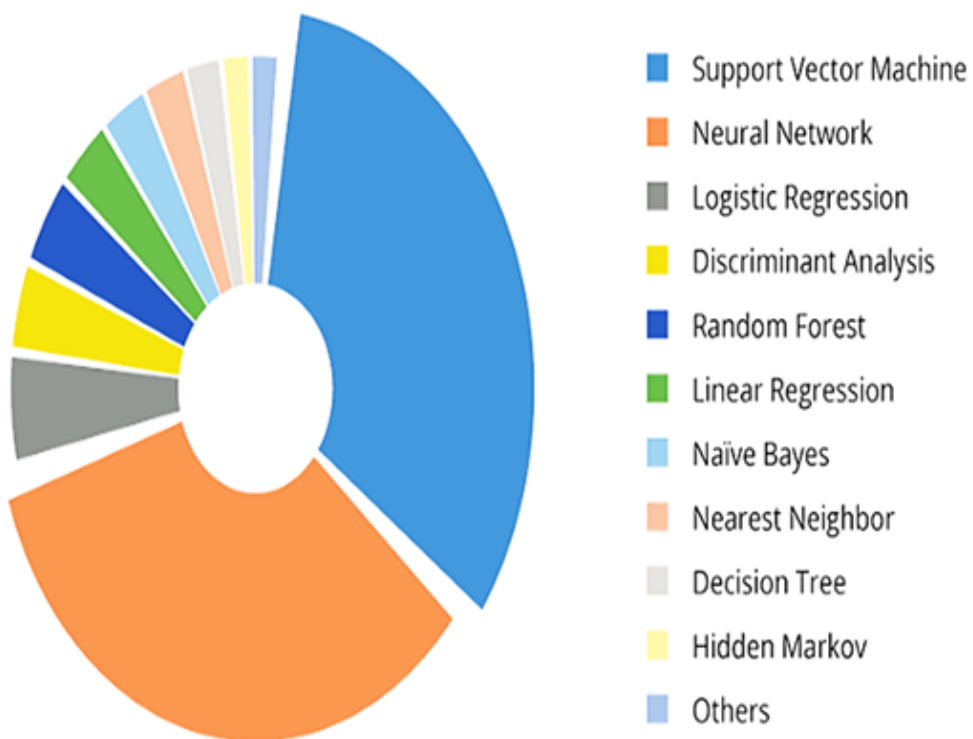
Dimensionality Redaction Algorithm (DRA)

DAR including a numbers of algorithms such as principal component analysis (PCA) and linear discriminant analysis (LDA) which aims to decrease the number of output data dimensions. The DAR's input which is take in large data sets is first identifies its correlations and patterns by removing discrepancy, excessive data, and highly

correlated data features, and with ensures to keep its critical information previously provided the output is provided in a much smaller data set (Hemantha et al. 2021).

Figure 9. Dimensionality redaction algorithm (DRA)
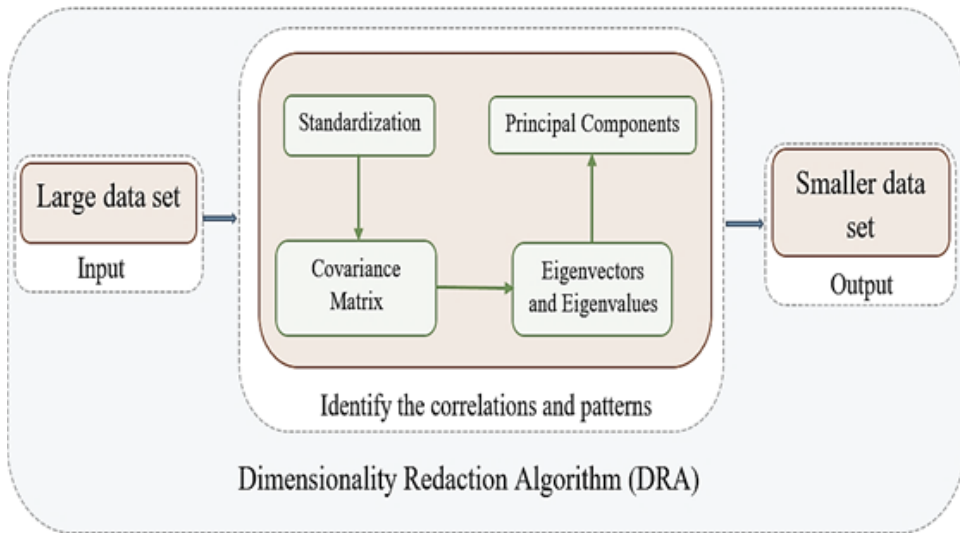
Dimensionality reduction is performed through; standardization, computing the covariance matrix, calculating the eigenvectors and eigenvalues, and computing the principal components. Significant promises is applied in (Lee et al. 2020) by combining IoT and DRA to diagnosis Parkinson's disease and breast cancer. Figure 9 represent DRA algorithm.

Discriminant Analysis

Discriminant analysis, which express data, points to a less dimensional space so that the categories are appropriately separated into non-overlapping groups (Essa et al. 2018). Based on the given class value the linear discriminant analysis is the probability density function probability density function. This function is based on the given class value with conditional probability and normal distribution (Neesha et al. 2015). Discriminant analysis is used in healthcare to finds applications to measuring the prognosis and severity of the patient's disease. For example based on discriminant analysis authors in (Armañanzas et al. 2013) establish the initial set of substantial risk factors for early warning of the chronic illness. In (Jen et al.

18

2012), authors uses scores of non-motor symptoms an algorithm proposed to help in predicting the severity staging of Parkinson's disease.

K-Means and K-Nearest Neighbouring

K-means aims to forming clusters containing the objects with the parameters of a certain class, which fall within the range of "similar or dissimilar "categories. After creating the classification categories and the clusters, the centroid of the clusters for each category is determined by the Euclidean distances. Based on the distances from each cluster, the new objects is also classified (Sood et al. 2017). K-mean is used in diseases diagnostics such as remote diagnostics for a chikungunya epidemic by tracking the disease transmission possibility. In (Kim et al. 2016), using k-means clustering on MRI images the brain tumors detection is speed up.

K-Nearest Neighbor (KNN) also is working based on the same strategy of K-mean; however, Euclidean instances of an object whose class is assigned to its nearest neighbor k are counted. KNN is proposed to increasing the efficiency of K-mean and finish its dependent on K by utilizing anew optimal and deferent K value every time. The new K value is selected by the dataset itself to annihilate the dependence on K without any intervening by the use (Durga et al. 2019).

Decision Tree

The decision tree (DT) structure is similar to the tree which including internal, sections, and leaf nodes. The DT structure help in decision making by stages until reaching the final decision stage. Internal nodes exemplify the features; decision represent the rules, and outcomes represented by branches (Chinmay et al. 2021). Gini index method is widely used to classify data in decision tree, which can be calculated by the following formula.1. Figure 10 indicates the decision tree classifier model.

$$Gini\ Index = 1 - \sum_{i=1}^{n} \left(p_i \right)^2 \tag{1}$$

Where: p_i is probability of the classified element. Decision tree learning is used in disease diagnosis such as arrhythmia.

Figure 10. The decision tree classifier model
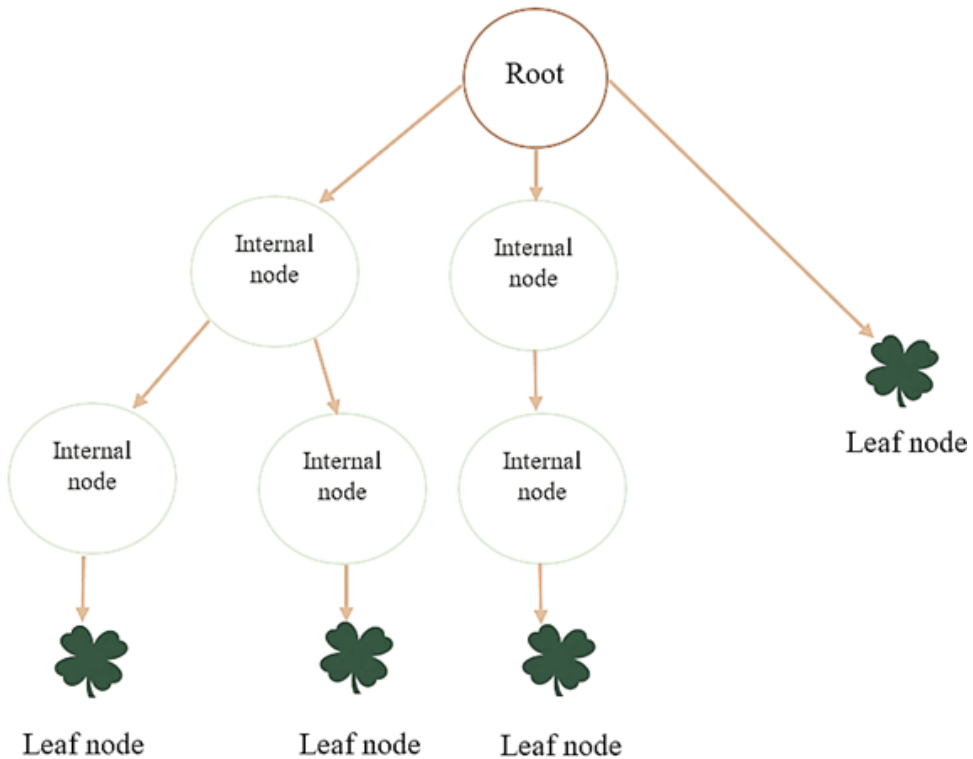
Authors in (Xie et al. 2019) develops heartbeat classification algorithms that identifies premature ventricular contraction (PVC) based on decision tree ML algorithm used to diagnose arrhythmia by take the amplitudes and heartbeat intervals as features.

Naïve Bayes

Naive Bayes classifier is supervised learning which applying Bayes' theorem. The word 'Naive' express the theorem clearly and it indicates the features independency of each other. The data is either a response vector or a feature matrix. The response vector's rows represents the outcome in classes, furthermore, in the rows of the feature matrix's the whole data collection is expressed as vectors (Suraj et al. 2018). The Naive Bayes classifier can be classified into Gaussian Naive Bayes, which use continuous predictor values, Bernoulli Naive Bayes, which use the Boolean variables as the predictors, and multinomial Naive Bayes, which is used for the document problems classification.

20

Figure 11. Naive bayes classifier
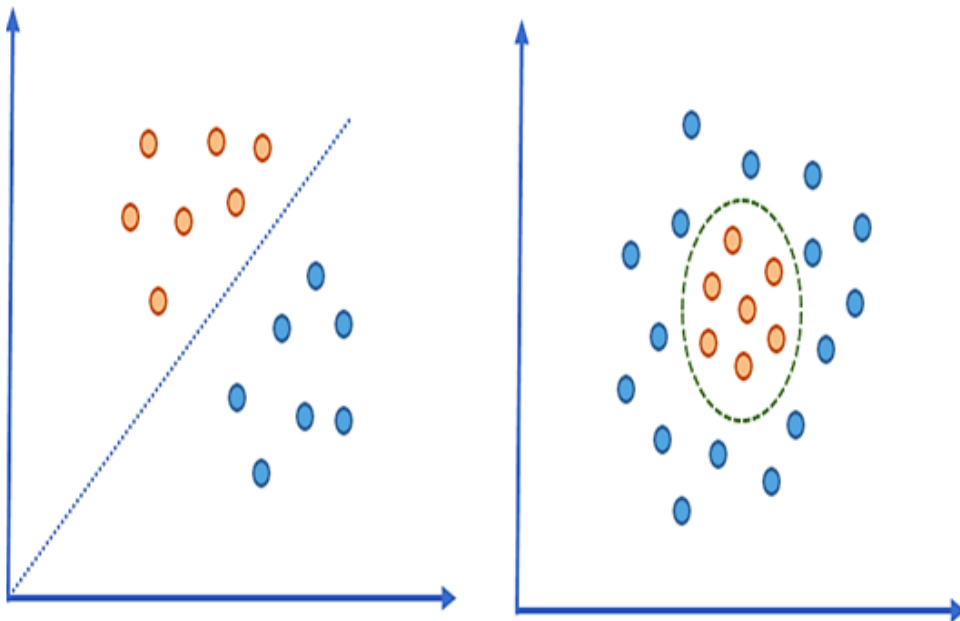
Naive Bayes classifier requires less number of training data, fast, and it is easy for implementation. However, its predictors must be independent (Chinmay et al. 2021). Naive Bayes classifier is used in medical institutes in treatment by determine the most useful drug with the minimum side effects by the aid of the sentimental analysis of the patients (Suraj et al. 2018). Figure 11 represent a general idea about Naive Bayes classifier.

Neural Networks

Neural networks are used to capture complex non-linear relationships between input variables and an outcome. Neural networks aim to minimize the average error between the outcome data and their prediction by estimating the weights through the input and outcome (see figure 12). This is done via depicting the associations between the outcome and the input variables through multiple hidden layer combinations of pre-specified functional (Fei et al. 2017).

21

Figure 12. Neural networks approach
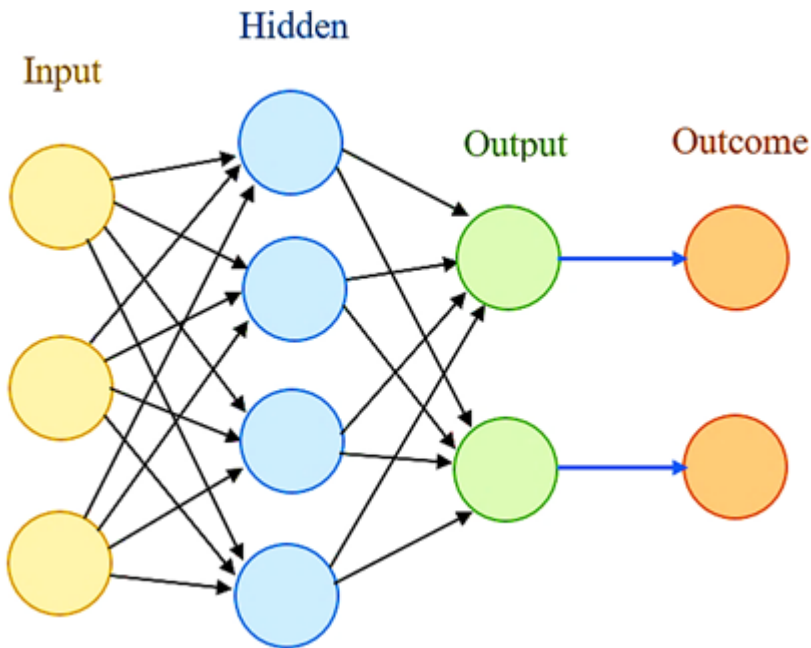
In (Elfatih et al. 2021) neural network are used to predict breast cancer and diagnose cancer in with the input being the texture information from mammographic images in the first case and the PCs estimation of numbers of genes in the second case. In the two cases, the desired output is the tumor indicators or categories. In addition, the neural network is used in (Hirschauer et al. 2015) to diagnose Parkinson's disease.

ML APPLICATIONS IN HEALTHCARE

Recently ML is contribute in improving the healthcare process from the beginning by early prediction before infections until the end of treatment. ML helps in increase the accuracy of the system as well as efficiency by using the machine in diseases predicting. During the diagnosis process, the physicians can be helped in detecting the disease by extracting and comparing the results with previously obtained results (Jiang et al. 2021). By using ML in monitoring the patients during the treatment, we can avoid the deterioration of the patient's condition and provide timely intervention. Using ML algorithms, the data is extracted analyzed, and used in accurse prediction of other patient in the future (Hemantha et al. 2021). The application of ML in healthcare can be inserted under the following categories.

Diagnosis of Disease

The process of identifying a medical condition, disease that the patient is currently facing, generally defines diagnosis. The identification process is carried based on the sensor measurements of symptoms examinations or others parameters such as the patient's health history (Assery et al. 2019). To diagnose a disease, the medical data is extracted using ML algorithms analyzed, and the decision will be make. The ML algorithms using has shown a remarkable results in many widely affecting chronic diseases diagnosis such as; Type 2 diabetes, Chronic kidney disease (CKD), Heart diseases, Lung cancer, and neurological disorders.

Smart Electronic Health Records

Electronic Health Records (EHRs) is a combined of digitized record of a medical occurrence called electronic health records (EMRs) which provide an overview of specific patient's health. By containing a complete patient's medical history, EHRs present a good method to track the patient health progression. EMR could be in the form of unstructured data such as radiology reports or structured data such as drug orders, which are taken either during or after the health issue by a medical professional in a medical environment (Adnan et al. 2020). To increases, the efficiency of the disease diagnosis process benefit from the EHRs number ML-based methods are applied. For example in (Zheng et al. 2017), ML is used for diabetes diagnosis from EHRs.

Medical Imaging Processing

Different imaging modalities such as magnetic resonance imaging (MRI), ultrasound, and positron emission tomography (PET) computed tomography (CT), etc. are the input data source in medical image analysis. Medical image analysis is so beneficial in diseases diagnosis and prognosis as it is the main reference to the clinicians and radiologists. By the aid of different ML algorithms, these modalities help in disease diagnosis by providing needed medical information about body organs (Adnan et al. 2020). Figure 13 present taxonomy of key medical imaging processing modalities. The basics tasks in medical image analysis include.

- Enhancement, which regarded as the important pre-processing step of the medical image processing and directly effects the disease diagnosis process. Enhancement is used to reduce the noise in the medical images by using different ML and DL methods.

- Identifying the patterns of a specific disease or abnormalities, which refer to Detection. Varies of ML and DL algorithms such as CNN are used for the detection of diseases.
- Classification and recognizing abnormalities in different body organs, from medical images.
- Partitioning images into multiple non-overlapping parts which known as segmentation.
- Medical image reconstruction, which is using the imaging sensor data to generating interpretable images.
- Retrieving medical images from a large database various ML/DL techniques.

Figure 13. The commonly used medical imaging processing

Medical Imaging Modalities

- Magnetic Resonance Imaging (MRI)
- Ultrasound
- X-Rays
- Histology
- Computed Tomography (CT)
- Positron Emission Tomography (PET)

24
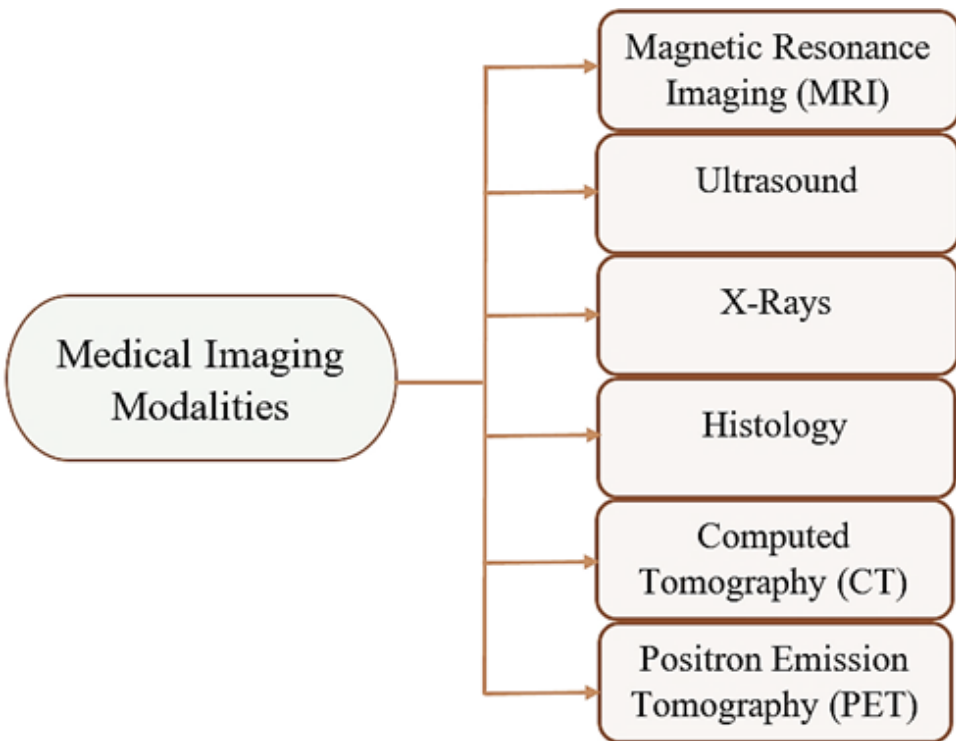
Figure 14. Wearable sensors based remote healthcare monitory
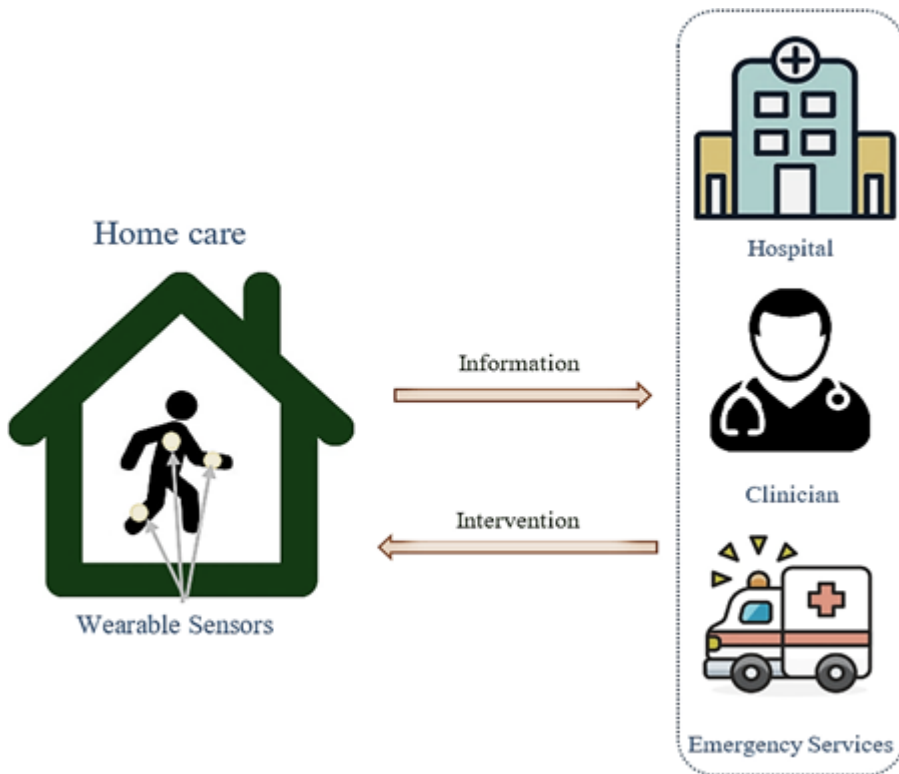
Patient and Hospital Monitoring

Critical patients monitoring is an important part of the treatment process, which could occurs during or after it. Continuous health monitoring also can include monitoring elderly people during their daily activities to interfere in the suitable time if there is sudden situation such as falling. The process of data from the gathering to the outcome in continuous health monitoring is start of collecting the data using wearable device and smartphone, followed by sending it to the cloud to be analysis (Zheng et al. 2017).

The general idea of remote health monitoring is illustrated in figure 14. After analysis the data using an ML/DL technique, the outcomes will be transmit back to the device and taking suitable procedure. In (Zech et al. 2018) others are proposed a framework which monitoring the heart rate using PPG signals. The framework is having a similar previous system architecture and it is developed using integrating mobile and cloud for monitoring.

ML TECHNOLOGY FOR IOT BASED
WEARABLE MEDICAL DEVICES

Wearable medical devices are an electronic biomedical equipment that can be used in collecting real- time medical information such as motion patterns, EMG, ECG, EEG, blood pressure ant etc. about a body, which can be displayed in LCD embedded devices. Wearable medical devices refer to as Wireless Body Area Network (W-BAN) (Brahmaji et al. 2020). WBAN is a network of wearable wirelessly inter-connected medical devices which. The network is consist of the sensors, which they are the wearable devices, and a near located gateway, which deliver the data to the server. By the recent advances, the artificial intelligence and its subfield ML is used in enhance the performance of WBAN interaction (Fadi et al. 2019). In addition, ML can improve WBAN outcome by take the necessary actions. By the cooperation with ML, WBAN is being capable of detecting hidden patterns and make smart decisions.

Figure 15. Wireless body area network structure (W-BAN)
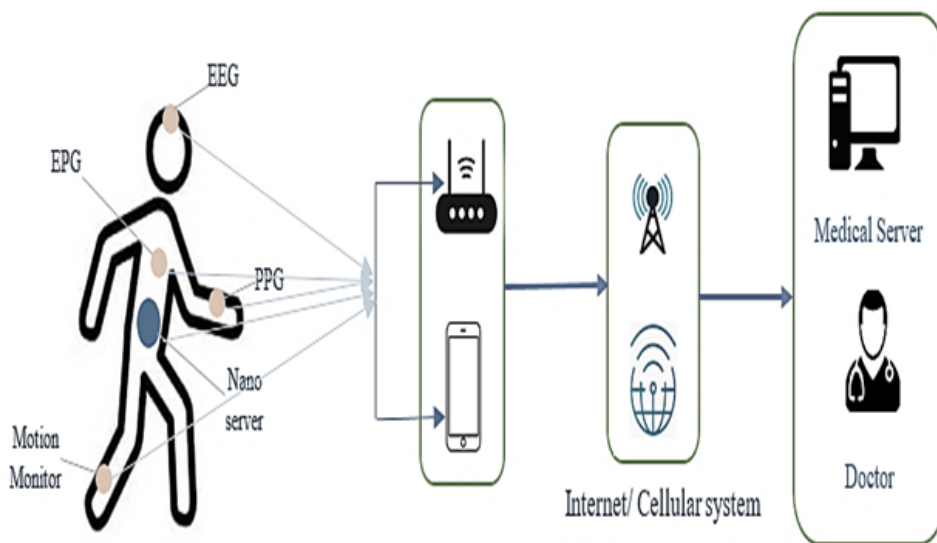
In the ML- based WBAN system, after collecting the wearable devices medical data by an intermediate connected device, the data will be transmitted to the desired health center (clinic) by mobile device via the internet. Before using the data, it will be analyzed and processed by the suitable ML method/ methods (Wang et al. 2020). Figure 15 giving a general idea about the IoT-based wearable system.

26

The most usable WBAN systems that are attached to the patient bodies (Chengwei et al. 2021). To monitor heart rate, calories burned, distance traveled, and other physiological parameters the smartwatch is used. The ear accessory device is connected to the ear as reasonable sensors and can be used to obtain heart rate and oxygen saturation level. T-shirt is used to obtain heart-activity-signal beside other numbers of physiological signals, applying electronic technologies and cloth materials it can cover a larger body area.

MACHINE LEARNING IN HEALTHCARE, CHALLENGES AND OPPORTUNITIES

Machine learning in Healthcare drives advances in many aspects including medical care, diagnosing, and treatment. ML enables to manage the data related to the diagnosing and observational of large-scale diseases phenotyping. Most of the current studies using machine learning in the medical field focus only on applications in biomedicine. However, the use of ML in health care and big data mining in precision medicine presents broader opportunities to develop health care delivery and operational needs such as care tracking and revenue cycle management.

Even that ML provides many advantages I healthcare applications, however, the use of ML in health care still has risks related to predictions of data being generated and managed across the medical system. Most of the challenges facing ML are in implementation and realization in medical applications, and the lack of training samples for the medical learning model leads to poor usability. In addition, the dimensions of medical data available for analysis, such as vital signs, medical imaging and patient data, are different, which is influences the ML performance (Ghassemi et al. 2020). Other consideration is related to the reliability of the analysis results related to machine learning techniques in healthcare data sets need to develop interactive techniques within the reliability and confidentiality of data with human intervention to validate the model (Adnan et al. 2020).

Another aspect related to training the medical models, which is that use of ML is generally done by training models on the largest possible data set, but the change in clinical settings does not enable continuous learning of models, especially when the treatment procedures for patients change after a period of time. This change in clinical settings leads to weakness and deterioration in predictive performance, so it required strong models for these changes (Ghassemi et al. 2020). The clinical procedures changes that affect the performance of ML techniques is related to different aspects, which are categorized as follows.

a.   Change in Internal Validity:

It is related to medical changes over time, which appear through medical assessments in some diseases due to changes in research behaviors. These changes may lead to the products medical estimates that are exaggerated in models, which causes a deviation in the expectations of disease development.

b. Change in External Validity:

It is related to the generalizability related to the practices of different local hospitals, in addition to the number of patients, existing equipment and electronic health records. For example, in the case of some transitions between electronic records occurred, it creates problems in assigning features, which may hinder the development of strong models due to the difference in data.

c. Clinical Data Type and Quality:

Compared to other data applications that use ML, health care data is well organized but highly heterogeneous, as it is vague and incomplete, so it represents a major challenge for machine and deep learning techniques, especially about big data.

d. Information Integration:

The gaps in healthcare information lead to inaccurate predictions when using machine learning, causing errors in medical decision-making and clinical settings.

With the presence of mentioned challenges related to the use of ML in healthcare applications, there is a greater imposition and a promising future in the possibility of improving and upgrading the performance of learning models to reduce the impact of most of the challenges (Riccardo et al. 2018). ML and deep learning able to offer a promising development in healthcare in important aspects.

a. Expert Knowledge:

The importance of current expert knowledge of medical and healthcare problems lies in the fact that medical data is limited and diversified as well as quality problems. Therefore, teaching techniques enable the incorporation of expert knowledge to guide it in the right direction and to obtain optimal conclusions. ML can enables to easy the use of the EHR management systems and provides a clinical decision support, in addition to integrating the disease diagnosis and analysis.

b. Time Modeling:

Time is one of the most important requirements related to health care and is highly sensitive, especially with procedures related to electronic health

records and monitoring devices. Deep learning models provide time-sensitive training to deliver timely patient clinical decisions.

c.   Predictive Analytics:

The use of ML in health informatics and predictive analytics presents promising opportunities to improve health care procedures, strengthen clinical decision-making, and help improve patient outcomes.

In general, ML applications will greatly influences positively in patient care delivery strategies. In addition to helping physicians identify, diagnose and treat disease, ML techniques are also involved in building interactive healthcare applications related to medical planning. According to a number of previous studies for the use of ML in health care, ML provides future opportunities in the development of a number of applications such as, disease identification and diagnosis, medical imaging diagnosis, personalized medicine, robotic surgery and patient support tasks.

MACHINE LEARNING FUTRUE TRENDS IN HEALTCARE

Recently, the professionals of health informatics care strongly about the possibility of enabling ML algorithms to play a vital role in medical processes and healthcare. Since the patient care, and healthcare industries are depend on the data outcomes, the use of ML and DL algorithms can reduce the reviewing time taken with patient and medical data, which will improves the process of diagnosis.

During the past two years, ML techniques have been widely included in studies about the global epidemic of Coronavirus disease (COVID-19), as they have contributed to improving the extraction of reports related to health analysis. Where these technologies have proven their effectiveness and can provide a significant improvement in the field of health care in the future, especially in the field of health informatics (Jiang et al. 2021). The ML technologies will also play a major role in innovating and developing technologies in various applications related to health care and diagnosis. Here are some examples in which machine learning techniques can play a large and vital roles.

a.   Wearable Devices:

ML technologies will help in the development of a number of devices that help monitor patients and their vital functions such as heart rate, temperature and pressure and other changes by integrating their data with doctors and linking them with various health information systems.

b.   Augmented Virtual Reality:

> Virtual reality technologies that rely on ML will offer solutions to facilitate patient health procedures and assist clinicians with vital testing, training and teaching.

c. Intelligent Medical Models:
> Artificial intelligence and ML techniques can provide models for medical analysis that have the ability to identify patterns in data that humans cannot realistically detect. It also enables them to make decisions that are more informed and detect abnormalities in patient examinations and diagnoses.

d. Improving Administrative Efficiency:
> The use of AI and ML helps to improve the provision of health services to support or complete the jobs and roles related to employees in the medical fields. It can also help in knowing the recovery rates of patients and their response to therapeutic procedures by doctors.

In the coming years, it expected that ML tools would use extensively in health systems for various purposes, such as recording the risks related to patients that arise from the occurrence of some variables, and determining the degree of attention according to the risk. There is also another aspect related to making decisions related to the planning of diagnosis and treatment related to patients. It expected that the use of ML tools would lead to the development of health care systems and raise their quality to deal with patients more accurately.

Due to the recent circumstances, that the world has experienced and still affected due to COVID-19 epidemic. Most countries attempt to confront the epidemic as they have turned to the use of digital technology, which has created greater opportunities to use ML algorithms for example, to help address the challenges of locating patients and managing the medical crisis, as well as predicting patient behaviors and characterizing interactions between medical instructions and the patient. Undoubtedly, there will be a great tendency to use artificial intelligence techniques in this vital and sensitive field.

CONCLUSION

Future Medical IoT architecture enables to manage the supervised remotely the performance of medical machines and devices in industrial healthcare applications. The AI, ML and IoT complement each other to build intelligent healthcare systems for patient's diagnosis and treatment. In healthcare, the use of ML with respect to patient records, treatment plans, and diagnosing data enable to provide an improved indicators like patient care accurately. ML provides powerful and accurate predictions for IoT Healthcare data being aggregated and artificially make decisions for many

30

healthcare services aspects. The security is a most important issue related to the Internet of medical things (IoMT) -based healthcare system, and being the most growing challenge regards to medical image analysis. Security and precision requirements in disease diagnose can be achieved by suing ML to provides the IoMT systems the capability of finding the solution to several diseases and managing various devices from various patients. The control decision of medical IoT devices in processing can be provides by deep learning (DL) method, which help to interact with the patient's environment to learn optimal policies, which will enable to increase the healthcare personalized services.

REFERENCES

Agarwal, N., Singh, P., Singh, N., Singh, K. K., & Jain, R. (2021). Machine Learning Applications for IoT Healthcare. In *Machine Learning Approaches for Convergence of IoT and Blockchain* (pp. 129–144). Scrivener Publishing LLC. doi:10.1002/9781119761884.ch6

Al-Turjman, F., & Baali, I. (2019). *Machine learning for wearable IoT-based applications: A survey*. Wiley. doi:10.1002/ett.3635

Aldahiri, A., Alrashed, B., & Hussain, W. (2021). *Trends in Using IoT with Machine Learning in Health Prediction System.* https://www.mdpi.com/journal/forecasting

Ali, E. S., Hassan, M. B., & Saeed, R. A. (2021). Machine Learning Technologies in Internet of Vehicles. In *Intelligent Technologies for Internet of Vehicles.* Springer. . doi:10.1007/978-3-030-76493-7_7

Almotiri, S. H., Khan, M. A., & Alghamdi, M. A. (2016). Mobile health (m-health) system in the context of IoT. *Proc. IEEE 4th Int. Conf. Future Internet Things Cloud Workshops (FiCloudW)*, 39–42.

Alnazir, A., Mokhtar, R. A., Alhumyani, H., Ali, E. S., Saeed, R. A., & Abdel-Khalek, S. (2021). Quality of Services Based on Intelligent IoT WLAN MAC Protocol Dynamic Real-Time Applications in Smart Cities. *Computational Intelligence and Neuroscience*, *2021*, 1–20. doi:10.1155/2021/2287531 PMID:34754301

Alsheikh, M. A., Lin, S., Niyato, D., & Tan, H.-P. (2016). Rate-distortion balanced data compression for wireless sensor networks. *IEEE Sensors Journal*, *16*(12), 5072–5083. doi:10.1109/JSEN.2016.2550599

Armañanzas, R., Bielza, C., Chaudhuri, K. R., Martinez-Martin, P., & Larrañaga, P. (2013). Unveiling relevant non-motor Parkinson's disease severity symptoms using a machine learning approach. *Artificial Intelligence in Medicine*, *58*(3), 195–202. doi:10.1016/j.artmed.2013.04.002 PMID:23711400

Assery, N., Xiaohong, Y., Almalki, S., Kaushik, R., & Xiuli, Q. (2019). Comparing learning-based methods for identifying disaster-related tweets. *Proc. 18th IEEE Int. Conf. Mach. Learn. Appl. (ICMLA)*, 1829–1836.

Baker, S. B., Xiang, W., & Atkinson, I. (2017). Internet of Things for Smart Healthcare: Technologies, Challenges, and Opportunities. *IEEE Access: Practical Innovations, Open Solutions*, *5*, 26521–26544. doi:10.1109/ACCESS.2017.2775180

Bharadwaj, H. K., Agarwal, A., Chamola, V., Lakkaniga, N. R., Hassija, V., Guizani, M., & Sikdar, B. (2021). A Review on the Role of Machine Learning in Enabling IoT Based Healthcare Applications. *IEEE Access: Practical Innovations, Open Solutions*, *9*, 38859–38890. doi:10.1109/ACCESS.2021.3059858

Bhardwaj, R., Nambiar, A. R., & Dutta, D. (2017). *A Study of Machine Learning in Healthcare*. IEEE. doi:10.1109/COMPSAC.2017.164

Borthakur, D., Dubey, H., Constant, N., Mahler, L., & Mankodiya, K. (2017). Smart fog: Fog computing framework for unsupervised clustering analytics in wearable internet of things. *2017 IEEE Global Conference on Signal and Information Processing (GlobalSIP)*, 472–476. 10.1109/GlobalSIP.2017.8308687

Carrio, A., Sampedro, C., Rodriguez-Ramos, A., & Campoy, P. (2017). *A review of deep learning methods and applications for unmanned aerial vehicles*. *Hindawi Journal of Sensors*. doi:10.1155/2017/3296874

Chakraborty, C., Banerjee, A., Kolekar, M. H., & Garg, L. (2021). *Internet of Things for Healthcare Technologies*. Springers. doi:10.1007/978-981-15-4112-4

Chen, X. A., Grossman, T., Wigdor, D. J., & Fitzmaurice, G. (2014). Duet: Exploring joint interactions on a smart phone and a smart watch. In The SIGCHI conference on human factors in computing systems (pp. 159–168). ACM.

Dhillon & Singh. (2019). *Machine Learning in Healthcare Data Analysis: A Survey*. doi:10.15412/J.JBTW.01070206

Dorsemaine, B., Gaulier, J.-P., Wary, J.-P., Kheir, N., & Urien, P. (2015). Internet of Things: a definition & taxonomy. In *9th International Conference on Next Generation Mobile Applications, Services and Technologies*. IEEE.

Dragorad, M. O., & Zoran, B. (2017). *Cloud-based IoT healthcare applications: Requirements and recommendations. International Journal of Internet of Things and Web Services*.

Durga, & Nag, & Daniel. (2019). Survey on Machine Learning and Deep Learning Algorithms used in Internet of Things (IoT) Healthcare. *IEEE Access: Practical Innovations, Open Solutions*.

Elfatih, N. M., Hasan, M. K., Kamal, Z., Gupta, D., Saeed, R. A., Ali, E. S., & Hosain, M. S. (2021). Internet of vehicle's resource management in 5G networks using AI technologies: Current status and trends. *IET Communications*, 1–21.

Elmustafa & Ahmed. (2021). Algorithms Optimization for Intelligent IoV Applications. In Handbook of Research on Innovations and Applications of AI, IoT, and Cognitive Technologies. IGI Global. doi:10.4018/978-1-7998-6870-5.ch001

Essa, Y. M., Attiya, G., El-Sayed, A., & ElMahalawy, A. (2018). Data processing platforms for electronic health records. *Health and Technology*, *8*(4), 271–280. doi:10.100712553-018-0219-5

Fei, C., Liu, R., Li, Z., Wang, T., & Baig, F. N. (2021). *Machine and Deep Learning Algorithms for Wearable Health Monitoring*. Springer. doi:10.1007/978-3-030-68723-6_6

Ghassemi, M., Naumann, T., Schulam, P., Beam, A. L., Chen, I. Y., & Ranganath, R. A. (2020). Review of Challenges and Opportunities in Machine Learning for Health. *AMIA Joint Summits on Translational Science Proceedings AMIA Summit on Translational Science*, *2020*, 191–200. PMID:32477638

Godi, Viswanadham, Muttipati, Samantray, & Gadiraju. (2020). E-Healthcare Monitoring System using IoT with Machine Learning Approaches. *IEEE Xplore.*

Gope, P., & Hwang, T. (2015). Bsn-care: A secure IoT-based modern healthcare system using body sensor network. *IEEE Sensors Journal*, *16*(5), 1368–1376. doi:10.1109/JSEN.2015.2502401

Hirschauer, T. J., Adeli, H., & Buford, J. A. (2015). Computer-Aided diagnosis of Parkinson's Disease Using Enhanced Probabilistic Neural Network. *Journal of Medical Systems*, *39*(11), 179. doi:10.100710916-015-0353-9 PMID:26420585

Jen, C.-H., Wang, C.-C., Jiang, B. C., Chu, Y.-H., & Chen, M.-S. (2021). Application of classification techniques on development an early-warning system for chronic illnesses. Expert Syst. Appl., 39(10), 8852–8858.

Jiang, Jiang, Zhi, Dong, Li, Ma, Wang, Dong, Shen, & Wang. (2017). *Artificial intelligence in healthcare: past, present and future*. doi:10.1136/svn-2017-000101

Jiang, L., Wu, Z., Xu, X., Zhan, Y., Jin, X., Wang, L., & Qiu, Y. (2021). Opportunities and challenges of artificial intelligence in the medical field: Current application, emerging problems, and problem-solving strategies. *The Journal of International Medical Research*, *49*(3). Advance online publication. doi:10.1177/03000605211000157 PMID:33771068

Jothi, Rashid, & Husain. (2015). Data Mining in Healthcare – A Review. Elsevier.

Kang. (2018). *Recent Patient Health Monitoring Platforms Incorporating Internet of Things-Enabled Smart Devices*. Korean Continence Society.

Khan, F., Rehman, A. U., Jan, M. A., & Rahman, I. U. (2019). efficient resource allocation for real time traffic in cognitive radio internet of things. *International Conference on Internet of Things (iThings),* 1143–1147.

Khan, F., Rehman, A. U., Zheng, J., Jan, M. A., & Alam, M. (2019). Mobile crowd sensing: A survey on privacy-preservation, task management, assignment models, and incentives mechanisms. *Future Generation Computer Systems*, *100*, 456–472. doi:10.1016/j.future.2019.02.014

Kim, J., Lee, S., Lee, G., Park, Y., & Hong, Y. (2016). Using a method based on a modified K-means clustering and mean shift segmentation to reduce file sizes and detect brain tumors from magnetic resonance (MRI) images. *Wireless Personal Communications*, *89*(3), 993–1008. doi:10.100711277-016-3420-8

Kumar, Jain, & Mahalakshmi. (2018). Enhancement of Healthcare Using Naïve Bayes Algorithm and Intelligent Data mining of Social Media. *International Journal of Applied Engineering Research.*

Lee, S.-J., Tseng, C.-H., Lin, G., Yang, Y., Yang, P., Muhammad, K., & Pandey, H. M. (2020). A dimension-reduction based multilayer perception method for supporting the medical decision making. *Pattern Recognition Letters*, *131*, 15–22. doi:10.1016/j.patrec.2019.11.026

Lin, Q., & Zhao, Q. (2021). *IoT Applications in Healthcare. In Internet of Things Cases and Studies*. Springer.

Machorro-Cano, I., Alor-Herna'ndez, G., Paredes-Valverde, M. A., Ramos-Deonati, U., Sánchez-Cervantes, J. L., & Rodríguez-Mazahua, L. (2019). PISIoT: A machine learning and IoT-based smart health platform for overweight and obesity control. *Applied Sciences (Basel, Switzerland)*, *9*(15), 3037. doi:10.3390/app9153037

Mahmud, R., Koch, F. L., & Buyya, R. (2018). Cloud-Fog Interoperability in IoT-enabled Healthcare Solution. *ICDCN*, *18*(January), 4–7.

Man, Na, & Kit. (2015). IoT-based Asset Management System for Healthcare-related Industries. *International Journal of Engineering Business Management, 7*(19). doi:10.5772/61821

Miotto, R., Wang, F., Wang, S., Jiang, X., & Dudley, J. T. (2018). Deep learning for healthcare: Review, opportunities and challenges. *Briefings in Bioinformatics*, *19*(6), 1236–1246. doi:10.1093/bib/bbx044 PMID:28481991

Moeen. (2015). Health Monitoring and Management Using Internet-of-Things (IoT) Sensing with Cloud-based Processing: Opportunities and Challenges. *IEEE International Conference on Services Computing*

Mohan Kumar, S., & Majumder, D. (2018). Healthcare solution based on machine learning applications in IoT and edge computing. *International Journal of Pure and Applied Mathematics*, *119*(16), 1473–1484.

Onasanya, A., & Elshakankiri, M. (2018). Secured Cancer Care and Cloud Services in IoT/WSN Based Medical Systems. *Second EAI International Conference, SGIoT*.

Padmavathi & Ran. (2016). Implementation of IOT Based Health Care Solution Based on Cloud Computing. *International Journal of Engineering and Computer Science, 5*(9), 17931-17937.

Papadokostaki, K., Mastorakis, G., Panagiotakis, S., & Mavromoustakis, C. X. (2016). Handling big data in the era of Internet of things (IoT). *Advances in Mobile Cloud Computing and Big Data in the 5G Era.*

Qayyum, Qadir, Bilal, & Al-Fuqaha. (2020). *Secure and Robust Machine Learning for Healthcare: A Survey.* doi:10.1109/RBME.2020.3013489

Raeesi Vanani, I., & Amirhosseini, M. (2021). IoT-Based Diseases Prediction and Diagnosis System for Healthcare. In *Internet of Things for Healthcare Technologies. Studies in Big Data* (Vol. 73). Springer. doi:10.1007/978-981-15-4112-4_2

Rameswari, R., & Divya, N. (2018). Smart Health Care Monitoring System Using Android Application: A Review. *International Journal of Recent Technology and Engineering.*

Sadhukhan, B. Das, & Sangaiah. (2018). Producing better disaster management plan in post-disaster situation using social media mining. In Computational Intelligence for Multimedia Big Data on the Cloud With Engineering Applications. Academic.

Salih Ahmed, R., Sayed Ali Ahmed, E., & Saeed, R. A. (2021). Machine Learning in Cyber-Physical Systems in Industry 4.0. In A. Luhach & A. Elçi (Eds.), *Artificial Intelligence Paradigms for Smart Cyber-Physical Systems* (pp. 20–41). IGI Global. doi:10.4018/978-1-7998-5101-1.ch002

Sethi, P., & Sarangi, S. R. (2017). Internet of things: Architectures, protocols, and applications. *Journal of Electrical and Computer Engineering*, 25. doi:10.1155/2017/9324035

Singh, R., & Rajesh, E. (2019). Prediction of heart disease by clustering and classification techniques Prediction of Heart Disease by Clustering and Classification Techniques. *International Journal on Computer Science and Engineering*, *7*(5), 861–866.

Song, Y. E., Liu, Y., Fang, S., & Zhang, S. (2015). Research on applications of the internet of things in the smart grid. *7th International Conference on Intelligent Human-Machine Systems and Cybernetics (IHMSC)*, 2, 178–181. 10.1109/IHMSC.2015.131

Sood, S. K., & Mahajan, I. (2017). Wearable IoT sensor based healthcare system for identifying and controlling chikungunya virus. *Computers in Industry*, *91*, 33–44. doi:10.1016/j.compind.2017.05.006 PMID:32287550

Teshome, A. K. (2018). A Review of Implant Communication Technology in WBAN: Progresses and Challenges. *IEEE Access: Practical Innovations, Open Solutions*.

Wang, H., Kadry, S. N., & Raj, E. D. (2020). *Continuous Health Monitoring of Sportsperson using IoT devices based Wearable Technology*. Elsevier.

Wood, C. S., Thomas, M. R., Budd, J., Mashamba-Thompson, T. P., Herbst, K., Pillay, D., Peeling, R. W., Johnson, A. M., McKendry, R. A., & Stevens, M. M. (2019). Taking connected mobile-health diagnostics of infectious diseases to the field. *Nature*, *566*(7745), 467–474. doi:10.103841586-019-0956-2 PMID:30814711

Xie, T., Li, R., Zhang, X., Zhou, B., & Wang, Z. (2019). Research on heartbeat classification algorithm based on CART decision tree. *Proc. 8th Int. Symp. Next Gener. Electron. (ISNE)*, 1–3.

Zech, J., Pain, M., Titano, J., Badgeley, M., Schefflein, J., Su, A., Costa, A., Bederson, J., Lehar, J., & Oermann, E. K. (2018). Natural language–based machine learning models for the annotation of clinical radiology reports. *Radiology*, *287*(2), 570–580. doi:10.1148/radiol.2018171093 PMID:29381109

Zeinab, K. A. M., & Elmustafa, S. A. A. (2017). Internet of Things Applications, Challenges and Related Future Technologies. *World Scientific News*, *67*(2), 126–148.

36

Zheng, T., Xie, W., Xu, L., He, X., Zhang, Y., You, M., Yang, G., & Chen, Y. (2017). A machine learning-based framework to identify type 2 diabetes through electronic health records. *International Journal of Medical Informatics*, *97*, 120–127. doi:10.1016/j.ijmedinf.2016.09.014 PMID:27919371

KEY TERMS AND DEFINITIONS

Acute Diseases: Know the diseases that evolve suddenly and at a short time such as fast infection, accident injuries, and poor drugs. Such diseases are attached specific symptoms, require urgent health care, and are improved as soon as the urgent intervention of appropriate treatment.

Chronic Diseases: Such diseases appear after a while, where they begin to slowly evolve and long term. These diseases appear from non-healthy lagging behaviors such as malignancy, physical idle, or overlooking specific materials for a long time. Some are classified as addictive symptoms such as smoking and others because of the age of patient, such as Alzheimer, diabetes, and heart disease. Such diseases need a special health pattern and exercise a specific healthy behavior with continuous monitoring.

E-Health: The concept is related to the health care that supported by electronics and communications technology, where it reflects the use of Internet, medical hardware, and computer relationship with the request in addition to health informatics. The term also refers to health services, information provided or strengthened through the Internet and related techniques.

Internet of Medical Things (IoMT): A technology that connects a many medical devices and applications with information technology systems online related to healthcare. It can also be described as the possibility of allowing medical devices that contain communication mechanisms such Wi-Fi to connect with other devices to the Internet and enable the storage of medical data through different cloud platforms.

Remote Health Monitoring (RHM): This term means providing health information related to patients. The techniques used to supply different data to the patient's equipment managers, and provide location and data analysis capabilities. This concept is also possible to deliver data through cellular communications to health centers or doctors, regardless of where it is for medical equipment.

Representational State Transfer (REST): An architectural way of building software that is designed to develop a IoT Web Architecture for Monitoring Field that defines a number of constraints on how the Internet's distributed hypermedia system architecture behaves. It also enables scalability in interactions between

components, unified interfaces, and the creation of a multi-layered architecture for storing components.

Service-Oriented Architecture (SOA): An architectural method that supports the routing of services provided through a network communication protocol. SOA enables to pass messages using description metadata through protocols services. It is also enables exchanging the information between similar and dissimilar applications and solve the problem of interoperability by using an external web services.

Section 2

Diagnosis and Treatment of Some Common Diseases Using AI

Chapter 2

A Mobile Health Application for Monitoring Children With Autism Spectrum Disorder:
ASD Monitoring by mHealth

Masud Rabbani
https://orcid.org/0000-0003-3058-3625
Ubicomp Lab, Department of Computer Science, Marquette University, USA

Munirul M. Haque
University of Indianapolis, USA

Dipranjan Das Dipal
Marquette University, USA

Md Ishrak Islam Zarif
Marquette University, USA

Anik Iqbal
Marquette University, USA

Shaheen Akhter
Bangabandhu Sheikh Mujib Medical University, Bangladesh

Shahana Parveen
National Institute of Mental Health, Dhaka, Bangladesh

Mohammad Rasel
Bangabandhu Sheikh Mujib Medical University, Bangladesh

Tanjir Rashid Soron
Telepsychiatry Research and Innovation Network Ltd., Bangladesh

Naveen Bansal
Marquette University, USA

Amy Schwichtenberg
https://orcid.org/0000-0002-8920-6798
Purdue University, USA

Syed Ishtiaque Ahmed
University of Toronto, Canada

Sheikh Iqbal Ahamed
Marquette University, USA

ABSTRACT

Currently, one out of 160 children have autism spectrum disorder (ASD) in the world. This problem is observed in both developed and low-middle-income countries (LMICs) around the globe. Usually, in developed countries, the number can be estimated, but in LMICs, this number is largely unknown, and in some cases, many children with ASD are not treated after identification of the problem. In these cases, both for the developed and LMICs, mobile technology can continuously monitor children with ASD. In this chapter, the authors describe the techniques of remote monitoring of the behavioral and milestone parameters development for children with ASD that care practitioners can use as an evidence-based tool to make the decision in the treatment process. Lastly, the authors describe the advantages and challenges of using the mHealth tools in the ASD treatment based on the NIH-funded successful completion project "mCARE" in Bangladesh.

INTRODUCTION

Autism Spectrum Disorder was first identified as the children's behavior (Kanner, 1968) by Kanner in 1943. Later it was recognized as children's neurodevelopmental disorder which is also known as "Autism Spectrum Disorder" or "ASD." Consistently, it creates a global problem, (Wallace et al., 2016), and people of all societal levels suffer from ASD (Organization, 2021). Now, Autism Spectrum Disorder is a heterogeneous disorder (Tariq et al., 2019), and all socioeconomic, racial, and ethnic groups in the world are impacted by autism.(Services, 2020; Therapy, 2021; Wallace et al., 2016) In 2020, worldwide, around one in 160 children had ASD (Elsabbagh et al., 2012; Organization, 2021), whereas, in the USA, the rate is one in 54. (A., 2020; DiGuiseppi et al., 2016; Maenner et al., 2020) Figure 1 shows the autism outbreak rate from 2004 to 2020 in the USA.(SARRC, 2021; Speaks, 2020) From the Figure 1, it can be seen that in the USA, in 2004, one ASD child was found on 166, whereas in 2020, this rate was one in 54. Currently, over 3.5 million people in the USA are taking autism diagnoses, and its cost is sometimes other one's lifespan. In 2015, in the USA, the diagnosis cost was $268 billion, and it is expected this cost will be reached to $461 billion by 2025.(Therapy, 2021) But it is a matter of regret that a family has ASD children mostly subject to stigma, discrimination, and human rights violation (Organization, 2021),46% of ASD children do not get the proper treatment even after identifying the ASD.(Happé et al., 2016) In developing countries, this scenario is worse, where they even know the "Autism Spectrum Disorder" term. (Therapy, 2021) Integrating the mHealth technology in this area

can improve this situation and reduce the diagnosis cost. (Haque et al., 2020; Haque et al., 2021; Maples-Keller et al., 2017).

Figure 1. Autism prevalence rate in the USA from 2004 to 2020 (SARRC, 2021; Speaks, 2020)

AUTISM PREVALENCE RATE
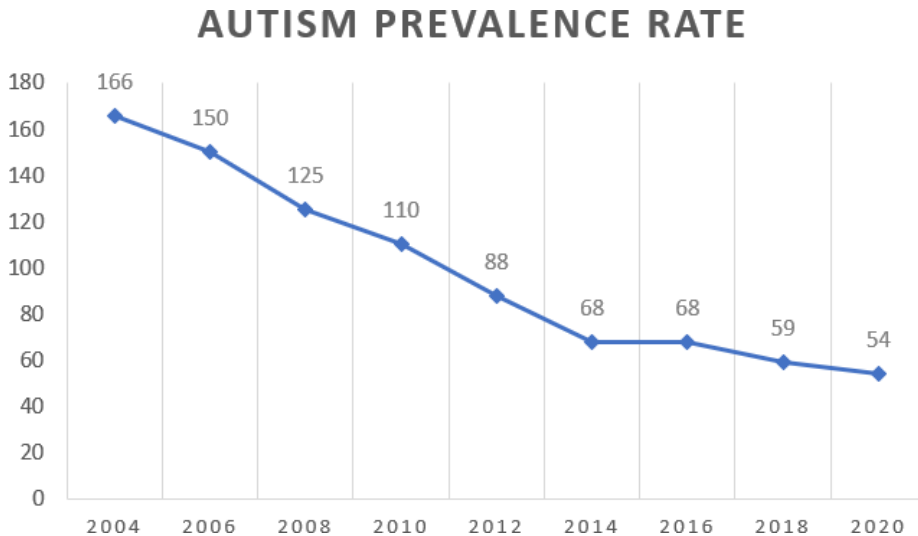
At present, mobile technology or mHealth is largely used in the early recognition or identification of the autism symbols or autism level in the children's' early age. Many mobile or web-based apps (Barbaro & Halder, 2016; Chakrabarti, 2009; Crais et al., 2006; Eaves & Ho, 2004; Guthrie et al., 2013; Webb & Jones, 2009; Zwaigenbaum et al., 2015) are now available online, where both caregiver and care practitioner can take the mHealth advantages from these mobile apps. Also, some other self-reported autism development tracker apps are available to track the development of children with ASD. In this chapter, the authors propose a new and innovative mobile-based and primary caregiver-reported application, where the children's (with ASD) longitudinal behavioral and milestone parameters are being tracked and monitored remotely by the care practitioners. These longitudinal data will then be shown graphically to the care practitioners so that the children's development can be easily visualized to the clinical or care professionals or care practitioners. By this system, the caregivers or parents will regularly get the update their children's developmental level by the app's report.

Many approaches have been developed to monitor children with ASD in many countries in recent years. (Shminan et al., 2017) (Khanam et al., 2019) (Sharmin

42

et al., 2018) (Ehsan et al., 2018) To monitor the children with ASD remotely, most of the approaches has faced many challenges like (i) they used external devices, (ii) developing and evaluating the architecture for a controlled environment, (iii) designing the architecture for a specific group, (iv) most of the approaches does not fit for low-and-middle-income-countries (LMICs). In this chapter, the authors described and proposed an architecture that is suitable for all populations in both developed and LMICs, also evaluated by an NIH-funded "mCARE" project for the Bangladesh population. In this architecture, the caregivers and care-practitioners can monitor the children with ASD for a long period. This approach is based on the mHealth technology, where the caregiver can regularly provide their children's (with ASD) behavioral and milestone data. The care-provider can see the longitudinal view that can help them make an evidence-based decision during the treatment process.

This chapter's main objective and contribution are to describe the detailed architecture of a mHealth application in the area of tracking the behavioral and milestone parameter development remotely by using the mobile application or mobile SMS. Also, describe this system's detailed components or user levels in this area with the advantages and challenges. At the end of this chapter, the authors of this chapter describe an NIH-funded project, mCARE's features, and contributions in this area. The rest of the chapter is structured as follows: Background of this mHealth work, then a comparison on previous studies and the detailed architecture and features of this mHealth application with advantages and challenges, after that a description of NIH-funded project named by "mCARE" with the recommendation, and the chapter concludes with the future research direction and conclusion.

BACKGROUND

The world has a revolution in the context of mobile phone technology and its uses in every step of human life. Now, mobile phone use is vital in all sectors of human life, such as education, entertainment, communication, and even in the health and medical area. According to Statista, in December 2021, about 7.10 billion mobile phone users (including both smart and feature phones) are in the world, which is about 89.76% population of the world. In the context of the smartphone user, this number is about 6.37 billion, which means approximately 80.63% of the population in the world has their own smartphone today. By 2025, the total number of smartphone users will be around 7.333 billion in the world. (BankMyCell, 2021; DataRePortal, 2021; Statista, 2021b) This number is not only growing in the developed countries like the USA or Europe but also in the low-middle-income countries (LMICs) (like Bangladesh) also has the revolution in mobile phone technology in recent years. The authors have noticed the digitization and revolution in mobile network coverage and

43

mobile phone users in Bangladesh in recent years. According to the survey report of Statista in 2016, in Bangladesh, about 99% population were connected by 2G mobile networks. (Statista, 2021a) mobile phone use and technology have been growing and updated in recent years. Now people in Bangladesh are being connected by a 4G mobile network, and 80% population in Bangladesh have the availability to connect with a 4G network. (Fenwick, 2020) Besides this technology, the number of smartphone users in Bangladesh is also growing exponentially; for example, currently, there are about 171.85 million mobile phone subscribers (Commission., 2021), and by 2025, 62% of the population of Bangladesh will use the smartphone. (Bhuiyan, 2021) This number is not an example of Bangladesh; this number represents the mobile phone used all over the LMICs. Initially, the mobile phone was used as communication media, then used as entertainment media with communication, but at present, it is not only a device for communication and entertainment; it is a device for all sectors like education, medical, therapy, business, and many other all sectors of human life. Using this technological expansion of mobile technology, the authors in this chapter propose mobile health (mHealth) technics in remote monitoring of children with ASD, which play a vital role in observing the long-time behavioral and milestone parameter development. Clinicians or care professionals always want to know the improvement level on the basis of the treatment action; this architecture mentioned in this chapter will be helpful for the clinicians or care professionals to make evidence-based decisions in the treatment process. Besides the care practitioners, the caregiver can also learn the improvement level of their children (with ASD) in the treatment process, which makes them more motivated to take care of their children (with ASD). The architecture proposed in this chapter is designed for children with ASD who live in a remote area or rural area and have less opportunity to make frequent visits to the care professionals or a clinic. In addition to that population, this mHealth architecture is also applicable in the urban and city area both in the developed and LMICs.

The treatment cost for children with ASD is very expensive throughout the world. In developed countries like the USA, the treatment reached $268 billion in 2015, and by 2025 it will reach $461 billion.(Speaks) And from the analysis of this cost, though most of the money cost for the adult ASD treatment service, about $61-$66 billion of money need for children with ASD every year in the USA. This is not only in the USA; in other countries like Bangladesh, the treatment of ASD is expensive((CRI)). And in the children's (with ASD) treatment process, their monitoring is vital. For this reason, by using mobile technology (as mobile technology has been revolved high in both developed and LMICs), we can easily monitor the children with ASD by minimal use of resources at low cost. And the described design in the chapter is based on the successfully implemented and completed "mCARE" project, (Haque

44

et al., 2020; Haque et al., 2021) funded by NIH (NIH) and deployed in remote monitoring for 300 children with ASD in 1 year in Bangladesh.

RELATED WORK

The ASD problem in Children is a global concern, and many research groups have experimented with many approaches for monitoring the children remotely. In this section, the authors described some previous studies or approaches in this area:

A picture exchange based mobile-application (AutiPECS) (Shminan et al., 2017) has been developed to monitor children with ASD remotely. This mobile-based framework established a picture exchange communication (PECS) between the caregivers and care-practitioners to monitor the children with ASD who suffers from communication and behavioral problem. Though this approach cloud able to bridge between the caregiver and care-practitioners, it had the challenge to monitor the children routinely and regularly by that current version of the AutiPECS app. And for the proper treatment and intervention, longtime and regular data is essential.

A computer vision technique has been described in (Khanam et al., 2019) to remote monitor the vital signs of children with ASD. This study deployed camera imaging technologies to capture the picture of the children with ASD and analysis their vital signs, for example, heart rate (HR), heart rate variability (HRV), blood pressure (BP), etc. Though the long-term vital signs are very crucial during the intervention time of the children with ASD, it is very difficult to measure the vital signs from the picture analysis from the children with ASD. In this study, authors explored and described the technics for measuring the vital signs from the picture analysis of the children with ASD, but most of the approaches are environment controlled with a limited number of children with ASD. To monitor a large number of children in a real environment is difficult by this approach.

Another remote monitoring approach for children with ASD is to deploy wearable devices with mobile. (Sharmin et al., 2018) Though this approach ensures the real-time and long-term data of the children with ASD, wearing a device all the time or a long period for children with ASD is a challenging issue. And this approach is not popular for a large number of children with ASD for remote monitoring in a long time.

A voice-based call management system has been introduced in (Ehsan et al., 2018) to monitor children with ASD. The described system in this study can make a group among the parents of the children with ASD through a moderator. This peer-supported system can be effective in removing the stigma towards ASD and ASD children. Still, for the treatment purpose, this system faces challenges for lacking evidence-based long-term behavioral data of the children.

To remote and non-invasive regular monitor of ASD children, the previous study faces a few challenges: (a) to evaluate the approach with a large number of children with ASD in a real environment for a long time, (ii) the effectiveness of the approach to monitoring the children with ASD, (iii) the data collection technics (most of them use an external camera or wearable devices) are not suitable and applicable for real patients to monitor a long time, and (iv) the cost of the approach, sometimes is not bearable for the people in the low-and-middle-income-countries (LMICs). After analyzing all of the challenges from the previous study, in this chapter authors proposed a mobile health (mHealth) application that can be applied to remote monitor for a long period without any external devices (only by mobile) both in the developed and LMICs.

MOBILE HEALTH APPLICATION FOR MONITORING THE CHILDREN WITH ASD

For remote monitoring the children with ASD both in the urban and rural areas, the authors proposed an Experience Sampling Method (ESM) (Larson & Csikszentmihalyi, 2014) based-mobile application that can monitor the progress of children's mental health. This proposed architecture aligned with the existing practice by allowing the caregivers (parents or legal guardians) to routinely report the development of their children's development (both the behavioral and milestone

Figure 2. mHealth architecture for remote monitoring of the children with ASD
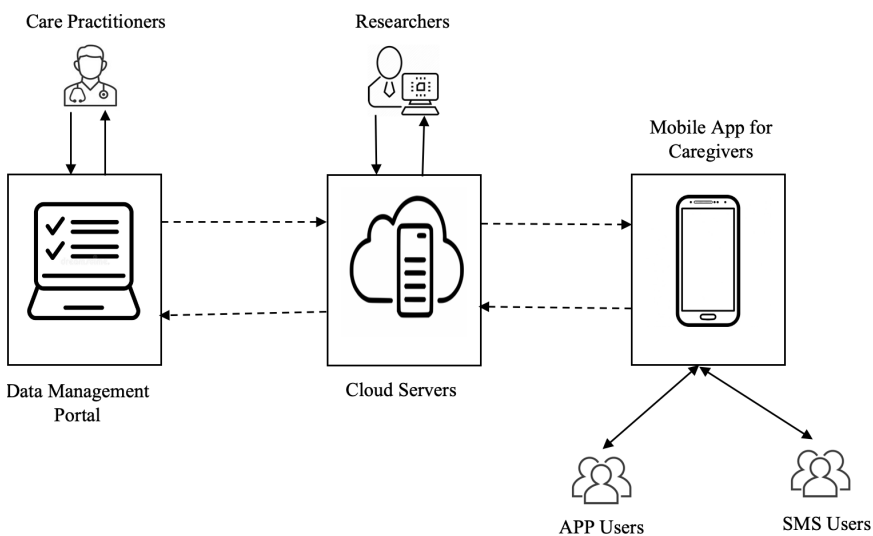
parameters) by the mHealth application. On the contrary, the data-driven platform from these parental-reported data can be useful to the care practitioners to increase efficacy in the treatment process. The proposed mHealth application architecture is shown in Figure 2.

In this architecture (shown in Figure 2), care-practitioners can remotely monitor the children with ASD who are registered in this system. They will monitor the children's longitudinal behavioral and milestone parameters data from the system. This data (behavioral and milestone parameters data of the children with ASD) will be provided by the caregivers (parents or primary caregivers of the children). Both the app user (or smart-phone user) and SMS user (or feature phone or non-smart-phone user) can provide the data to the system. After providing the data, the authorized research and care practitioners can visualize the provided data. From the visualization data, the care-practitioners can make an evidence-based decision in the treatment process, and research can analyze the important findings that can be helpful for future research. This architecture (described in Figure 2) is based on an NIH-funded project, "mCARE", which has been implemented in Bangladesh in a year for remote monitoring of children with ASD. The details of the architect is described in the following sections.

Architecture

The proposed architecture of this mHealth application can be described as follows:

- **Components:**
  - **Could Servers:** In this mHealth application, this cloud server is the heart of all processes. The authors recommend the Amazon Web Services (AWS) (Amazon, 2021) server for controlling the data flow and data storage purposes in this cloud server. All interfaces of the proposed mHealth architecture have been connected with this cloud server. The authors also recommend integrating the HIPPA compliance (Chen & Benusa, 2017; Compliancy-Group, 2021) guidelines in the server to ensure the children's (with ASD) data security. Researchers will be directly connected with the server for updating and maintaining the server. And other interfaces will be connected for data flowing, monitoring, or storing purposes. The care practitioners will connect to the server via Data Management Portal, whereas the caregivers will connect through the mHealth application (by APP or SMS).
  - **Data Management Portal (DMP):** The Data Management Portal (DMP) will be used as the visualization and analyzing tool for the data submitted by the caregivers. This visualization and analyzing tool can

assist the care provider in making evidence-based decisions during the treatment procedure for children with ASD. This also reduces intervention time when the care providers visually see all the previous records and developmental progress reports in a single platform. The DMP's this visualization tool will provide care practitioners with two important functionalities: a) Longitudinal view: they can see any single or multiple behavioral parameter developmental report (graphically) for over a certain period in a single graph. Besides the care practitioners, the caregivers can also see this report from their portal (only available for the APP group). b) Real-time SMS feedback: The care practitioners can select particular behavioral parameters. If the aggressive level of the behavior is higher than a certain level for certain consecutive days, then a pre-selected SMS will be automatically triggered to the care practitioners. This feature will help the caregiver to know the instances (higher aggressive behavior) so that they can take that rapid action to minimize the aggressive behavior. Besides that, the caregiver can recruit participants, input their demographical information, update or change their monitoring data (behavioral and milestone parameter) based on the children's situation, input the treatment action plan for certain children, or parental-report frequency by this DMP. And all this information will be stored in the cloud server via DMP.

  ○ **mHealth APP (APP/ SMS):** The caregivers can provide the developmental data to the system by these mHealth applications (APP or SMS). The authors suggest to provide both the mHealth: APP (for the smart-phone user) and mHealth: SMS (for the non-smart phone users). And for the mHealth: APP, the authors recommend to develop both the Android (Developers, 2011) and iOS (Apple, 2021) versions. By integrating all these versions, this mHealth application will be accessible by smart-non smartphone users, Android-iOS operated phone users, in developed-LMICs, in rural-urban areas. So, this removes most of the technological infrastructure barriers for using this mHealth application to monitor children with ASD. By using these mHealth applications, caregivers can provide their children's behavioral, developmental data once/twice (predefined by the care providers) in a week. They will also get the bi-weekly progress report from the DMP so that they learn their children's progression graph over the intervention time through the mHealth application.

● **Monitoring Parameters:** In this mHealth Architecture, the authors proposed two major categories of children's data that the system can monitor. The major two types are following:

48

- ◦ **Behavioral Parameters:** Here, the children's parameters which can be developed over a long intervention time, for example, social interaction, communication,, and sensory sensitivities. The care practitioners will set these behavioral parameters to a specific child based on the children's age and baseline data.
- ◦ **Milestone Parameters:** The milestone parameter will be those children's parameters that can be developed in a short intervention time. Those are very important to develop in the children's daily living. The authors this milestone parameters into four areas: (i) socialization, (ii) motor skills, (iii), communication and (iv) daily living skills. Similar to the behavioral parameters, the care practitioners will set these milestones parameters to a specific child based on the children's age and baseline data.

- **Users:** To monitor and intervene the children with ASD through this mHealth application, there need three types of users. They are:
  - ◦ **Care Practitioners:** Care practitioners are the clinicians or care professionals of children with ASD. Here clinical or individual care providers can use this system. The main roles of the care practitioners are: (i) recruit the patients to the system, (ii) store the children's demography and baseline data, (iii) set or update the behavioral and milestone data to the system for monitoring based upon the children's (with ASD) state, (iv) regularly monitor the children's behavioral and milestone progress data by graphical from the DMP, (v) based on the observation from the DMP make evidence-based action in the treatment or intervention time.
  - ◦ **Researchers:** The researchers are the only group in this system who can be directly connected to the server for (i) updating the system if needed, (ii) maintaining the server to proper data flow from server to user-interface or user-interface to the server, (iii) sometimes analysis the data for research purposes with taking proper consent from the caregivers as well as the care practitioners.
  - ◦ **Caregivers (APP/SMS Users):** The caregivers are the prime users in this system. Here caregiver can be two categories: (i) the mHealth: APP user (the smartphone user), and (ii) the mHealth: SMS user (the non-smartphone or feature phone users). On behalf of the children with ASD, their parents or legal guardians, that is, the caregivers will provide the behavioral or milestone parameters' developmental data to the system by this mHealth: APP or mHealth: SMS. Based on their children's condition, their children's monitoring parameters will be set by the care practitioners to the system. Besides following the treatment

plan by the care practitioners, the caregivers will regularly and remotely provide their children's (with ASD) developmental data to the system by the mHealth: APP or mHealth: SMS. They will also get the bi-weekly developmental progress report so that they can be motivated to take care of their children in their treatment process.

- **Recruitment process of User:** The recruitment process in the system can be done in several ways. The care practitioners can be involved in this system by any organization or individual. On the other hand, the caregivers with their children with ASD can be recruited in this system by volunteering or by any clinic or organization. But in anyways of the recruitment, the authors suggest to get proper Institutional Review Board (IRB) and consent from the caregivers before monitoring the children with ASD by this mHealth system.
- **Theory:** For designing and deploying this mHealth application, authors suggest to integrate different theories in the developmental phase of this mHealth application. They are:
  ◦ **Value-Sensitive Design (VSD) Framework.** Value-Sensitive Design (VSD) (Friedman, 1996; Friedman et al., 2002; Friedman et al., 2013) ensures the tight integration of this technology with local culture through conceptual alignments, empirical evidence, and technical compatibility.
  ◦ **Fogg's model for behavioral change (FBM):** This persuasive model (FBM) (Fogg, 2009) recommends building habits through motivations, ability, and triggers. The authors suggest to integrate this model in this mHealth application to incorporate culturally situated motivations and simplicity in the system.
- **Application Area:** The proposed mHealth application can be deployed in both developed or LMICs and urban or remote areas.
  ◦ **Rural Area:** This mHealth Application has a prime design agenda to use this application in any rural or remote area where only a mobile network (at least 2G) is available. In rural areas, the feature phone or non-smartphone user can also use this mHealth application and take the mHealth technological advantages by SMS.
  ◦ **Urban Area:** Unlike the rural area, smartphone users are more than feature phone users in an urban area. And this group (the smartphone users) are used to in mobile APP rather than SMS, so they can also use this mHealth technology by mHealth: APP.

Features

For a successful mHealth application of monitoring the children's (with ASD) behavioral progress, a system should have the following features:

50

(i) **Monitoring the Children's Development:** The primary feature of any mHealth monitoring system for children with ASD is monitoring the children's development in all possible ways. The most common monitoring areas area the children's: behavioral development and milestone parameters development, which are described in the previous mHealth architecture section.

(ii) **Providing the Children's Summary Report to the Caregivers:** To motivate the caregiver or update their knowledge about the ASD problem, a mHealth system should provide a regular (weekly or bi-weekly) summary report from the system. This summary should have the concise progress report of their children from the previous intervention, so if the developmental level is not satisfactory, they will know it very quickly. And they can also contact with care practitioners to solve the problem or to update the treatment action if needed for their children's development. Besides this progress report, the summary should have the "know-how" information about the ASD so that they can transfer from caregivers to skilled care providers for their children in the home settings.

(iii) **Customization of the Parameters:** Based on the children's development, the care practitioners always update or replace any behavioral and milestone parameters in the treatment process. For the assistance of the care-practitioners, the system should have an automatic recommendation system to provide the children's list with the parameters that need to change or updated. Here the system should include the data mining approaches to get this recommendation value for the care practitioners.

(iv) **Multi-Subject Parameters Comparison:** For monitoring the behavioral parameters of the ASD children by mHealth application, it is very important to have a robust data management platform where the care practitioners can compare more than one behavioral or milestone parameter for a child. In the behavioral parameter development of the children with ASD, one behavioral parameter sometimes depends on the other behavioral parameter, so this multi-subject parameter comparison is essential for a mHealth system. And the comparison should have been observed by graphically.

(v) **Graphical Interface for Data Observation:** To monitor the developmental progress of children with ASD, the mHealth system should have a data-driven graphical interface for the care practitioners to easily know the children's developmental progress report. This will also assist the health care professional to take proper decisions more easily and quickly during the treatment process.

(vi) **Multi-level and time-feature base query system:** Multi-level and time-feature base query means have the ability to find one or all children's (ASD) behavioral or milestone parameters in different levels of query for a specific period or the whole intervention period. By integrating these features, a caregiver can

51

visually observe the treatment impact on specific children and all children's development for a specific time or whole treatment time. This feature makes the treatment process more robust and evidence-based both for the caregivers and care-practitioners.

(vii) **Real-Time Monitoring and Feedback:** Real-time monitoring is very important for health care professional to get immediate feedback. By integrating this system, care practitioners can acknowledge the condition of the children with ASD till the next visit. Every mHealth system should have this facility, where care practitioners can know the caregivers' feedback by the system after taking any intervention. The system should have the automatic trigger option for the care providers if the children's behavior changes negatively after the intervention or if the caregiver does not consecutively provide their children's developmental data.

(viii) **HIPAA Compliance-based Monitoring System:** The mHealth application should build with the HIPAA compliance guidelines. That is, the system should be hosted on an AWS cloud server to provide and ensure data security by server-side encryption. The Database should have password protection with the encryption of the AWS server. Only the authorized and two-factored verified user's data can be accessed or updated in the Database.

(ix) **Easy to find the Patient's Status and Show the Previous Intervention Records:** The health care professional can update the patient's (children with ASD) status based on the condition. So, without investigating the details, any health care professional in this system can easily understand any patient's updated condition by observing the current status. Based on the demand, the health care professional can also look at all the previous medical records or intervention records for each patient date-wise or appointment-wise.

(x) **Virtual Appointment and Intervention:** This feature makes this mHealth application more unique in pandemic and lockdown periods. With this feature, the caregiver takes the "Telehealth" advantages in the mental health area. In this mHealth application, the caregiver can take the appointment with a health care professional by online, and the whole intervention process can also be done virtually. Based on the intervention, the health care professional can update the mHealth: DMP for that particular patient after the appointment.

(xi) **Easy to Check Patient's Status by Search:** In this mHealth system, a care professional should have an option to check the children's (with ASD) status by searching in three different ways (by participant's id, participant's last name, and participant's first name) based on their convenience.

52

Advantages

The main advantages of using mHealth technology in monitoring the children with ASD's development are. This advantage motivated the caregivers to provide the data regularly.

- **Virtual communication between the caregivers and care practitioners:** This is the most important advantage of a mHealth application to make a virtual bridge between the caregiver (or patients) and care-providers (clinical). And it is helpful for both groups, as caregivers feel that s/he always observed by care-providers; on the other hand, care-providers can always know the updated patients' data without any physical intervention.
- **Provide the telehealth facility in any unavoidable condition like pandemic:** This feature is proven after the breakout of the COVID-19, and many mHealth applications got the advantage to use the mHealth technics in the pandemic time. And many treatment systems have been converted into mHealth system to get the advantages of the mHealth system in the pandemic time.
- **Provide the opportunity to make an evidence-based decision:** If the mHealth system has the time-series data analysis platform, then it creates the opportunity for the care providers to make the evidence-based decision based on the patients' previous data with the mHealth system.
- **Provide the visualization for long-term longitudinal development of the patient:** This is another important advantage to use the mHealth system for a long time. The mHealth visualization system can provide a long-term longitudinal development of the patient, motivating both the caregiver and care provider to use the mHealth system in the treatment process.
- **Reduce the intervention time and ensure the quality of treatment:** The main objective of a mHealth application should be ensured to reduce intervention time with quality. This advantage will be helpful for the low-and-middle-income countries (LMICs), where recourses are constrained but need to treat a large number of patients.
- **Provide the opportunity to get the proper treatment of the children with ASD from the distant area:** This is a unique advantage of this mHealth system, as in many cases, the children with ASD could not visit a clinic frequently in the context of rural or long distance; but using the mHealth technology, they can get the proper treatment from their home setting.

Challenges

The main challenges for a mHealth application to screen the behavioral development of children with ASD are as follow:

- **The lack of motivation to regularly use and provide data to the system by the caregivers:** The main problem of a mobile health application is to retain the user or patients' motivation for a long time. For that reason, it will be a challenge to get proper and regular data from the user after a certain time. Most of the users in the mHealth system want to get rapid improvement by using any mHealth application; if any mHealth application fails to do that, the user could not keep their motivation to use the system. For that reason, each mHealth application should have both short-term and long-term deliverables to the user and need to understand their user about the short and long-term facility to use the system. So, in the mHealth system, the user motivation to use the system is always important; otherwise, it cannot get the regular data, and eventually, the system will fail in the long run.
- **The improper or less equipped mobile and mobile network infrastructure:** Most of the mHealth applications are based on smartphone users, so it is a barrier for non-smartphone users to deploy the mHealth application. So, before designing any mHealth application, researchers should analyze their user's device, and according to user devices' statistical information (how many percentages of users use a smartphone or non-smartphone user), they should design their mHealth application. Moreover, there needs additional information, for example, users' accessibility to use the internet (if the mHealth application is could-based), which operating system they use (iOS or Android), is they are affordable to use the internet cost for using the mHealth application, and etc.
- **The difficulties for the data validation:** This is another vital challenge to make a successfully mHealth application for a large number of users in a mHealth application in a long time; there needs to be a system for data validation. But for a large amount of data is quite impossible to do manually. So before designing the mHealth system, the researcher should provide a model to validate the large data automatically and regularly.

APPLICATIONS BY DEPLOYING M-HEALTH TECHNOLOGY

"mCARE" the mHealth Application for Monitoring the Children with ASD in LMICs: Based on the proposed mHealth architecture in the previous section,

54

an NIH-funded (grant number: 1R21MH116726-01) mobile-care-based monitoring application (mCARE) (Haque et al., 2020; Haque et al., 2021) of children with ASD has been developed and deployed in the low-and-middle-incomes-countries like Bangladesh. This project has been deployed to monitor the milestone parameters and behavioral development for 300 children with ASD for a year. This cohort of children has been recruited from four centers of different geological areas of Bangladesh. The prime aim of that project was to implement a remote monitoring mHealth application of the rural area of LMICs to monitor the behavioral and milestone parameter developmental data by mCARE: APP and mCARE: SMS. And to observe how mCARE can assist the care practitioners in making evidence-based decisions in their treatment procedure of children with ASD.

The mCARE Population: A total of 300 patients (children with ASD) were recruited by volunteering in this project from four centers of Bangladesh. For monitoring the data from this cohort, on July 9, 2020, we got the Institutional Review Board (protocol number HR-1803022959) of the Marquette University . mCARE collected the behavioral and milestone data from its cohort for one year (from November 2019 to November 2020). The participants of this project were divided into two groups: (i) test group: 150 children were monitored by the mCARE system regularly. (ii) control group: 150 children who were not monitored by the mCARE system regularly. They were in the system to find out the impact of mCARE in the treatment process of the children with ASD. The children for these two groups were selected randomly from the 300 cohorts. The center-wise participant of the mCARE project is shown in Table 1.

Table 1. The distribution of mCARE participants among the four centers in Bangladesh

Serial	Center Name	Participants Distribution	
		Test Group	**Control Group**
1	The National Institute of Mental Health (NIMH)	50	50
2	The Institute of Pediatric Neuro-disorder & Autism (IPNA)	50	50
3	Autism Welfare Foundation (AWF)	25	25
4	Nishpap Autism Foundation	25	25
In Total		**150**	**150**

The Demography of the mCARE Population

In the total cohort (300) of mCARE, children were aged from 2 to 9, and where male were 79.7%, and female were 20.3%. And among the user (caregivers), active

Table 2. mCARE participants' demographic information

Features		mCARE (%)	mCARE: APP		mCARE: SMS	
			Test Group (%)	Control Group (%)	Test Group (%)	Control Group (%)
Demographics of children						
Age	2-6	25.9	7.5	6.6	4.6	7.2
	6-9	74.1	24.9	23.0	13.1	13.1
Sex	Male	79.7	27.2	21.6	14.4	16.4
	Female	20.3	5.2	7.9	3.3	3.9
Education	Never went to school	28.9	6.6	8.2	5.6	8.5
	Went to usual academic school but failed to continue study	13.1	3.6	3.0	3.6	3.0
	Went to specialized school but failed to continue study	3.0	1.0	0.3	0.3	1.3
	Currently he/she is going to usual academic school	6.2	2.3	1.6	1.6	0.7
	Currently he/she is going to specialized academic school	48.9	19.0	16.4	6.6	6.9
Demographics of primary caregivers						
Education	Primary	19.7	3.3	4.4	5.6	6.4
	Secondary	20.5	5.7	6.4	4.1	4.3
	Higher secondary	59.8	23.5	18.7	8	9.7
Occupation	Housewife	81.7	25.6	22.6	15.1	18.4
	Service	13	4.9	5.2	1.6	1.3
	Others	5.3	2.0	1.6	1.0	0.7
Average family spending/month (Thousand BDT)	<15	13.4	3.9	1.6	3.3	4.6
	15-30	29.5	8.5	8.2	5.9	6.9
	30-50	22.3	5.2	7.5	4.9	4.6
	>50	34.8	14.8	12.1	3.6	4.3
Family Type	Nuclear	75.7	24.9	22.6	12.1	16.1
	Extended	24.3	7.5	6.9	5.6	4.3
Geographic Location	Urban	76.7	27.2	24.3	12.1	13.1
	Semi-urban	12.1	3.3	3.0	2.6	3.3
	Rural	11.1	2.0	2.3	3.0	3.9

smartphone users (APP users) were 61.9%, and non-smartphone users (SMS users) were 38.1%. From the observation and focus group discussion among the parents, it is mentioned that caregivers were more satisfied and feel easier the APP than the SMS user. After one year of completion of the project, mCARE could able to collect in total 56,290 behavioral data points, and the average data collection rate was 152.19 per week. And after analyzing the data, it is also noted that mCARE: APP users provided more accurate responses than mCARE: SMS users. The mCARE project recruits all kinds of children with ASD, for example single parents who have only mothers or fathers. The legal guardians volunteered to participate in the recruitment process, which the care practitioners would carry out. This project analyzed its participants' satisfaction level based on paired t-test. (Hsu & Lachenbruch, 2014) The participants' detailed demography of the mCARE project is shown in Table 2.

mCARE Contribution during the COVID-19 Lockdown Time

The care practitioners could continue the treatment process of "test group" participants of mCARE during the lockdown period due to the pandemic of COVID-19. Based on the ASD children's behavioral data through the mCARE system, the health care professionals could take the proper decision for each ASD child during the COVID-19 lockdown and other emergency. So, in the mCARE total population (both in the control and test group), it is observed a better improvement rate in the test group than in the control group. As in the study, only the test group was intervened by mCARE. Figure 3 shows the comparison of behavioral parameters improvement rate between the test and control group by calculating the average first and last month's improvement rate.

Figure 3. Overall improvement level analysis by deploying mCARE in (a) test group, (b) control group
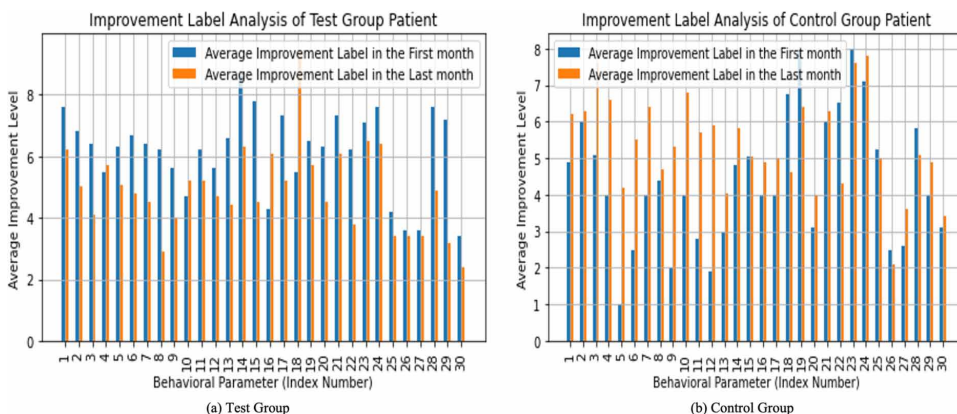
From Figure 3 (a), it is observed that 18-behavioral parameters were improved out of 30 (60%) from the "test group," and from Figure 3(b), 13-behavioral parameters were improved out of 30 (43.33%) from the "control group."

The improvement level among the "test group" in the mCARE project has been observed because of the use of mHealth technology. During the COVID-19 period, all physical intervention of the children with ASD was almost closed. But using the mCARE app (a mHealth application), the caregiver could provide their children's (with ASD) data to the system, and care-providers could know the patients' status and update the treatment by knowing the status. For this reason, the treatment of the children with ASD (in the test group of mCARE) was running, and their development had happened (shown in fig 3).

RECOMMENDATIONS FOR FUTURE RESEARCH DIRECTIONS

Based on the proposed mHealth model and mCARE project experience, the authors recommend some future directions in monitoring the children's (with ASD) behavior. They are:

- **Integration of EMR with mHealth application:** The integration of the EMR with the mHealth monitoring application will complete the whole treatment process of the children with ASD. Furthermore, to the mHealth monitoring application, the EMR feature will reduce the care practitioners' treatment hassle and intervention time. Thus, this will help to provide more care among children with ASD with quality in the LMICs where the number of care professionals is very limited. The virtual appointment feature with the intervention will make this mHealth application as a "telehealth" system. And this system will be very helpful during any natural disaster or any pandemic time. Besides this, in remote areas in LMICs, children with ASD can able to be treated by an expert with a long distance. And any care practitioner can easily refer children with ASD to another expert by creating the EMR link to that expert. Thus, integrating the EMR with the mHealth monitoring application will create a robust ASD treatment system in both developed and LMICs.
- **Arrange Focus Group Discussion (FGD) with the mHealth application:** The authors mentioned that the lack of motivation among the caregivers is the main problem to completing a successful mHealth application for monitoring the children with ASD. And the Focus Group Discussion (FGD) helps to create a bridge between the caregivers and care practitioners, which keeps the caregivers' motivational level high. But arranging an FGD in a

58

physical place is sometimes very difficult due to managing time, money, and other resources constraint. So the authors recommend to arrange short and quick FGD among the caregivers regularly and remotely in virtual mode. The arrangement can be done inside the mHealth application or using third-party meeting platforms like ZOOM, Google Meet, or Teams. Besides that, the system can also recommend the caregivers information based on the data analysis who does not respond to the system by mHealth: APP or SMS. Then the care practitioner can directly call to the caregivers and do an FGD to find out the problem and provide the solution. This FDG discussion with the mHealth application can help the caregivers to keep their motivation though out the study time or intervention time.

- **Arrange the motivational programs for the caregivers:** Besides the FGD, a mHealth application needs a regular program or approach to motivate the caregivers. It can be by sending motivational videos or providing different incentives levels by achieving different milestones. The reinforcement approach can be applied in the mHealth application to motivate its participants.
- **Create an infrastructure for ASD knowledge sharing:** The knowledge sharing approach or creating the infrastructure for creating ASD knowledge will be very helpful for the long-term ASD development in a society. The integration of ASD knowledge sharing approach in a mHealth application will create knowledge among the caregivers and also help to remove the stigma or other barriers towards the proper ASD treatment. A mHealth application can create this ASD knowledge-sharing infrastructure by providing regular short SMS or short videos. This also creates skilled care providers from the caregivers, who can professionally and properly treat their children (with ASD) in the home setting in any rural area without any help from clinical or professionals.

CONCLUSION

In this chapter, the authors proposed and described a mHealth application for monitoring the longitudinal behavioral and milestone parameters development of children with ASD. This parental report and remote experience sample-based method can be developed and deployed both for the developed and LMICs. This proposed mHealth application will be helpful for both the caregivers and care practitioners to (a) monitor the longitudinal behavioral development data, (b) to track the milestone parameters, (c) to make the evidence-based decision by the care practitioners, (d) to provide the care or treatment in any unavoidable situation like a natural disaster or pandemic time, and (e) to take proper treatment for the children with ASD. The authors

also mentioned a successful NIH-funded mHealth based application, "mCARE," in this field which had been developed by the proposed mHealth architecture model in this chapter. At the of the chapter, the authors recommend some future directions that integration with the proposed mHealth architecture will make a robust monitoring tool for children's (with ASD) behavioral development and also an effective mHealth application for the ASD treatment process.

ACKNOWLEDGMENT

REFERENCES

A., S. (2020). *Autism Statistics and Facts. autism speaks*. Retrieved 9th June from https://www.autismspeaks.org/autism-statistics-asd

Amazon. (2021). *Cloud computing with AWS*. Amazon Web Services. Retrieved 3rd December from https://aws.amazon.com/what-is-aws/

Apple. (2021). *iOS 15*. Retrieved 3rd December from https://www.apple.com/ios/ios-15/

BankMyCell. (2021). *Number of mobile phone & smartphone users*. Retrieved 3rd December from https://www.bankmycell.com/blog/how-many-phones-are-in-the-world

Barbaro, J., & Halder, S. (2016). Early identification of autism spectrum disorder: Current challenges and future global directions. *Current Developmental Disorders Reports*, *3*(1), 67–74.

Bhuiyan, M. (2021). 62% Bangladeshi users to have smartphones by 2025: Report. *The Business Standard*. Retrieved 3rd December from https://www.tbsnews.net/tech/62-bangladeshi-users-have-smartphones-2025-report-294121

Chakrabarti, S. (2009). Early identification of autism. *Indian Pediatrics*, *46*(5).

Chen, J. Q., & Benusa, A. (2017). HIPAA security compliance challenges: The case for small healthcare providers. *International Journal of Healthcare Management*, *10*(2), 135–146.

Commission, B. T. R. (2021). *The total number of Mobile Phone subscribers*. Retrieved 19th November from http://www.btrc.gov.bd/content/mobile-phone-subscribers-bangladesh-january-2021

Compliancy-Group. (2021). *What is HIPAA Compliance?* Retrieved 3rd December from https://compliancy-group.com/what-is-hipaa-compliance/

Crais, E. R., Watson, L. R., Baranek, G. T., & Reznick, J. S. (2006). Early identification of autism: How early can we go? *Seminars in Speech and Language*.

CRI. (n.d.). *Global Autism Movement and Bangladesh*. Retrieved February 11 from https://cri.org.bd/2014/09/03/global-autism-movement-and-bangladesh/

DataRePortal. (2021). *Digital Around The World*. Kepios. Retrieved 3rd December from https://datareportal.com/global-digital-overview#:~:text=There%20are%20 5.29%20billion%20unique,of%201.9%20percent%20per%20year

Developers, A. (2011). *What is android?* Dosegljivo: http://www. academia. edu/ download/30551848/andoid--tech. pdf

DiGuiseppi, C. G., Daniels, J. L., Fallin, D. M., Rosenberg, S. A., Schieve, L. A., Thomas, K. C., Windham, G. C., Goss, C. W., Soke, G. N., & Currie, D. W. (2016). Demographic profile of families and children in the Study to Explore Early Development (SEED): Case-control study of autism spectrum disorder. *Disability and Health Journal*, *9*(3), 544–551.

Eaves, L. C., & Ho, H. H. (2004). The very early identification of autism: Outcome to age 41/2–5. *Journal of Autism and Developmental Disorders*, *34*(4), 367–378.

Ehsan, U., Sakib, N., Haque, M. M., Soron, T., Saxena, D., Ahamed, S., Schwichtenberg, A., Rabbani, G., Akter, S., & Alam, F. (2018). Confronting autism in urban Bangladesh: unpacking infrastructural and cultural challenges. *EAI Endorsed Transactions on Pervasive Health and Technology, 4*(14).

Elsabbagh, M., Divan, G., Koh, Y. J., Kim, Y. S., Kauchali, S., Marcín, C., Montiel-Nava, C., Patel, V., Paula, C. S., & Wang, C. (2012). Global prevalence of autism and other pervasive developmental disorders. *Autism Research*, *5*(3), 160–179.

Fenwick, S. (2020). *Bangladesh Mobile Network Experience Report*. Opensignal Limited. Retrieved 19th November from https://www.opensignal.com/ reports/2020/07/bangladesh/mobile-network-experience

61

Fogg, B. J. (2009). A behavior model for persuasive design. *Proceedings of the 4th international Conference on Persuasive Technology*.

Friedman, B. (1996). Value-sensitive design. *Interactions, 3*(6), 16-23.

Friedman, B., Kahn, P., & Borning, A. (2002). *Value sensitive design: Theory and methods.* University of Washington Technical Report (2-12).

Friedman, B., Kahn, P. H., Borning, A., & Huldtgren, A. (2013). Value sensitive design and information systems. In *Early engagement and new technologies: Opening up the laboratory* (pp. 55–95). Springer.

Guthrie, W., Swineford, L. B., Nottke, C., & Wetherby, A. M. (2013). Early diagnosis of autism spectrum disorder: Stability and change in clinical diagnosis and symptom presentation. *Journal of Child Psychology and Psychiatry, and Allied Disciplines*, *54*(5), 582–590.

Happé, F. G., Mansour, H., Barrett, P., Brown, T., Abbott, P., & Charlton, R. A. (2016). Demographic and cognitive profile of individuals seeking a diagnosis of autism spectrum disorder in adulthood. *Journal of Autism and Developmental Disorders*, *46*(11), 3469–3480.

Haque, M. M., Dipal, D. D., Rabbani, M., Zarif, M. I. I., Iqbal, A., Akhter, S., Parveen, S., Rasel, M., Muhuri, B. R., & Soron, T. (2020). Towards Developing A Mobile-Based Care for Children with Autism Spectrum Disorder (mCARE) in low and middle-income countries (LMICs) like Bangladesh. *2020 IEEE 44th Annual Computers, Software, and Applications Conference (COMPSAC)*.

Haque, M. M., Rabbani, M., Dipal, D. D., Zarif, M. I. I., Iqbal, A., Akhter, S., Parveen, S., Rasel, M., Rabbani, G., & Alam, F. (2021). Grant Report on mCARE: Mobile-Based Care for Children with Autism Spectrum Disorder (ASD) for Low-and Middle-Income Countries (LMICs). *Journal of Psychiatry and Brain Science, 6*.

Hsu, H., & Lachenbruch, P. (2014). *Paired t test.* Wiley.

Kanner, L. (1968). Autistic disturbances of affective contact. *Acta Paedopsychiatrica*, *35*(4), 100–136.

Khanam, F.-T.-Z., Al-Naji, A., & Chahl, J. (2019). Remote monitoring of vital signs in diverse non-clinical and clinical scenarios using computer vision systems: A review. *Applied Sciences (Basel, Switzerland)*, *9*(20), 4474.

Larson, R., & Csikszentmihalyi, M. (2014). The experience sampling method. In *Flow and the foundations of positive psychology* (pp. 21–34). Springer.

Maenner, M. J., Shaw, K. A., & Baio, J. (2020). Prevalence of autism spectrum disorder among children aged 8 years—Autism and developmental disabilities monitoring network, 11 sites, United States, 2016. *MMWR. Surveillance Summaries*, *69*(4), 1.

Maples-Keller, J. L., Bunnell, B. E., Kim, S.-J., & Rothbaum, B. O. (2017). The use of virtual reality technology in the treatment of anxiety and other psychiatric disorders. *Harvard Review of Psychiatry*, *25*(3), 103.

NIH. (n.d.). Retrieved February 11 from https://www.nih.gov/

Organization, W. H. (2021). *Autism spectrum disorders*. Retrieved 30th June from https://www.who.int/news-room/fact-sheets/detail/autism-spectrum-disorders

SARRC. (2021). *Prevalence of Autism Increases by 10%, to 1 in 54 Children*. Retrieved 9th June from https://autismcenter.org/prevalence-autism-increases-10-1-54-children

Services, C.-U. S. D. o. H. H. (2020). *Data & Statistics on Autism Spectrum Disorder*. Retrieved 5th June from https://www.cdc.gov/ncbddd/autism/data.html

Sharmin, M., Hossain, M. M., Saha, A., Das, M., Maxwell, M., & Ahmed, S. (2018). From research to practice: Informing the design of autism support smart technology. *Proceedings of the 2018 CHI Conference on Human Factors in Computing Systems.*

Shminan, A. S., Adzani, R. A., Sharif, S., & Lee, N. K. (2017). AutiPECS: Mobile based learning of picture exchange communication intervention for caregivers of autistic children. *2017 International Conference on Computer and Drone Applications (IConDA).*

Speaks, A. (2020). *CDC estimate on autism prevalence increases by nearly 10 percent, to 1 in 54 children in the U.S.* Retrieved 9th June from https://www.autismspeaks.org/press-release/cdc-estimate-autism-prevalence-increases-nearly-10-percent-1-54-children-us

Speaks, A. (n.d.). *Autism Statistics and Facts*. Retrieved February 11 from https://www.autismspeaks.org/autism-statistics-asd

Statista. (2021a). *Mobile network coverage as share of population in Bangladesh in 2016, by type*. Statista Research Department. Retrieved 3rd December from https://www.statista.com/statistics/898413/bangladesh-mobile-network-coverage-by-type/

Statista. (2021b). *Number of smartphone users from 2016 to 2021*. S. O'Dea. Retrieved 3rd December from https://www.statista.com/statistics/330695/number-of-smartphone-users-worldwide/

Tariq, Q., Fleming, S. L., Schwartz, J. N., Dunlap, K., Corbin, C., Washington, P., Kalantarian, H., Khan, N. Z., Darmstadt, G. L., & Wall, D. P. (2019). Detecting developmental delay and autism through machine learning models using home videos of Bangladeshi children: Development and validation study. *Journal of Medical Internet Research*, *21*(4), e13822.

Therapy, S. (2021). *Autism Statistics & Rates in 2021*. Retrieved 5th June from https://www.joinsprouttherapy.com/studio/autism/statistics-and-rates

Wallace, G. L., Kenworthy, L., Pugliese, C. E., Popal, H. S., White, E. I., Brodsky, E., & Martin, A. (2016). Real-world executive functions in adults with autism spectrum disorder: Profiles of impairment and associations with adaptive functioning and co-morbid anxiety and depression. *Journal of Autism and Developmental Disorders*, *46*(3), 1071–1083.

Webb, S. J., & Jones, E. J. (2009). Early identification of autism: Early characteristics, onset of symptoms, and diagnostic stability. *Infants and Young Children*, *22*(2), 100.

Zwaigenbaum, L., Bauman, M. L., Stone, W. L., Yirmiya, N., Estes, A., Hansen, R. L., McPartland, J. C., Natowicz, M. R., Choueiri, R., & Fein, D. (2015). Early identification of autism spectrum disorder: Recommendations for practice and research. *Pediatrics*, *136*(Supplement 1), S10–S40.

ADDITIONAL READING

Brock, S. E., Jimerson, S. R., & Hansen, R. L. (2006). *Identifying, assessing, and treating autism at school*. Springer.

Haque, M. M., Rabbani, M., Dipal, D. D., Zarif, M. I. I., Iqbal, A., Schwichtenberg, A., ... Ahamed, S. I. (2021). Informing Developmental Milestone Achievement for Children With Autism: Machine Learning Approach. *JMIR Medical Informatics*, *9*(6), e29242.

Kanner, L. (1943). Autistic disturbances of affective contact. *Nervous Child*, *2*(3), 217–250.

Mohammadi, M. R. (Ed.). (2011). *A comprehensive book on autism spectrum disorders*. BoD–Books on Demand.

Prizant, B. M., Wetherby, A. M., Rubin, E., Laurent, A. C., & Rydell, P. J. (2006). *The SCERTS model: A comprehensive educational approach for children with autism spectrum disorders* (Vol. 1). Paul H Brookes Publishing.

Rabbani, M., Haque, M. M., Das Dipal, D., Zarif, M. I. I., Iqbal, A., Schwichtenberg, A., ... Ahamed, S. I. (2021). An mCARE study on patterns of risk and resilience for children with ASD in Bangladesh. *Scientific Reports*, *11*(1), 1–11.

Rahman, A., Divan, G., Hamdani, S. U., Vajaratkar, V., Taylor, C., Leadbitter, K., ... Green, J. (2016). Effectiveness of the parent-mediated intervention for children with autism spectrum disorder in south Asia in India and Pakistan (PASS): A randomised controlled trial. *The Lancet. Psychiatry*, *3*(2), 128–136.

Shic, F., Bradshaw, J., Klin, A., Scassellati, B., & Chawarska, K. (2011). Limited activity monitoring in toddlers with autism spectrum disorder. *Brain Research*, *1380*, 246–254.

KEY TERMS AND DEFINITIONS

ASD: Autism Spectrum Disorder or ASD is the behavioral development disability among children's early age.

Demography of Children With ASD: In a mHealth application, children's demography is very important to make proper evidence-based decisions in the treatment process.

mCARE: Mobile-Based Care or mCARE is an NIH-funded project to monitor children with ASD in Bangladesh by mHealth technology. This project was accomplished for one year to monitor behavioral and milestone parameter development.

mHealth: Mobile Health or mHealth is a set of mobile apps or devices that can be used to monitor or track diseases and provide information to the population, especially in remote areas.

MP: Milestone Parameter or MP is the record of early age children's behavioral act.

RESM: Remote Experience Sampling Method or RESM theory was used to design the mCARE app to remote monitor children with ASD in urban and rural areas.

VSD: Value Sensitive Design or VSD theory was also deployed for designing the mCARE app to ensure a robust, verifiable, and replicable strategy for cultural adoption.

Chapter 3

Artificial Intelligence Aiding Medical Diagnosis Focusing on Diabetic Retinopathy

Sakshi Juneja
Panjab University, Chandigarh, India

Alka Bali
Panjab University, Chandigarh, India

Nishu Bali
Chitkara University, Punjab, India

ABSTRACT

Artificial intelligence (AI) is a set of technologies that allows robots to detect, understand, act, and learn at human-like levels. The vast bulk of the AI that surrounds us now is powered by ineffective AI. This sort of AI is demonstrated by IBM Watson, self-driving cars, and Apple's Siri. Machine learning includes deep learning as a subset which is commonly utilised in predictive modelling. It functions in the same manner that neurons do in our brains. Its structure and networking are also influenced by neural networks found in our brains. Since the 1950s, artificial intelligence (AI) has been applied in medicine. The use of artificial intelligence in ophthalmology is mostly focused on high-incidence illnesses such as diabetic retinopathy, glaucoma, age-related macular degeneration, and cataract. The chapter reviews research demonstrating AI enhancing medical diagnosis with a focus on diabetic retinopathy.

INTRODUCTION

Artificial intelligence (AI) is a collection of technologies that work in concert to enable the machines to detect, interpret, work, and learn at the levels of intelligence of human brain (Accenture, 2021). The artificial intelligence categorized as Weak AI, also termed as Artificial Narrow Intelligence (ANI), or simply as Narrow AI, is a form of artificial intelligence that has been trained and fixated on performing narrow tasks. The majority of the AI that surrounds us now is driven by weak AI. IBM Watson, autonomous vehicles and Apple's Siri are all examples of this type of AI. Strong AI, also known as Artificial Super Intellect, is a speculative kind of AI in which a machine has an intelligence equivalent to humans, something that surpasses the intelligence and capacity of the human brain. Strong AI is purely a theoretical concept as yet and there are no real instances in use presently (Education, 2021).

Complex computing's capacity to do pattern recognition by building complex associations on the basis of incoming data, followed by its comparison with performance standards is a significant step forward towards dealing with such vast amount of data. This technology has the potentiality to ameliorate healthcare pricing, efficiency, and availability. It is essentially a digital system's capacity to demonstrate cognitive abilities. AI is much more than a massive collection of database. Just as people need to learn to execute things, AI systems need to be first exposed to a database that allows them to initially "learn" elementary targets related to a certain discovery or condition. Following the early learning stages, the machine or the system is taught to "develop," i.e., to modify its original learning to be much more efficient and precise. This learning is augmented by the application of sophisticated differential algorithms to help the system grasp complex correlations between diverse variables *via* an information dissemination called "neural network." (Doi, 2007; Hamet, 2017; Jiang, 2017).

Machine learning (ML) is basically, a subset of Artificial intelligence (AI) and deep learning (DL) is further, a subset of machine learning (Darcy et al., 2016). Deep learning has been widely used in predictive analysis. It works in a similar way as neurons work in our brain. Its structure and networking is also rooted on the neural networks in our brain. It is composed of the artificial neural network which when introduced with a vast amount of learning data understands it and makes a memory of it and when the test data similar to it is inputted, it recognizes and produces the output. It works similar to our brain that learns when introduced to new information, by first trying to compare with known information and recognizing it with the stored memory. Structurally, it is made up of many layers of artificial neurons, thus giving it the name 'deep learning'. The basic structure comprises of deep neural network, constituted with an input layer of artificial neurons, few hidden layers and finally, the output layer, all arranged hierarchically. All these layers consist of the structural unit

called 'node', analogous to a biological neuron. Function conducted by neurons of each layer is termed as activation function which is then forwarded to the connected neuron. The input is received and worked upon only when it is above threshold just like how our biological neurons work (Jigsaw Academy, 2021)

Artificial intelligence has a widespread utilization in the health and medical sciences. AI has been in use in medicine since the early 1950s, when the physicians sought to enhance the accuracy of their diagnostics by employing computer-aided algorithms. (Secinaro et al., 2021).These technologies are used to discover novel medications for health-care management and patient-care therapies (Burton, 2019; Howard, 2019; Murff et al., 2011; Yang, 2019).

Researchers in biomedical sciences have been actively attempting to apply AI to aid enhance analysis and treatment outcomes, hence, raising the overall utility of the health sector (Rong et al., 2021). Application of AI in the arena of ophthalmology is mostly concentrated on disorders with high prevalence rates, including diabetic retinopathy (DR), glaucoma, age-related macular degeneration (ARMD), cataract etc. (Kumar et al., 2019). Supply-and-demand issues could be addressed with the efficient utilization of various contemporary technologies in medicine, including artificial intelligence because of the rising accessibility of inter data, combined with technological advancements in smartphone, internet, online data storage, and data security. All these usher a moment of integration between medicine and innovation that will radically transform public healthcare concepts through Digital medical systems as these will help in treating the large patient load and the efficient management of the whole medical organization (Rong et al., 2020).

There have been several instances of utilization of Deep learning (DL) algorithms for the identification and detection of (DR) with expert-level precision (Ting et al., 2017) . The machine learning process in general is divided into two components: development of the training set and the validation set. For application of deep learning in DR, the training set includes a large quantity of training data which encompassing thousands of retinal pictures with varied degrees of DR. This training set is provided to the machine for learning process to be executed. The majority of the data is tagged in advance by competent specialists based on characteristics. After seeing a large number of labelled retinal pictures, the machine learns to perform the grading of DR on its own by constructing a model of intricate correlations between the input data and extrapolating a standard of performance.

In comparison to human graders, the deep learning systems have demonstrated much superior levels of sensitivity coupled with specificity of greater than 95% for recognizing referable DR (Ruamviboonsuk et al., 2019). Deep learning algorithms could turn out to be highly beneficial tools for carrying out the screening for DR, particularly, in poor countries with a high patient load. The key challenge in such organizations is the grading of retinal images by the qualified personnel

68

(ophthalmologists), the number of which is severely restricted in proportion to the number of patients who require screening. In developing countries, several of these patients reside in distant areas and are unable to consult qualified ophthalmologists. Moreover, because long-term follow-ups are required, patients' attitudes and/or behavioral components have a negative impact on their career, despite being aware of the consequences. These issues can be remedied by placing an automated imaging equipment within the patient's reach. In recent times, there has been an heightening interest in the creation of artificial intelligence (AI) software for analyzing the retinal pictures in diabetic patients (Noriega et al., 2020; Quinn et al., 2021). The goal of this chapter is to investigate the use of artificial intelligence in medical diagnosis, with a particular focus on diabetic retinopathy. It assesses the efficacy of currently existing diagnostic tools and forecasts future prospects.

Background

Diabetic retinopathy (DR) is a major consequence of diabetes which impairs the eyesight of afflicted patients. Diabetes impairs the body's capacity of utilization and storage of glucose. The condition is characterized by an excess of glucose in the bloodstream, which can induce damage all through body, which includes the eyes as well. Diabetes wreaks havoc on the body's tiny blood vessels, especially the retina, over time. DR develops when small blood vessels bleed blood and other substances. This results in the expansion of the retinal tissue, leading to foggy or impaired vision (Fong et al., 2004).

DR normally affects both eyes at the same time. DR seems to be more likely to develop as a person's diabetes progresses. Diabetic retinopathy can lead to blindness if left untreated. When people with this condition have high blood sugar levels for an extended length of time, fluid can build up in the lens of the eyes, which governs focalization. This alters the lens shape, resulting in visual alterations. However, if glucose levels are under control, the lens will normally revert to its former shape and eyesight will improve. Diabetics who are able to regulate their blood sugar levels in a more effective manner have a slower initiation and growth of diabetic retinopathy.

There are two major forms of DR, i.e., proliferative DR and non-proliferative DR. The non-proliferative form of DR (NPDR) is characterized by the disease symptoms that are non-existent or minor in intensity or severity. The retinal blood vessels are known to be afflicted in NPDR. Small bulges in arterial blood vessels termed as microaneurysms can result that can cause the leakage of fluid into the retina. This leakage can further induce the enlargement of macula. The most problematic and advanced form of the illness is called proliferative DR (PDR). Here, problems in circulation restrict the oxygen supply of retina (Ferris et al., 2013) and as a consequence, new, weak blood vasculature can emerge in the retina, the

69

blood vessels may cause blood to flow into the vitreous humor present in the rear portion of the eye obscuring vision. Other PDR problems include detached retina owing to generation of scar tissue and the emergence of glaucoma. Glaucoma is an ophthalmic condition in which the optic nerve gradually deteriorates. In PDR, fresh blood vasculature form in the region of the eyes which discharges fluid (Diabetic retinopathy, 2021).

Artificial Intelligence (AI) has been greatly employed for diagnosing Diabetic retinopathy and lot of research has been done depicting its potential in increasing the diagnostic efficiency (Burlina et al., 2017; Tong et al., 2020). Its promising results have made medical practitioners to employ these new technologies and improve the prognosis (Education, 2021).

ARTIFICIAL INTELLIGENCE AIDING DIAGNOSIS OF DIABETIC RETINOPATHY

Diabetes affects around 73 million people in India (Gadkari, 2018; Sosale, 2020). DR is the leading cause of avoidable blindness. Screening is hampered by a lack of knowledge, restricted accessibility to good qualified ophthalmologists, the requirement for costly equipment, and various types of socioeconomic constraints (Graham et al., 2018; Imani et al., 2015).

DR is characterized as the presence of illness that is more severe than mild non-proliferative DR or by the existence of macular edema (ME) associated with diabetes (DME). Image diagnosis is often used to assess severe forms of NPDR (STDR) or diabetic macular edema (DME).

In individuals with uncontrolled diabetes, at least yearly fundus screening is recommended for early detection and treatment in order to lessen the mortality and morbidity in the community. Unfortunately, only half of these individuals get screened. (Murchison et al., 2017; Pratt et al., 2016). Individuals with sight-threatening DR would need to see an eye expert. Because DR affects people generally in their youth, it is vital that these patients be referred as soon as possible. (Rajalakshmi et al., 2014; Scanlon et al., 2013; Zheng et al., 2012). Diabetes-related macular edema (DME) is the major cause behind the loss of vision in diabetic people. The gold standard for identifying this issue is a stereoscopic macular evaluation combined with computed optical tomography. (Browning, 2004; Litvin et al., 2017; Murchison et al., 2017; Virgili et al., 2015; Pratt et al., 2016).

Traditionally, retinopathy detection is carried out by ophthalmologists by fundus evaluation or through color fundus photography using traditional fundus cameras by trained eye technicians or optometrists (Rosenberg & Tsui, 2017). Here, major concern is to grade the retinal pictures skillfully by trained ophthalmologists, whose number

70

is extremely limited in comparison to the number of patients requiring screening. There has been an increasing interest in the creation of artificial intelligence (AI) softwares for accurate and precise evaluation of retinal pictures in diabetic patients as it can greatly aid in those circumstances where easy accessibility to healthcare professionals is not existing and patients have to traverse long distances for their healthcare needs (Abramoff et al., 2007; Fong et al., 2004; Gulshan et al., 2016; Mintz & Brodie, 2019; Namperumalsamy et al., 2003; Ryan et al., 2015; Taylor et al., 2007; Yadav & Jadhav, 2019; Vashist et al., 2011; Walton et al., 2016). The convolutional neural network (CNN) along with MTANN (massive-training artificial neural network) are two primary deep learning models that have been defined to be vital in the diagnosis of DR (Rajalakshmi, 2019; Lee et al., 2017; Suzuki, 2017). The utilization of AI in detecting referable diabetic retinal disease (DR) seems promising, with numerous studies showing excellent sensitivity and specificity values of over 90%. (Raman et al., 2018).

IDx-DR

IDx- DR is the very first AI system to be approved by the United States Food and Drug Administration (USFDA or FDA) for the non-ophthalmic screening of DR in offices of healthcare professionals. (Office of the Commissioner, 2019). The FDA has authorised IDx-DR as the first completely autonomous diagnostic system based on artificial intelligence. It delivered a diagnostic result to 819 individuals (96.1 percent) out of 900 in a study carried out by Abramoff et al. (2018). The level of sensitivity for diagnosing more severe DR was 87.2 percent, with a specificity of 90.7 percent (Abràmoff et al., 2018).

The gadget is linked to a non-mydriatic retinal sensor, and the pictures it captures are uploaded to a cloud-based database. Based on an automated analysis with a huge collection of typical fundus pictures, the server then employs deep learning algorithm to discover retinal abnormalities. The program produces one of two outcomes: if more than moderate DR is discovered, it advises to see an eyecare expert (ECP); if the findings for more than mild DR are negative, subsequent application in 12 months.

The previous versions of IDx-DR were investigated as constituent of a detection program (Iowa Detection Programme or IDP. This has been validated employing a de-identified set of 1748 digital fundus colour photographs from 874 diabetic individuals (Messidor-2 dataset). The sensitivity for diagnosing referable DR was found to be 96.8 percent when compared to the agreement of three retinal experts, while the specificity was 59.4 percent. The inclusion of DL features to the IDX-DR system improves on the IDP. It was tested against publicly available Messidor-2 dataset to see if the inclusion of DL methods gave any advantage, and it was found that there was a significant enhancement in specificity and IDX-DR was capable

71

of attaining 87 percent specificity, thus significantly lowering the number of false-positive examinations (Abràmoff et al., 2016; Grzybowski et al., 2019; Hansen et al., 2015; van der Heijden et al., 2017).

EyeArt-Remidio

Artificial Intelligence algorithms designed for DR screening, including IDx-DR and EyeArt, run on cloud-based systems. The collected photographs are sent to the internet, and the algorithm generates a response in a reasonable amount of time (Abramoff et al., 2016). To assess the effectiveness of the fundus imaging system of an AI-based screening, assessment has also been obtained from the medical clinic during study conducted by Bhaskaranand et al. (2016). The research has claimed excellent sensitivity for detecting DR > 95% while using the EyeArt programme on retinal pictures taken over the phone with Fundus (FOP). In another recent study conducted by EyeNuk with retinal pictures captured on typical desktop computer, EyeArt's sensitivity to DR was demonstrated using fundus cameras. A smartphone-based screening trial which was conducted during a study done by Bhaskaranand (2016) found sensitivity levels of 91.7 percent and a high specificity of 91.5 percent (Rajalakshmi et al., 2018)

Restricted internet connectivity or bandwidth hinders the use of these solutions in low-income and middle-economy nations. Furthermore, majority of cameras that are coupled with AI systems are the usual pricey, big fundus cameras that need the operator to take dilated retinal pictures (Gulshan,2016). Medios Technologies' AI model is the foremost offline programme for screening of DR linked with a fundus camera based on smart phone, the Remidio non-mydriatic fundus-on-phone (FOP) (Rajalakshmi, 2015). Scikit-learn is a commercially accessible example of machine learning (ML) software, with a prerequisite necessity of computer languages such as Python, that has been designed to identify diabetic retinopathy (Kumar, 2019). Convolutional Neural Networks underpin the Medios Technology system. It comprises of one neural network for assessing picture quality along with additional two different neural networks for detecting lesions in DR. The outputs resulting from both these DR neural networks are used to compute a final DR diagnostic for the patient, which is then spread to all photos of that patient (Sosale, 2020). The neural networks have been built on an Inception-V3 architecture and these have been trained to distinguish between healthy pictures and those of patients suffering from DR (moderate NPDR and greater) needing medical referral. The outcome is thus, a binary recommendation of referring or consultating an ophthalmologist. During the AI's training, no mild NPDR photos were employed. As a result, the system has been designed to optimize the sensitivities for DR needing referral and specificities for any type of DR (Sosale, 2020).

72

Another example is The LVPEI and MIT Public Indirect Ophthalmoscope which provides a built-in choice for diagnosis of DR through Machine Learning. Further, Kavya Kopparapu's Eyagnosis app, created in 2016 coupled with a 3D printed mobile fundus camera has been evaluated in various prominent eye institutions (Kopparapu, 2021).

A study by Sosale et al (2020) was conducted on 900 patients to evaluate the offline use of this software. In their study, a skilled technician collected undilated retinal pictures with the smartphone-based 'Remidio FOP camera'. From each patient's eye, two pictures, i.e., disc and macula centered, were obtained. In the study, low cost cameras were used to take the images. The 4350 nm photos were obtained with the Remidio FOP during screening camps, a total of 14266 images were taken employing the KOWA vx-10 mydriatic camera, and 34278 pictures were taken from the EyePACS dataset. Patients suffering from DR made up fifty percent of the training set, while the healthy individuals made up the remaining part of the set. The study was done with the primary goal of determining the sensitivity, precision, predictive values (both positive and negative) of the AI algorithm in successful detection of all DR when compared to the validated assessment by eye experts. The secondary goal was to determine the sensitivity, precision, PPV, and NPV of the algorithm for effectively diagnosing RDR. Here, RDR was specified as having moderate NPDR or severe form of the disease, or having DME. The algorithm's capacity to accurately detect all cases of sight-threatening DR (STDR) indicated by picture diagnosis was additionally tested. STDR was characterized as having major NPDR or even more severe illness, or having DME. They found the performance of this offline software to be very promising with a sensitivity of 83.3% (80.9% to 85.7%), precision of 95.5% (94.1% to 96.8%), PPV of 87.8% (85.7% to 90%) and NPV of 93.6% (92% to 95.2%) in determining all DR and for RDR sensitivity was found to be 93% (91.3% to 94.7%) with a precision of 92.5% (90.8% to 94.2%), PPV of 78.2% (75.5% to 80.9%) and NPV of 97.8% (96.9% to 98.8%).

Another research assessed the performance of the Medios AI utilising dilated retinal pictures taken from 231 diabetics, which were collected with the Remidio FOP (Natarajan et al., 2019). The photos were taken by a healthcare provider from a community health screening camp. The AI's sensitivity in the diagnosis of RDR was found to be 100 percent coupled with a very good specificity of 88.4 percent. Further, the corresponding value of sensitivity for DR was 85.2 percent along with 92 percent specificity.

Bosch DR Algorithm

Bosch DR Algorithm has been utilized for detecting DR from non-mydriatic pictures. Patients aged 18 years or older, suffering from diabetes lasting for a minimum of 5

years, were enrolled in the trial. Patients who had already been identified with DR were not eligible. A Mobile Eye Care fundus camera by Bosch was used to take the photographs. For the identification of DR, the pictures were processed using the Retinal Imaging Bosch DR Algorithm. The ETDRS (Early Treatment DR) values were utilized as the standard for determining the device's sensitivity as well as its specificity. A total of 564 individuals were enrolled from six Indian locations. Each person was assessed during a solitary outpatient appointment. The system cannot identify 3.9 percent of the photographs, hence, they were classified as unconvincing. Four of the individuals had no satisfactory picture by either eye, thus, they were removed from the study. These photos were then analyzed by AI software based on CNN to provide a disease present/disease absent or inadequate quality result. Remaining 560 subjects were examined. 531 out of 560 cases were accurately identified by the system. The Bosch DR Program produced remarkable results, including 91% sensitivity, 96% specificity, with PPV and NPV rates of 94%, and 95%, respectively. Thus, the Bosch DR Algorithm demonstrated a good sensitivity and a high specificity for detecting DR in pictures of non-mydriatic retina, making testing for DR easier. It has huge ramifications for telehealth in the application of retinal monitoring in diabetics (Bawankar et al., 2017; Grzybowski et al., 2019)

Google

In 2016, a Google-sponsored study that validated a novel DR detection technique based on CNN was released. The system, like IDX-DR, yields a value ranging from 0 to 1, indicating the possibility of referable DR existing in the examined picture (Gulshan et al., 2016). In the study, the authors tested their technique for detecting DR using the Messidor-2 dataset. The sets were graded by board-certified ophthalmologists in the United States. For both datasets, the algorithm attained a sensitivity of more than 95 percent and a specificity of 90.3 percent/98.1 percent. A large-scale validation research conducted in Thailand to assess the effectiveness of a Deep Learning (DL) algorithm created by Google compared with grading by regional retina specialists or ophthalmologists revealed that the DL algorithm has a high specificity and sensitivity for identification of RDR and STDR (Raman et al., 2018). A total of more than twenty five thousand gradable retinal pictures from 7517 diabetic individuals were evaluated for DR severity levels .The reference data set for this investigation was adjudicated gradings by retinal professionals from India, United States and Thailand. Their collaborative project is with their subsidiary Deep Mind, UCL and an established eye Hospital. DeepMind has developed a prototype gadget that scans a patient's retina in real time to identify possible abnormalities. The equipment examines the retina, then DeepMind's analytics evaluate the pictures to deliver a diagnostic and a "priority score."

74

The system is developed based on well-established deep learning concepts, which employ methods to find similar trends in information. The data in this example is 3D images of patients' eyes taken with an OCT (Optical coherence tomography) technology. This produces a three-dimensional snapshot of the epithelium, and that is a standard approach to evaluate eye wellness. OCT scans are an important health check tool, as early detection of the eye condition could save a patient's vision. Almost 15,000 OCT scans of 7,500 patients were used to train the program. All of these people were diagnosed at an established eye Hospital. Their scans were input into the system with assessments from human doctors. It taught the identification of different elements of the eye anatomy before recommending clinical intervention depending on the numerous indicators of pathology which the scans revealed (Vincent, 2018).

FUTURE RESEARCH DIRECTIONS

Diabetes-related vision loss can be prevented if diabetic eye disease (or DR) is detected and treated early. Over the last decade, significant progress has been achieved in the introduction of automated eye analysis tools. These rely on various image processing approaches, which are often based on human designed algorithms for classification of lesions, Machine Learning, or a combination of the two. DR detection techniques that are mechanized offer various benefits over screening by qualified ophthalmologists. For starters, these don't weary and can be used to grade hundreds of photographs every day, typically providing findings within a very short span of time ranging in minutes or even seconds, after capturing the photographs. Expanding automated DR screening procedures is thus primarily a question of purchasing more gear. Even after making significant progress in developing the AI systems and algorithms outlined above, which produce high accuracy, their implementation for practical application lacks the necessary infrastructure. As an example, Google Medical investigators in eleven clinics spanning Thailand found multitude of factors linked to socio-environmental issues which hampered accuracy and its acceptance in practical use. To count few of the challenges; Hospital screening environments (poorly lightened clinics produce less efficient pictures), picture gradability and internet bandwidth. All these issues caused the retaking of the images and thus, causing a delay in the diagnosis, something it was aimed to reduce. (Beede et al., 2020; He et al., 2020)

Nonetheless, it is unclear that fully automated DR testing will be available very soon, and professional graders will continue to be required to interpret abnormal or low-quality photos. Regardless of the expense of the automation itself, such type of screening still necessitates considerable investment with respect to equipment, trained personnel fo0r efficient equipment handling, and other costs. The efficiency

of presently existing commercially accessible systems also shows that certain degree of professionally qualified professional verification is essential, especially due to the poor specificity of most systems. The key to building cost-efficient screening and treatment is to strike an appropriate balance between high specificity and sensitivity. With decreased sensitivity, more DR cases are overlooked, which contradicts the primary goal of a DR screening program, that is, the early diagnosis of DR. If specificity is poor, a disproportionate amount of false positives are obtained, that require additional investigation, wasting the resources, which computerized Diabetic retinopathy screening is attempting to save. The newer DL systems are being credited with plausible high levels of sensitivity and specificity. Though, these are yet to be realized, and their effectiveness in realistic screening situations needs to be included after more validation. A variety of technologies for rapid recognition of DR are now commercially available, and several others are also on the way with some of them in the works. Irrespective of their evolution stage, many of these systems are being dynamically developed, with updates and enhancements in user interface, portability, improved detection of DME. One of the most challenging obstacles to be surmounted in developing these systems is obtaining an adequate number of retinal pictures which could be employed to train and evaluate such algorithms. Some of the challenges in getting a sufficiently big dataset include privacy and data security as most of the algorithm system used cloud based system, they collect the data from patients and stores on cloud datasets which can put patients' privacy on risk. Furthermore, such photographs must be professionally graded and labeled as a standard reference, which takes a substantial amount of time and money. This adds to the ambiguity around the assessors' sort of precision.

Some of the investigations were validated and compared using the publicly accessible Messidor-2 dataset, which has over 1700 tagged retinal pictures. This dataset, on the other hand, comprises photos of exceptional quality, at a level which is not indicative of real-world invited applications. Lastly, creating DL algorithms using the criterion of human grading restricts the system's potential efficacy to those of professional evaluators. It is not impossible for computerized retinal image processing systems to outperform professional graders in times to come; nevertheless, this cannot be measured if manual marking is considered the ultimate goal. Currently available systems include specialized computer programmes, web solutions, and even smartphone apps for integration with new or current screening activities. It is unknown how well these various platforms impact the performance or processes of routine screening, especially as more of these systems come into use.

The Artificial intelligence-based DR tool can help the doctor with fundus picture processing, which can help determine more quickly, the progression of disease in the patient. Doctors can also attend to even more patients who require assistance without suffering from mydriasis. New health care techniques aim to reduce

ophthalmologist visits, lowering total healthcare expenditures, and increasing the patients served by each health practitioner. AI can assist the health-care provider in reaching his or her objective. Though technology helps in the healthcare system, it cannot be used to replace a clinician at this time. Artificial intelligence has made significant strides in recent years and is laying the foundation for new possibilities. AI - powered advancements are opening up novel opportunities for implementing DR detection and scoring systems (Kumar et al., 2019). The inclusion of more costly data from OCT angiography or wide field imaging can also be utilized for future AI applications instead of the conventionally employed fundus images. Coming future can prospect us with compact devices which may enable patients to accomplish retinopathy diagnostic screening by using their personal devices at home which can result in a significant reduction in the number of trained medical personnel as well as medical infrastructure necessary to make diagnosis.

Automation systems may be developed which are able to cover lot more variety of disease indicators . Currently for now simultaneous usage of AI technology and physicians seemed to be most efficient solution. (Li et al., 2021)

Early screening and surveillance of various illnesses including diabetic retinopathy is also being researched by employing serum biomarkers (Al-Rubeaan et al., 2017; Jenkins et al., 2015; Markan et al., 2020; Motawi et al., 2018; Zhang et al., 2019) and these can also be used to provide better perceptivity to conclude better than human intelligence.

CONCLUSION

This chapter gives an overview of the current infrastructure and the potential of artificial intelligence as a diagnostic tool in future, with an emphasis on diabetic retinopathy. The Artificial intelligence-based DR tools may aid the doctor with retina image interpretation, allowing the physician to immediately advise the next stages in the patient's care. In addition, without mydriasis, clinicians could be able to attend to greater number of patients. New medical care advancements based on AI place a premium on decreasing visits to ophthalmologist, lowering gross treatment expenses, and expand the count of patients treated by every physician. AI can be a valuable tool to assist health care professionals in reaching their objectives. However, given its existing limitations, it cannot be used to replace clinicians at least at this point of time. New advancements in the field of AI technology are bringing new opportunities for deploying DR identification and rating systems.

REFERENCES

Abràmoff, M., Lavin, P., Birch, M., Shah, N., & Folk, J. (2018). Pivotal trial of an autonomous AI-based diagnostic system for detection of diabetic retinopathy in primary care offices. *NPJ Digital Medicine*, *1*(1), 39. Advance online publication. doi:10.103841746-018-0040-6 PMID:31304320

Abràmoff, M., Lou, Y., Erginay, A., Clarida, W., Amelon, R., Folk, J., & Niemeijer, M. (2016). Improved Automated Detection of Diabetic Retinopathy on a Publicly Available Dataset Through Integration of Deep Learning. *Investigative Ophthalmology & Visual Science*, *57*(13), 5200. doi:10.1167/iovs.16-19964 PMID:27701631

Abramoff, M., Niemeijer, M., Suttorp-Schulten, M., Viergever, M., Russell, S., & van Ginneken, B. (2007). Evaluation of a System for Automatic Detection of Diabetic Retinopathy From Color Fundus Photographs in a Large Population of Patients With Diabetes. *Diabetes Care*, *31*(2), 193–198. doi:10.2337/dc07-1312 PMID:18024852

Abràmoff, M. D., Lou, Y., Erginay, A., Clarida, W., Amelon, R., Folk, J. C., & Niemeijer, M. (2016). Improved automated detection of diabetic retinopathy on a publicly available dataset through integration of Deep Learning. *Investigative Ophthalmology & Visual Science*, *57*(13), 5200. doi:10.1167/iovs.16-19964 PMID:27701631

Accenture. (2021). *What Is Artificial Intelligence*. Retrieved 17 November 2021, from https://www.accenture.com/us-en/insights/artificial-intelligence-summary-index

Al-Rubeaan, K., Siddiqui, K., Al-Ghonaim, M. A., Youssef, A. M., Al-Sharqawi, A. H., & AlNaqeb, D. (2017). Assessment of the diagnostic valueMarkan, A., Agarwal, A., Arora, A., Bazgain, K., Rana, V., & Gupta, V. (2020). Novel imaging biomarkers in diabetic retinopathy and diabetic macular edema. *Therapeutic Advances in Ophthalmology*, *12*, 251584142095051. doi:10.1177/2515841420950513

Bawankar, P., Shanbhag, N., K, S. S., Dhawan, B., Palsule, A., Kumar, D., Chandel, S., & Sood, S. (2017). Sensitivity and specificity of automated analysis of single-field non-mydriatic fundus photographs by Bosch DR Algorithm—Comparison with mydriatic fundus photography (ETDRS) for screening in undiagnosed diabetic retinopathy. *PLoS One*, *12*(12), e0189854. doi:10.1371/journal.pone.0189854 PMID:29281690

Beede, E., Baylor, E., Hersch, F., Iurchenko, A., Wilcox, L., & Ruamviboonsuk, P., & Vardoulakis, L. M. (2020). A human-centered evaluation of a deep learning system deployed in clinics for the detection of diabetic retinopathy. *Proceedings of the 2020 CHI Conference on Human Factors in Computing Systems*. 10.1145/3313831.3376718

Bhaskaranand, M., Ramachandra, C., Bhat, S., Cuadros, J., Nittala, M., Sadda, S., & Solanki, K. (2016). Automated Diabetic Retinopathy Screening and Monitoring Using Retinal Fundus Image Analysis. *Journal of Diabetes Science and Technology*, *10*(2), 254–261. doi:10.1177/1932296816628546 PMID:26888972

Browning, D. (2004). Comparison of the clinical diagnosis of diabetic macular edema with diagnosis by optical coherence tomography*1. *Ophthalmology*, *111*(4), 712–715. doi:10.1016/j.ophtha.2003.06.028 PMID:15051203

Burlina, P., Pacheco, K. D., Joshi, N., Freund, D. E., & Bressler, N. M. (2017). Comparing humans and deep learning performance for grading AMD: A study in using universal deep features and transfer learning for automated AMD analysis. *Computers in Biology and Medicine*, *82*, 80–86. doi:10.1016/j.compbiomed.2017.01.018 PMID:28167406

Burton, R. J., Albur, M., Eberl, M., & Cuff, S. M. (2019). Using artificial intelligence to reduce diagnostic workload without compromising detection of urinary tract infections. *BMC Medical Informatics and Decision Making*, *19*(1), 171. Advance online publication. doi:10.118612911-019-0878-9 PMID:31443706

Darcy, A. M., Louie, A. K., & Roberts, L. W. (2016). Machine Learning and the Profession of Medicine. *Journal of the American Medical Association*, *315*(6), 551. doi:10.1001/jama.2015.18421 PMID:26864406

Diabetic retinopathy. (2021). Retrieved 17 November 2021, from https://www.aoa.org/healthy-eyes/eye-and-vision-conditions/diabetic-retinopathy?sso=y

Doi, K. (2007). Computer-aided diagnosis in medical imaging: Historical Review, current status and future potential. *Computerized Medical Imaging and Graphics*, *31*(4-5), 198–211. doi:10.1016/j.compmedimag.2007.02.002 PMID:17349778

Education, I. (2021). *What is Artificial Intelligence (AI)?* Retrieved 17 November 2021, from https://www.ibm.com/cloud/learn/what-is-artificial-intelligence

Ferris, F. L. III, Wilkinson, C. P., Bird, A., Chakravarthy, U., Chew, E., Csaky, K., & Sadda, S. R. (2013). Clinical Classification of Age-related Macular Degeneration. *Ophthalmology*, *120*(4), 844–851. doi:10.1016/j.ophtha.2012.10.036 PMID:23332590

Fong, D., Aiello, L., Ferris, F. III, & Klein, R. (2004). Diabetic Retinopathy. *Diabetes Care*, *27*(10), 2540–2553. doi:10.2337/diacare.27.10.2540 PMID:15451934

Fong, D. S., Aiello, L. P., Ferris, F. L. III, & Klein, R. (2004). Diabetic Retinopathy. *Diabetes Care*, *27*(10), 2540–2553. doi:10.2337/diacare.27.10.2540 PMID:15451934

Gadkari, S. S. (2018). Diabetic retinopathy screening: Telemedicine, the way to go! *Indian Journal of Ophthalmology*. Retrieved from https://pubmed.ncbi.nlm.nih.gov/29380754/

Graham-Rowe, E., Lorencatto, F., Lawrenson, J. G., Burr, J. M., Grimshaw, J. M., Ivers, N. M., Presseau, J., Vale, L., Peto, T., Bunce, C., & Francis, J. (2018). Barriers to and enablers of diabetic retinopathy screening attendance: A systematic review of published and Grey Literature. *Diabetic Medicine*, *35*(10), 1308–1319. doi:10.1111/dme.13686 PMID:29790594

Grzybowski, A., Brona, P., Lim, G., Ruamviboonsuk, P., Tan, G., Abramoff, M., & Ting, D. (2019). Artificial intelligence for diabetic retinopathy screening: A review. *Eye (London, England)*, *34*(3), 451–460. doi:10.103841433-019-0566-0 PMID:31488886

Gulshan, V., Peng, L., Coram, M., Stumpe, M., Wu, D., Narayanaswamy, A., Venugopalan, S., Widner, K., Madams, T., Cuadros, J., Kim, R., Raman, R., Nelson, P. C., Mega, J. L., & Webster, D. R. (2016). Development and Validation of a Deep Learning Algorithm for Detection of Diabetic Retinopathy in Retinal Fundus Photographs. *Journal of the American Medical Association*, *316*(22), 2402. doi:10.1001/jama.2016.17216 PMID:27898976

Gulshan, V., Peng, L., Coram, M., Stumpe, M. C., Wu, D., Narayanaswamy, A., Venugopalan, S., Widner, K., Madams, T., Cuadros, J., Kim, R., Raman, R., Nelson, P. C., Mega, J. L., & Webster, D. R. (2016). Development and validation of a deep learning algorithm for detection of diabetic retinopathy in retinal fundus photographs. *Journal of the American Medical Association*, *316*(22), 2402. doi:10.1001/jama.2016.17216 PMID:27898976

Hamet, P., & Tremblay, J. (2017). Artificial Intelligence in medicine. *Metabolism: Clinical and Experimental*, *69*, S36–S40. Advance online publication. doi:10.1016/j.metabol.2017.01.011 PMID:28126242

Hansen, M., Abràmoff, M., Folk, J., Mathenge, W., Bastawrous, A., & Peto, T. (2015). Results of Automated Retinal Image Analysis for Detection of Diabetic Retinopathy from the Nakuru Study, Kenya. *PLoS One*, *10*(10), e0139148. doi:10.1371/journal.pone.0139148 PMID:26425849

He, M., Li, Z., Liu, C., Shi, D., & Tan, Z. (2020). Deployment of artificial intelligence in real-world practice: Opportunity and challenge. *Asia-Pacific Journal of Ophthalmology*, *9*(4), 299–307. doi:10.1097/APO.0000000000000301 PMID:32694344

Howard, J. (2019). Artificial intelligence: Implications for the future of work. *American Journal of Industrial Medicine*, *62*(11), 917–926. doi:10.1002/ajim.23037 PMID:31436850

Imani, E., Pourreza, H.-R., & Banaee, T. (2015). Fully automated diabetic retinopathy screening using morphological component analysis. *Computerized Medical Imaging and Graphics*, *43*, 78–88. doi:10.1016/j.compmedimag.2015.03.004 PMID:25863517

Jenkins, A., Joglekar, M., Hardikar, A., Keech, A., O'Neal, D., & Januszewski, A. (2015). Biomarkers in Diabetic Retinopathy. *The Review of Diabetic Studies; RDS*, *12*(1-2), 159–195. doi:10.1900/RDS.2015.12.159 PMID:26676667

Jiang, F., Jiang, Y., Zhi, H., Dong, Y., Li, H., Ma, S., Wang, Y., Dong, Q., Shen, H., & Wang, Y. (2017). Artificial Intelligence in healthcare: Past, present and future. *Stroke and Vascular Neurology*, *2*(4), 230–243. doi:10.1136vn-2017-000101 PMID:29507784

Jigsaw Academy. (2021). *Deep Neural Network: An Easy Introduction for 2021*. Retrieved 17 November 2021, from https://www.jigsawacademy.com/blogs/ai-ml/deep-neural-network/

Kopparapu, K. (2021). *16: 2017 WebMD Health Hero, Inventor*. WebMD. Retrieved 17 November 2021, from https://www.webmd.com/healthheroes/2017-inventor-kavya-kopparapu

Kumar, A., Padhy, S., Takkar, B., & Chawla, R. (2019). Artificial intelligence in diabetic retinopathy: A natural step to the future. *Indian Journal of Ophthalmology*, *67*(7), 1004. doi:10.4103/ijo.IJO_1989_18 PMID:31238395

Lee, A., Taylor, P., Kalpathy-Cramer, J., & Tufail, A. (2017). Machine Learning Has Arrived! *Ophthalmology*, *124*(12), 1726–1728. doi:10.1016/j.ophtha.2017.08.046 PMID:29157423

Li, S., Zhao, R., & Zou, H. (2021). Artificial Intelligence for Diabetic retinopathy. *Chinese Medical Journal*. Publish Ahead of Print. doi:10.1097/CM9.0000000000001816

Litvin, T., Bresnick, G., Cuadros, J., Selvin, S., Kanai, K., & Ozawa, G. (2017). A Revised Approach for the Detection of Sight-Threatening Diabetic Macular Edema. *JAMA Ophthalmology*, *135*(1), 62. doi:10.1001/jamaophthalmol.2016.4772 PMID:27930756

Markan, A., Agarwal, A., Arora, A., Bazgain, K., Rana, V., & Gupta, V. (2020). Novel imaging biomarkers in diabetic retinopathy and diabetic macular edema. *Therapeutic Advances in Ophthalmology*, *12*, 251584142095051. doi:10.1177/2515841420950513 PMID:32954207

Mintz, Y., & Brodie, R. (2019). Introduction to artificial intelligence in medicine. *Minimally Invasive Therapy & Allied Technologies*, *28*(2), 73–81. doi:10.1080/13 645706.2019.1575882 PMID:30810430

Motawi, T., Shehata, N., ElNokeety, M., & El-Emady, Y. (2018). Potential serum biomarkers for early detection of diabetic nephropathy. *Diabetes Research and Clinical Practice*, *136*, 150–158. doi:10.1016/j.diabres.2017.12.007 PMID:29253627

Murchison, A., Hark, L., Pizzi, L., Dai, Y., Mayro, E., Storey, P., Leiby, B. E., & Haller, J. A. (2017). Non-adherence to eye care in people with diabetes. *BMJ Open Diabetes Research & Care*, *5*(1), e000333. doi:10.1136/bmjdrc-2016-000333 PMID:28878930

Murff, H. J., FitzHenry, F., Matheny, M. E., Gentry, N., Kotter, K. L., Crimin, K., Dittus, R. S., Rosen, A. K., Elkin, P. L., Brown, S. H., & Speroff, T. (2011). Automated Identification of Postoperative Complications Within an Electronic Medical Record Using Natural Language Processing. *Journal of the American Medical Association*, *306*(8). Advance online publication. doi:10.1001/jama.2011.1204 PMID:21862746

Namperumalsamy, P., Nirmalan, P., & Ramasamy, K. (2003). Developing a Screening Program to Detect Sight-Threatening Diabetic Retinopathy in South India. *Diabetes Care*, *26*(6), 1831–1835. doi:10.2337/diacare.26.6.1831 PMID:12766118

Natarajan, S., Jain, A., Krishnan, R., Rogye, A., & Sivaprasad, S. (2019). Diagnostic accuracy of community-based diabetic retinopathy screening with an offline artificial intelligence system on a smartphone. *JAMA Ophthalmology*, *137*(10), 1182. doi:10.1001/jamaophthalmol.2019.2923 PMID:31393538

Noriega, A., Meizner, D., Camacho, D., Enciso, J., Quiroz-Mercado, H., Morales-Canton, V., & ... . (2020). Screening Diabetic Retinopathy Using an Automated Retinal Image Analysis System in Mexico: Independent and Assistive use Cases (Preprint). *JMIR Formative Research*. Advance online publication. doi:10.2196/25290 PMID:34435963

Office of the Commissioner. (2019). *FDA permits marketing of artificial intelligence-based device to detect certain diabetes-related eye problems*. U.S. Food and Drug Administration. https://www.fda.gov/news-events/press-announcements/fda-permits-marketing-artificial-intelligence-based-device-detect-certain-diabetes-related-eye

Pratt, H., Coenen, F., Broadbent, D., Harding, S., & Zheng, Y. (2016). Convolutional Neural Networks for Diabetic Retinopathy. *Procedia Computer Science*, *90*, 200–205. doi:10.1016/j.procs.2016.07.014

Pros and cons of using an AI-based diagnosis for diabetic retinopathy. (n.d.). *Optometry Times*. Retrieved November 19, 2021, from https://www.optometrytimes.com/view/pros-and-cons-using-ai-based-diagnosis-diabetic-retinopathy

Quinn, N., Brazionis, L., Zhu, B., Ryan, C., D'Aloisio, R., Lilian Tang, H., Peto, T., & Jenkins, A. (2021). Facilitating diabetic retinopathy screening using automated retinal image analysis in underresourced settings. *Diabetic Medicine*, *38*(9). Advance online publication. doi:10.1111/dme.14582 PMID:33825229

Rajalakshmi, R. (2019). The impact of artificial intelligence in screening for diabetic retinopathy in India. *Eye (London, England)*, *34*(3), 420–421. doi:10.103841433-019-0626-5 PMID:31827270

Rajalakshmi, R., Amutha, A., Ranjani, H., Ali, M., Unnikrishnan, R., Anjana, R., Narayan, K. M. V., & Mohan, V. (2014). Prevalence and risk factors for diabetic retinopathy in Asian Indians with young onset Type 1 and Type 2 Diabetes. *Journal of Diabetes and Its Complications*, *28*(3), 291–297. doi:10.1016/j.jdiacomp.2013.12.008 PMID:24512748

Rajalakshmi, R., Arulmalar, S., Usha, M., Prathiba, V., Kareemuddin, K. S., Anjana, R. M., & Mohan, V. (2015). Validation of smartphone based retinal photography for diabetic retinopathy screening. *PLoS One*, *10*(9), e0138285. Advance online publication. doi:10.1371/journal.pone.0138285 PMID:26401839

Rajalakshmi, R., Subashini, R., Anjana, R., & Mohan, V. (2018). Automated diabetic retinopathy detection in smartphone-based fundus photography using artificial intelligence. *Eye (London, England)*, *32*(6), 1138–1144. doi:10.103841433-018-0064-9 PMID:29520050

Raman, R., Srinivasan, S., Virmani, S., Sivaprasad, S., Rao, C., & Rajalakshmi, R. (2018). Fundus photograph-based deep learning algorithms in detecting diabetic retinopathy. *Eye (London, England)*, *33*(1), 97–109. doi:10.103841433-018-0269-y PMID:30401899

Raman, R., Srinivasan, S., Virmani, S., Sivaprasad, S., Rao, C., & Rajalakshmi, R. (2018). Fundus photograph-based deep learning algorithms in detecting diabetic retinopathy. *Eye (London, England)*, *33*(1), 97–109. doi:10.103841433-018-0269-y PMID:30401899

Researchers Reveal New Biomarkers for Early Detection of Diabetic Vision Loss. (2021). *Chinese Academy of Sciences.* Retrieved 19 November 2021, from https://english.cas.cn/newsroom/cas_media/202010/t20201019_244966.shtml

Rong, G., Mendez, A., Bou Assi, E., Zhao, B., & Sawan, M. (2021). *Artificial Intelligence in Healthcare: Review and Prediction Case Studies*. Academic Press.

Rosenberg, J. B., & Tsui, I. (2017). Screening for Diabetic Retinopathy. *The New England Journal of Medicine*, *376*(16), 1587–1588. doi:10.1056/NEJMe1701820 PMID:28423293

Ruamviboonsuk, P., Krause, J., Chotcomwongse, P., Sayres, R., Raman, R., Widner, K., Campana, B. J. L., Phene, S., Hemarat, K., Tadarati, M., Silpa-Archa, S., Limwattanayingyong, J., Rao, C., Kuruvilla, O., Jung, J., Tan, J., Orprayoon, S., Kangwanwongpaisan, C., Sukumalpaiboon, R., ... Webster, D. R. (2019). Deep learning versus human graders for classifying diabetic retinopathy severity in a nationwide screening program. *NPJ Digital Medicine*, *2*(1), 25. Advance online publication. doi:10.103841746-019-0099-8 PMID:31341955

Ryan, M., Rajalakshmi, R., Prathiba, V., Anjana, R., Ranjani, H., Narayan, K., Olsen, T., Mohan, V., Ward, L., Lynn, M., & Hendrick, A. (2015). Comparison Among Methods of Retinopathy Assessment (CAMRA) Study. *Ophthalmology*, *122*(10), 2038–2043. doi:10.1016/j.ophtha.2015.06.011 PMID:26189190

Scanlon, P., Aldington, S., & Stratton, I. (2013). Epidemiological issues in diabetic retinopathy. *Middle East African Journal of Ophthalmology*, *20*(4), 293. doi:10.4103/0974-9233.120007 PMID:24339678

Secinaro, S., Calandra, D., Secinaro, A., Muthurangu, V., & Biancone, P. (2021). The role of artificial intelligence in healthcare: A structured literature review. *BMC Medical Informatics and Decision Making*, *21*(1), 125. Advance online publication. doi:10.118612911-021-01488-9 PMID:33836752

Shi, L., Wu, H., Dong, J., Jiang, K., Lu, X., & Shi, J. (2015). Telemedicine for detecting diabetic retinopathy: a systematic review and meta-analysis. *British Journal of Ophthalmology, 99*(6), 823-831. doi:10.1136/bjophthalmol-2014-305631

Sosale, B., Aravind, S., Murthy, H., Narayana, S., Sharma, U., Gowda, S., & Naveenam, M. (2020). Simple, Mobile-based Artificial Intelligence Algorithm in the detection of Diabetic Retinopathy (SMART) study. *BMJ Open Diabetes Research & Care*, *8*(1), e000892. Advance online publication. doi:10.1136/bmjdrc-2019-000892 PMID:32049632

Sosale, B., Sosale, A. R., Murthy, H., Sengupta, S., & Naveenam, M. (2020). Medios–an offline, smartphone-based artificial intelligence algorithm for the diagnosis of diabetic retinopathy. *Indian Journal of Ophthalmology*, *68*(2), 391. doi:10.4103/ijo.IJO_1203_19 PMID:31957735

Suzuki, K. (2017). Overview of deep learning in medical imaging. *Radiological Physics and Technology*, *10*(3), 257–273. doi:10.100712194-017-0406-5 PMID:28689314

Taylor, C., Merin, L., Salunga, A., Hepworth, J., Crutcher, T., O'Day, D., & Pilon, B. (2007). Improving Diabetic Retinopathy Screening Ratios Using Telemedicine-Based Digital Retinal Imaging Technology: The Vine Hill Study. *Diabetes Care*, *30*(3), 574–578. doi:10.2337/dc06-1509 PMID:17327323

Ting, D. S. W., Cheung, C. Y.-L., Lim, G., Tan, G. S. W., Quang, N. D., Gan, A., Hamzah, H., Garcia-Franco, R., San Yeo, I. Y., Lee, S. Y., Wong, E. Y. M., Sabanayagam, C., Baskaran, M., Ibrahim, F., Tan, N. C., Finkelstein, E. A., Lamoureux, E. L., Wong, I. Y., Bressler, N. M., & Sivaprasad, S. (2017). Development and Validation of a Deep Learning System for Diabetic Retinopathy and Related Eye Diseases Using Retinal Images From Multiethnic Populations With Diabetes. *Journal of the American Medical Association*, *318*(22), 2211. doi:10.1001/jama.2017.18152

Tong, Y., Lu, W., Yu, Y., & Shen, Y. (2020). Application of machine learning in ophthalmic imaging modalities. *Eye and Vision*, *7*(1). Advance online publication. doi:10.118640662-020-00183-6

Van der Heijden, A., Abramoff, M., Verbraak, F., van Hecke, M., Liem, A., & Nijpels, G. (2017). Validation of automated screening for referable diabetic retinopathy with the IDx-DR device in the Hoorn Diabetes Care System. *Acta Ophthalmologica*, *96*(1), 63–68. doi:10.1111/aos.13613 PMID:29178249

Vashist, P., Gupta, N., Singh, S., & Saxena, R. (2011). Role of early screening for diabetic retinopathy in patients with diabetes mellitus: An overview. *Indian Journal of Community Medicine*, *36*(4), 247. doi:10.4103/0970-0218.91324 PMID:22279252

Vincent, J. (2018, August 13). DeepMind's AI can detect over 50 eye diseases as accurately as a doctor. *The Verge*. https://www.theverge.com/2018/8/13/17670156/deepmind-ai-eye-disease-doctor-moorfields

Virgili, G., Menchini, F., Casazza, G., Hogg, R., Das, R., Wang, X., & Michelessi, M. (2015). Optical coherence tomography (OCT) for detection of macular oedema in patients with diabetic retinopathy. *Cochrane Database of Systematic Reviews*. Advance online publication. doi:10.1002/14651858.CD008081.pub3 PMID:25564068

Walton, O. IV, Garoon, R., Weng, C., Gross, J., Young, A., Camero, K., Jin, H., Carvounis, P. E., Coffee, R. E., & Chu, Y. I. (2016). Evaluation of Automated Teleretinal Screening Program for Diabetic Retinopathy. *JAMA Ophthalmology*, *134*(2), 204. doi:10.1001/jamaophthalmol.2015.5083 PMID:26720694

Yadav, S., & Jadhav, S. (2019). Deep convolutional neural network based medical image classification for disease diagnosis. *Journal of Big Data*, *6*(1), 113. Advance online publication. doi:10.118640537-019-0276-2

Yang, X., Wang, Y., Byrne, R., Schneider, G., & Yang, S. (2019). Concepts of Artificial Intelligence for computer-assisted drug discovery. *Chemical Reviews*, *119*(18), 10520–10594. doi:10.1021/acs.chemrev.8b00728 PMID:31294972

Zhang, D., Ye, S., & Pan, T. (2019). The role of serum and urinary biomarkers in the diagnosis of early diabetic nephropathy in patients with type 2 diabetes. *PeerJ*, *7*, e7079. Advance online publication. doi:10.7717/peerj.7079 PMID:31218128

Zheng, Y., Lamoureux, E., Lavanya, R., Wu, R., Ikram, M., Wang, J., Mitchell, P., Cheung, N., Aung, T., Saw, S.-M., & Wong, T. Y. (2012). Prevalence and Risk Factors of Diabetic Retinopathy in Migrant Indians in an Urbanized Society in Asia. *Ophthalmology*, *119*(10), 2119–2124. doi:10.1016/j.ophtha.2012.04.027 PMID:22709419

ADDITIONAL READING

Approval of artificial intelligence and machine learning-based medical devices in the USA and Europe (2015–20): a comparative analysis. (2021). *The Lancet Digital Health, 3*(3), e195–e203. doi:10.1016/S2589-7500(20)30292-2

Bajwa, J., Munir, U., Nori, A., & Williams, B. (2021). Artificial intelligence in healthcare: Transforming the practice of medicine. *Future Healthcare Journal*, *8*(2), e188–e194. doi:10.7861/fhj.2021-0095 PMID:34286183

Bellemo, V., Lim, G., Rim, T. H., Tan, G. S. W., Cheung, C. Y., Sadda, S., He, M., Tufail, A., Lee, M. L., Hsu, W., & Ting, D. S. W. (2019). Artificial Intelligence Screening for Diabetic Retinopathy: The Real-World Emerging Application. *Current Diabetes Reports*, *19*(9), 72. Advance online publication. doi:10.100711892-019-1189-3 PMID:31367962

Bellemo, V., Lim, Z. W., Lim, G., Nguyen, Q. D., Xie, Y., Yip, M. Y. T., Hamzah, H., Ho, J., Lee, X. Q., Hsu, W., Lee, M. L., Musonda, L., Chandran, M., Chipalo-Mutati, G., Muma, M., Tan, G. S. W., Sivaprasad, S., Menon, G., Wong, T. Y., & Ting, D. S. W. (2019). Artificial intelligence using deep learning to screen for referable and vision-threatening diabetic retinopathy in Africa: A clinical validation study. *The Lancet. Digital Health*, *1*(1), e35–e44. doi:10.1016/S2589-7500(19)30004-4 PMID:33323239

Gadekallu, T. R., Khare, N., Bhattacharya, S., Singh, S., Maddikunta, P. K. R., & Srivastava, G. (2020). Deep neural networks to predict diabetic retinopathy. *Journal of Ambient Intelligence and Humanized Computing*. Advance online publication. doi:10.100712652-020-01963-7

Legg, S., & Hutter, M. (2007). Universal Intelligence: A Definition of Machine Intelligence. *Minds and Machines*, *17*(4), 391–444. doi:10.100711023-007-9079-x

Reddy, S., Fox, J., & Purohit, M. P. (2018). Artificial intelligence-enabled healthcare delivery. *Journal of the Royal Society of Medicine*, *112*(1), 22–28. doi:10.1177/0141076818815510 PMID:30507284

Rong, G., Mendez, A., Bou Assi, E., Zhao, B., & Sawan, M. (2020). Artificial Intelligence in Healthcare: Review and Prediction Case Studies. *Engineering.*, *6*(3), 291–301. Advance online publication. doi:10.1016/j.eng.2019.08.015

Sajda, P. (2006). Machine learning for detection and diagnosis of disease. *Annual Review of Biomedical Engineering*, *8*(1), 537–565. doi:10.1146/annurev.bioeng.8.061505.095802 PMID:16834566

Wong, T., & Sabanayagam, C. (2019). Strategies to Tackle the Global Burden of Diabetic Retinopathy: From Epidemiology to Artificial Intelligence. *Ophthalmologica*, *243*(1), 9–20. doi:10.1159/000502387 PMID:31408872

Wong, T. Y., & Sabanayagam, C. (2019). The War on Diabetic Retinopathy. *Asia-Pacific Journal of Ophthalmology*, *8*(6), 448–456. doi:10.1097/APO.0000000000000267 PMID:31789647

Chapter 4

Fully Automatic Epiretinal Membrane Segmentation in OCT Scans Using Convolutional Networks

Mateo Gende
CITIC, INIBIC, Universidade da Coruña, Spain

Joaquim de Moura
iD https://orcid.org/0000-0002-2050-3786
CITIC, INIBIC, Universidade da Coruña, Spain

Jorge Novo
CITIC, INIBIC, Universidade da Coruña, Spain

Marcos Ortega
CITIC, INIBIC, Universidade da Coruña, Spain

ABSTRACT

The epiretinal membrane (ERM) is an ocular pathology that can cause visual distortions. To prevent a loss of vision, symptomatic ERM needs to be removed before it can cause irreversible damage. In order to do this, the ERM needs to be located early, so that it can be peeled from the retina. This chapter explores an automatic methodology for ERM segmentation, as well as its intuitive visualization in the form of colour maps. To do this, visual features that are compatible with ERM presence are extracted from ophthalmologic images by using computer vision algorithms and deep learning models. This methodology achieved satisfactory results, reaching a dice coefficient of 0.826 and a Jaccard index of 0.714, contributing to highlight the applicability of deep learning models for the detection of pathological signs in medical images.

INTRODUCTION

Thanks to recent advances in computation architectures and in the development of new and improved artificial intelligence algorithms, Computer-aided Diagnosis (CAD) systems are becoming increasingly relevant in healthcare services, finding application in fields such as audiometry (Fernández, et al., 2018), radiology (Romeny et al., 1998) or encephalography (Hosny et al., 2018). Among the different domains of application of CAD systems, the analysis of medical images stands out.

Deep learning is a subset of machine learning focused on the development of artificial neural network models that have multiple layers in order to progressively extract higher-level features from data (LeCun et al., 2015). Convolutional neural networks are artificial neural networks that use the convolution operation in order to be able to extract visual features from images (Lecun et al., 1998). Thanks to the advent of deep convolutional neural networks, deep learning models are nowadays used for several tasks in the field of image analysis. These tasks can range from image classification (Krizhevsky et al., 2017), in which images are separated in classes according to their content; to image segmentation (Long et al., 2015), where images are partitioned into multiple segments, or every pixel in their content is labelled; to regression (Lv et al., 2014), where a value or a set of values are extracted from the images. With a focus on healthcare, deep convolutional neural networks have successfully been used to analyze and study anatomical structures as well as pathological signs in medical images of several types (Shen et al., 2017; Litjens et al., 2017). In particular, deep learning-based CAD systems have found uses in medical imaging techniques such as magnetic resonance imaging (Kamnitsas et al., 2017), conventional radiography (Lakhani & Sundaram, 2017), ultrasound (Cheng et al., 2016) or computed tomography scans (Setio et al., 2016). These systems have demonstrated that their performance can be on par with, or even exceed that of human experts in different diagnosis-related tasks (Litjens et al., 2017; Lee et al., 2020; Ting et al., 2017; Gulshan et al., 2016).

In ophthalmology, Optical Coherence Tomography (OCT) is an imaging technique that allows the in-depth visualization of tissue (Huang et al., 1991). By shining a beam of low coherence (high bandwidth) light over the tissue and measuring the differences in phase and amplitude in the reflected beam compared to a reference one, a one-dimensional reading or A-Scan can be acquired at every scanned spot. This A-Scan contains depth-wise information about the reflectivity of the scanned tissue. If this beam is swept through the surface of the tissue, these readings can be combined into a two-dimensional reading or B-Scan (Figure 1). These B-Scans can be visualized as high-resolution images which show a cross-sectional view of the tissue, like a tomogram containing the histological information of the scanned tissue. Furthermore, these B-Scans can be laterally combined to produce a volumetric

representation of the underlying tissue. This makes OCT a remarkably useful technique for the analysis of healthy or pathological ocular structures since these volumes allow the complete histological visualisation of the retinal tissue *in vivo* and in a non-invasive manner. For reference, OCT images can be used for the study of the vascular structure of the eye (Kashani et al., 2017; de Moura et al., 2016, 2017a; Spaide et al., 2018); for the diagnosis of glaucoma (Hood, 2017) (Tan et al., 2009; Jaffe & Caprioli, 2004), which is the most common cause of blindness in the developed world for people over 50; exudative macular disease (de Moura et al., 2017b), one of the most common causes of blindness in the developed world; or that of diabetic macular oedema (Hee, 1995; de Moura et al., 2019, 2020; Mookiah et al., 2013), the leading cause of blindness in patients of diabetes mellitus.

Figure 1. Example of an OCT slice or B-Scan, illustrated over an eye fundus image showcasing its location
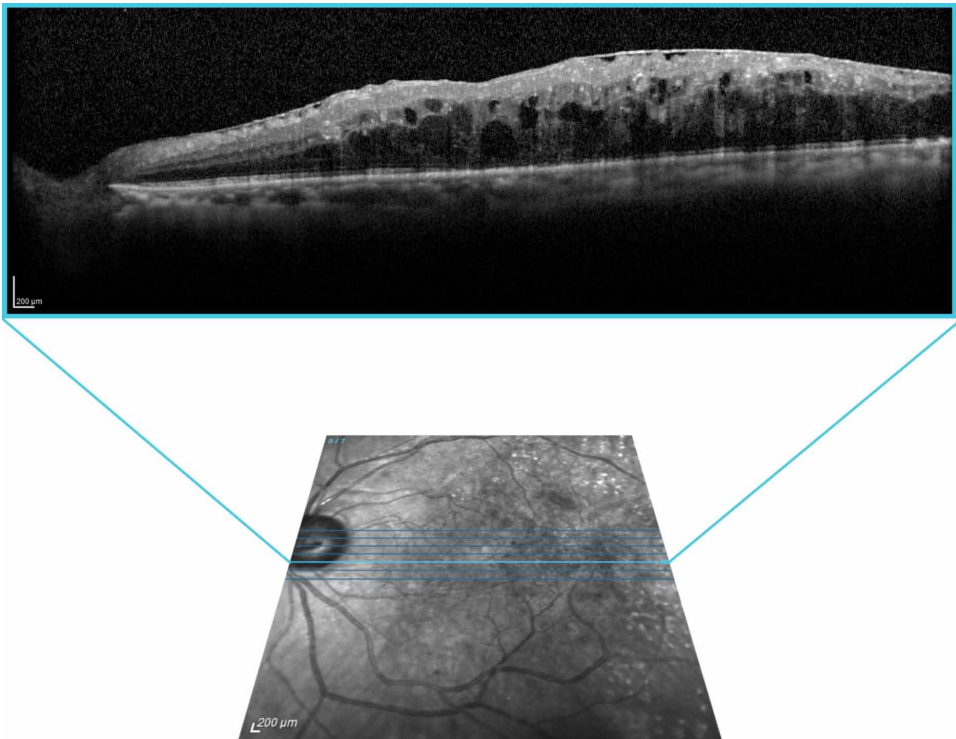
This chapter explores a methodology developed for the automatic detection and segmentation of one such ocular pathology, the Epiretinal Membrane (ERM). The ERM is a thin fibrocellular sheet that may appear over the retina surface. This layer

90

is mostly transparent and can be imagined as a thin film of cellophane stuck to the fundus of the eye. It is known by different names such as cellophane maculopathy, macular pucker, macular fibrosis, or surface wrinkling retinopathy. These names reference the effects that this layer can have over the tissue of the retina. While it is mostly transparent and may not cause any symptoms, the ERM may also start to harden and contract after appearing. This causes mechanical traction over the underlying tissue, which in turn may start to deform and wrinkle the retina. The ERM is typically formed over the boundary between the vitreous body and the retina tissue, this area is known as the Inner Limiting Membrane (ILM). If the ERM is positioned over the retinal macula, these deformations may cause metamorphopsia (Matsumoto et al., 2003), a visual distortion that can manifest itself as a bowing in the centre of the visual field. For example, when observing parallel lines such as in an Amsler grid, these may appear to bow and bend to a patient suffering from metamorphopsia (Figure 2). Additionally, the deformations provoked by the ERM can also cause a thickening of the macular tissue, and in severe cases, the disappearance of the foveal pit. Although it is normally idiopathic, the ERM can also appear as a secondary factor to other related ocular pathologies. Diabetic macular oedema has a high prevalence of related ERM, with studies reporting that between 27 and 34% of oedema patients present ERM (Yamamoto et al., 2001; Ghazi et al.,2007). It can also appear as a response to external trauma to the eye, as a response to surgery or as a posterior complication of vitreous detachment or macular hole, among others. Generally, its appearance is caused by the retraction of the vitreous gel from the macula.

Figure 2. Example of the visual distortions that the metamorphopsia may cause to patients suffering from ERM over an Amsler grid
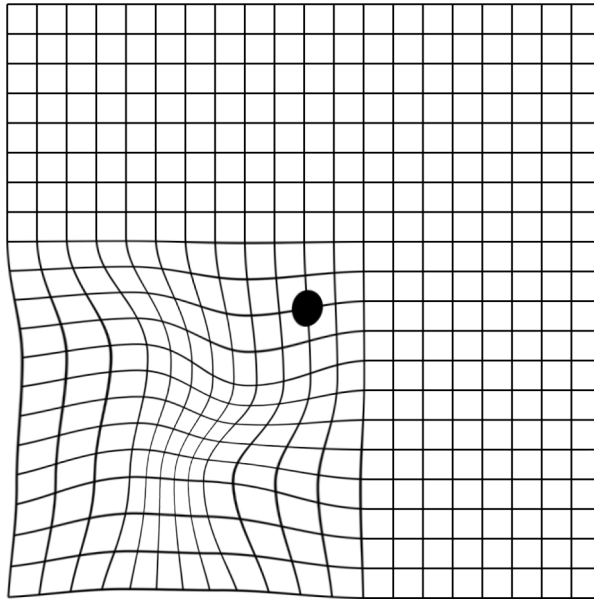
If the ERM is allowed to contract and deform the retina for long, some of the deformations it produces may become permanent. Treatment for symptomatic ERM involves a surgery known as *pars plana* vitrectomy (Suh et al., 2009), where a series of instruments are used to scrape the surface of the retina and peel away the fibrocellular layer. This surgery has higher chances of preserving the vision of the patients if performed early, before the exerted traction can further deform the tissue (Massin et al., 2000; Rahman & Stephenson, 2014), and it requires that the expert determines the extent and location of the ERM. This underscores the relevance of an early and accurate diagnosis of the ERM. Due to its transparency, the ERM is difficult to detect in eye fundus images (Figure 3). Often, only the deformations the ERM causes over the retina are visible in this imaging technique, and even then, only those that are very prominent. In OCT images, however, the ERM appears as a bright layer over the ILM (Figure 4). This imaging modality makes it much easier for the experts to detect and diagnose the ERM, as its high reflectivity facilitates its visualisation. Because of this, ERM diagnosis is usually performed by experts visually inspecting OCT images.

Figure 3. Example of a case of symptomatic ERM in an eye fundus image. Small creases over the tissue can be observed in the highlighted area
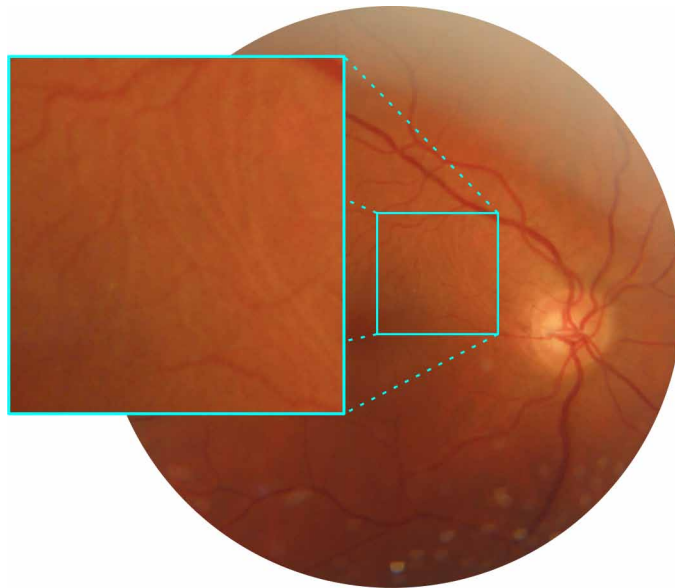
While the ERM is easier to detect in OCT slices, the visual inspection of images with the intention of screening for ERM signs is a time-consuming and inherently subjective process. Furthermore, the ERM is not the only reflective surface that can appear in OCT images, since visual artefacts caused by the forwards and backwards scattering of light can produce noise and bright spots in this image modality, making the visual detection of the ERM in OCT a non-trivial task.

Figure 4. OCT slice displaying the ERM and ERM-related lesions
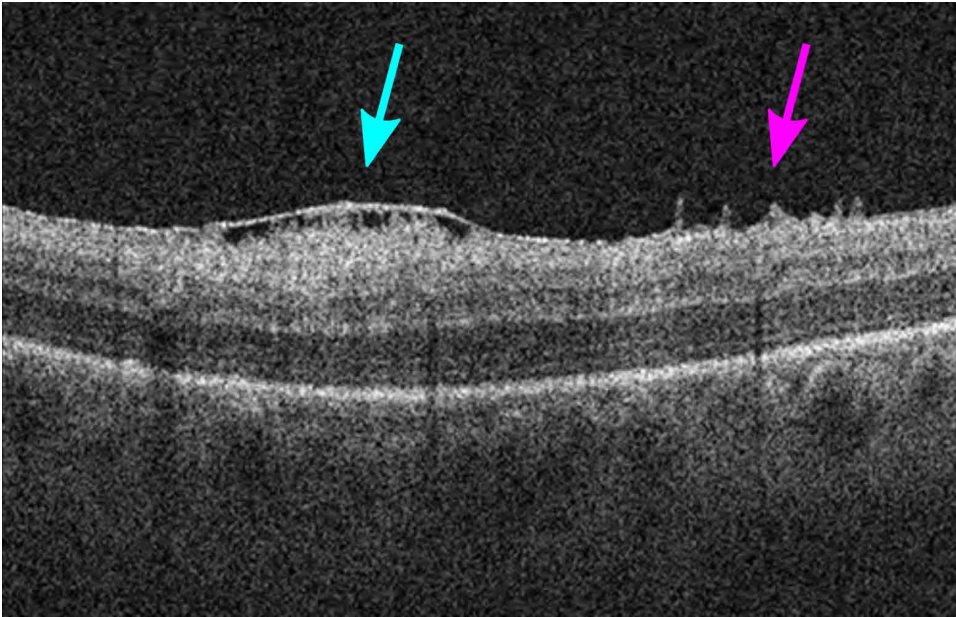
In this chapter, a methodology developed for the automatic segmentation of the ERM in OCT images is explored. The aim of this methodology is to provide the experts with an intuitive visualisation of the ERM presence (or lack thereof) in OCT volumes. To do this, the methodology consists of a series of three steps aimed at the preliminary detection of our Region of Interest (ROI), the segmentation of the ERM and, finally, the generation of intuitive segmentation maps that display the ERM overlaid on a reconstruction of the eye fundus, generated based on the original OCT volumes. These maps are also post-processed to incorporate cross-slice information into the segmentation results, helping minimise the stochastic errors that may be produced by the visual artefacts that are present in OCT images. The complete methodology makes use of different computer vision techniques, as well as deep learning algorithms in order to extract and analyse visual features which are relevant for the detection and diagnosis of the ERM. Moreover, thanks to the use of machine learning models, the segmentation process can be trained directly from annotated images, implicitly learning which visual features are relevant for the task at hand. This greatly simplifies the development process of CAD systems making use of this methodology.

The layout of this chapter is as follows: The Background section introduces how other works in the literature have approached the problem of the diagnosis of this pathology. The Epiretinal Membrane Segmentation section explains how each

94

of the steps that comprise this methodology are performed, the data that was used for its development, the deep learning model training details and the results that were obtained from evaluating the methodology. Solutions and Recommendations covers some of the solutions that were designed for the issues that arose during the development of this methodology. Future Research Directions indicates the different approaches that may be taken to further advance in the detection of this pathology. Finally, in Conclusion, the main ideas exposed in this chapter are summed up.

BACKGROUND

Due to the relevance of a disease such as the ERM, various works have addressed the challenge presented by its detection as an opportunity for the application of CAD systems that can aid in its diagnosis. This section shares an overview of how different works in the literature have approached the problem of detecting the ERM in medical imaging, a brief description of each one, as well as a summary of the advantages they may provide to the field of study and the shortcomings they might suffer from.

In the beginning, works such as the proposal by Wilkins *et al.* (1996) offered semi-automatic approaches for ERM diagnosis. These, however, relied on an initial manual annotation made by the expert indicating the location of the ERM in order to measure the macular thickening that it caused and assess the ERM.

Later works have introduced automatic methods, aiming to overcome the reliance on an initial expert annotation. As reference, Lu *et al.* (2018) used deep learning models for the detection of different pathologies, the ERM being one of them. A convolutional neural network was trained to classify images according to which of the four considered pathologies was present. The results obtained by this convolutional model were compared to those produced by two experts on the same task. These results showed that the system achieved a performance that was competitive with or better than that of human experts. In the work by Fang *et al.* (2017), the authors propose the detection of multiple macular lesions in OCT images. Among these lesions, the ERM was also considered. In order to perform this detection, a conventional feature extraction process was performed in segmented regions of interest. Using a machine learning-based system, these regions were then classified into the different macular lesions. Kuwayama *et al.* (2019) also proposed a system based on the classification of OCT slices. In a similar manner to the work by Lu *et al.*, the authors used a convolutional neural network for the classification into four different pathologies, achieving competitive results.

Sonobe *et al.* (2018) presented a study in which they compare the performance of support vector machines and deep learning models at detecting ERM cases in OCT

volumes. Images from the surface of the eye fundus, obtained from the software provided by the OCT scanner were used as input and a classification was performed by making use of the two proposed approaches. The results achieved by the deep learning model were higher than those obtained by the support vector machine approach. More recently, Lo *et al.* (2020) used a residual neural network architecture to screen for ERM in OCT images. Non-retinal specialised ophthalmologists were asked to participate in a test where their results were compared to those achieved by the residual neural network. In this comparison, the deep learning models performed slightly better than the ophthalmologists. More recently, Parra-Mora *et al.* (2021) described the use of four Deep learning-based classification architectures for the screening of the ERM. In the results, the authors claim a high discriminative performance by the deep learning models at classifying between OCT slices that displayed healthy eyes and slices showing ERM presence.

The results that were obtained in these works collectively show the potential that deep learning models possess for the screening of the ERM. These models have been proven to achieve a performance that can be on par with human experts and, in some cases, even exceed that of certified specialists. Additionally, comparisons between classical machine learning-based approaches that use conventional feature extraction and selection and deep learning models have shown that the latter may have the upper hand in terms of results. All of the previously mentioned approaches are based on the classification of OCT slices into whether they show healthy tissue or if signs compatible with the ERM are visible in the images. Furthermore, many of these proposals are focused on the screening of several pathologies, the ERM just being one of those considered and hardly the main focal point of these works.

Conversely, the works by Baamonde *et al.* (2017a, 2017b, 2019a) showcase a series of methods for the characterization of the ERM tissue in OCT images. These studies are completely focused on the detection of this pathology by means of different approaches such as local luminosity patterns or hand-crafted visual features. Moreover, in (Baamonde, et al., 2019b), the authors present the first approach for the segmentation of the ERM. This segmentation is done by means of the classification of patches. From every patch, the authors extracted a set of 452 conventional visual features, grey-level co-occurrence matrices, Gabor features, local binary patterns, Laws features) to intensity-based (intensity global features, grey-level intensity histograms, histograms of oriented gradients), as well as a set of domain-specific hand-crafted features. From this set of original features, the authors used the Spatial Uniform ReliefF algorithm to select the ones that contributed the most to the classification process. Finally, they provide a comparison between using random forests, k-nearest neighbours, and support vector machines for the classifications of different sets of selected features.

In this chapter, a refinement of the ERM segmentation methodology proposed by Baamonde *et al.* is explained (Gende et al., 2021). This methodology is refined by incorporating deep learning models into the classification process and providing an intuitive visualisation of the diseased tissue over a projection of the eye fundus.

EPIRETINAL MEMBRANE SEGMENTATION

This section explains the step-by-step process in which the presented methodology for the ERM segmentation in OCT images is subdivided. A visual summary of this methodology can be found in Figure 5. As previously mentioned, this segmentation methodology consists of a set of three steps, namely: the segmentation of the ROI, the classification of image patches and the final reconstruction of the intuitive representation. These will be explained in detail in the following subsections, as well as the data that was used to develop and test this methodology and the details of the neural network model training process.

Figure 5. Graphical summary of the methodology that is explored in this chapter. The original OCT volume is first subdivided into 2-dimensional B-Scans. Then, the ROI is segmented, and a series of windows centred on the ILM are extracted. These windows are classified by a convolutional neural network. Based on this classification, the segmentation map is reconstructed and postprocessed. A reconstruction of the eye fundus can be generated from the OCT volume. In parallel, this reconstruction and the segmentation map are overlaid to create the intuitive visualisation of ERM presence over the eye fundus.
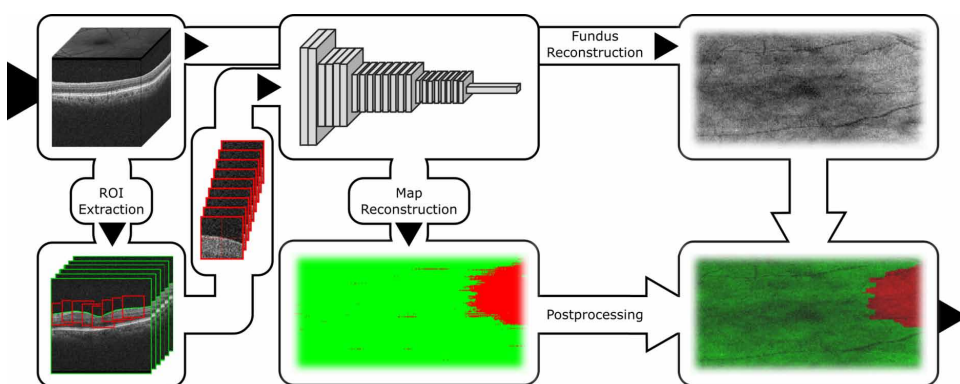
Region of Interest Segmentation

The first step is to segment the ROI location. In order to narrow down the area in which to look for the ERM, the boundary in which the ERM may appear if present must first be detected. This region is known as the Inner Limiting Membrane. Fortunately, due to the transparency of the vitreous body, the ILM is easy to detect in OCT slices. In these images, the retinal tissue is visible as are its internal structures, while the vitreous body appears as a slightly noisy background. This conveniently simplifies the task of detecting the position of the ILM.

Since the ILM appears as a continuous horizontal layer in these images, its position can be modelled as a height value. That is, for every image column in any OCT slice, there will be a pixel in which the ILM will begin. Thanks to this continuity, it is possible to convert this segmentation problem into a problem of determining the height of the ILM in every image column, which is much simpler.

To take advantage of the contrast that the ILM possesses in OCT images and the fact that the ILM can be modelled as a height value for every vertical column of pixels, active contour models can be used to segment the ROI (Gawlik et al., 2018). Active contour models, or snakes, are a computer vision framework used for determining the outlines of objects in images. One of the advantages of this framework is its robustness to noise. An active contour model can be defined as a set of n points v_i for $i=0,\ldots,n-1$. The contour model is moderated by a set of two energies: $E_{external}$, the external energy which pulls the contour outwards toward the edges that are visible in the image and $E_{internal}$, the internal energy which elastically contracts the contour in order to preserve a smooth curve. Thus, the energy function of the snake can be described by Equation 1.

$$E^{*}_{snake} = \int_0^1 E_{snake}\left(\boldsymbol{v}\left(s\right)\right)ds = \int_0^1 E_{internal}\left(\boldsymbol{v}\left(s\right)\right) + E_{external}\left(\boldsymbol{v}\left(s\right)\right)ds \tag{1}$$

$E_{external}$ draws the snake towards visible edges in the image. It measures how well the curve matches image data. it can be described by Equation 2:

$$E_{external}(v) = -|G_y(v)|^2 \tag{2}$$

where G_y is the gradient in the y-axis. This makes it so that the active contour adjusts itself to edges in the image. Since the ILM describes an approximately horizontal line, only those pixels that possess the highest gradient in the y-axis are of interest.

On the other hand, $E_{internal}$ (Equation 3) reflects curve tension and curvature. Minimising the internal energy favours smooth, continuous curves.

$$E_{internal}\left(\boldsymbol{v}\right) = E_{continuity}\left(\boldsymbol{v}\right) + E_{curvature}\left(\boldsymbol{v}\right)$$

$$E_{continuity}\left(\boldsymbol{v}\right) = \frac{1}{2}\left(\alpha\left(s\right)\left|\boldsymbol{v}_s\left(s\right)\right|^2\right) = \frac{1}{2}\left(\alpha\left(s\right)\left\|\frac{\partial\overline{\boldsymbol{v}}}{\partial s}\left(s\right)\right\|^2\right) \tag{3}$$

$$E_{curvature}\left(\boldsymbol{v}\right) = \frac{1}{2}\left(\beta\left(s\right)\left|\boldsymbol{v}_{ss}\left(s\right)\right|^2\right) = \frac{1}{2}\left(\beta\left(s\right)\left\|\frac{\partial^2\overline{\boldsymbol{v}}}{\partial s^2}\left(s\right)\right\|^2\right)$$

where $\alpha(s)$ and $\beta(s)$ are weights which control the sensitivity of the internal energy. $\alpha(s)$ penalises the separation between points in the contour. $\beta(s)$ penalises oscillations between the positions of consecutive points, preserving curve smoothness.

OCT images generally present speckle noise due to the effects of light back-scattering (Samagaio et al., 2017). This noise can cause the active contours to fixate on bright spots that don't correspond to the real ILM location. In order to get rid of this noise, each original OCT slice is first pre-processed using a median filter. This filter assigns the median of the surrounding neighbours to each pixel. This way, the effects of isolated bright pixels can be minimised. To obtain the horizontal filters, a convolution using a y-axis Sobel filter is applied. This pre-processing stage can be visualised in Figure 6.

Figure 6. Initial pre-processing of an OCT slice prior to ILM segmentation. The image is filtered in order to remove noise and a Sobel operator in the y-axis is applied. This way the ILM can be highlighted over the fundus.
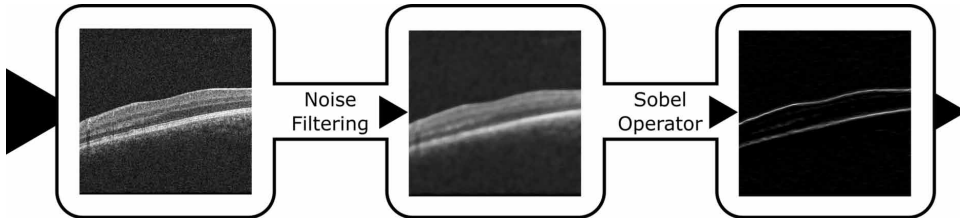
Once an image highlighting the horizontal edges in the original OCT slice has been obtained, the active contour can be adjusted. As previously indicated, since only the horizontal edge of the ILM is of relevance for this task, the active contour is initialised to the top of the image, with a contour point for every image column. These are allowed to iteratively move in the vertical axis, minimising the aforementioned internal and external energies until convergence. Once the active contour has settled over the ILM surface, its vertical position for every image column can be obtained,

effectively producing the segmentation of this layer. At this point, to proceed with the segmentation of the ERM, each ILM pixel will have to be classified into whether it is positioned over healthy or diseased tissue. Since a single pixel does not contain sufficient information about whether the tissue point it displays is diseased or not, a standard image window must first be extracted around each of these pixels. These windows contain the visual information surrounding the ILM pixel that is necessary for its correct classification. A summary of this process of window extraction can be visualised in Figure 7.

Figure 7. ILM segmentation. The active contour is allowed to contract downward until it converges on the ILM surface. Once the position of the ILM is determined, a window is extracted around each ILM pixel. These are to be classified on the next step.
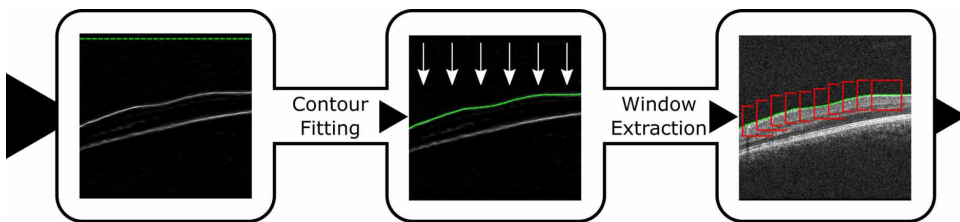
Window Classification

Once the region of interest has been segmented and the windows around each pixel of the ILM have been extracted, the second step is the classification of each of these windows according to whether they are centred around pathological or healthy tissue. The classification of these images can be accomplished by employing a convolutional neural network. These deep learning models can use the convolution operation (Figure 8) in order to make use of the visual information contained in images as features. These models are able to learn a number of convolutional filters that can extract visual features from the images. The progressive stacking of these convolutional filters in depth yields gradually higher-level features. This ability to learn high-level visual representations of information directly from images enables deep learning models to perform a variety of computer vision tasks.

Figure 8. Convolution operation. A convolution filter is applied centred on every image element. The values of the image and the filter are multiplied and gathered in order to obtain the resulting value at each point.
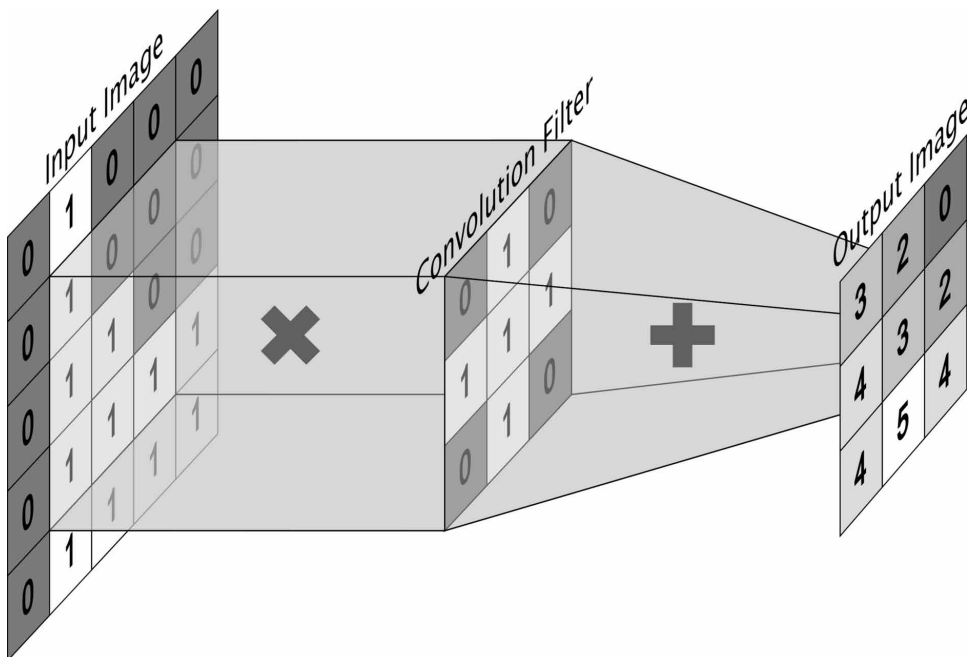
To classify the image windows, Densely Connected Convolutional Neural Networks can be employed (Huang et al., 2017). These deep learning models use dense blocks and the progressive concatenation of lower-level features in order to propagate these further into the architecture. This aids to mitigate the vanishing gradient problem by allowing it to flow directly from the layer closest to the loss to the early ones. This way, the layers close to the original data can be updated more efficiently than in a conventional convolutional neural network. From among the different DenseNet variants, a DenseNet-121 was used for the methodology described in this chapter. A schematic representation of this architecture can be found in Figure 9.

Figure 9. Basic structure of a DenseNet-121 model, detailing the composition of the dense blocks, their dense layers, and the progressive concatenation of visual features
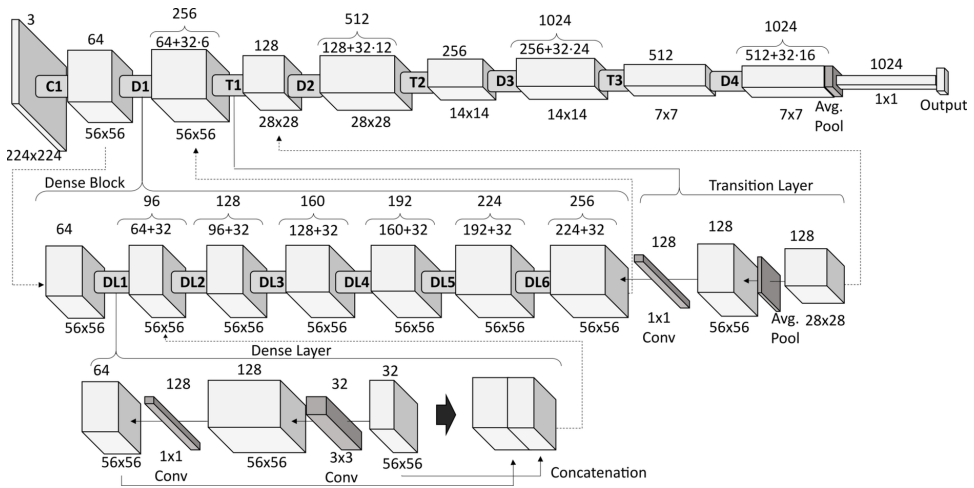
The labels that result from each window classification can be assigned to the original central pixels around which the image windows were extracted. This way, by combining the location of the ILM with its classification into healthy or diseased tissue, a segmentation of the ERM can be effectively produced (Figure 10).

Figure 10. Second step of ERM segmentation. The windows that were extracted in the previous step are classified into healthy or pathological. The resulting labels are assigned to the original pixels around which the windows were extracted.
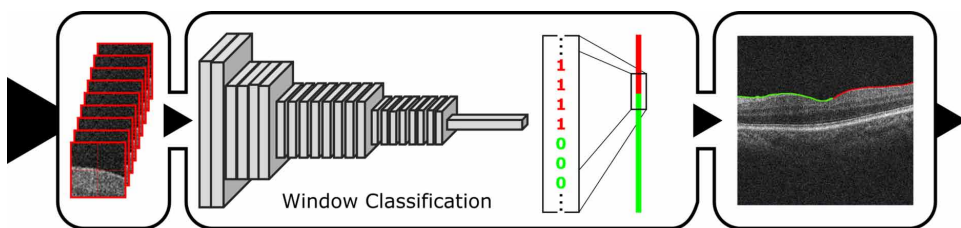
INTUITIVE MAP RECONSTRUCTION

The third and final step is the reconstruction and post-processing of the segmentation maps. In order to provide the experts with an intuitive visualisation of the results, these are reconstructed in the form of a colour map indicating ERM presence or absence overlaid over a representation of the eye fundus. This way, the zone that is

102

affected by the ERM can be easily interpreted, bypassing the need to observe each of the OCT slices.

For this reconstruction, the information contained in the 3D OCT volumes is leveraged by taking advantage of the consecutive organisation of the 2D OCT slices. These advantages are harnessed in two ways. First, since each OCT tomogram represents a parallel slice of the analysed section of the eye fundus, there is a structural relation between the information contained in consecutive slices. This information can be used to further refine the ERM segmentation by providing a consensus of the classifications of the surrounding boundary points. This way, each image pixel contributes not only to the classification of the spot where it is located and the surrounding pixels in the same slice, but also to the classifications of pixels in the surrounding slices, adding an additional cross-slice dimension through which visual information can be integrated in the segmentation process. This helps to correct spurious misclassifications that may occur due to lighting differences in consecutive slices and softens the segmented boundary region. Second, due to the organisation of the 2D OCT slices, the visual information contained in each of them can be combined in order to recreate a visualisation of the analysed retina section. This visualisation allows for the information contained in the whole cube to be summed up in order to provide a quick analysis and reference of the location of the analysed tissue. This way, the segmentation results and the equivalent location in the eye fundus can be viewed at a glance in the form of colour maps.

To obtain these maps, the one-dimensional classification tag arrays of every slice are laterally stacked together according to their original location. This creates a two-dimensional spatial representation of the classification of every original image column, which can be interpreted as an overview of the eye fundus. In these images, green represents an ILM spot that was classified as healthy, while red represents a diseased one.

Since every image patch was isolated from its context, some outlying pixels classified as ERM can appear. These are mainly caused by a few misclassifications produced by image artefacts and reflections in the original OCT images. In order to correct these, and with the aim to produce a visualisation that better represents the appearance that the ERM has over the eye fundus, a post-processing step is applied. This step incorporates into the classification of every pixel the information contained in the classification of its surrounding neighbours. Additionally, it aims to preserve the softer boundaries that the ERM actually presents.

Figure 11. Third step of ERM segmentation. The 1D classification arrays are converted to colour pixels are stacked in the original order. The resulting segmentation maps are then post-processed in order to filter spurious pixels and produce a regular boundary.
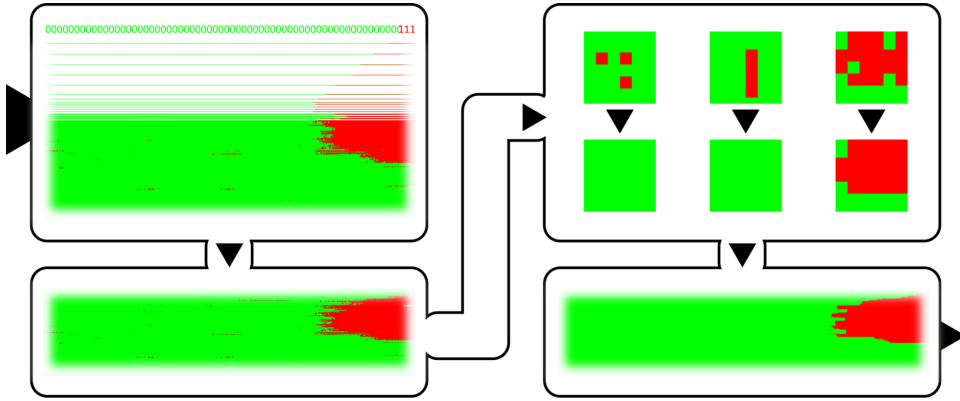
This post-processing step consists of the filtering of any ERM-classified contour under a certain size threshold and morphological filtering. Expert knowledge determines that isolated ERM patches of a very small size are extremely unlikely. Because of this, the first step of this post-processing stage is to filter out any isolated ERM-classified contour under 25 pixels in size. Furthermore, in order to correct spurious misclassifications and preserve the regularity of the boundary region, a morphological opening is performed on the segmentation map using a 10×4 pixel horizontal rectangle as structuring element. This operation is described by Equation 4, where A_b denotes the translation of A by b. Since consecutive OCT slices may show differences in reflectivity, incorporating cross-slice information via this morphological filtering helps preserve boundary regularity. This results in an image where the isolated ERM pixels are filtered out and with a continuous boundary region. The complete reconstruction and the post-processing stage are summed up in Figure 11.

$$A \circ B = \left(A \ominus B \right) \oplus B$$
$$A \ominus B = \bigcap_{b \in B} A_{-b} \qquad\qquad (4)$$
$$A \oplus B = \bigcup_{b \in B} A_b$$

104

Finally, in order to provide a reference for this map, a representation of the eye fundus is created from the original OCT volume. This representation is created by averaging every image column in the volume. That is, for every slice in the volume, the average value of the pixels in every column is calculated. This value is translated into a pixel brightness value, which can be combined with its neighbours in an orderly manner, in the same way in which the segmentation map is reconstructed. The resulting two-dimensional image shows a representation of the fundus of the eye, allowing a visualisation of the foveal pit, the vascular structure of the eye and any relevant deformations that may be present in the retina (Figure 12). By overlaying the segmentation colour map over the eye fundus reconstruction, the final intuitive visualisation of the ERM is produced.

Figure 12. Reconstruction of the eye fundus representation to be used as reference. The average brightness value of each image column of every OCT slice contained in the original volume is calculated. These values are then combined to produce a 2D image representing the retina of the eye.
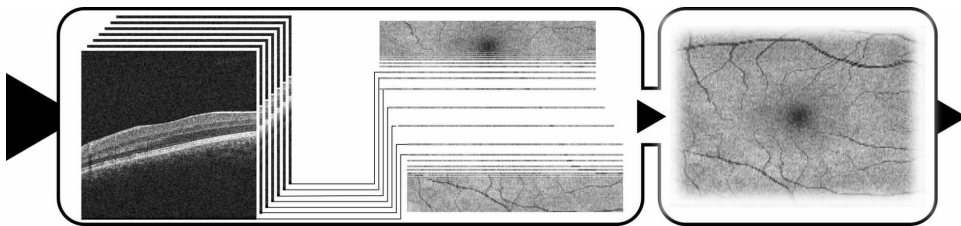
Dataset

The methodology presented in this chapter was comprehensively validated with a representative dataset. Specifically, this dataset consisted of 20 OCT volumes obtained from different patients. Each of these volumes represents an eye. Out of the 20 eyes, 12 belonged to healthy patients, while 8 displayed signs of ERM. These volumes contained a total of 2428 2D OCT slices, with 1,536 belonging to healthy eyes and 892 to eyes with ERM. The platform used to produce these images was a CIRRUS ™ HD-OCT Carl Zeiss Meditec confocal scanning laser ophthalmoscope. These images were obtained in accordance with the Declaration of Helsinki, as approved by the Ethics Committee of Investigation from A Coruña/ Ferrol (2014/437) the 24th of November 2014. All of the images showing ERM signs were manually annotated by an expert indicating the location of the diseased tissue, which served as the dataset ground truth. This dataset was partitioned using a 4-fold cross-validation, with each fold being divided into three sets, using 50% of

105

the eyes for training, 25% for validation and the remaining 25% for test. In order to preserve a balance between ERM-positive and negative cases, as well as to avoid oversampling the training set, 40 equispaced windows were extracted from every slice belonging to diseased eyes, and 8 from every slice taken from a healthy eye. This resulted in a total of 21,667 pathological samples and 27,536 healthy samples. These were used to train and validate this methodology, ensuring each eye appears in a testing set once.

Training Details

The DenseNet-121 models were trained on the available dataset following the 4-fold cross-validation. This way, 4 models were trained on their corresponding training sets. The training process was allowed to run for a maximum of 100 epochs, selecting the epoch that produced the smallest loss on its corresponding validation set for testing. Cross-entropy loss was used for training, while Adaptive Moment Estimation (Adam) was used for optimisation, with a learning rate of 1×10^{-5}, $\beta 1 = 0.9$ and $\beta 2 = 0.999$. The 112×112 pixel windows extracted from the images were resized to a standard 224×224 resolution. Furthermore, in order to take a better advantage of the available data, online augmentation was used on the training samples, combining random horizontal flipping, random vertical and horizontal shearing between -15° and 15° as well as random rotation of the windows between -15° and 15° (Figure 13). The borders of the images were reflected with the intention to preserve image continuity after the augmentation.

Figure 13. Example of different augmented variations of the same spot showing signs of ERM
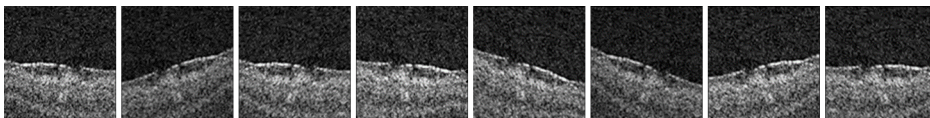
RESULTS AND DISCUSSION

This methodology achieved generally favourable results, both in terms of the classification of image patches and the segmentation of the ERM in the images as a whole. In this sense, this methodology can provide an accurate and robust diagnosis of this pathology. In this section, the results that were obtained by making use of the presented methodology are described and discussed. These results correspond to those produced by the convolutional neural networks when trained and cross-

validated on the previously described dataset. Commonly reported metrics for similar image segmentation tasks such as the Accuracy (Equation 5), Sensitivity or Recall (Equation 6), Specificity (Equation 7), Sørensen-Dice Coefficient (Equation 8) and Jaccard Index (Equation 9) were used.

$$Accuracy = \frac{TP + TN}{TP + TN + FP + FN} \tag{5}$$

$$Sensitivity = Recall = \frac{TP}{TP + FN} \tag{6}$$

$$Specificity = \frac{TN}{TN + FP} \tag{7}$$

$$Dice = \frac{2 \times TP}{2 \times TP + FP + FN} \tag{8}$$

$$Jaccard = \frac{TP}{TP + FP + FN} \tag{9}$$

Figure 14. Accuracy, Precision and Recall of the samples contained in the test sets and by extracting a window around every ILM pixel of the images in this set
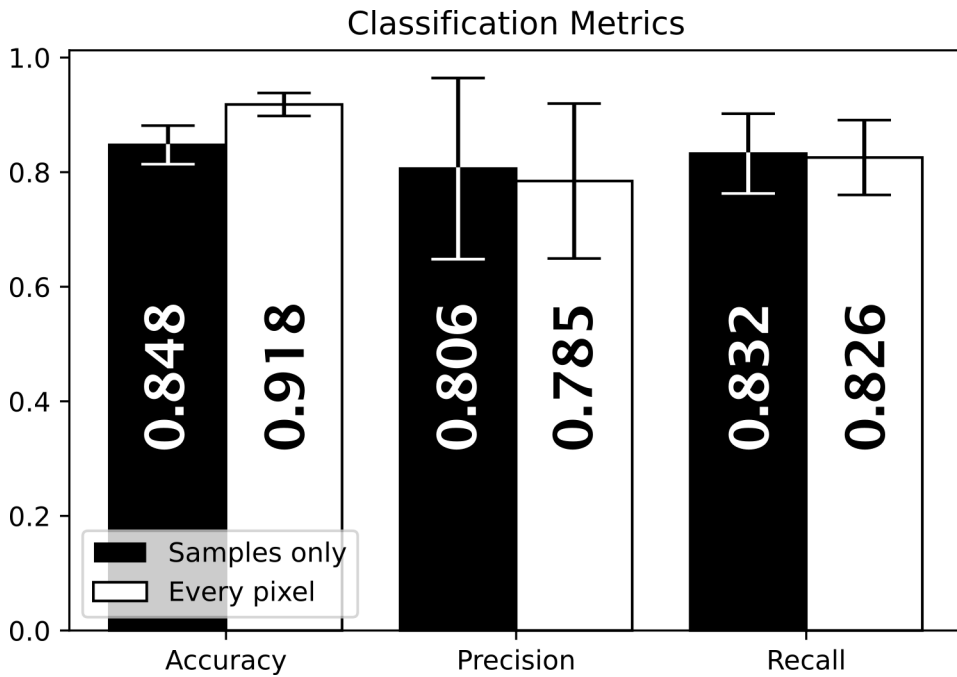
In terms of the classification of the image windows, Figure 14 shows the results that were obtained by every model classifying the window samples contained in the test set. This figure also displays the results obtained from the classification of every window extracted from every pixel contained in the volumes included in the test sets, analogously to how this model would perform when analysing an OCT volume. Respecting the segmentation maps of the ERM, Figure 15 illustrates the Receiver Operating Characteristic as well as the Precision Recall curves described by the models. The Dice Coefficient and the Jaccard Index before and after applying the post-processing stage can be found in Figure 16.

Figure 15. Receiver Operating Characteristic (left) and Precision Recall (right) curves corresponding to the results of the proposed methodology
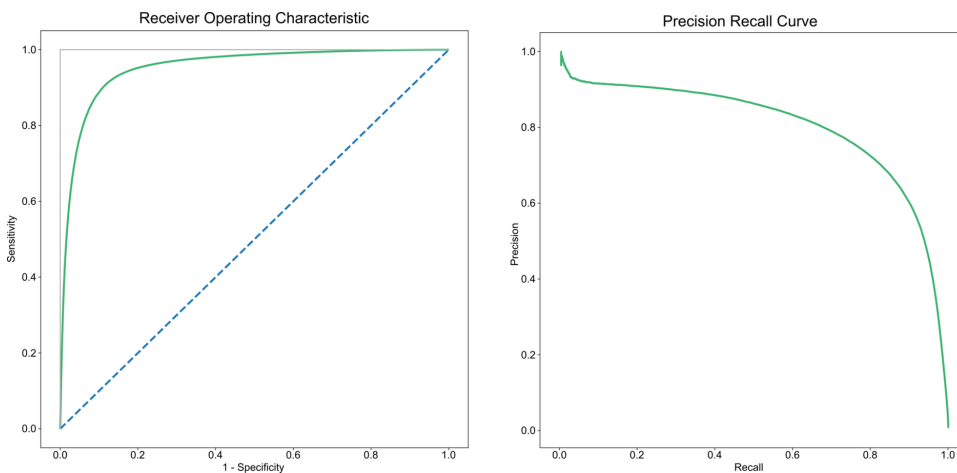
These results show that this methodology can provide a robust and objective segmentation of the ERM in OCT images. By making use of deep learning models, the visual features that are visible at different scales in the images can be used for an accurate characterisation of the ERM. Furthermore, by incorporating the information contained in the surrounding slices into the classification results, these can be refined. Thanks to this post-processing stage, it is possible to achieve better results and provide a segmentation that preserves the actual appearance of the ERM over the eye fundus. The resulting colour maps overlaid over the eye fundus reference have the potential to simplify the analysis process and provide an intuitive diagnosis of this disease.

Figure 16. Dice Coefficient and Jaccard Index corresponding to the segmentation maps before and after the application of the post-processing stage

Segmentation Metrics

Before post-processing (black bars): Dice Coefficient 0.800, Jaccard Index 0.676
After post-processing (white bars): Dice Coefficient 0.826, Jaccard Index 0.714
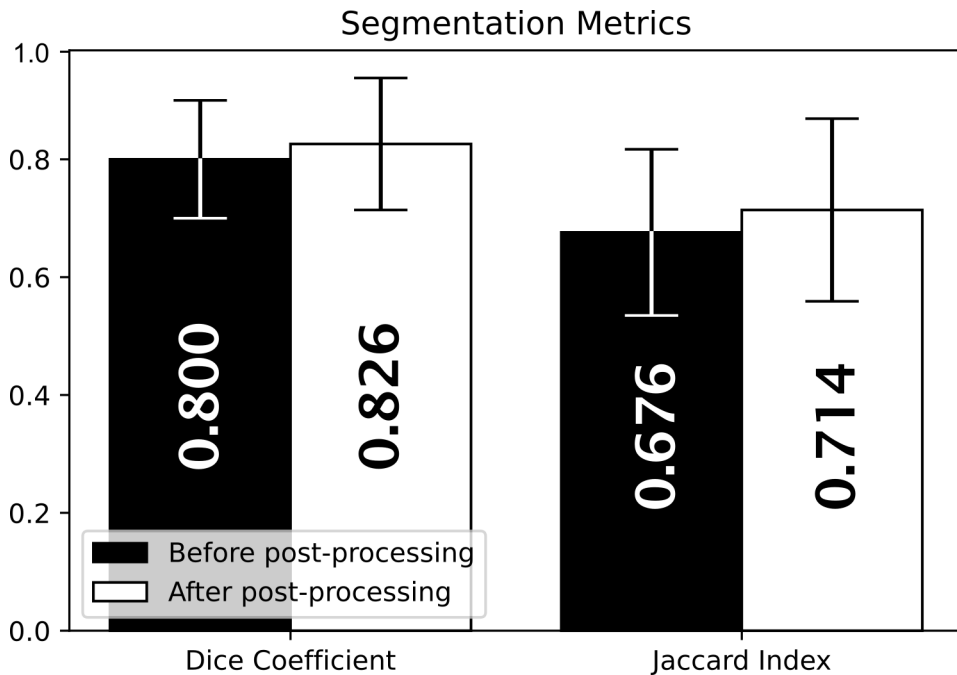
SOLUTIONS AND RECOMMENDATIONS

During the development process of this methodology, the authors identified a number of possible issues and proposed a series of solutions. For the problem of determining the balance between the positive and the negative samples in the dataset, preliminary testing was performed. In this testing, different sampling conditions were compared, with the best results being obtained with the strategy that was described. This strategy consisted in sampling 40 equispaced windows from every image belonging to a pathological eye and 8 from every image in a healthy eye. This relation between samples was chosen in order to preserve a balance between the classes, since the healthy eyes are more numerous and do not contain diseased tissue while the diseased ones are fewer and do contain healthy tissue. Moreover, by using this sampling strategy, there is already a consistent overlap between consecutive windows. Increasing the number of samples extracted from the images further would provide little to no benefit at the risk of overrepresenting the visual information that was already sampled.

The post-processing stage was incorporated to the methodology partially as a solution to the problem of isolated bright pixels caused by image artefacts being

110

misclassified as ERM-positive spots. Furthermore, there are some differences in lighting and overall image quality between consecutive slices, which can lead to irregular boundary regions when only the information that is contained in a single slice is used to classify ILM pixels. By filtering out the small, isolated spots which are not adjacent to any ERM region and by using morphological filtering to incorporate cross-slice information into the classification of every ILM pixel, these problems can be corrected, resulting in a more uniform segmentation map without isolated ERM-positive pixels and with a more regular boundary between ERM and healthy regions.

FUTURE RESEARCH DIRECTIONS

Future work dedicated to address ERM diagnosis could focus on leveraging the information contained in OCT volumes. This chapter exposed the advantages of combining cross-slice information into the segmentation of each ILM spot. These advantages could be further exploited in the form of three-dimensional analysis by employing 3D convolutional models for the detection of this pathology. This way, the convolutional models can better integrate more of the surrounding slice information into classifying each of the ILM pixels.

Moreover, this methodology could be simplified significantly by training models to perform the automatic segmentation of the ERM tissue. It may be possible to train convolutional neural networks to return segmentation masks directly from the data, bypassing the series of steps described in this chapter and the over reliance on the ILM segmentation pre-processing stage.

Furthermore, the problem of automatically assessing the different stages of ERM and its severity remains to be addressed. By performing a multiclass classification of each segmented ERM pixel into the stages the ERM may present, a more complete evaluation of this relevant eye disease can be produced. In order to achieve many of the tasks that are proposed here, a more comprehensive annotated dataset focused entirely on the segmentation of the ERM may be required.

CONCLUSION

This chapter explores a detailed explanation of a fully automatic methodology for the segmentation of the ERM in OCT images. This methodology takes advantage of computer vision techniques and makes use of state-of-the-art deep learning models in order to provide an accurate and objective detection of the visual features that characterise this disease.

The first step in the proposed methodology is to limit the area that is to be analysed to only that which is susceptible to ERM apparition. To do this, the ILM region is segmented from the images by using active contours. This region is modelled as a height value for every image column, since the ILM appears as a mostly horizontal boundary line in the OCT slices. Due to its horizontality, the ILM region can be highlighted using border detection techniques such as a convolution using the y-axis Sobel operator. The active contour is then allowed to contract downward from the top of the image, eventually converging over the ILM location.

At this point, an image window is extracted around every segmented ILM pixel. These windows are then classified by a DenseNet-121 architecture. This deep learning model returns a label determining whether each image displays healthy or ERM-related tissue. These labels are then assigned to the original ILM pixels, marking whether they should be considered healthy or diseased tissue. This way, an effective segmentation of the ERM can be produced by means of a classification of windows.

The arrays containing the labels of each OCT slice segmentation are then combined with those of the consecutive slices. This produces a two-dimensional segmentation map which shows the ERM presence in an overhead view. In order to further refine these maps, a post-processing stage based on expert clinical knowledge is applied. After this post-processing stage, the maps display a uniform ERM region, according to its real appearance. This post-processing stage also contributes to improve the results, since it filters out many misclassifications that may occur due to image artefacts.

Finally, an overhead visualisation of the eye fundus is generated based on the original OCT volume. This visualisation is synthesised by calculating the average brightness value of every image column in the set. This visualisation clearly displays the foveal pit as well as the vascular structure of the retina and any irregularities that may be present. This representation serves as a reference with which to interpret the ERM segmentation maps. As a final step, these two images are overlaid in order to present the segmentation results in an intuitive and simple manner, helping provide robustness and objectivity to the diagnosis of this relevant pathology.

ACKNOWLEDGMENT

REFERENCES

Baamonde, S., de Moura, J., Novo, J., Charlón, P., & Ortega, M. (2019a). Automatic identification and characterization of the epiretinal membrane in OCT images. *Biomedical Optics Express*, *10*(8), 4018. doi:10.1364/BOE.10.004018 PMID:31452992

Baamonde, S., de Moura, J., Novo, J., Charlón, P., & Ortega, M. (2019b). Automatic Identification and Intuitive Map Representation of the Epiretinal Membrane Presence in 3D OCT Volumes. *Sensors (Basel)*, *19*(23), 5269. doi:10.339019235269 PMID:31795480

Baamonde, S., de Moura, J., Novo, J., & Ortega, M. (2017a). Automatic Detection of Epiretinal Membrane in OCT Images by Means of Local Luminosity Patterns. In I. Rojas, G. Joya, & A. Catala (Eds.), *Advances in Computational Intelligence* (pp. 222–235). Springer International Publishing. doi:10.1007/978-3-319-59153-7_20

Baamonde, S., de Moura, J., Novo, J., Rouco, J., & Ortega, M. (2017b). Feature Definition and Selection for Epiretinal Membrane Characterization in Optical Coherence Tomography Images. In *Image Analysis and Processing - ICIAP 2017* (pp. 456–466). Springer International Publishing. doi:10.1007/978-3-319-68548-9_42

Borrelli, E., Sarraf, D., Freund, K. B., & Sadda, S. R. (2018, November). OCT angiography and evaluation of the choroid and choroidal vascular disorders. *Progress in Retinal and Eye Research*, *67*, 30–55. doi:10.1016/j.preteyeres.2018.07.002 PMID:30059755

Cheng, J.-Z., Ni, D., Chou, Y.-H., Qin, J., Tiu, C.-M., Chang, Y.-C., Huang, C.-S., Shen, D., & Chen, C.-M. (2016, April). Computer-Aided Diagnosis with Deep Learning Architecture: Applications to Breast Lesions in US Images and Pulmonary Nodules in CT Scans. *Scientific Reports*, *6*(1), 24454. Advance online publication. doi:10.1038rep24454 PMID:27079888

de Moura, J., Novo, J., & Ortega, M. (2019). Deep Feature Analysis in a Transfer Learning-based Approach for the Automatic Identification of Diabetic Macular Edema. In *2019 International Joint Conference on Neural Networks (IJCNN)* (pp. 1-8). Institute of Electrical and Electronics Engineer. 10.1109/IJCNN.2019.8852196

de Moura, J., Novo, J., Ortega, M., & Charlón, P. (2016). 3D retinal vessel tree segmentation and reconstruction with OCT images. In *Image Analysis and Recognition* (pp. 716–726). Lecture Notes in Computer Science. Springer. doi:10.1007/978-3-319-41501-7_80

de Moura, J., Novo, J., Rouco, J., Penedo, M. G., & Ortega, M. (2017). *Automatic detection of blood vessels in retinal OCT images*. International Work-Conference on the Interplay Between Natural and Artificial Computation. doi:10.1007/978-3-319-59773-7_1

de Moura, J., Samagaio, G., Novo, J., Almuina, P., Fernández, M. I., & Ortega, M. (2020, June). Joint Diabetic Macular Edema Segmentation and Characterization in OCT Images. *Journal of Digital Imaging*, *33*(5), 1335–1351. doi:10.100710278-020-00360-y PMID:32562127

de Moura, J., Vidal, P. L., Novo, J., Rouco, J., & Ortega, M. (2017). Feature definition, analysis and selection for cystoid region characterization in Optical Coherence Tomography. In *Knowledge-Based and Intelligent Information & Engineering Systems: Proceedings of the 21st International Conference* (pp. 1369-1377). Elsevier. 10.1016/j.procs.2017.08.043

Doi, K. (2007, June). Computer-aided diagnosis in medical imaging: Historical review, current status and future potential. *Computerized Medical Imaging and Graphics*, *31*(4-5), 198–211. doi:10.1016/j.compmedimag.2007.02.002 PMID:17349778

Fang, L., Yang, L., Li, S., Rabbani, H., Liu, Z., Peng, Q., & Chen, X. (2017, June). Automatic detection and recognition of multiple macular lesions in retinal optical coherence tomography images with multi-instance multilabel learning. *Journal of Biomedical Optics*, *22*(6), 066014. doi:10.1117/1.JBO.22.6.066014 PMID:28655052

Fernández, A., Ortega, M., de Moura, J., Novo, J., & Penedo, M. G. (2018, June). Detection of reactions to sound via gaze and global eye motion analysis using camera streaming. *Machine Vision and Applications*, *29*(7), 1069–1082. doi:10.100700138-018-0952-9

Gawlik, K., Hausser, F., Paul, F., Brandt, A. U., & Kadas, E. M. (2018, December). Active contour method for ILM segmentation in ONH volume scans in retinal OCT. *Biomedical Optics Express*, *9*(12), 6497–6518. doi:10.1364/BOE.9.006497 PMID:31065445

Gende, M., Moura, J. D., Novo, J., Charlon, P., & Ortega, M. (2021). Automatic Segmentation and Intuitive Visualisation of the Epiretinal Membrane in 3D OCT Images Using Deep Convolutional Approaches. *IEEE Access: Practical Innovations, Open Solutions*, *9*, 75993–76004. doi:10.1109/ACCESS.2021.3082638

Ghazi, N. G., Ciralsky, J. B., Shah, S. M., Campochiaro, P. A., & Haller, J. A. (2007). Optical coherence tomography findings in persistent diabetic macular edema: The vitreomacular interface. *American Journal of Ophthalmology*, *144*(5), 747–754. doi:10.1016/j.ajo.2007.07.012 PMID:17869207

Gulshan, V., Peng, L., Coram, M., Stumpe, M. C., Wu, D., Narayanaswamy, A., Venugopalan, S., Widner, K., Madams, T., Cuadros, J., Kim, R., Raman, R., Nelson, P. C., Mega, J. L., & Webster, D. R. (2016, December). Development and Validation of a Deep Learning Algorithm for Detection of Diabetic Retinopathy in Retinal Fundus Photographs. *Journal of the American Medical Association*, *316*(22), 2402. doi:10.1001/jama.2016.17216 PMID:27898976

Hee, M. R. (1995, August). Quantitative Assessment of Macular Edema With Optical Coherence Tomography. *Archives of Ophthalmology*, *113*(8), 1019. doi:10.1001/archopht.1995.01100080071031 PMID:7639652

Hood, D. C. (2017, March). Improving our understanding, and detection, of glaucomatous damage: An approach based upon optical coherence tomography (OCT). *Progress in Retinal and Eye Research*, *57*, 46–75. doi:10.1016/j.preteyeres.2016.12.002 PMID:28012881

Hosny, A., Parmar, C., Quackenbush, J., Schwartz, L. H., & Aerts, H. J. (2018, May). Artificial intelligence in radiology. *Nature Reviews. Cancer*, *18*(8), 500–510. doi:10.103841568-018-0016-5 PMID:29777175

Huang, D., Swanson, E. A., Lin, C. P., Schuman, J. S., Stinson, W. G., Chang, W., Hee, M. R., Flotte, T., Gregory, K., Puliafito, C. A., & Fujimoto, J. G. (1991). Optical Coherence Tomography. *Science*, *254*(5035), 1178–1181. doi:10.1126cience.1957169 PMID:1957169

Huang, G., Liu, Z., Van Der Maaten, L., & Weinberger, K. Q. (2017). Densely Connected Convolutional Networks. *2017 IEEE Conference on Computer Vision and Pattern Recognition (CVPR)*, 2261-2269. 10.1109/CVPR.2017.243

Jaffe, G. J., & Caprioli, J. (2004, January). Optical coherence tomography to detect and manage retinal disease and glaucoma. *American Journal of Ophthalmology*, *137*(1), 156–169. doi:10.1016/S0002-9394(03)00792-X PMID:14700659

Kamnitsas, K., Ledig, C., Newcombe, V. F., Simpson, J. P., Kane, A. D., Menon, D. K., Rueckert, D., & Glocker, B. (2017, February). Efficient multi-scale 3D CNN with fully connected CRF for accurate brain lesion segmentation. *Medical Image Analysis*, *36*, 61–78. doi:10.1016/j.media.2016.10.004 PMID:27865153

Kanopoulos, N., Vasanthavada, N., & Baker, R. L. (1988). Design of an image edge detection filter using the Sobel operator. *IEEE Journal of Solid-State Circuits*, *23*(2), 358–367. doi:10.1109/4.996

Kashani, A. H., Chen, C.-L., Gahm, J. K., Zheng, F., Richter, G. M., Rosenfeld, P. J., Shi, Y., & Wang, R. K. (2017, September). Optical coherence tomography angiography: A comprehensive review of current methods and clinical applications. *Progress in Retinal and Eye Research*, *60*, 66–100. doi:10.1016/j.preteyeres.2017.07.002 PMID:28760677

Kass, M., Witkin, A., & Terzopoulos, D. (1988, January). Snakes: Active contour models. *International Journal of Computer Vision*, *1*(4), 321–331. doi:10.1007/BF00133570

Kim, J., Hong, J., & Park, H. (2018, June). Prospects of deep learning for medical imaging. *Precision and Future Medicine*, *2*(2), 37–52. doi:10.23838/pfm.2018.00030

Kingma, D. P., & Ba, J. (2015). Adam: A Method for Stochastic Optimization. In Y. Bengio, & Y. LeCun (Ed.), *3rd International Conference on Learning Representations, ICLR 2015*, *San Diego, CA, USA*, *May 7-9, 2015*, *Conference Track Proceedings.* Retrieved from https://arxiv.org/abs/1412.6980

Krizhevsky, A., Sutskever, I., & Hinton, G. E. (2017, May). ImageNet classification with deep convolutional neural networks. *Communications of the ACM*, *60*(6), 84–90. doi:10.1145/3065386

Kuwayama, S., Ayatsuka, Y., Yanagisono, D., Uta, T., Usui, H., Kato, A., Takase, N., Ogura, Y., & Yasukawa, T. (2019, April). Automated Detection of Macular Diseases by Optical Coherence Tomography and Artificial Intelligence Machine Learning of Optical Coherence Tomography Images. *Journal of Ophthalmology*, *2019*, 1–7. doi:10.1155/2019/6319581 PMID:31093370

Lakhani, P., & Sundaram, B. (2017, August). Deep Learning at Chest Radiography: Automated Classification of Pulmonary Tuberculosis by Using Convolutional Neural Networks. *Radiology*, *284*(2), 574–582. doi:10.1148/radiol.2017162326 PMID:28436741

LeCun, Y., Bengio, Y., & Hinton, G. (2015, May). Deep learning. *Nature*, *521*(7553), 436–444. doi:10.1038/nature14539 PMID:26017442

Lecun, Y., Bottou, L., Bengio, Y., & Haffner, P. (1998). Gradient-based learning applied to document recognition. *Proceedings of the IEEE*, *86*(11), 2278–2324. doi:10.1109/5.726791

Lee, J.-H., Kim, Y.-T., Lee, J.-B., & Jeong, S.-N. (2020, November). A Performance Comparison between Automated Deep Learning and Dental Professionals in Classification of Dental Implant Systems from Dental Imaging: A Multi-Center Study. *Diagnostics (Basel)*, *10*(11), 910. doi:10.3390/diagnostics10110910 PMID:33171758

Litjens, G., Kooi, T., Bejnordi, B. E., Setio, A. A., Ciompi, F., Ghafoorian, M., van der Laak, J. A. W. M., van Ginneken, B., & Sánchez, C. I. (2017, December). A survey on deep learning in medical image analysis. *Medical Image Analysis*, *42*, 60–88. doi:10.1016/j.media.2017.07.005 PMID:28778026

Lo, Y.-C., Lin, K.-H., Bair, H., Sheu, W. H.-H., Chang, C.-S., Shen, Y.-C., & Hung, C.-L. (2020, May). Epiretinal Membrane Detection at the Ophthalmologist Level using Deep Learning of Optical Coherence Tomography. *Scientific Reports*, *10*(1), 8424. Advance online publication. doi:10.103841598-020-65405-2 PMID:32439844

Long, J., Shelhamer, E., & Darrell, T. (2015, June). Fully convolutional networks for semantic segmentation. In *2015 IEEE Conference on Computer Vision and Pattern Recognition*. IEEE. 10.1109/CVPR.2015.7298965

Lu, W., Tong, Y., Yu, Y., Xing, Y., Chen, C., & Shen, Y. (2018, December). Deep Learning-Based Automated Classification of Multi-Categorical Abnormalities From Optical Coherence Tomography Images. *Translational Vision Science & Technology*, *7*(6), 41. doi:10.1167/tvst.7.6.41 PMID:30619661

Lv, Y., Duan, Y., Kang, W., Li, Z., & Wang, F.-Y. (2014). Traffic Flow Prediction With Big Data: A Deep Learning Approach. *IEEE Transactions on Intelligent Transportation Systems*, 1–9. doi:10.1109/TITS.2014.2345663

Massin, P., Allouch, C., Haouchine, B., Metge, F., Paques, M., Tangui, L., Erginay, A., & Gaudric, A. (2000, December). Optical coherence tomography of idiopathic macular epiretinal membranes before and after surgery. *American Journal of Ophthalmology*, *130*(6), 732–739. doi:10.1016/S0002-9394(00)00574-2 PMID:11124291

Matsumoto, C., Arimura, E., Okuyama, S., Takada, S., Hashimoto, S., & Shimomura, Y. (2003, September). Quantification of Metamorphopsia in Patients with Epiretinal Membranes. *Investigative Ophthalmology & Visual Science*, *44*(9), 4012. doi:10.1167/iovs.03-0117 PMID:12939323

Mitchell, P., Liew, G., Gopinath, B., & Wong, T. Y. (2018, September). Age-related macular degeneration. *Lancet*, *392*(10153), 1147–1159. doi:10.1016/S0140-6736(18)31550-2 PMID:30303083

Mookiah, M. R., Acharya, U. R., Chua, C. K., Lim, C. M., Ng, E. Y., & Laude, A. (2013, December). Computer-aided diagnosis of diabetic retinopathy: A review. *Computers in Biology and Medicine*, *43*(12), 2136–2155. doi:10.1016/j.compbiomed.2013.10.007 PMID:24290931

Parra-Mora, E., Cazañas-Gordon, A., Proença, R., & da Silva Cruz, L. A. (2021). Epiretinal Membrane Detection in Optical Coherence Tomography Retinal Images Using Deep Learning. *IEEE Access: Practical Innovations, Open Solutions*, *9*, 99201–99219. doi:10.1109/ACCESS.2021.3095655

Rahman, R., & Stephenson, J. (2014, January). Early surgery for epiretinal membrane preserves more vision for patients. *Eye (London, England)*, *28*(4), 410–414. doi:10.1038/eye.2013.305 PMID:24406414

Romeny, B. M., Zuiderveld, K. J., Waes, P. F., Walsum, T. V., Weijden, R. V., Weickert, J., ... Viergever, M. A. (1998, October). Advances in three-dimensional diagnostic radiology. *Journal of Anatomy*, *193*(3), 363–371. doi:10.1046/j.1469-7580.1998.19330363.x PMID:9877291

Samagaio, G., de Moura, J., Novo, J., & Ortega, M. (2017). Optical Coherence Tomography Denoising by Means of a Fourier Butterworth Filter-based Approach. In *Image Analysis and Processing - ICIAP 2017* (pp. 422–432). Lecture Notes in Computer Science. Springer. doi:10.1007/978-3-319-68548-9_39

Setio, A. A., Ciompi, F., Litjens, G., Gerke, P., Jacobs, C., van Riel, S. J., Wille, M. M. W., Naqibullah, M., Sanchez, C. I., & van Ginneken, B. (2016, May). Pulmonary Nodule Detection in CT Images: False Positive Reduction Using Multi-View Convolutional Networks. *IEEE Transactions on Medical Imaging*, *35*(5), 1160–1169. doi:10.1109/TMI.2016.2536809 PMID:26955024

Shen, D., Wu, G., & Suk, H.-I. (2017, June). Deep Learning in Medical Image Analysis. *Annual Review of Biomedical Engineering*, *19*(1), 221–248. doi:10.1146/annurev-bioeng-071516-044442 PMID:28301734

Sonobe, T., Tabuchi, H., Ohsugi, H., Masumoto, H., Ishitobi, N., Morita, S., Enno, H., & Nagasato, D. (2018, September). Comparison between support vector machine and deep learning, machine-learning technologies for detecting epiretinal membrane using 3D-OCT. *International Ophthalmology*, *39*(8), 1871–1877. doi:10.100710792-018-1016-x PMID:30218173

Spaide, R. F., Fujimoto, J. G., Waheed, N. K., Sadda, S. R., & Staurenghi, G. (2018, May). Optical coherence tomography angiography. *Progress in Retinal and Eye Research*, *64*, 1–55. doi:10.1016/j.preteyeres.2017.11.003 PMID:29229445

Suh, M. H., Seo, J. M., Park, K. H., & Yu, H. G. (2009, March). Associations Between Macular Findings by Optical Coherence Tomography and Visual Outcomes After Epiretinal Membrane Removal. *American Journal of Ophthalmology*, *147*(3), 473–480.e3. doi:10.1016/j.ajo.2008.09.020 PMID:19054492

Tan, O., Chopra, V., Lu, A. T.-H., Schuman, J. S., Ishikawa, H., Wollstein, G., Varma, R., & Huang, D. (2009, December). Detection of Macular Ganglion Cell Loss in Glaucoma by Fourier-Domain Optical Coherence Tomography. *Ophthalmology*, *116*(12), 2305–2314.e2. doi:10.1016/j.ophtha.2009.05.025 PMID:19744726

Ting, D. S., Cheung, C. Y.-L., Lim, G., Tan, G. S., Quang, N. D., Gan, A., Hamzah, H., Garcia-Franco, R., San Yeo, I. Y., Lee, S. Y., Wong, E. Y. M., Sabanayagam, C., Baskaran, M., Ibrahim, F., Tan, N. C., Finkelstein, E. A., Lamoureux, E. L., Wong, I. Y., Bressler, N. M., ... Wong, T. Y. (2017, December). Development and Validation of a Deep Learning System for Diabetic Retinopathy and Related Eye Diseases Using Retinal Images From Multiethnic Populations With Diabetes. *Journal of the American Medical Association*, *318*(22), 2211. doi:10.1001/jama.2017.18152 PMID:29234807

Vidal, P. L., de Moura, J., Novo, J., Penedo, M. G., & Ortega, M. (2018, September). Intraretinal fluid identification via enhanced maps using optical coherence tomography images. *Biomedical Optics Express*, *9*(10), 4730. doi:10.1364/BOE.9.004730 PMID:30319899

Wilkins, J. R., Puliafito, C. A., Hee, M. R., Duker, J. S., Reichel, E., Coker, J. G., Schuman, J. S., Swanson, E. A., & Fujimoto, J. G. (1996, December). Characterization of Epiretinal Membranes Using Optical Coherence Tomography. *Ophthalmology*, *103*(12), 2142–2151. doi:10.1016/S0161-6420(96)30377-1 PMID:9003350

Yamamoto, T., Akabane, N., & Takeuchi, S. (2001). Vitrectomy for diabetic macular edema: The role of posterior vitreous detachment and epimacular membrane. *American Journal of Ophthalmology*, *132*(3), 369–377. doi:10.1016/S0002-9394(01)01050-9 PMID:11530050

ADDITIONAL READING

Bowling, B. (2015). *Kanski's clinical ophthalmology* (8th ed.). W B Saunders.

De Fauw, J., Ledsam, J. R., Romera-Paredes, B., Nikolov, S., Tomasev, N., Blackwell, S., Askham, H., Glorot, X., O'Donoghue, B., Visentin, D., van den Driessche, G., Lakshminarayanan, B., Meyer, C., Mackinder, F., Bouton, S., Ayoub, K., Chopra, R., King, D., Karthikesalingam, A., ... Ronneberger, O. (2018). Clinically applicable deep learning for diagnosis and referral in retinal disease. *Nature Medicine*, *24*(9), 1342–1350. doi:10.103841591-018-0107-6 PMID:30104768

Doi, K. (2007, June). Computer-aided diagnosis in medical imaging: Historical review, current status and future potential. *Computerized Medical Imaging and Graphics*, *31*(4-5), 198–211. doi:10.1016/j.compmedimag.2007.02.002 PMID:17349778

Gende, M., de Moura, J. D., Novo, J., Charlón, P., & Ortega, M. (2021). Automatic segmentation and intuitive visualisation of the epiretinal membrane in 3D OCT images using deep convolutional approaches. *IEEE Access: Practical Innovations, Open Solutions*, *24*, 75993–76004. doi:10.1109/ACCESS.2021.3082638

Keane, P. A., Patel, P. J., Liakopoulos, S., Heussen, F. M., Sadda, S. R., & Tufail, A. (2012). Evaluation of age-related macular degeneration with optical coherence tomography. *Survey of Ophthalmology*, *57*(5), 389–414. doi:10.1016/j.survophthal.2012.01.006 PMID:22898648

LeCun, Y., Bengio, Y., & Hinton, G. (2015, May). Deep learning. *Nature*, *521*(7553), 436–444. doi:10.1038/nature14539 PMID:26017442

Schmidt-Erfurth, U., Sadeghipour, A., Gerendas, B. S., Waldstein, S. M., & Bogunović, H. (2018). Artificial intelligence in retina. *Progress in Retinal and Eye Research*, *67*, 1–29. doi:10.1016/j.preteyeres.2018.07.004 PMID:30076935

Vidal, P. L., de Moura, J., Novo, J., Penedo, M. G., & Ortega, M. (2018, September). Intraretinal fluid identification via enhanced maps using optical coherence tomography images. *Biomedical Optics Express*, *9*(10), 4730. doi:10.1364/BOE.9.004730 PMID:30319899

KEY TERMS AND DEFINITIONS

Artificial Neural Network: Computing system inspired by neurons which can learn to convert a series of input features into a meaningful output.

Epiretinal Membrane (ERM): Thin fibrocellular layer that may appear over the eye macula idiopathically or as a secondary factor of other pathologies. May cause irreversible visual distortions.

Fovea: Central pit in the middle of the macula of the retina. Composed of closely packed cones, it is responsible for approximately half of the visual information produced by the whole retina.

Inner Limiting Membrane (ILM): Layer that serves as a boundary between the vitreous body and the retina. It is the layer over which the ERM may appear.

Macula: Pigmented area near the centre of the ocular retina that is responsible for the acute, high-resolution colour vision.

Optical Coherence Tomography (OCT): Medical imaging technique that uses low coherence light to produce cross-sectional visualisations of tissue. It can produce volumes that display the tissue of the patient in three dimensions.

Retina: Light-sensitive layer of tissue located at the back of the eye. It is responsible for the translation of light into electrical neural impulses that can be interpreted by the brain.

Segmentation: In computer vision, the process of partitioning an image into multiple zones, areas, or segments, according to their content.

Chapter 5

A Lightweight CNN to Identify Cardiac Arrhythmia Using 2D ECG Images

Sara El Omary

IMAGE Laboratory, Higher School of Technology, Moulay Ismail University of Meknes, Morocco

Souad Lahrache

Faculty of Sciences, Ibn Zohr University, Morocco

Rajae El Ouazzani

IMAGE Laboratory, Higher School of Technology, Moulay Ismail University of Meknes, Morocco

ABSTRACT

Worldwide, cardiac arrhythmia disease has become one of the most frequent heart problems, leading to death in most cases. In fact, cardiologists use the electrocardiogram (ECG) to diagnose arrhythmia by analyzing the heartbeat signals and utilizing electrodes to detect variations in the heart rhythm if they show certain abnormalities. Indeed, heart attacks depend on the treatment speed received, and since its risk is increased by arrhythmias, in this chapter the authors create an automatic system that can detect cardiac arrhythmia by using deep learning algorithms. They propose a deep convolutional neural network (CNN) to automatically classify five types of arrhythmias then evaluate and test it on the MIT-BIH database. The authors obtained interesting results by creating five CNN models, testing, and comparing them to choose the best performing one, and then comparing it to some state-of-the-art models. The authors use significant performance metrics to evaluate the models, including precision, recall, sensitivity, and F1 score.

INTRODUCTION

Today, heart disease is responsible for numerous deaths, and on the report of the World Heart Federation, more than 17 million people die each year (Namara et al., 2019). In fact, Cardiac Arrhythmia is one of the most frequent diseases that affect a very large number of people around the world; it is more prevalent in people over the age of 60, as they often use medications that affect the functioning of the heart. Arrhythmia can be defined as irregular or changing heartbeats, and these changes are felt by people most of the time (Sahoo & Prakach, 2011), it can be harmless and occur to healthy people, but some abnormal rhythms can be serious and even cause death. Besides, irregular heartbeats can lead to poor blood flow that can affect other organs, injuring or stopping them permanently (Humphreys et al., 2013)). Moreover, cardiac arrhythmias may be undetected, because it does not have any indications or symptoms until the doctor examines the patient and notice the heartbeats disorder. In general, arrhythmias can be manifested by certain signs such as: chest pain, breathing problems, slow heartbeats, fast heartbeats, pounding in the chest, anxiety, fatigue, dizziness, sweating and fainting (Mayo Clinic, 2021). In addition, knowing how the heart normally works can help to figure out the reason behind cardiac arrhythmias. The heart has four chambers, two upper chambers are named atria and two lower chambers named ventricles (Mayo Clinic, 2021). Actually, the cardiac rhythm is managed by a cardiac stimulator named sinoatrial node, situated in the right atria called atrium. Then, the sinoatrial node addresses the signals produced by each heartbeat; these signals pass through the atria, which compresses the heart muscles and pumps the blood into the ventricles (Mayo Clinic, 2021). Afterward, the signals arrive at a group of cells named the AV node, where they slacken off; this minor delay allows the ventricles to be able to fill with blood (Mayo Clinic, 2021). Finally, when signals attain the ventricles, the chambers of the heart push the blood to the lungs or the rest of the body (Mayo Clinic, 2021). Furthermore, this cardiac signaling occurs at a rate of 60 to 100 beats per minute in a healthy heart. An irregular heartbeat can be caused by a variety of factors, including: recent heart attack, heart arteries that are clogged, cardiomyopathy, a high blood pressure, COVID-19 infection, stress, certain medications without prescription, etc. (Mayo Clinic, 2021). However, people can avoid arrhythmias by making some lifestyle changes, adding modifications that minimize the heat disease risks. The following are examples of a heart healthy lifestyle: a heart-healthy diet is one of the most important things for health, staying physically active, maintaining a healthy weight, caffeine and alcohol should be consumed in moderation or not at all, smoking cessation, take medications exactly as prescribed and inform the doctor about prescriptions, even those purchased without a prescription (Mayo Clinic, 2021). The ECG is a cardiology technique utilized to record the electrical impulses of the heart's contraction and

relaxation (Isin & Ozdalili, 2017), these recordings are widely used to diagnose and detect heart diseases, and it is a one-dimensional (1D) signal that represents a heartbeat. Additionally, an ECG can be performed by numerous methods; this test usually requires placing electrodes which are a certain number of sensors on different place of the body particularly the chest, arms, and legs and these sensors are attached to an ECG recording device (NHS choices, 2022). Normally, patients need to remove upper clothes before connecting the electrodes and the chest need to be cleaned, this test often needs few minutes (NHS choices, 2022). Moreover, there are three main types of ECG; doctors specify the type based on the patient's symptoms and problem. At first, a resting ECG performed while the patient is in a relaxed situation, next, a stress ECG is done while the body is exercising, finally, Holter monitor where the electrodes monitoring the heart for one of more days at home (NHS choices, 2022). In fact, each heartbeat includes three different waves P, QRS which consists of the Q wave, R wave, S wave, and T wave. Firstly, the P wave corresponds to the atrial depolarization, next, the QRS is triggered, and each QRS complex does not completely present the three Q, R or S waves; it is the ventricular depolarization, then the T wave represents the ventricular repolarization (Ullah et al., 2021). Classifying Arrhythmia using ECG is distinguishing between normal and abnormal heartbeats that are represented by ECG recording signals. However, the enormous challenge) with manual ECG signals analysis is to detect and categorize wave-forms that clinical experts and doctors might take hours to realize and are susceptible to errors (World Health Organization, 2022). Thus, the automatic detection and categorization of cardiac arrhythmias could significantly reduce the morbidity and mortality rates. Therefore, the authors propose a new workflow for arrhythmia detection using ECG images, and as mentioned earlier, these images are provided by the well-known public MIT-BIH arrhythmia database (Moody et al., 2021). To the authors' knowledge, they are among the few papers to have used ECG signal recordings as 2D images to classify cardiac arrhythmia using a deep CNN. The suggested workflow starts with loading the transformed ECG signals into 2D images. Then, unifying and resizing the shape of these images. Next, the pre-processed images are divided into three parts, namely training, validation and test sets. Thereafter, the authors build and train the models to find out the best-performing one by evaluating their scores. Finally, they evaluate the scores of the best model. Figure 1 exposes the authors suggested workflow with some details.

124

Figure 1. The workflow of the suggested model to detect heart arrhythmia
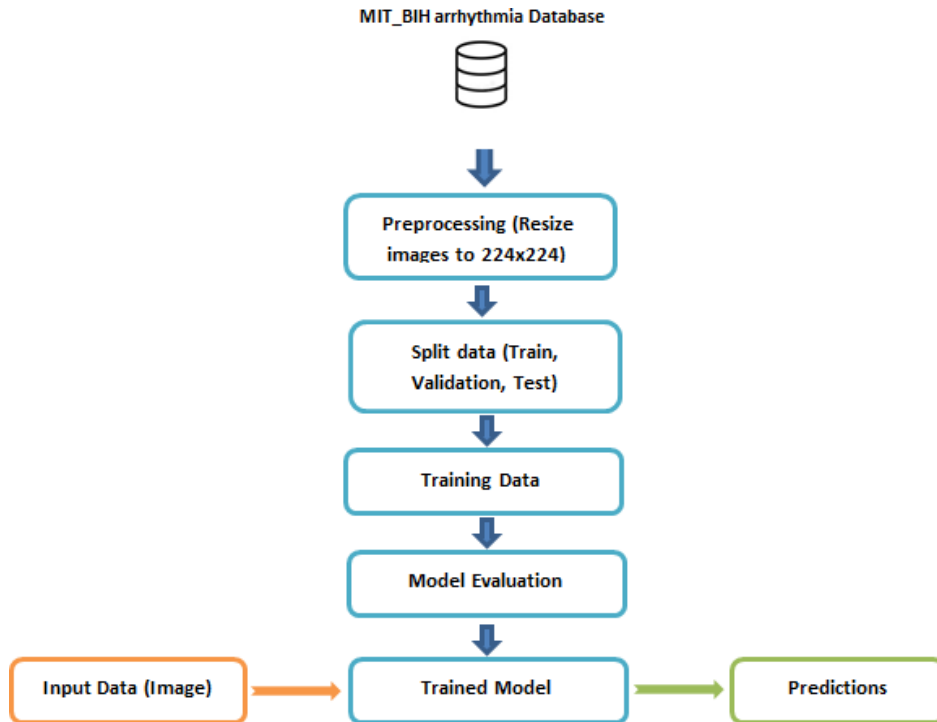
The rest of this chapter is structured in the following way. Section 2 provides the background about deep learning, deep learning architectures, and previous works related to arrhythmia detection. Then, section 3 focuses on the proposed CNN model; it discusses the signal transformation, the database details, the data preparation, as well as the implementation of the CNN model. Later, section 4 consists of the experimental findings and results and some performances analysis. Finally, section 5 contains the conclusion and future work.

BACKGROUND

Deep Learning

Deep learning is a subset of the artificial intelligence Neural Networks (NNs) family, and it differs from typical machine learning in several ways (Grossi & Buscema, 2007). In fact, deep learning algorithms work as the human brain and are able to learn without any human supervision. Mainly, these algorithms can be divided into

two categories, and each one of them could be subdivided into subtypes, supervised and unsupervised deep learning algorithms (Alloghani et al., 2019). Supervised learning is the first type where the data used for learning is labeled, and this refers to inputs that already have proper outputs, and based on this data, the model can be used to predict outputs to new (test) data (Guru99, 2022). Supervised learning can solve several problems (Analytics Vidhya, 2021), (Sidey-Gibbons, 2019), (Toh & Brody, 2021). For example, it has the ability to know the classes of objects by making predictions based on experiments (Esteva et al., 2021). Supervised learning has some disadvantages like requiring much computer resources, knowledge about object classes, and cannot give a correct prediction if the test data are too different from data in the training set (Airon, 2022). In addition to supervised learning algorithms, there is unsupervised learning one which handles to discover the patterns within the data that have not been detected; it basically works on unlabeled data sets. Unsupervised learning has many advantages, for example, it does not require labeled data for processing. In fact, labeling data requires much manual work and expertise, and solving this problem by learning the data and classifying it without any labels make data classification much easier (Culurciello, 2018). Moreover, unsupervised learning systems can perform more complex treatment tasks than unsupervised learning systems (Explorium, 2021).

Algorithms Used for Cardiac Arrhythmia Classification

Over the years, a variety of machine and deep learning techniques have been used to classify arrhythmias. The most commonly used arrhythmia classification methods and algorithms are shown in Figure 2.

Figure 2. Cardiac Arrhythmia classification algorithms
Source: Complexity (2021)
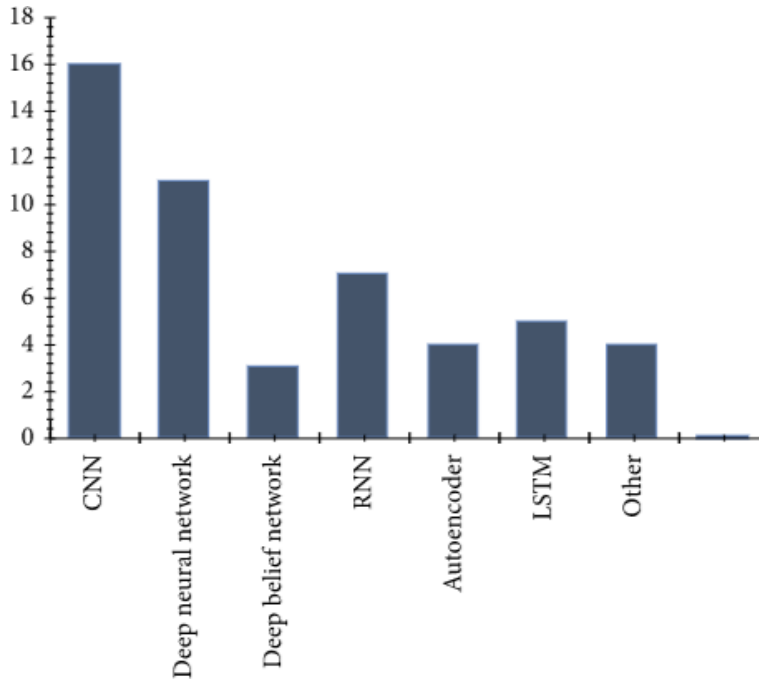
Deep Learning Architectures

Medical image analysis is a broad field that commonly uses deep learning algorithms (El Omary et al. 2021). Based on Figure 2, the authors will describe NNs algorithms that are widely used for Cardiac Arrhythmia classification. There are listed as the following:

- Recurrent Neural Networks (RNNs)
- Long Short-Term Memory (LSTM)
- Autoencoders
- Deep Neural Networks (DNNs)
- Deep Belief Networks (DBNs)
- Convolutional Neural Network (CNNs)

RNNs and LSTM

The RNN is a member of NNs family (Sherstinsky, 2020). In fact, the RNN architecture has added the potential to preserve the semantic dependence between data; it allows

127

the memorization and recursive propagation during the learning process. Since the previous output is reused as an input when adding hidden states, this is called recursive (Sherstinsky, 2020). In order to update the weights, back propagation is applied, and the computation carried out between the units may produce a large or small value, which may reduce the gradient descent to zero or vanish. As a result, it will be difficult for the network to preserve the data memorization, which means poor predictions (Sherstinsky, 2020). This briefly means that this architecture suffered from the vanishing gradient problem (SuperDataScience, 2020). Therefore, to resolve the issue of gradient vanishing, an architecture called Long Short-Term Memory (LSTM) was introduced (Staudemeyer & Morris, 2019). The LSTM architecture is a form of RNN, and it is commonly referred as the cell state (Staudemeyer & Morris, 2019). The cell state is changed by the forgetting gate, that are placed under the cell state and it is also adjusted by the input modulation gate. And, the precedent cell state is then forgotten by multiplying it by the forgetting gate, and the fresh information is added to the input gates outputs. The output of the forgetting gate informs the cell state what information should be forgotten by multiplying 0 with a position in the matrix. If the output of the forgetting gate is equal to 1, the information is retained in the cell state (Staudemeyer & Morris, 2019). Additionally, and as shown in Figure 3, ht-1 refers to previous hidden state, Ct-1 refers to current input, ht is the hidden state and Ct is the current output.

Figure 3. The architecture of LSTM
Source: Complexity (2021)
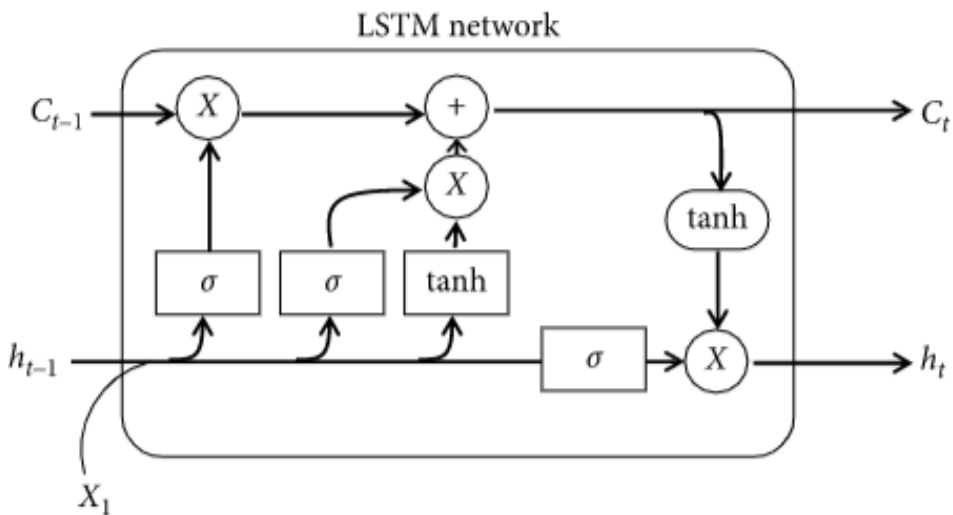
Autoencoders

Autoencoders are a type of feedforward neural networks (NNs) that use an unsupervised method for learning. The autoencoders reduce the data from a higher-dimensional encoding to a lower dimensional representation by training the model to catch the main areas of the input data (Bank et al., 2021). This architecture has three main parts including encoder, bottleneck and decoder (Bandyopadhyay, 2022). First, the encoder is an ensemble of convolutional and pooling blocks that compress the model's input in a small area named bottleneck. Then, the bottleneck which is the main part of this network, allows the flow of data from the encoder to the decoder, and lets through only the most critical data. The bottleneck is built to capture the maximum information contained in an image (Bandyopadhyay, 2022). Additionally, very tiny bottlenecks would limit the quantity of data that could be stored, increasing the risk of vital data leaking through the encoder's pooling layers. Finally, the decoder reconstructs the output of the bottleneck using oversampling and convolutional blocks (Bandyopadhyay, 2022). When training autoencoders, four hyperparameters need to be fixed which are the code size, number of layers, number of nodes per layer and reconstruction (Bandyopadhyay, 2022). Furthermore, there are five famous autoencoders including denoising autoencoders, undercomplete autoencoders, contractive autoencoders, sparse autoencoders, and variational autoencoders (Bandyopadhyay, 2022). Figure 4 displays the architecture of an autoencoder.

Figure 4. The architecture of autoencoder
Source: Complexity (2021)
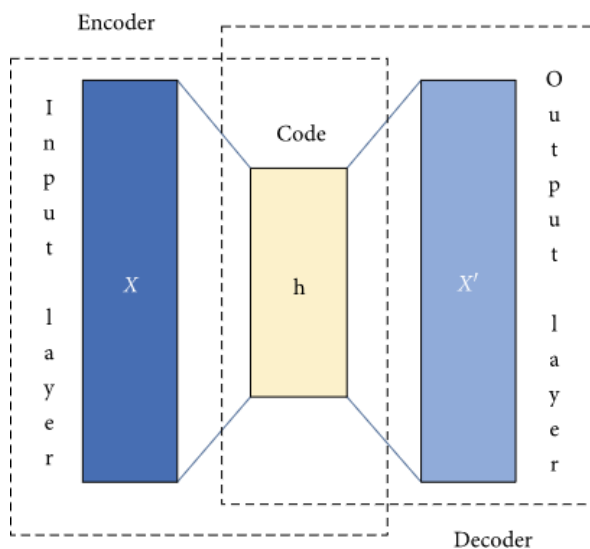
DNNs

DNNs are a type of machine learning where many layers of nodes are used to extract some high-level functions from the incoming data; it transforms the data into a more creative one (Huang et al., 2016). The DNN is capable of recognizing various types of unstructured data. In this chapter, the authors presented many types of NNs for arrhythmia classification, but the components of the proposed networks are the same: neuron, weight, bias, and function (Huang et al., 2016). All of these components have the ability to behave in the same way as the human brain. Besides, DNNs are a well-known method for ECG image categorization (Huang et al., 2016).

DBNs

A DBN is a sophisticated generative model that uses a deep architecture consisting of numerous stacks of Restricted Boltzmann machines (RBM)) (Montufar, 2018). Each RBM model conducts a non-linear transformation on its input and outputs vectors that will be used as input for the next RBM model in the sequence (Montufar, 2018). While DBNs are generative models, they acquire a lot of flexibility and are easier to extend, and can also be used in unsupervised or supervised manner. Additionally, DBNs can also learn, extract, and categorize features, which can be beneficial in a wide range of applications (Yuming et al., 2015). During the feature learning task, an unsupervised pre-training is performed on each layer in the individual MBRs that make up a DBN, and then the back-propagation technique is used to refine classification and other tasks on a small labeled data set (Labs, 2018).

CNNs

The CNN is a subcategory of Artificial Neural Networks (ANNs), which is particularly designed for image processing, and it is composed of two main phases (Wu, 2021). The first phase is feature extraction. In fact, the application of convolutional operations of CNN returns various feature maps, which are then normalized or resized using an activation function (Wu, 2021). The second phase consists of converting the output of the previous phases into a new vector; the latter contains the probabilities of an input image to be classified into one of the output classes (Wu, 2021). CNN is composed of four types of layers, including convolutional, pooling, ReLU (Rectified Linear Unit), and fully connected (FC) (Ke et al., 2018). Actually, the convolutional layer is the key of a CNN success; it can detect a set of features from an input image by using a convolutional filter. The latter is a simple window used to drag on the input image to calculate the product between the input image and the filter. In addition, the convolutional filters are used to maintain the detected features in

130

the input image (Ke et al., 2018). For each product, the result is a feature map that presents the location of features in the image. Next, the pooling layer receives the set of feature maps that were produced by the convolutional layer and then it applies a pooling operation in order to reduce the image shape while conserving the main characteristics. Pooling operations can be divided into two categories; maximum and average. The pooling operation consists of dividing the input image into cells, and then keeping the maximum value if maximum pooling is applied, or the average value in the cell if average pooling is chosen (Prabhu, 2019). The main role of the pooling layer is to improve the efficiency of the architecture by reducing the number of parameters. Subsequently, ReLU layer introduces the non-linearity to the used model; it replaces the negative values that are presented in the dataset by zeros (Prabhu, 2019). Finally, the FC layer is often the last layer of a Neural Network; and it gets the output of the CNN model in a form of the vector from the previous layer and produces a new one. The latter has a certain shape, which is the number of classes that have been given in the dataset, and each number in this vector assigns a predicted probability about the chosen image (Prabhu, 2019). CNN has a strategy that is similar to traditional supervised learning algorithms.

Figure 5. The CNN architecture
Source: Machine Learning Mastery (2019)
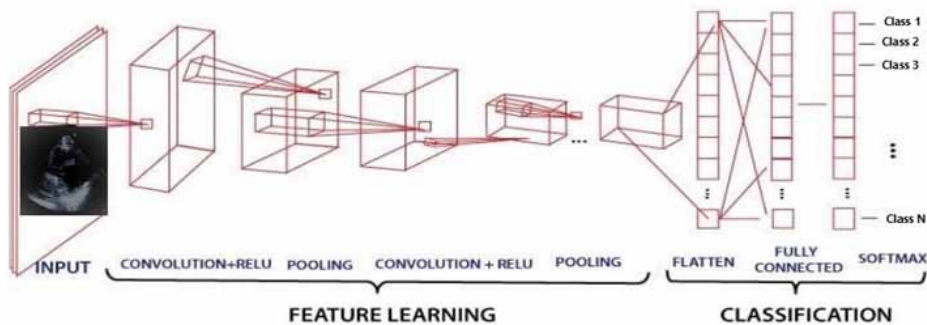
CNN is the most typical image analysis architecture; and it outperforms other ANNs by sharing weights at each position in the image. CNNs drastically decrease the weights number in the network when compared to ordinary ANNs. In fact, CNNs are applied in several types of medical scans; like cardiac ultrasound, cardiac Magnetic Resonance Imaging (MRI), and cardiac Computed Tomography (CT). Actually, CT and MRI terms may refer to the same thing, however, CT scans are less expensive and more common but MRI gives more information details. Moreover, Cardiac ultrasound or echocardiography involves obtaining ultrasound images of the

deep heart within the body. In addition, MRI is a scan as well; it uses radio waves and magnetic fields to capture heart images and their components in detail. Then, cardiac CT refers to scans that use X-rays to produce detailed images of the heart and its vessels. With cardiac ultrasound for example, (Abdi et al., 2017) used CNNs to predict the quality of echo series and they used the Mean Absolute Error (MAE) as a metric of evaluation and they obtained a value of 71%. Then, (Dezaki et al., 2019) used a CNN combined with a RNN to predict end-systolic and end-diastolic frames and they get 98% coefficient of determination (R2). Next, (Diller et al., 2019) have used CNN to detect underlying diagnoses in complex congenital heart disease and U-Net to segment the systemic ventricle, they utilized Dice Coefficient (DC) as an evaluation metric, and they obtained a value between 0.794–0.881 DC. Thereafter, (Jun et al., 2018) utilized a CNN network to classify Understanding Intravascular Ultrasound (IVUS) frames as normal or Thin-Cap FibroAtheroma (TCFA), and they obtained an accuracy rate of 91.1%. Later, (Moradi et al., 2018), used a combination of models based on CNNs to generate text descriptions for Doppler US images of cardiac valves using doc2vec, and they get an accuracy rate of 96% for valve classification. In addition, (Østvik et al., 2019) classified seven classes of cardiac views by using a real time CNN model, as an evaluation metric, and they obtained an accuracy rate of 98%. After that, CNNs have various applications in Cardiac CT, for example, (Commandeur et al., 2018) used two subsequent CNNs to segment Adipose tissue, they used DC as an evaluation metric and they get values in a range of 71%-82%. Later, (Gülsün et al., 2016) treated coronary centerline extraction in Coronary Computed Tomography Angiography (CCTA), and they used CNN to classify paths into correct or not and they got a classification rate between 90.8%–92.7%. Next, (Green et al., 2018) used a CNN model for per voxel prediction of routine-dose hydroxyurea (HU) values, and as an evaluation metric, they get a Peak Signal-to-Noise Ratio (PSNR) rate of 41.47. Then, (Jin et al., 2018) used CCTA to segment the left atrial appendage, and CNN with the conditional random field, and they obtained a DC rate of 95%. In addition, (Lessmann et al., 2018) utilized CT of the chest to classify voxel calcium scoring in low dose, and they get 91% of Linear Weighted Kappa (LWK). Later, (López-Linares et al, 2018) have used the CNN model to localize the Region of Interest (ROI), and another CNN to segment abdominal aortic thrombus, and they obtained 82% DC. Next, (Lossau et al., 2019) treated motion artifacts in coronary CCTA, they used the CNN model to classify coronary cross-sectional images, and they obtained a classification accuracy of 99.3%. Finally, CNNs are applied on MRI as well, for example, (Avendi et al., 2015) used a model that combines CNN and Autoencoders (AE) to segment the left ventricle, and they obtained a DC value of 94%. Next, (Du et al., 2020) used images of congenital heart disease images with CNN and deep supervision to segment blood pool and myocardium, and they achieved a DC value of 93%. Thereafter, (Emad et al., 2015)

132

applied a multiscale CNN to localize the bounding box of the left ventricle in short axis MRI slice, and they achieved a classification accuracy of 99%.

Arrhythmia is a cardiac disturbance that can cause damage to the other organs in the human body due to the inefficient blood pumping, and can sometimes lead to death (Humphreys et al., 2013; Klein, 2018). To detect cardiac arrhythmia, clinical experts use ECG signals by recording the electrical heart activity in the form of signals (Klein, 2018; Hadjem, 2015). The latter include different kinds of waves; some of these waves can be extracted to diagnose arrhythmia such as QRS, P, T and other waves as shown in Figure 4 (Sun, 2005).

Figure 6. ECG waves
Source: BMC Cardiovascular Disorders (2005)
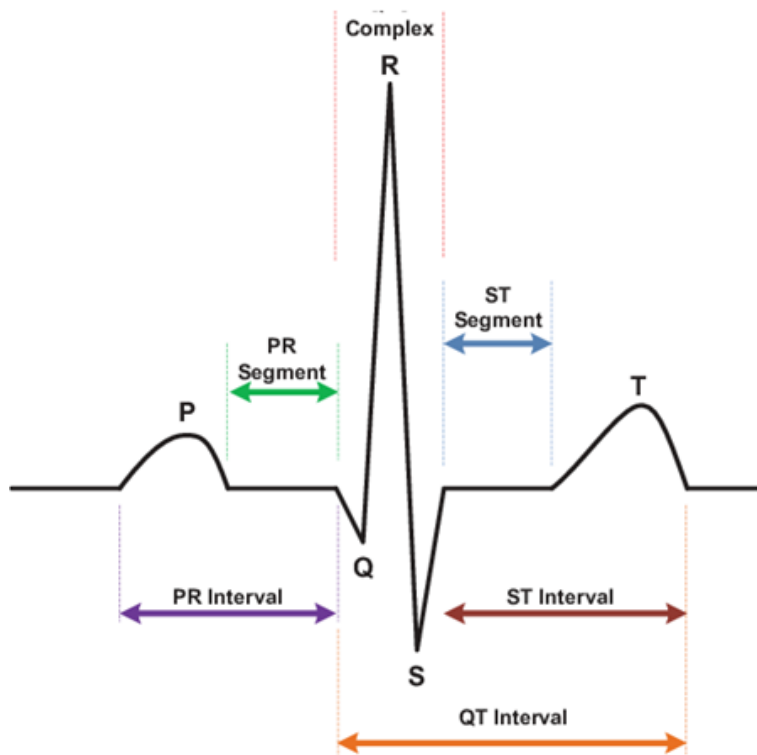
ECG Signals

The analysis of ECG signals reveals cardiac dysfunctions if there are any and sometimes they are difficult to detect (Anwar, 2018). Determining the specific type of arrhythmia that causes illness is a difficult task because analyzing a patient's ECG signal may

133

take hours (critical cases); moreover, cardiologists need to identify the correct type of arrhythmia before prescribing a specific treatment. Several algorithms have been developed and implemented to improve the duration of disease diagnosis. Recent studies have focused on machine learning algorithms to detect cardiac arrhythmia, and the proposed approaches achieved good results. For example, (Ye et al., 2010) applied a Support Vector Machine (SVM) with Wavelet Transform (WT) and Independent Component Analysis (ICA) using the MIT-BIH database for arrhythmia detection, and they achieved a classification accuracy of 99.66%. In addition, (Mustaqeem et al., 2017) have used SVM and ECG, and their model has achieved classification accuracies of 81.11% when using 80/20 data split and 92.07% when using 90/10 data split. Recently, and due to the advances in deep learning, different approaches are proposed for ECG-supported arrhythmia classification. It is well known that deep learning methods do not require manual feature extraction, in contrast to machine learning classic algorithms (Salem et al., 2018). However, the recent discoveries indicate that deep learning algorithms can directly extract representative features from the input data, because of the convolutional layers (Brownlee, 2020). First, (Yıldırım, 2018) proposed a deep learning approach that uses bidirectional LSTM with wavelet layers on the MIT-BIH database and they achieved a classification accuracy of 99.39% on 5 types of arrhythmias. Next, (Yao et al., 2020) introduced and proposed an Attention-based Time Incremental CNN (ATI-CNN) which preserves spatial and temporal information of ECG signals. They achieved a classification accuracy of 81.2% on paroxysmal arrhythmias classification. Later, (Rahhal et al., 2016) proposed a new method based on Deep Neural Networks and Stacked De-noising Auto-Encoders (SDA) for ECG signal classification, and they obtained high accuracies on three different databases. After that, (Hannun et al., 2019) have proposed a new Deep Neural Networks, and they achieved a classification accuracy rate of 83.7%. However, CNNs are the most widely used networks for arrhythmia detection, and they use as input 1D data, 2D, and 3D images that represent the ECG signals. In addition, (Kiranyaz et al., 2016) proposed a 1D CNN model that had a high accuracy on the MIT-BIH arrhythmia database. Later, (Yıldırım et al., 2018) have used a new 1D CNN model for arrhythmia classification and they achieved a classification accuracy of 91.33% on the MIT-BIH database. Afterward, (Jun et al., 2018) have proposed 2D CNN using grayscale ECG images for arrhythmia classification, and they achieved a classification accuracy of 99.05% on the MIT-BIH database. Finally, (Huang et al., 2019) have proposed a 2D CNN to detect five different types of arrhythmias and they achieved an accuracy of 99% on the MIT-BIH database. Hence, in this chapter, the authors propose a deep CNN model that classifies 2D ECG images into different types of arrhythmia; the proposed model uses ECG images as inputs and provides the specific type of arrhythmia (classes) as an output. The experiments were carried out on images from the MIT-BIH database,

134

and the reached results show that the model performed well in the classification of arrhythmia types. In fact, the proposed model differs from existing approaches that treat Cardiac Arrhythmia detection in three points. First, the authors use a 2D representation of the ECG signals to detect arrhythmia, which is different from the most widely used techniques, which are based on 1D representation. Second, the strategy used by the authors differs from existing ones; the proposed model makes a classification learning tasks to assign a class or category to each object. Thus, in this chapter, the authors have built 5 deep CNN models from scratch. At the beginning, they classify whether there is a cardiac problem or not, then, they move on to detect three abnormal types of arrhythmia. Next, the authors extended the number of classes to four types of abnormal rhythms, and finally, the authors classify five classes that combine the four abnormal classes mentioned above in addition to the normal class.

THE PROPOSED CNN MODEL

Dataset

The ECG images came from the MIT-BIH arrhythmia dataset (Moody & Mark, 2005), which holds signals from 48 participants with different types of beats. The ECG recordings were measured at 360Hz from 1970; each one has 30 minutes duration and bandpass filtered at 0.1- 100Hz. The used images were selected from the modified limb II, and each one contains a heartbeat which can be classified into five different types as shown in Table 1 (Yamada, 2006).

Table 1. MIT-BIH database arrhythmia types

Arrhythmia type	MIT-BIH heartbeat classes
Non-Ectopic Beats (N)	Normal Beat Left Bundle Branch Block Beat Right Bundle Branch Block Beat Nodal (Junctional) Escape Beat Atrial Escape Beat
Supraventricular Ectopic Beats (S)	Aberrated Atrial Premature Beat Premature or Ectopic Supraventricular Beat Atrial Premature Contraction Nodal (Junctional) Premature Beat
Ventricular Ectopic Beats (V)	Ventricular flutter Wave Ventricular Escape Beat Premature Ventricular Contraction
Fusion Beats (F)	Fusion of Ventricular and Normal Beat
Unknown Beats (Q)	Paced Beat Unclassifiable Beat Fusion of Paced and Normal Beat

Source: MIT-BIH arrhythmia database (2005)

Figure 7. 2D image classes
Source: Encyclopedia of Mathematical Physics (2006)
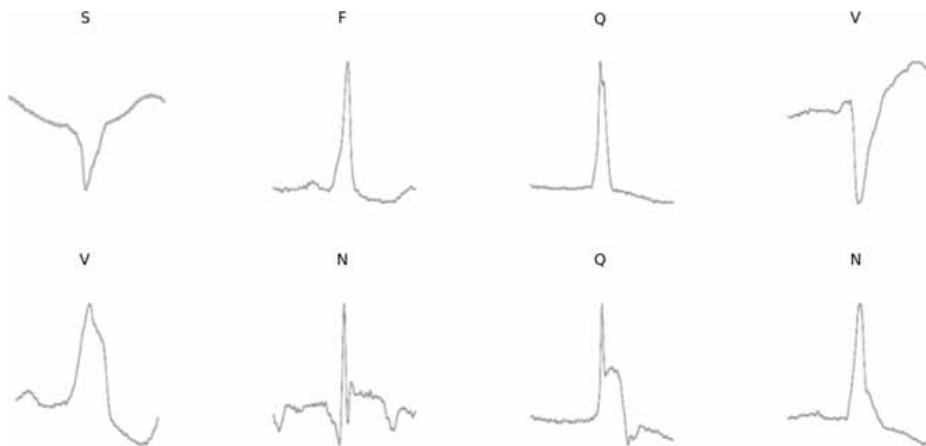
Transformation of Signals into Images

Actually, the processing of signals is a vast engineering field that includes extracting, converting, and storing information that are encoded in signals and images (Byrne, 2005). Signal processing methods include information compression; analog-to-digital conversion; signal and image reconstruction or restoration; adaptational filtering; distributed sensing and processing; and automatic pattern analysis. From the first days of the Fast Fourier Transform (FFT) (Brigham & Morrow, 1967) to today's omnipresent of MP3, JPEG, and MPEG compression algorithms, signal processing is behind several products and devices that have evolved the whole world technology, including scanners for 3D medical images, audio in digital format); cell phones with GPS and geolocation; intelligent automotive sensors (airbag sensors and collision warning systems, and others). Thereafter, signal processing is a science that involves mathematical derivation and implementation of new processing methods based on the first principles that anticipate the performance limitations and strength of methods (Byrne, 2005). Currently, images are used in different fields in medicine, education, communication, and others. Basically, an image is a signal, and the 1D medical data presentation is the most used format in various studies (Nguyen, 2021; Rim, 2020), but recently, ECG employing transform algorithms has been prominent. For signal conversion, numerous transform algorithms such as Fourier, discrete cosine, and wavelet transforms are commonly used (Brigham & Morrow, 1967; Ahmed, 1974; Antoine, 2003). Hence, (Hatipoglu et al., 2018) have proposed a new method to transform a 1D signal of magnetoencephalography (MEG) and electroencephalography (EEG) to images; they used Time Series to convert the signals to an angle-amplitude graph image. Next, (Azad et al., 2019) introduced a new approach as well to convert a 1D signal to a 2D grayscale image. They started by collecting wave signals, then, they applied empirical mode decomposition, after that, they calculated the energy of signals which is carried out to convert signals into 2D images, thereafter they converted the energy spectrum of signals into 2D grayscale images. Finally, this conversion, may simplify the tasks of the Artificial Intelligence (AI) community in medical image analysis.

The design and creation of a new 2D CNN model is the major key contribution in this chapter. The proposed model is efficient, lightweight which makes it applicable in real time applications, non-complex, and easy to implement. Therefore, this study aims to seek out an efficient model for arrhythmia detection based on heartbeat 2D images, which could reduce the clinical expert analysis time. The process of research starts by posing and determining the background of the problem in order to be able to define a set of research objectives. Thereafter, the model is built using deep learning techniques. Finally, this model is validated by comparing it with other models using the same data characteristics. The authors have tested several

image sizes until they found that the best size is 32 x 32, which consumes the least amount of computer resources. Therefore, the images were resized into 32 x 32 and given as inputs to the model. The used images are grouped into 4 groups which are:

- Group 1: Consists of two classes Normal and Abnormal (Other).
- Group 2: Contains three abnormal classes which are F, V, and Q.
- Group 3: Contains the following four classes F, S, V, and Q.
- Group 4: Contains five classes which are N, F, S, Q, and V.

Architecture

CNN is one of the most popular deep learning architectures that the authors choose due to its performance and success on 2D data classification (Analytics Vidhya, 2020). However, deep learning architectures have a high level of features extraction, hence, the ECG images were directly used as inputs without features extraction or de-noising processes.

The proposed CNN model for classifying different Cardiac Arrhythmia types is presented in Table 1. The workflow of the model is described in Figure 6, while Table 2 provides a complete representation of the model layers. In effect, the used architecture includes three 2D convolutional layers; each one is succeeded by a pooling layer, fully connected layers, and dropout layers. The convolution and pooling layers make features extraction, the dropout layer prevents the model from over-fitting and pooling layers reduce the input dimensions in order to protect representative features (Brownlee, 2019). As shown in Table 2, the first 2D convolutional layer is made up with 896 parameters, and in the maximum pooling layer, the maximum values in the region is specified on the feature maps that are acquired from the previous layers. In fact, the pooling layer reduces the size of the feature maps obtained from the previous convolutional layers. Moreover, reducing the size of feature maps is a crucial step to decrease the computational cost of the deep learning architecture. Various methods, such as mean values, are used for this purpose (Brownlee, 2019). Subsequently, the process is repeated until the sixth layer of the architecture. In addition, a dropout parameter is employed to avoid overfitting, and finally, the softmax layer is added to make the prediction regarding the output classes.

Figure 8. The proposed CNN model
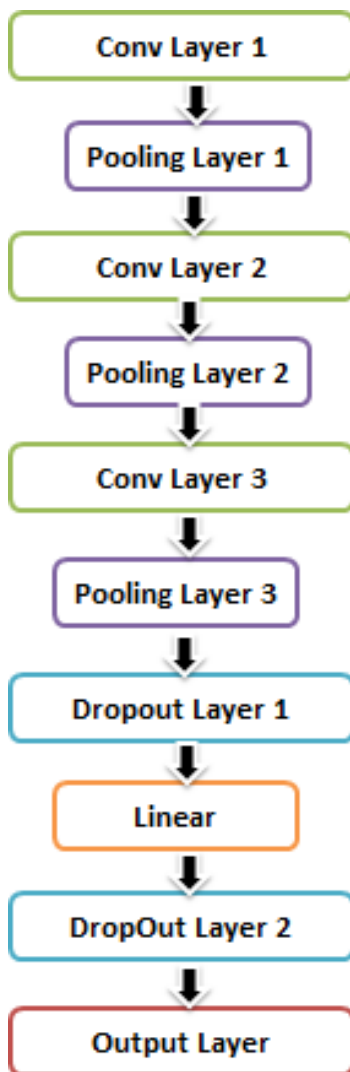
Table 2. Details of the layers used in the proposed CNN model

Layer	Filter size	Parameters
Conv2d	3 x 3.	896
MaxPool2d	2 x 2.	-
Conv2d	3 x 3.	9248
MaxPool2d	2 x 2.	-
Conv2d	3 x 3	18 496
MaxPool2d	2 x 2	-
Dropout	-	-
Linear	-	123 000
Dropout	-	-
Output layer	-	242

Evaluation Parameters

One of the most investigated fields in the research world is classification problems, several use cases are present in various areas, face recognition (Berrahal & Azizi, 2021), emergency car classification (Kherraki et al., 2021), etc. Hence, certain metrics are needed to evaluate the model's performance to distinguish between excellent and terrible classification models. Accuracy, Confusion matrix, Precision and Recall, Specificity, F1 score and AU-ROC are the significant metrics that are employed when solving classification problems. In the following, the formula of calculation for each metric is presented. Let's consider Tp the true positives, Fp the false positives, Tn the true negatives, and Fn the false negatives, s is the class index and M is the total number of classes.

The accuracy is calculated as follows (Joshi, 2016):

$$Accuracy = \frac{1}{M} \sum\nolimits_{s=1}^{M} \left(\frac{Tp^s + Tn^s}{Tp^s + Tn^s + Fp^s + Fn^s} \right) \qquad [1]$$

The recall (sensitivity) and precision are calculated as follows (Joshi, 2016):

$$Recall = \frac{1}{M} \sum\nolimits_{s=1}^{M} \left(\frac{Tp^s}{Tp^s + Fn^s} \right) \qquad [2]$$

$$Precision = \frac{1}{M} \sum\nolimits_{s=1}^{M} \left(\frac{Tp^s}{Tp^s + Fp^s} \right) \qquad [3]$$

The specificity is also called the true negative rate, and is calculated as follows (Joshi, 2016):

$$Specifity = \frac{1}{M} \sum\nolimits_{s=1}^{M} \left(\frac{Tn^s}{Tn^s + Fp^s} \right) \qquad [4]$$

The F1 score is calculated using the recall and precision as follows (Joshi, 2016):

$$F1score = 2 * \frac{Precision * Recall}{Precison + Recall} \qquad [5]$$

The ROC-AUC curve is a performance indicator that is used to assess the classification issues at various thresholds. The ROC curve demonstrates how well the model can distinguish between the various classifications; the AUC indicates how well the model can discriminate between classes; furthermore, the higher the AUC, the better is (Bradley, 1997).

Finally, the confusion matrix summarizes the prediction results after training the model and testing it on the test set. The diagonal values in the matrix present the number of elements that are correctly classified by the model. The upper right corner represents the predicted positive false items, as well as the down left corner of the diagonal (Joshi, 2016). The matrix follows show the confusion matrix of a binary classification:

$$\begin{bmatrix} True\ Poositive(\mathrm{TP})\ False\ positive(\mathrm{FP}) \\ False\ Negative(\mathrm{FN})\ True\ Negative(TN) \end{bmatrix}$$

[6]

While the used classes in the training set are unbalanced, the authors choose the significant performance metrics that perform well on this type of databases to evaluate the models, including precision, recall, sensitivity, and F1 score.

CLASSIFICATION RESULTS AND DISCUSSION

Actually, the proposed CNN classifier and all the experiments were implemented in Python language using PyTorch, the open-source machine learning library, developed by Facebook for deep learning, on the Kaggle simulator including GPU. The authors have implemented several CNN models.

The authors used ECG images classification dataset containing 54,378 images in order to evaluate the performance of the proposed 2D CNN model. While some of the ECG classes in the dataset do not have enough sample number, the authors created four subsets of data including two, three, and four classes in addition to the original five classes of the dataset. Additionally, the subsets are divided into 70%, 20%, and 10%, respectively, to be used for the training, validation, and testing sets. The proposed model was trained for each subset separately using training and validation sets. The validation data set is carried out to choose the best values of hyper-parameters. Next, the test set, which contains the data that had never been seen by the generated, is used to evaluate the given predictions. Besides, the performance of the proposed CNN model was assessed using a set of evaluation metrics, which are described in the Evaluation metrics subsection, such as recall, precision, sensitivity, specificity, and F1 score.

Results

The proposed CNN has been evaluated based on different experiments using several values of learning parameters, and it is shown that the significant parameters that should be carefully tuned are batch size and learning rate (Kandel & Castelli, 2020; Wilson & Martinez, 2020). Therefore, the authors use three values of learning rate; a small (i.e. 0.0001) and a large (i.e. 0.01) learning rate values, which greatly affect the behavior of the performance metrics. For the large value of 0.01, the model converges slowly, however, for a value of 0.0001, the model converges too fast. Thus, the authors have selected a learning rate value of 0.001, which achieves the best performance metrics as shown in the tables in the next subsections.

Results of Two Classes

Group 1 contains two classes, which are Normal and Abnormal (Other). Table 4 shows the scores for each class, where the highest precision value is for the Normal class with 97% versus 91% for abnormal class, which means that 97% of the predicted labels are correct as well as 91% of the abnormal class. Then, the highest Recall is for the Abnormal class (Other) with 95% which means that 95% of the predicted labels are incorrect, besides to 94% for the labels in the Normal class labels. Furthermore, the high precision and recall rates mean that the model labeled the images of Normal and Abnormal classes correctly. In addition, the good F1 score value goes to the Normal class with 95% which means that the model predicts the Normal class better than the Abnormal one (Other).

Table 3. Learning rates and performance metrics for a batch size of 32 (two classes)

Batch size	Learning rate	Precision	Recall	F1 score
32	0.01	30.60%	50.0%	37.96%
32	0.001	**93.78%**	**94.56%**	**94.13%**
32	0.0001	83.60%	85.04%	82.13%

Table 4. Average scores for two classes

Class	Precision	Recall	F1 score
Normal	97%	94%	95%
Abnormal (Other)	91%	95%	93%

143

Results of Three Classes

Group 2 contains three classes, which are Q class, F class, and V class. Table 6 shows that the F class gets the highest precision value of 100% which means that 100% of the predicted labels are correct, 99% are correct labels for Q class and 86% for V class. In addition, class V gets the highest Recall value and 100% of the predicted labels are incorrect, 96% for Q class and 85% for F class. Moreover, Q class gets the best F1 score value with 98% which means that the model predicts the class Q better than the other classes.

Table 5. Learning rates and performance metrics for a batch size of 32 (three classes)

Batch size	Learning rate	Precision	Recall	F1 score
32	0.01	11.79 %	33.33 %	17.42 %
32	0.001	**95.14 %**	**93.65 %**	**94.01 %**
32	0.0001	90.71 %	86.88 %	87.54 %

Table 6. Average scores for three classes

Class	Precision	Recall	F1 score
F	100 %	85 %	92 %
Q	99 %	96 %	98 %
V	86 %	100 %	92 %

144

Results of Four Classes

Group 3 contains four classes, which are F class, Q class, S class, and V class. Table 8 shows that the highest precision goes for Q class with 100% of correct predicted labels versus 99% for F and S classes and 87% for V class. Next, the highest Recall value is for S and V classes with 100% of incorrect predicted labels, 96% for Q class and 86% for F class. And the best F1 score value is for S class with 100%, which means that S class is predicted well than the other classes.

Table 7. Learning rates and performance metrics for a batch size of 32 (four classes)

Batch size	Learning rate	Precision	Recall	F1 score
32	0.01	88.10%	87.27%	87.39%
32	0.001	**96.44%**	**95.57%**	**95.77%**
32	0.0001	93.75%	91.96%	92.27%

Table 8. Average scores for four classes

Class	Precision	Recall	F1 score
F	99 %	86 %	92 %
Q	100 %	96 %	98 %
S	99 %	100 %	100 %
V	87 %	100 %	93 %

Results of Five Classes

The last group contains five classes, which are F class, Q class, S class, V class, and N class. Table 10 shows that the highest precision goes for F, S, and Q classes with 100% of correct predicted labels, versus 85% for N class and 91% for V class. Then, the highest Recall value is for S and N classes with 100% of incorrect predicted class, against 87% for F class, 94% for Q class and 99% for V class. And the best F1 score value is for S class with 100%, the model classify well S class than the other classes.

Table 9. Learning rates and performance metrics for a batch size of 32 (five classes)

Batch size	Learning rate	Precision	Recall	F1 score
32	0.01	24.74 %	21.96 %	13.74 %
32	**0.001**	**95.14 %**	**93.97 %**	**94.10 %**
32	0.0001	87.02 %	80.80 %	80.44 %

Table 10. Average scores for five classes

Class	Precision	Recall	F1 score
F	100 %	87 %	87 %
N	85 %	100 %	92 %
Q	100 %	94 %	97 %
S	100 %	100 %	100 %
V	91 %	99 %	95 %

To show the model's detailed performances, the confusion matrices of the whole classes are presented in Figures 7 and 8, the dark color of the diagonal elements shows the correct classifications, while the other elements represent incorrect classifications.

The confusion matrices of the proposed model were created using the test data set. The proposed CNN model correctly classified 1733 of the 1840 images belonging to the five test classes. These results are reached by using the best weights values.

Figure 9. The confusion matrix in the right presents the binary classification (Normal and abnormal (other class)), and the left confusion matrix shows the three abnormal classes (F, Q, and F)
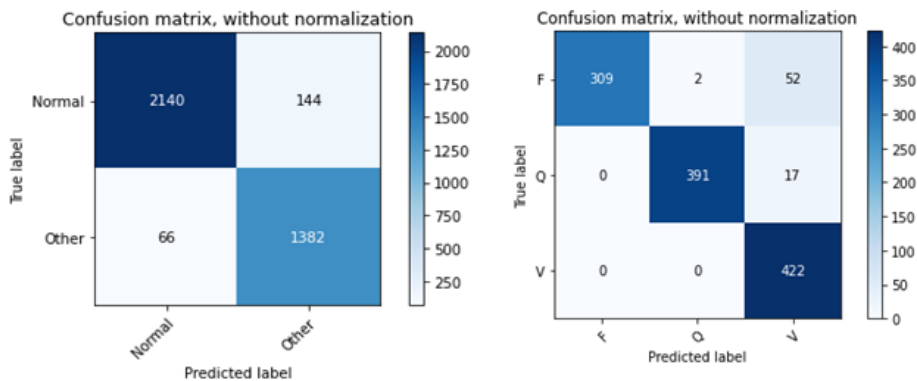
Figure 10. The confusion matrix in the right shows four abnormal classes (F, Q, S, and V), and the left confusion matrix shows five classes (F, Q, S, N, and N)

147
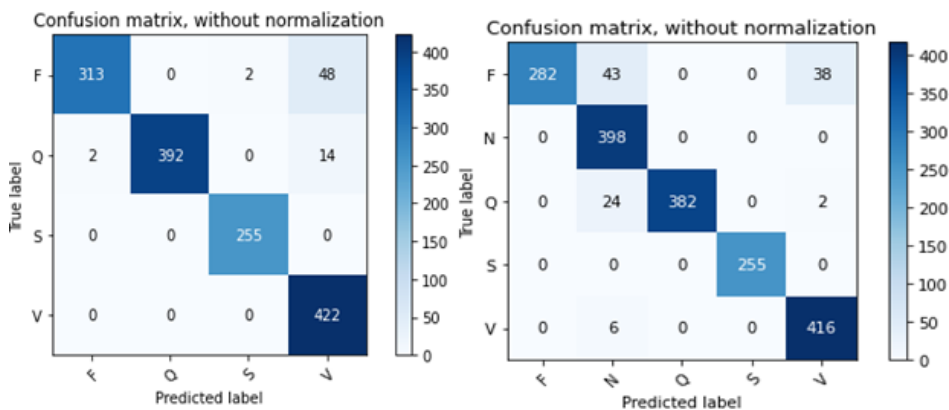
Discussion

As mentioned in the related work section, 2D CNN models are most commonly used for arrhythmia classification, therefore, the proposed CNN model used the 2D representation, by converting the ECG signals from 1D to 2D form in order to reap the benefits of the success of CNNs. Table 11 shows the performance of the proposed model compared to others, using 2D ECG images with different approaches. The authors mention that the comparison of the proposed CNN model with other existing algorithms and methods may be inappropriate due to variations in the size of the used ECG images, the architecture of the models, the number of classes used for classification, and the dataset. Therefore, they create different models and test them with the same data characteristics to make a fair comparison. The results of these latter are almost equal, but as shown in Table 11, the proposed CNN (2) is the model that gets the highest metrics when compared to the other models. The proposed CNN model (2) has achieved good results compared to the handcrafted other CNNs in terms of sensitivity, precision, recall, and F1 score for the whole classes among the other CNN hand-built models. The proposed CNN model achieves a better sensitivity in three classes in comparison with CNN, a better recall value than the SVM algorithm, and a better sensitivity rate in four classes in comparison with Feedforward Neural Network (FFNN).

148

Table 11. Comparison of the proposed model with other classification techniques

Model	Classes	Sensitivity %	Recall %	Precision %	F1 Score %
LS-SVM [84]	3	86.16	99.17	97.01	91
SVM [85]	6	93.83	90.49	-	-
FFNN [86]	4	96.31	97.78	-	-
RNN [87]	4	98.15	97.78	-	-
KNN(88)	17	96.60	95.80	-	-
Proposed Model (1)	2	94.71	94.71	93.64	94.12
	3	93.51	92.10	93.80	92.50
	4	93.87	91.19	93.87	90.81
	5	93.00	91.03	93.00	91.26
Proposed Model (2)	2	**93.78**	**94.56**	**93.78**	**94.13**
	3	**95.14**	**93.65**	**95.14**	**94.01**
	4	**96.44**	**95.57**	**96.57**	**96.77**
	5	**95.14**	**93.97**	**95.14**	**94.10**
Proposed Model (3)	2	86.60	88.54	86.60	86.38
	3	91.11	88.32	91.11	88.84
	4	94.96	93.40	94.96	93.71
	5	91.89	89.32	91.89	89.46
Proposed Model (4)	2	71.26	73.5	76.20	67.82
	3	94.35	92.61	94.35	92.96
	4	93.48	91.07	93.48	91.54
	5	88.75	86.82	88.69	86.70
Proposed Model (5)	2	92.48	90.24	92.48	91.12
	3	84.85	76.75	84.85	77.31
	4	91.14	86.94	91.14	87.52
	5	91.04	88.00	91.04	87.94

Detecting cardiac arrhythmias is a task that needs hours and careful observations of ECG recording by clinical experts. Automating this task using the author's best model could improve the performance of cardiologists' diagnosis.

After training and compiling the proposed model, the performance scores are generated for each class. In Figure 11, many examples of image classification are presented, the actual class is above each image, and the model prediction and model's confidence for each class are put below. It also shows the actual class and the set of confidence assigned by the model to each class. Sometimes, it is noticed that the confidence score is high, which means a good prediction, and in other times, it is low, which is normal because of the error rate margin, and the model will learn by experience.

Figure 11. Results of predicted classes

Actual Class : V

Class: V , confidence: 97.34
Class: Q , confidence: 2.001
Class: F , confidence: 0.655
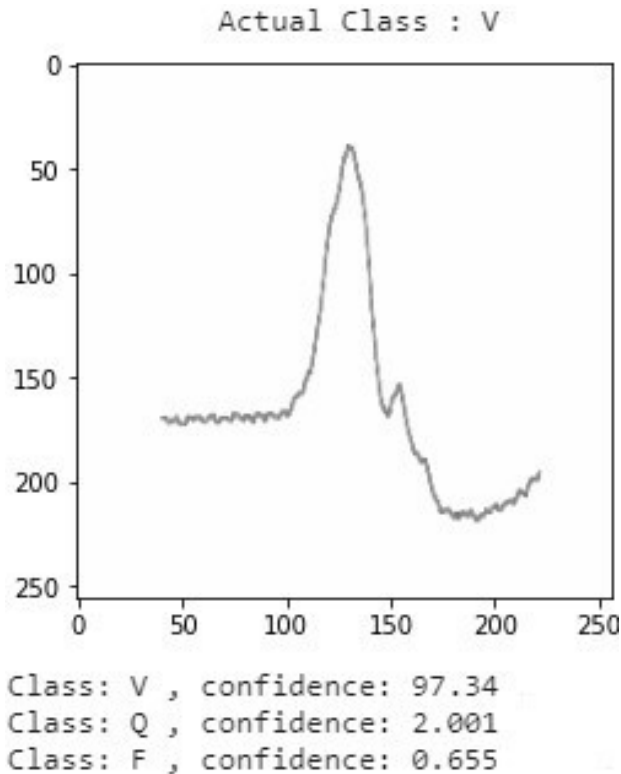
CONCLUSION

The use of deep learning models like CNN in medicine has a great utility while it can widely simplify the work of clinical experts and doctors. For example, the authors have proposed a 2D CNN model that can classify heart arrhythmias of different types based on 2D ECG images. Hence, the model was given 2D representation as input instead of 1D representation, which minimizes the signal noise, thus, the authors do not apply any method of data pre-processing. The proposed model contains three convolutional layers to extract the relevant information from images, three pooling layers to down-sample the feature maps obtained from the previous layer, two dropout layers to avoid over-fitting, and a final fully connected layer. This model gives good results for the whole arrhythmia classes detection, for instance, the classification of four classes gives a precision rate of 96.44% and an F1 Score rate of 95.77%. Reached results show that the proposed model performs well in Cardiac Arrhythmia diagnosis. Moreover, the authors should mention that the model

150

has a total of 151,882 parameters, which makes it a lightweight model that can be applied in real time uses. In the future, the authors can integrate a huge number of arrhythmia types and increase the complexity of the CNN architecture; they can also add multiple ECG leads.

REFERENCES

Abdi, A. H., Luong, C., Tsang, T., Allan, G., Nouranian, S., Jue, J., Hawley, D., Fleming, S., Gin, K., Swift, J., Rohling, R., & Abolmaesumi, P. (2017). Automatic quality assessment of echocardiograms using convolutional neural networks: Feasibility on the apical four-chamber view. *IEEE Transactions on Medical Imaging*, *36*(6), 1221–1230. doi:10.1109/TMI.2017.2690836 PMID:28391191

Ahmed, N., Natarajan, T., & Rao, K. R. (1974). Discrete cosine transform. *IEEE Transactions on Computers*, *C-23*(1), 90–93. https://doi.org/10.1109/t-c.1974.223784

Alloghani, M., Al-Jumeily, D., Mustafina, J., Hussain, A., & Aljaaf, A. J. (2019). A systematic review on supervised and unsupervised machine learning algorithms for Data Science. *Unsupervised and Semi-Supervised Learning*, 3–21. doi:10.1007/978-3-030-22475-2_1

An Introduction to Autoencoders: Everything You Need to Know. (n.d.). Retrieved February 16, 2022, from https://www.v7labs.com/blog/autoencoders-guide#autoencoders-intro

Analytics Vidhya. (2020, October 19). *CNN image classification: Image Classification using CNN*. Retrieved February 16, 2022, from https://www.analyticsvidhya.com/blog/2020/02/learn-image-classification-cnn-convolutional-neural-networks-3-datasets/

Analytics Vidhya. (2021, May 27). *Supervised deep learning algorithms*: *Types and applications*. Retrieved November 18, 2021, from https://www.analyticsvidhya.com/blog/2021/05/introduction-to-supervised-deep-learning-algorithms/

Antoine, J.-P. (2003). Wavelet transforms and their applications wavelet transforms and their applications, Lokenath Debnath, Birkhäuser, Boston, 2002. $79.95 (565 pp.). ISBN 0-8176-4204-8. *Physics Today*, *56*(4), 68–68. https://doi.org/10.1063/1.1580056

Anwar, S. M., Gul, M., Majid, M., & Alnowami, M. (2018). Arrhythmia classification of ecg signals using hybrid features. *Computational and Mathematical Methods in Medicine*, *2018*, 1–8. doi:10.1155/2018/1380348 PMID:30538768

Avendi, M. R., Kheradvar, A., & Jafarkhani, H. (2016). A combined deep-learning and deformable-model approach to fully automatic segmentation of the left ventricle in cardiac MRI. *Medical Image Analysis*, *30*, 108–119. doi:10.1016/j.media.2016.01.005 PMID:26917105

Azad, M., Khaled, F., & Pavel, M. I. (2019). A novel approach to classify and convert 1D signal to 2D grayscale image implementing support vector machine and empirical mode decomposition algorithm. *International Journal of Advanced Research*, *7*(1), 328–335. https://doi.org/10.21474/ijar01/8331

Bank, D., Koenigstein, N., & Giryes, R. (2021, April 3). *Autoencoders*. Retrieved November 19, 2021, from https://arxiv.org/abs/2003.05991

Berrahal, M., & Azizi, M. (2021). Augmented binary multi-labeled CNN for practical facial attribute classification. *Indonesian Journal of Electrical Engineering and Computer Science*, *23*(2), 973. https://doi.org/10.11591/ijeecs.v23.i2.pp973-979

Bradley, A. P. (1997). The use of the area under the ROC curve in the evaluation of machine learning algorithms. *Pattern Recognition*, *30*(7), 1145–1159. https://doi.org/10.1016/s0031-3203(96)00142-2

Brigham, E. O., & Morrow, R. E. (1967). The fast fourier transform. *IEEE Spectrum*, *4*(12), 63–70. https://doi.org/10.1109/mspec.1967.5217220

Brownlee, J. (2019, July 5). *A gentle introduction to pooling layers for Convolutional Neural Networks*. Machine Learning Mastery. Retrieved November 19, 2021, from https://machinelearningmastery.com/pooling-layers-for-convolutional-neural-networks/

Brownlee, J. (2020, April 16). *How do convolutional layers work in Deep Learning Neural Networks?* Machine Learning Mastery. Retrieved October 15, 2021, from https://machinelearningmastery.com/convolutional-layers-for-deep-learning-neural-networks/

Commandeur, F., Goeller, M., Betancur, J., Cadet, S., Doris, M., Chen, X., Berman, D. S., Slomka, P. J., Tamarappoo, B. K., & Dey, D. (2018). Deep learning for quantification of epicardial and thoracic adipose tissue from Non-Contrast CT. *IEEE Transactions on Medical Imaging*, *37*(8), 1835–1846. doi:10.1109/TMI.2018.2804799 PMID:29994362

Culurciello, E. (2018, December 24). *Navigating the unsupervised learning landscape*. Medium. Retrieved November 19, 2021, from https://medium. com/intuitionmachine/navigating-the-unsupervised-learning-landscape-951bd5842df9#:~:text=Unsupervised%20learning%20is%20the%20Holy,be%20 trained%20with%20little%20data.&text=Today%20Deep%20Learning%20 models%20are,there%20is%20a%20corresponding%20label

Diller, G.-P., Babu-Narayan, S., Li, W., Radojevic, J., Kempny, A., Uebing, A., Dimopoulos, K., Baumgartner, H., Gatzoulis, M. A., & Orwat, S. (2019). Utility of machine learning algorithms in assessing patients with a systemic right ventricle. *European Heart Journal Cardiovascular Imaging*, *20*(8), 925–931. doi:10.1093/ ehjci/jey211 PMID:30629127

Du, X., Song, Y., Liu, Y., Zhang, Y., Liu, H., Chen, B., & Li, S. (2020). An integrated deep learning framework for joint segmentation of Blood Pool and myocardium. *Medical Image Analysis*, *62*, 101685. doi:10.1016/j.media.2020.101685 PMID:32272344

El Omary, S., Lahrache, S., & El Ouazzani, R. (2021). Detecting heart failure from chest X-ray images using deep learning algorithms. *2021 3rd IEEE Middle East and North Africa COMMunications Conference (MENACOMM)*. 10.1109/ MENACOMM50742.2021.9678291

Emad, O., Yassine, I. A., & Fahmy, A. S. (2015). Automatic localization of the left ventricle in cardiac MRI images using Deep Learning. *2015 37th Annual International Conference of the IEEE Engineering in Medicine and Biology Society (EMBC)*. 10.1109/EMBC.2015.7318454

Esteva, A., Chou, K., Yeung, S., Naik, N., Madani, A., Mottaghi, A., Liu, Y., Topol, E., Dean, J., & Socher, R. (2021, January 8). *Deep learning-enabled Medical Computer Vision*. Nature News. Retrieved November 19, 2021, from https://www. nature.com/articles/s41746-020-00376-2

Explorium. (2021, July 11). *Unsupervised learning wiki*. Retrieved November 19, 2021, from https://www.explorium.ai/wiki/unsupervised-learning/

Green, M., Marom, E. M., Konen, E., Kiryati, N., & Mayer, A. (2018). 3-D neural denoising for low-dose coronary CT angiography (CCTA). *Computerized Medical Imaging and Graphics*, *70*, 185–191. doi:10.1016/j.compmedimag.2018.07.004 PMID:30093171

Grossi, E., & Buscema, M. (2007). Introduction to artificial neural networks. *European Journal of Gastroenterology & Hepatology*, *19*(12), 1046–1054. doi:10.1097/ MEG.0b013e3282f198a0 PMID:17998827

Güler, İ., & Übeylı˙, E. D. (2005). ECG beat classifier designed by combined neural network model. *Pattern Recognition*, *38*(2), 199–208. https://doi.org/10.1016/j.patcog.2004.06.009

Gülsün, M. A., Funka-Lea, G., Sharma, P., Rapaka, S., & Zheng, Y. (2016). Coronary centerline extraction via optimal flow paths and CNN path pruning. *Lecture Notes in Computer Science*, *9902*, 317–325. doi:10.1007/978-3-319-46726-9_37

Hadjem, M., & Nait-Abdesselam, F. (2015). An ECG T-wave anomalies detection using a lightweight classification model for WIRELESS body sensors. *2015 IEEE International Conference on Communication Workshop (ICCW)*. 10.1109/ICCW.2015.7247191

Hannun, A. Y., Rajpurkar, P., Haghpanahi, M., Tison, G. H., Bourn, C., Turakhia, M. P., & Ng, A. Y. (2019). Cardiologist-level arrhythmia detection and classification in ambulatory electrocardiograms using a deep neural network. *Nature Medicine*, *25*(1), 65–69. doi:10.103841591-018-0268-3 PMID:30617320

Hatipoglu, B., Yilmaz, C. M., & Kose, C. (2018). A signal-to-image transformation approach for EEG and Meg Signal Classification. *Signal, Image and Video Processing*, *13*(3), 483–490. https://doi.org/10.1007/s11760-018-1373-y

Hua, Y., Guo, J., & Zhao, H. (2015). Deep belief networks and Deep Learning. *Proceedings of 2015 International Conference on Intelligent Computing and Internet of Things*. 10.1109/ICAIOT.2015.7111524

Huang, J., Chen, B., Yao, B., & He, W. (2019). ECG arrhythmia classification Using STFT-Based spectrogram and convolutional neural network. *IEEE Access: Practical Innovations, Open Solutions*, *7*, 92871–92880. https://doi.org/10.1109/access.2019.2928017

Humphreys, M., Warlow, C., & McGowan, J. (2013). Arrhythmias and their management. *Nursing the Cardiac Patient,* 132–155. doi:10.1002/9781118785331.ch10

Introduction to convolutional neural networks. (n.d.). Retrieved November 19, 2021, from https://cs.nju.edu.cn/wujx/paper/CNN.pdf

Isin, A., & Ozdalili, S. (2017). Cardiac arrhythmia detection using deep learning. *Procedia Computer Science*, *120*, 268–275. doi:10.1016/j.procs.2017.11.238

Jin, C., Feng, J., Wang, L., Yu, H., Liu, J., Lu, J., & Zhou, J. (2018). Left atrial appendage segmentation and quantitative assisted diagnosis of atrial fibrillation based on fusion of temporal-spatial information. *Computers in Biology and Medicine*, *96*, 52–68. doi:10.1016/j.compbiomed.2018.03.002 PMID:29547711

Johnson, D. (2022, February 12). *Supervised vs unsupervised learning: Key differences*. Guru99. Retrieved February 16, 2022, from https://www.guru99.com/supervised-vs-unsupervised-learning.html

Jun, T., Nguyen, H.M., Kang, D., Kim, D., Kim, D., & Kim, Y. (2018). *ECG arrhythmia classification using a 2-D convolutional neural network*. ArXiv, abs/1804.06812.

Jun, T., Nguyen, H.M., Kang, D., Kim, D., Kim, D., & Kim, Y. (2018). *ECG arrhythmia classification using a 2-D convolutional neural network*. ArXiv, abs/1804.06812.

Kandel, I., & Castelli, M. (2020). The effect of batch size on the generalizability of the Convolutional Neural Networks on a histopathology dataset. *ICT Express*, *6*(4), 312–315. doi:10.1016/j.icte.2020.04.010

Ke, Q., Liu, J., Bennamoun, M., An, S., Sohel, F., & Boussaid, F. (2018). Computer vision for human–machine interaction. *Computer Vision for Assistive Healthcare*, 127–145. doi:10.1016/B978-0-12-813445-0.00005-8

Kherraki, A., Maqbool, M., & El Ouazzani, R. (2021). Traffic scene semantic segmentation by using several deep convolutional neural networks. *2021 3rd IEEE Middle East and North Africa COMMunications Conference (MENACOMM)*. doi:10.1109/menacomm50742.2021.9678270

Kiranyaz, S., Ince, T., & Gabbouj, M. (2016). Real-Time patient-specific ECG classification BY 1-D convolutional neural networks. *IEEE Transactions on Biomedical Engineering*, *63*(3), 664–675. doi:10.1109/TBME.2015.2468589 PMID:26285054

Klein, G. J. (2018). *Strategies for Ecg arrhythmia Diagnosis: Breaking down complexity*. Cardiotext Publishing.

Labs, I. C. (2018, August 8). *Deep belief networks - all you need to know*. Medium. Retrieved November 19, 2021, from https://medium.com/@icecreamlabs/deep-belief-networks-all-you-need-to-know-68aa9a71cc53

Lessmann, N., van Ginneken, B., Zreik, M., de Jong, P. A., de Vos, B. D., Viergever, M. A., & Isgum, I. (2018). Automatic calcium scoring in low-dose chest CT using deep neural networks with dilated convolutions. *IEEE Transactions on Medical Imaging*, *37*(2), 615–625. doi:10.1109/TMI.2017.2769839 PMID:29408789

López-Linares, K., Aranjuelo, N., Kabongo, L., Maclair, G., Lete, N., Ceresa, M., García-Familiar, A., Macía, I., & González Ballester, M. A. (2018). Fully automatic detection and segmentation of abdominal aortic thrombus in post-operative CTA images using deep convolutional neural networks. *Medical Image Analysis*, *46*, 202–214. doi:10.1016/j.media.2018.03.010 PMID:29609054

Lossau, T., Nickisch, H., Wissel, T., Bippus, R., Schmitt, H., Morlock, M., & Grass, M. (2019). Motion artifact recognition and quantification in coronary ct angiography using Convolutional Neural Networks. *Medical Image Analysis*, *52*, 68–79. doi:10.1016/j.media.2018.11.003 PMID:30471464

Mayo Foundation for Medical Education and Research. (2021, October 1). *Heart arrhythmia*. Mayo Clinic. Retrieved February 15, 2022, from https://www.mayoclinic.org/diseases-conditions/heart-arrhythmia/symptoms-causes/syc-20350668

Montufar, G. (2018, June 19). *Restricted Boltzmann machines: Introduction and review*. Retrieved November 19, 2021, from https://arxiv.org/abs/1806.07066

Moody, G., & Mark, R. (2005, February 24). *MIT-BIH arrhythmia database*. MIT-BIH Arrhythmia Database v1.0.0. Retrieved September 26, 2021, from https://physionet.org/content/mitdb/1.0.0/

Moradi, M., Madani, A., Gur, Y., Guo, Y., & Syeda-Mahmood, T. (2018). Bimodal network architectures for automatic generation of image annotation from text. Medical Image Computing and Computer Assisted Intervention, 449–456. doi:10.1007/978-3-030-00928-1_51

Mustaqeem, A., Anwar, S. M., Khan, A. R., & Majid, M. (2017). A statistical analysis based recommender model for heart disease patients. *International Journal of Medical Informatics*, *108*, 134–145. doi:10.1016/j.ijmedinf.2017.10.008 PMID:29132619

Namara, K. M., Alzubaidi, H., & Jackson, J. K. (2019). Review of Cardiovascular disease as a leading cause of death: How are pharmacists getting involved? *Integrated Pharmacy Research & Practice*.

Nguyen, K. (2021, October 12). *Detecting heart abnormalities using 1D CNN on data you cannot see*. Medium. Retrieved November 19, 2021, from https://towardsdatascience.com/detecting-heart-abnormalities-using-1d-cnn-on-data-you-cannot-see-with-pysyft-735481a952d8

NHS. (n.d.). *NHS choices*. Retrieved February 16, 2022, from https://www.nhs.uk/conditions/electrocardiogram/

Open Data Science. (2020, November 5). *The A – Z of supervised learning, use cases, and disadvantages*. Retrieved November 19, 2021, from https://opendatascience.com/the-a-z-of-supervised-learning-use-cases-and-disadvantages/

Østvik, A., Smistad, E., Aase, S. A., Haugen, B. O., & Lovstakken, L. (2019). Real-time standard view classification in transthoracic echocardiography using Convolutional Neural Networks. *Ultrasound in Medicine & Biology*, *45*(2), 374–384. doi:10.1016/j.ultrasmedbio.2018.07.024 PMID:30470606

Park, J., Lee, K., & Kang, K. (2013). Arrhythmia detection from heartbeat using k-nearest neighbor classifier. *2013 IEEE International Conference on Bioinformatics and Biomedicine*. doi:10.1109/bibm.2013.6732594

Prabhu. (2019, November 21). *Understanding of convolutional neural network (CNN) - Deep learning*. Medium. Retrieved November 21, 2021, from https://medium.com/@RaghavPrabhu/understanding-of-convolutional-neural-network-cnn-deep-learning-99760835f148

Rahhal, M. M. A., Bazi, Y., AlHichri, H., Alajlan, N., Melgani, F., & Yager, R. R. (2016). Deep learning approach for active classification of electrocardiogram signals. *Information Sciences*, *345*, 340–354. doi:10.1016/j.ins.2016.01.082

Rim, B., Sung, N.-J., Min, S., & Hong, M. (2020). Deep learning in Physiological Signal Data: A survey. *Sensors (Basel)*, *20*(4), 969. https://doi.org/10.3390/s20040969

Sahoo, J. P. (2011). Analysis of ECG signal for Detection of Cardiac Arrhythmias. National Institute of Technology, Rourkela.

Salem, M., Taheri, S., & Yuan, J.-S. (2018). ECG arrhythmia classification using transfer learning From 2- DIMENSIONAL Deep CNN Features. *2018 IEEE Biomedical Circuits and Systems Conference (BioCAS)*. 10.1109/BIOCAS.2018.8584808

Sherstinsky, A. (2020). Fundamentals of Recurrent Neural Network (RNN) and long short-term memory (LSTM) network. *Physica D. Nonlinear Phenomena*, *404*, 132306. doi:10.1016/j.physd.2019.132306

Sidey-Gibbons, J. A., & Sidey-Gibbons, C. J. (2019). Machine learning in medicine: A practical introduction. *BMC Medical Research Methodology*, *19*(1), 64. Advance online publication. doi:10.118612874-019-0681-4 PMID:30890124

Signal Processing: A mathematical approach, second. (n.d.). Retrieved November 19, 2021, from https://library.oapen.org/bitstream/id/3eb04f39-67d7-4b4d-8569-3185fbefd944/1005624.pdf

Solutions, E. (2016, November 11). *Accuracy, precision, recall & f1 score: Interpretation of performance measures.* Exsilio Blog. https://blog.exsilio.com/all/accuracy-precision-recall-f1-score-interpretation-of-performance-measures/

Staudemeyer, R. C., & Morris, E. R. (2019, September 12). *Understanding LSTM — a tutorial into long short-term memory recurrent neural networks.* Retrieved February 16, 2022, from https://arxiv.org/abs/1909.09586

Sun, Y., Chan, K. L., & Krishnan, S. M. (2005). Characteristic wave detection In ECG signal using Morphological transform. *BMC Cardiovascular Disorders*, *5*(1), 28. Advance online publication. doi:10.1186/1471-2261-5-28 PMID:16171531

SuperDataScience. (n.d.). Retrieved November 19, 2021, from https://www.superdatascience.com/blogs/recurrent-neural-networks-rnn-the-vanishing-gradient-problem

Taheri Dezaki, F., Liao, Z., Luong, C., Girgis, H., Dhungel, N., Abdi, A. H., Behnami, D., Gin, K., Rohling, R., Abolmaesumi, P., & Tsang, T. (2019). Cardiac phase detection in echocardiograms with densely gated recurrent neural networks and global extrema loss. *IEEE Transactions on Medical Imaging*, *38*(8), 1821–1832. doi:10.1109/TMI.2018.2888807 PMID:30582532

Takalo-Mattila, J., Kiljander, J., & Soininen, J. P. (2018). Inter-patient ECG classification using deep convolutional neural networks. In N. Konofaos, M. Novotny, & A. Skavhaug (Eds.), *2018 21st Euromicro Conference on Digital System Design* (pp. 421-425). IEEE Institute of Electrical and Electronic Engineers. doi:10.1109/DSD.2018.00077

Toh, C., & Brody, J. (2021). Applications of machine learning in Healthcare. *Smart Manufacturing - When Artificial Intelligence Meets the Internet of Things*. doi:10.5772/intechopen.92297

Übeyli, E. D. (2009). Combining recurrent neural networks WITH eigenvector methods for classification of ECG beats. *Digital Signal Processing*, *19*(2), 320–329. https://doi.org/10.1016/j.dsp.2008.09.002

Ullah, W., Siddique, I., Zulqarnain, R. M., Alam, M. M., Ahmad, I., & Raza, U. A. (2021). Classification of arrhythmia in Heartbeat detection using deep learning. *Computational Intelligence and Neuroscience*, *2021*, 1–13. doi:10.1155/2021/2195922 PMID:34712316

Wilson, D. R., & Martinez, T. R. (2020). The need for small learning rates on large problems. IJCNN'01. *International Joint Conference on Neural Networks. Proceedings.* doi:10.1109/ijcnn.2001.939002

World Health Organization. (n.d.). *Cardiovascular diseases*. World Health Organization. Retrieved February 16, 2022, from https://www.who.int/health-topics/cardiovascular-diseases#tab=tab_1

Yamada, M. (2006). Wavelets: Applications. *Encyclopedia of Mathematical Physics*, 420–426. doi:10.1016/b0-12-512666-2/00242-x

Yao, Q., Wang, R., Fan, X., Liu, J., & Li, Y. (2020). Multi-class arrhythmia detection from 12-lead varied-length ECG using Attention-based time-incremental convolutional neural network. *Information Fusion*, *53*, 174–182. doi:10.1016/j.inffus.2019.06.024

Ye, C., Coimbra, M. T., & Vijaya Kumar, B. V. (2010). Arrhythmia detection and classification using morphological and dynamic features of ECG signals. *2010 Annual International Conference of the IEEE Engineering in Medicine and Biology*. 10.1109/IEMBS.2010.5627645

Yi, H., Sun, S., Duan, X., & Chen, Z. (2016). A study on Deep Neural Networks Framework. *2016 IEEE Advanced Information Management, Communicates, Electronic and Automation Control Conference (IMCEC)*. 10.1109/IMCEC.2016.7867471

Yildirim, Ö. (2018). A novel wavelet sequence based on deep bidirectional LSTM network model for ECG signal classification. *Computers in Biology and Medicine*, *96*, 189–202. doi:10.1016/j.compbiomed.2018.03.016 PMID:29614430

Yıldırım, Ö., Pławiak, P., Tan, R.-S., & Acharya, U. R. (2018). Arrhythmia detection using deep convolutional neural network with long duration ECG signals. *Computers in Biology and Medicine*, *102*, 411–420. doi:10.1016/j.compbiomed.2018.09.009 PMID:30245122

ADDITIONAL READING

Hernández-Madrid, A., Paul, T., Abrams, D., Aziz, P. F., Blom, N. A., Chen, J., Chessa, M., Combes, N., Dagres, N., Diller, G., Ernst, S., Giamberti, A., Hebe, J., Janousek, J., Kriebel, T., Moltedo, J., Moreno, J., Peinado, R., Pison, L., ... Dubin, A. (2018). Arrhythmias in congenital heart disease: A position paper of the European Heart Rhythm Association (EHRA), association for European paediatric and congenital cardiology (AEPC), and the European Society of Cardiology (ESC) Working Group on grown-up congenital heart disease, endorsed by HRS, paces, APHRS, and Solaece. *EP Europace*, *20*(11), 1719–1753. doi:10.1093/europace/eux380 PMID:29579186

Moulay, S., Morocco, M., Slimane, M., & Morocco, B. M. (2012). AR Modeling for Cardiac Arrhythmia Classification using MLP. *Neural Networks*.

Raach, O., Pillai, T. R., & Abdullah, A. B. (2018). GARMA Modeling of ECG and Classification of Arrhythmia. *2018 8th International Conference on Intelligent Systems, Modelling and Simulation (ISMS)*, 26-31.

Singh, A. (2018, October 24). *ECG arrhythmia classification using a 2-D convolutional neural network*. Medium. Retrieved March 4, 2022, from https://medium.datadriveninvestor.com/ecg-arrhythmia-classification-using-a-2-d-convolutional-neural-network-33aa586bad67

Sraitih, M., Jabrane, Y., & Hajjam El Hassani, A. (2021). An automated system for ECG arrhythmia detection using machine learning techniques. *Journal of Clinical Medicine*, *10*(22), 5450. doi:10.3390/jcm10225450 PMID:34830732

KEY TERMS AND DEFINITIONS

2D Images: A number of pixels that are presented in a 2 dimensional space that includes horizontal and vertical dimensions. In this chapter the authored used CNNs with 2D images.

Arrhythmia Disease: It is a disturbance of the heartbeat that does not necessarily follow a slow or fast rhythm. Most people experience this, but sometimes it can be serious and lead to different types of illness.

Artificial Intelligence: It is widely used in various applications and can be defined as an ensemble of algorithms that make computers and machines capable to learn by themselves.

Artificial Neural Networks (ANNs): ANNs are a set of units that are connected to each other in a way that mimics the human brain and form the basis of every deep learning architecture.

Classification Issues: Classification problems in deep learning refer to the assignment of a specific label to a specific image. In this chapter the authors classify 2D images into different types of classes.

Convolutional Neural Networks (CNNs): CNNs are a class of deep learning models; they perform well on image issues due to convolutional blocks that extract the main part of the images. CNNs are the category of models used in this chapter.

Deep Learning: It is a category of artificial intelligence that combines a variety of models that are fundamentally based on artificial neural networks.

ECG Signals: ECG signals are the signals produced by electrocardiograms that represent the electrical activity of the heart. Based on these signals, cardiologists can identify various cardiovascular problems and diseases.

160

Section 3

COVID−19 Diagnosis and Treatment Using AI

Chapter 6

Intelligibility of Nonparametric Survival Analysis for Health Security Policy Evaluation:
Application to the Analysis of COVID-19 Data

Hamlili Ali
Mohammed V University of Rabat, Morocco

ABSTRACT

Survival analysis is one of the most important research topics in probability and statistics applications to health and medical data. Its implementation has caught the attention of a large community of researchers from several skills including data analysis, statistical modeling, data mining, data science, and artificial intelligence. Survivor function and death intensity allow the analyst to assess the dynamics of the proportion of deaths and the risk of death over time. This chapter proposes an approach to the analysis of interval-censored survival data based on plug-in estimation as well as tools to assess the predictive quality of these estimators. Graphical tests are provided to support the choice between health security policies with the objective of leading to low mortality. The intertwining of this method with artificial intelligence tools paves the way for both personalized, precise, and efficient medicine and automated, informed, and rapid decision-making in health security.

INTRODUCTION

To meet the needs of collecting and interpreting medical and health data, it is necessary more than ever to introduce methods of machine learning (ML) and artificial intelligence (AI). This will allow medicine to enter a new era where diagnoses will be more precise, clinical dashboards more complete and treatments more personalized. Also, it will allow health services and governments to fully exploit health data, share information, evaluate health security policies, improve them and fight effectively together against serious diseases and pandemics. The volume of data thus collected and shared could reach very large sizes. This is what, alongside the particularity (incomplete, censored, truncated) of this data, would require the intervention of very advanced methods of analysis. Survival analysis constitutes one of ML methods to meet this kind of need. It helps to answer questions that traditional data analysis methods are unable to resolve.

The use of ML for the analysis of medical and public health survival data is not new. There are various works that have referred to since the end of the twentieth century (Ripley & Ripley, 1998; Zupan et al., 2000). However, despite the abundance of tools offered today by ML, we notice that most recent works on these subjects continue to rely for decades on very old non-parametric (Kaplan & Meier, 1958), semi-parametric (Cox, 1972) and parametric (Emura & Chen, 2018; Rezaul & Ataharul, 2019) methods to drive their estimations. Thus, usually Kaplan-Meier estimate is used to evaluate the survivor function and a variant of Cox's regression model is used to measure the influence of explanatory variables on the risk of death or the survivor function itself. In this regard, we can cite various works where these approaches was used in order to analyze survival data. In (Elandt-Johnson & Johnson, 1980), the authors provide a general overview of survival data analysis methods and their applications for medical data modeling purposes. In order to conduct their analyses, they defined different disease onset distributions and several models for aging, chronic disease and mortality and they were interested in determining the proportions of deaths in some groups of individuals under well-defined conditions. To do this, they assumed that the period of exposure to the risk was known for each individual and must be recorded. For census-type data, this period was generally unknown and had to be estimated. In (Zupan et al., 2000) survival analysis is applied with the objective to investigate a particular problem of building prognostic models for prostate cancer recurrence. In this study, the authors estimated the probability of the event of interest and assigned a resulting distribution to it under censorship and to show the utility of their technique, they studied the construction of prognostic models for prostate cancer recurrence. In (Selvin, 2008) the author gives a global mathematical and practical presentation of the application of parametric statistical models to survival analysis and he answered

to various problems raised by research in the fields of epidemiology and medicine. On several occasions, the author considered AIDS data as examples to illustrate the statistical techniques he has examined. In (Hans & Hein, 2012), after reviewing the specific nature of survival data, the authors studied the properties of several survival prediction models including those of Kaplan-Meier and Cox in the case of clinical data and they presented how to implement these models. In (Léger et al., 2017), the authors studied 11 ML algorithms with 12 methods of feature selection through the concordance index for survival analysis. In this study, the authors used parametric and non-parametric survival models including the Kaplan-Meier estimator and the Cox' hazard function regression method. To illustrate their methods, they considered data extracted from CT scans of patients with head and neck squamous cell carcinoma. In (Jakobsen et al., 2020), the authors have reviewed several existing methods for estimating the cure point and discuss new clinically relevant measures for quantifying the mortality. Then they were interested in the study of the bias of the point of cure estimator and in the determination of the point of cure confidence interval through survival analysis of cancer data. Ernesto and Lusmeralis (Ernesto & Lusmeralis, 2021) studied the role played by vaccination in the dynamics of a given COVID-19 compartmental model. They have developed a computational code to mimic the first wave of the coronavirus pandemic in the state of New York and they show how a vaccine with 95% efficacy could reduce the number of deaths. In (Calabuig et al., 2021), the authors propose a complete health system management tool based on Kaplan-Meier curves. They showed on the basis of data from the first COVID-19 wave (February-June) that it is possible to deduce useful information on the dynamics of the pandemic in different countries. They also showed that the differences in pandemic evolution between countries are reflected in such curves. Jnanendra et al. used ML classification methods and survival analysis to predict certain biomarkers specific to breast cancer (Jnanendra et al., 2021). Thus, they showed how certain biomarkers' characteristics are used to select breast cancer subtypes and provide further categorization of the biomarkers.

Survival analysis considers the duration of occurrence of a given event called death. This chapter proposes an original ML method as an alternative to classical methods for analyzing survival data. The main contribution of our approach covers two main areas. The formalism used aims to provide data scientists with an in-depth knowledge of the application of inferential statistical theory and ML methods for survival analysis. Validation tools are thus developed in order to demonstrate the adequacy of the proposed models. All the methods we have exposed here have been adapted for numerical evaluation and thus proposed for computer implementation. Their implementation will be assessed against daily data of COVID-19 deaths.

DATA REPRESENTATION, MANAGEMENT AND ANALYSIS

Good data management is essential for any further analysis. The slightest defect in data collection or storage processes can make happen their loss, corrupt their integrity or distort any analysis. Thus, in medical and public health fields, poor data management can compromise the monitoring of the evolution of diseases for patients, epidemics on a national scale and pandemics on an international scale. Most data collection, and in particular the collection of survival data, is usually spread over long periods of time. To allow their storage and then their analysis, it is important that they are correctly represented. Each new data item requires to be recorded in its representation format in one or more databases. These records may depend heavily on a compilation before any analysis (Selvin, 2008).

Influence of the Nature of the Pandemic on Data Collection

During the monitoring of a disease or an epidemic, the medical or public health services concerned collect periodically (by day, week, month or year) measurements of the physical signs of the disease in a patient or separately the number of confirmed infections and deaths related to the epidemic.

Figure 1. Covid-19 transmission/illness scheme
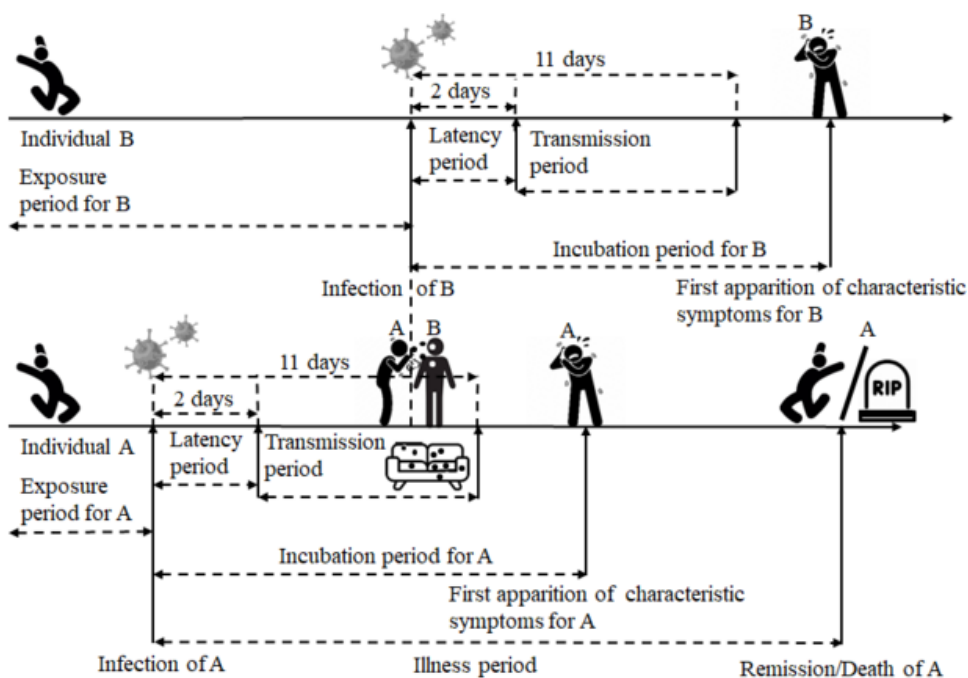
Data records are then communicated to government authorities and made available to the public (universities, laboratories, pharmaceutical industries, people) and concerned international organizations. As the reporting of isolated data is irrelevant to monitoring and analysis processes, medical and epidemic data is rarely reported in real time. This approach is also supported by the fact that for many diseases and epidemics, the absence of symptoms at the beginning of the infection makes it difficult to become aware of them. For example, like different variants of influenza, Covid-19 pandemic is a respiratory disease that is transmitted either directly after a direct exposure when a confirmed patient and the future carrier are quite close to each other, or indirectly by touching objects handled by a confirmed patient (Liu et al., 20). As the virus can survive for some time on the supports and the more specific symptoms of this disease do not appear until two weeks after infection, transmissions to other people continue to occur silently for a few days by the indirect exposure and between the second and eleventh day of the infection of a confirmed patient by direct exposure while he is still unaware of his illness (Khalik, 2020). Figure 1 illustrates the transmission cycle of the disease.

Lifetime and Data Assumptions

Lifetime Modeling

As we are mainly interested here in the statistical description of durations, we will consider the time as a random variable, from a sampling universe Ω to $\mathbb{R}_+$. So, let Ω be a sampling universe, $\mathcal{A}$ the σ-algebra of all possible events on Ω and $\mathcal{B}(\mathbb{R}_+)$ the Borel σ-algebra on $\mathbb{R}_+$. Thus, time T is a non-negative $(\Omega, \mathcal{A}) - (\mathbb{R}_+, \mathcal{B}(\mathbb{R}_+))$ measurable function, i.e.

$$\forall B \in \mathcal{B}(\mathbb{R}_+): \quad T^{-1}(B) \in \mathcal{A}$$

So, it suffices to define a probability distribution on the probability space $(\Omega, \mathcal{A})$ to deduce a probability distribution induced by T on the probability space $(\mathbb{R}_+, \mathcal{B}(\mathbb{R}_+))$. Time T might represent the lifetime which is by definition the instant when a specific event occurs and which is marked by the end of a process that began long before. In medical and health contexts, lifetime can be broadly thought of as the time elapsed until the occurrence of an event marked by the onset of infection, development of disease, disappearance of symptoms, recovery following treatment, relapse after recovery or simply death.

166

Hypotheses on the Data Model

Depending on the application framework and the objectives of the analysis, different hypotheses can be made on the analyzed data. To fix the ideas, we will assume that the following five hypotheses are always verified:

1. The event of interest is the death of an individual.
2. The regeneration of the event of interest defines a point process.
3. The observed (or monitored) feature is lifetime.
4. Lifetime observations are interval-censored.
5. Survival data is provided all at once for the purpose of the analysis.

The first four hypotheses from 1 to 4 concern the analysis of censored lifetime data. Diverse common reasons can lead to censorship. These include the fact that a concerned individual with the event of interest is lost from sight or abandoned by the follow-up, or that an individual has not experienced the event before the follow-up ends, or that an individual has experienced an unrelated event excluding him from any further follow-up. The fifth hypothesis concerns aspects of statistical inference in ML. This last hypothesis assumes a batch learning mode where all the data proposed for the training process are provided at once.

Data as a Point Process

In many areas, the data model is represented as a point stochastic process. The stochastic nature comes into play each time we wish to represent a discrete or continuous evolution of hazard. A point process representation of temporal data is a specific type of stochastic process such that each data is the realization of an isolated time random point. Survival analysis uses this type of models by referring to the end-of-duration event as "death" and the time-to-event as "lifetime". Let's consider that lifetime is represented by a non-negative random variable T. We can adopt one or both of the two following stochastic processes to model survival data:

1. The process $T \equiv \left\{ T_i \mid i \in \mathbb{N} \right\}$ of times-to-event,
2. The counting process $N \equiv \left\{ N_t \mid t \in \mathbb{R}_+ \right\}$ of event observations where N_t signifies the number of events occurring in the interval $[0,t]$.

To avoid any confusion, we will assume throughout the rest of this chapter that the indices T_i are indexed in the chronological order of occurrence of the events, $T_0=0$ and $N_0=0$.

Censoring Issues

Censoring is an essential property which characterizes time-to-event data. It arises from ignorance of the exact values of this type of data. In practice, we can find different models of censorship: right-censoring, left-censoring and interval-censoring (van den Hout, 2017; Bogaerts et al., 2018; Rezaul & Ataharul, 2019). Interval-censoring model is used when the time-to-event is not specified, but a time interval where the event occurs is known. This phenomenon is characteristic of follow-up problems and in particular of problems where event data is regularly reported.

Interval-Censoring

As is often the case with monitoring the evolution of serious diseases and pandemics, after lifetime data is collected, it is used as a single batch in the analysis. As mentioned above, rarely events are detected and their data is analyzed in real time. Thus, lifetimes are only known through their belonging to some intervals instead to be observed individually. They are said to be interval-censored. In this regard, we are led to consider a discretization grid $\{\tau_k$, k=0,1,…,Jt_j of the observation window [0,t] of time where the events are supposed to be observed and such that for Jt_j,

$$0 = \tau 0 < \tau 1 <_< \tau 2 <_{...} < \tau j \leq _t$$

Jt $d_e$notes the random number of censoring subintervals of the window of time [0,t] such that $]\tau_{k-1}, \tau_k]$ defines the kth ^{c}ensoring subinterval of this subdivision. In general, the grid $\{\tau k|_k=0,1,…,j\}$ $m$ay embody a sequence of random or deterministic finding thresholds τk wi$_t$h k=0,1,…,j. A special case of such a deterministic grid arises when [0,t] is broken down into j al$i$quots a>0, i.e.,

$$\tau_1 - \tau_0 = \tau_2 - \tau_1 = \cdots = \tau_j - \tau_{j-1} = a \text{ and } \tau j \leq t_< \tau j + a$$

In the case of recording COVID-19 data, τk re$_f$ers to the time where a compilation of the daily data is communicated. In these conditions, the grid $\{\tau k|$ k=$_0$,1,…,j$\}$ ca$n$ be identified to j con$s$ecutive days (or aliquots) of the window [0,t].

*C*ounting Process under Censoring Assumption

As above, let consider Nt=n be the number of deaths recorded until time t and Jt=j be the number of aliquots in the window [0,t]; with t>0 and n≥j. The idea is similar

168

to sectioning the interval [0,t] *i*nto j s*u*bintervals or aliquots. According to such a discretization of the window [0,t], we can write

$$
]0,t] = \begin{cases} \bigcup_{k=1}^{J_t}]\tau_{k-1}, \tau_k] & \text{if } \tau_j = t \\[2ex] \left(\bigcup_{k=1}^{j}]\tau_{k-1}, \tau_k] \right) \cup]\tau_j, t] & \text{otherwise} \end{cases}
$$

Because the available data is collected by intervals $]\tau_{k-1}, \tau_k]$, if $\tau j_{<} t$, the data recorded during the period $]\tau j,_t]$ is not yet compiled and communicated and then it is not yet considered for counting. Then, the known number of deaths communicated until time t *i*s truncated to the interval $[0, \tau j]$

$$
n = \sum_{k=1}^{j} N_{]\tau_{k-1}, \tau_k]} \tag{1}
$$

Censored survival data consist then of considering the set $\{(T_i, \delta i_{k)}|$ i=1,2,…,n; k=1,2,…,j$\}$, where T*i* denotes as described above the i*t*h event's time and δik_denotes a censoring indicator such that

$$
\delta_{ik} = \begin{cases} 1 & \text{if the } i^{\text{th}} \text{ event occurs in the interval }]\tau_{k-1}, \tau_k] \\ 0 & \text{otherwise} \end{cases} \tag{2}
$$

So, event times T_i are observable but unknown or not available for i=1,2,…,*n* and the censoring indicators δi_k are perfectly known for i=1,2,…,n and k=1,2,…,j. In these conditions, we define the indicators

$$
\delta_{i\bullet} = \sum_{k=1}^{j} \delta_{ik} \text{ for } i=1,2,…,n \tag{3}
$$

which are 1 or 0 depending on whether the ith event is censored by one interval of the grid $\left\{]\tau_{k-1}, \tau_k] \middle| k = 1, 2, \cdots, j \right\}$ or not and the indicators

$$
\delta_{\bullet k} = \sum_{i=1}^{n} \delta_{ik} \text{ for } k=1,2,…j \tag{4}
$$

which count the number of deaths registered in the associated intervals $]\tau_{k-1}, \tau_k]$ for $k=1,2,\ldots,j$. Another way to calculate indicators $\delta_{\bullet k}$ consists in writing the number $N_{]\tau_{k-1},\tau_k]}$ of events found between the thresholds τ_{k-1} and τk as

$$\delta_{\bullet k} = N_{]\tau_{k-1},\tau_k]}$$
$$= N_{\tau_k} - N_{\tau_{k-1}} \tag{5}$$

For $k=1,2,\ldots,j$. Thus, we can deduce that from equations (1) and (5), the sum

$$\sum_{k=1}^{j} \delta_{\bullet k} = \sum_{k=1}^{j} N_{]\tau_{k-1},\tau_k]}$$
$$= n \tag{6}$$

counts all the n death cases occurred in the interval $[0,\tau\mathrm{j}_j$ without knowing their exact dates.

SOME INFERENCE AND ML ISSUES

Inference is a compelling operation based on induction. Thus, inferential statistics are often defined as a set of methods that make it possible to generalize, at the level of the population, conclusions drawn from the realization of a sample. Thus, inference tries to estimate certain characteristics of data on a statistical basis, without necessarily making predictions (Paolella, 2018).

Role of Inference in ML Algorithmics

While inference refers to learning the structure of the process that gives rise to data, prediction is a method of ML that uses this structure to forge the outputs associated with new inputs. Inference can thus be a useful process for identifying predictors associated with model responses. The goal of ML algorithmics is to merge statistical computing with the computing power of contemporary computers for the purpose of processing large datasets. We will see in sections 6 to 8 how to develop specialized ML algorithms on the basis of learning model induced by the functional estimation of the important factors for interval-censored survival analysis. Thus, after the determination of an estimator of a given function trained on the available data, the inference operation will allow to make predictions.

170

Preparing Data for ML

At the start of any ML problem, data may be found distributed across multiple datasets. This is indeed the case for most medical and public health data. Data is thus real empirical data such that duplicate recordings which relate to a same individual can be found at the same time on multiple storage media. This requires to take into account this eventual duplicity of same data. To be able to analyze them as a whole, the different datasets are first brought together in the same set of data which could of course give rise to Big Data which may need cleaning (see figure 2).

Figure 2. Data gathering and cleansing
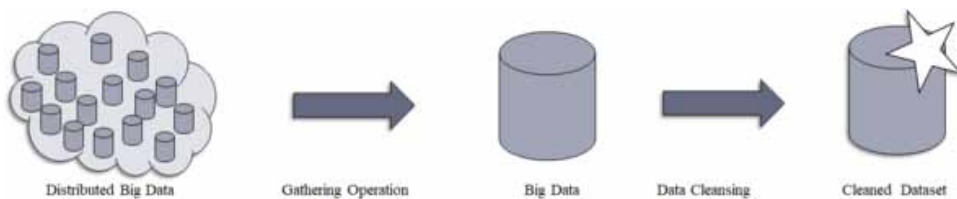
Recall here that depending on the nature of the dataset to be exploited and the objectives of the planned processing operations, the steps and techniques for cleaning data vary significantly from one dataset to another and there is no specific roadmap to determine the exact steps to follow during this operation. However, we can state unequivocally that the first step in data cleaning consists in removing all unwanted observations (duplicate observations) as well as any irrelevant information other than the information targeted by the analysis.

Outliers must be filtered out since their occurrence could interfere with certain calculations and analyses (mean values, error calculation, regressions) and missing data must be corrected. Indeed, many ML algorithms may not deal with such issues. In addition, structural errors such as those that occur during reporting, transfer as well as any other type of mismanagement or corrupted labeling of data should be corrected at this stage.

SURVIVAL ANALYSIS ISSUES

The central idea of survival analysis is to first determine a probabilistic model of the lifetime data and then extract the hidden information from it. Thus, it seeks

to evaluate the distribution of survival data and the intensity of occurrence of the event of interest.

Lifetime Cumulative Distribution Function

Let consider time T to be the lifetime. Its cumulative distribution function (CDF) at time $t \in \mathbb{R}_+$ defines the probability that a death happens before time t. Formally, the CDF is written as

$$F_T(t) = \Pr(T \le t) \tag{7}$$

where $\Pr(A)$ is the probability of event $A \in \mathcal{A}$. CDF defines Under the assumption that there are no deaths at time $t=0$, the CDF is a non-negative function, i.e.,

$$F_T(t) \begin{cases} > 0 & \text{if } t \in \mathbb{R}_+^* \\ = 0 & \text{otherwise} \end{cases}$$

Survivor Function

The survivor function (SF) is considered as the complement of the probability that a death occurs inside the interval $[0,t]$ under the assumption that there are no deaths at the origin of time $t=0$. This probability is expressed as

$$\begin{aligned} S_T(t) &= 1 - F_T(t) \\ &= \Pr(T > t) \end{aligned} \tag{8}$$

It represents the proportion of individuals of the population still alive after time t.

Probability Distribution Function

In the case where the time is supposed to vary continuously, the lifetime probability distribution function (pdf) can be defined as the ratio of the probability of death into the interval $]t,t+\eta]$ over the variation of time η, when η tends positively to zero, i.e.,

$$f_T(t) = \lim_{\eta \to 0^+} \frac{\Pr(t < T \le t + \eta)}{\eta} \tag{9}$$

172

and it is

$$f_T(t)\begin{cases} > 0 & \text{if } t \in \mathbb{R}_+^* \\ = 0 & \text{otherwise} \end{cases}$$

In general, all possible useful information on the random variable T is transcribed by its pdf. A new event will happen before a death time $t \in \mathbb{R}_+$ as soon as the conditions favorable to its occurrence will meet. The pdf and CDF of T are interrelated by the following equation

$$\forall t \in \mathbb{R}: \quad F_T(t) = \int_{-\infty}^{t} f_T(s)\,ds \tag{10}$$

where the CDF is expressed as the integral of the pdf with respect to time and

$$\forall t \in \mathbb{R}: \quad f_T(t) = \frac{d}{dt} F_T(t) \tag{11}$$

which expresses the pdf f_T as the first derivative of the CDF F_T with respect to time. Likewise, by bringing into play equations (8), (10) and (11), we can establish an expression of the SF as a function of the density function and vice-versa. So, we write

$$\forall t \in \mathbb{R}: \quad S_T(t) = 1 - \int_{-\infty}^{t} f_T(s)\,ds \tag{12}$$

and

$$\forall t \in \mathbb{R}: \quad f_T(t) = -\frac{d}{dt} S_T(t) \tag{13}$$

Hazard Function

The hazard function (HF) at time t is defined as the intensity of death at this time

$$h : \mathbb{R} \to \mathbb{R}$$
$$t \mapsto \lambda_t$$

where

$$\lambda_t = \frac{f_T(t)}{S_T(t)}$$

$$= -\frac{d}{dt}\log\big[S_T(t)\big]$$

(14)

The real quantity λ_t is called hazard rate or intensity of mortality. It should be noted that equation (14) suggests the two following properties of h:

1. The HF h is non-negative, i.e., $\forall t \in \mathbb{R}_+ : h(t) \geq 0$,

2. The function $t \mapsto \int_0^t h(s)ds$ is increasing and not superiorly bounded, i.e., $\lim_{t \to +\infty} \int_0^t h(s)ds = +\infty$.

Indeed, property 1 follows obviously from equation (14) and the fact that λ_t is the ratio of two positive quantities. Now, to show property 2, we can see from property 1 that the integral $\int_0^t h(s)ds$ defines an increasing function of time. For the second part of property 2, we know from the equation (14) that

$$\lim_{t \to +\infty} \int_0^t h(s)ds = -\lim_{t \to +\infty} \log\big[S_T(t)\big]$$

but, because $\lim_{t \to +\infty} S_T(t) = 0$, this gives the desired result.

Also, from equation (14), we can rewrite the SF as

$$S_T(t) = \exp\left(-\int_0^t \lambda_s \, ds\right)$$

(15)

The hazard function plays an important role in survival analysis. On the one hand, it provides an active means to analyze how the risk of death varies over time and on the other hand, when we know the expression of the hazard function, it makes it possible to calculate the survivor functions.

Cumulative Hazard Function

Sometimes it is more convenient to work in terms of the cumulative hazard function (CHF). This function is conventionally denoted Λ_t and defined as

174

$$\forall t \in \mathbb{R}_+ : \; \Lambda_t = \int_0^t \lambda_s \; ds \tag{16}$$

In other words, in terms of the SF, from equation (15) we write

$$\Lambda_t = -\log S_T(t) \tag{17}$$

Case of Improper Distribution

Until now, we've assumed that anyone who survives the disease or the pandemic must die one day in the very distant future. This is expressed mathematically as

$$\lim_{t \to +\infty} F_T\left(t\right) = 1 \tag{18}$$

or similarly

$$\lim_{t \to +\infty} S_T\left(t\right) = 0 \tag{19}$$

Under these conditions, the probability distribution of the lifetime *T* verifies all the good probabilistic properties. It is called appropriate or proper.

However, the follow-up time may not be long enough to observe the death of all patients who are considered by the study. Thus, in this section, we are going to assume that due to different treatments or because the cellular immunity of some people, many patients in the population under consideration end up surviving the severe disease or pandemic under study. For example, we observed many people get sick from the Corona virus, but for reasons of the medical management of their illness or because their excellent immunity, they end up surviving this disease. Mathematically speaking, this can be written as

$$\lim_{t \to +\infty} F_T\left(t\right) < 1 \tag{20}$$

and by abuse of notation, we note $F_T(+\infty)$ this probability. In other words, the associated SF is such that

$$S_T\left(+\infty\right) = \lim_{t \to +\infty} S_T\left(t\right) > 0 \tag{21}$$

This means that for a part of the population, the lifetime T can be infinite with a positive probability which is not negligible. In this case, the probability distribution of T is said inappropriate or improper. Although we can always consider the median lifetime as the time at which half of the population in question would be decimated, there are two unfortunate effects of assuming that a non-negligible proportion of the population would never die, to know:

1. The mean lifetime is indefinite for such a population, i.e., $E(T)=+\infty$.
2. The pdf does not satisfy the normalization condition, i.e., $\int_{-\infty}^{+\infty} f_T(t)\,dt \neq 1$.

This last remark characterizes improper distributions. In order to always bring the reasoning back to a population which would have an appropriate lifetime distribution, it suffices to consider the conditional distribution which considers only the subpopulation of patients who end up dying, i.e. the subpopulation with a lifetime with the pdf

$$
\begin{aligned}
\tilde{f}(t) &= \frac{f_T(t)}{F_T(+\infty)} \\
&= \frac{f_T(t)}{1 - S_T(+\infty)}
\end{aligned}
\tag{22}
$$

So, from equations (10) and (22) we can deduce the associate conditional CDF defined as

$$
\begin{aligned}
\tilde{F}(t) &= \int_0^t \tilde{f}(s)\,ds \\
&= \frac{1}{F_T(+\infty)} \int_0^t f_T(s)\,ds \\
&= \frac{F_T(t)}{F_T(+\infty)}
\end{aligned}
\tag{23}
$$

and the SF associated with this distribution is then

$$
\begin{aligned}
\tilde{S}(t) &= 1 - \tilde{F}(t) \\
&= \frac{S_T(t) - S_T(+\infty)}{1 - S_T(+\infty)}
\end{aligned}
\tag{24}
$$

176

In this way, according to (21) and (24), we obtain

$$\lim_{t \to +\infty} \tilde{S}(t) = \frac{\lim_{t \to +\infty} S_T(t) - S_T(+\infty)}{1 - S_T(+\infty)}$$
$$= 0 \qquad (25)$$

Equation (25) shows that the distribution of lifetime over the subpopulation of patients that end up dying during the study period is appropriate. The proper HF is still written as the ratio of the proper pdf by the proper SF

$$\tilde{h}(t) = \frac{\tilde{f}(t)}{\tilde{S}(t)}$$
$$= \frac{f_T(t)}{S_T(t) - S_T(+\infty)} \qquad (26)$$

Under these conditions, the proper SF $\tilde{S}$ can be rewritten according to the equation (15) under the form

$$\tilde{S}(t) = \exp\left(-\int_0^t \tilde{h}(s)\, ds\right) \qquad (27)$$

Conditional Survivor Function

In this section, we will characterize the SF by conditioning the lifetime distribution differently. Indeed, until now, the SF was introduced under the assumption that there were no deaths at the origin of time $t=0$. Now, let's consider an individual that survives until time t (fix) and which is still surviving until $t+x$. Formally, the probability of this conditional event can be expressed as

$$\Pr\left(T > t + x \mid T > t\right) = \frac{\Pr\left(\{T > t + x\} \cap \{T > t\}\right)}{\Pr\left(T > t\right)}$$
$$= \frac{\Pr\left(T > t + x\right)}{\Pr\left(T > t\right)} \qquad (28)$$

According to equation (8), we can rewrite equation (28) as the ratio of the values of the SF at times $t+x$ and t,

$$\Pr\left(T > t + x \mid T > t\right) = \frac{S_T\left(t + x\right)}{S_T\left(t\right)} \tag{29}$$

and according to equation (15), we can rewrite equation (29) in terms of the cumulative HF

$$\Pr\left(T > t + x \mid T > t\right) = \exp\left(-\int_t^{t+x} \lambda_s \, ds\right)$$

This probability is called conditional SF (CSF) and we note this function as

$$S_t^\star\left(x\right) = \exp\left(-\int_t^{t+x} \lambda_s \, ds\right) \tag{30}$$

So, taking into account equation (29), the conditional pdf associated with CSF $S_t^\star\left(x\right)$ is given by

$$\begin{aligned} f_t^\star\left(x\right) &= -\frac{dS_t^\star\left(x\right)}{dx} \\ &= \frac{f_T\left(t + x\right)}{S_T\left(t\right)} \end{aligned} \tag{31}$$

This function is such that for all $x \in \mathbb{R}_+$

$$\begin{aligned} S_t^\star\left(x\right) &= 1 - \int_{-\infty}^{x} f_t^\star\left(s\right) ds \\ &= \int_x^{+\infty} f_t^\star\left(s\right) ds \end{aligned} \tag{32}$$

Average of Remaining Time until Death

If X defines the random time to survive beyond time $t>0$, the average of the remaining time until death is calculated as

$$E_\star(X) = \int_0^{+\infty} x f_t^\star(x)\,dx$$

$$= \frac{1}{S_T(t)} \int_0^{+\infty} x f_T(t+x)\,dx \tag{33}$$

$$= \frac{1}{S_T(t)} \int_t^{+\infty} S_T(s)\,ds$$

The rigorous proof of the last equality in equation (33) involves the use of the fundamental theorem of Fubini-Tonelli. Otherwise, to make sure that the proof works correctly with the integration by parts, you have to assume that $\lim_{s \to +\infty} s\, S_T(s) = 0$.

NONPARAMETRIC ESTIMATION OF SURVIVAL CHARACTERISTICS

The assessment of the SF through the Kaplan-Meier estimator and the estimation of the HF through the Cox's regression model are the subject of the majority of papers reporting on the application of ML in health and medical fields (Hans & Hein, 2012). These models being much more suited to model situations where survival data is completely known, we give in this section an alternative method dedicated to contexts where data is censored and compiled. The approach we propose in this section promotes the use of nonparametric point estimators of the survivor and hazard functions on the basis of the plug-in method and the use of the theorem of Glivenko-Cantelli.

Point Estimation

Estimating a given quantity consists of looking for an approximate value which is based on the observation of a sample according to which this value is calculated. In the context of parametric statistics, it is generally assumed that the probability distribution sought has a particular form which is expressed using a number of parameters. In such cases, to fully determine such a behavior model, it suffices to estimate its parameters (Emura & Chen, 2018; Rezaul & Ataharul, 2019). In the case where there is no a priori on the form of the unknown probability distribution, we search for estimating functional quantities, and no longer the distribution parameters. This way of doing things is the subject of nonparametric statistics. It requires less a priori knowledge about the studied probabilistic behaviors of considered data. But, in return, it requires more data in order to obtain estimation precisions similar to those of the parametric framework.

Nonparametric Probability Distribution Estimation

Regardless of the origin of data and the functions considered for the estimation, we can speak of an approximation of one probability distribution by another in the nonparametric framework when their respective cumulative distribution functions are close to each other. Obviously, the design perception of such an approximation or neighborhood of distribution remains to be specified.

Thus, if F_1 and F_2 are two CDFs associated with two probability distributions, the distance defined as

$$d_\infty \left(F_1, F_2 \right) = \sup_{x \in \mathbb{R}} \left| F_1 \left(x \right) - F_2 \left(x \right) \right| \tag{34}$$

on the metric space of functions with one real variable could serve as a basis for the design of the approximation of functions.

However, precisely, the fundamental theorem of Glivenko-Cantelli uses such a distance to establish the convergence of the empirical distribution function towards the CDF of the probability distribution from which a sample is randomly selected.

Theorem of Glivenko-Cantelli

Almost surely the empirical distribution function $\widehat{F}_n$ based on an n-sample of the CDF F converges almost surely towards this function uniformly and we write

$$\Pr \left(\lim_{n \to +\infty} d_\infty \left(F, \widehat{F}_n \right) = 0 \right) = 1 \tag{35}$$

The proof of this theorem involves the strong law of large numbers and Donsker's theorem (Donsker, 1952). This last theorem gives an idea of the speed of convergence expressed by the Glivenko-Cantelli theorem. The reader concerned with these points of demonstration will find more details and discussions in (Dvoretzky et al., 1956), (Massart, 1990) and (Billingsley, 1999).

Plug-In Estimation

Plug-in method is an estimation procedure that proceeds by substitutions. It makes it possible to approximate the value of an unknown characteristic of an unknown probability distribution. Plug-in estimation can thus be used to determine an expected value, a variance or any percentile from the observation of a sample or a given dataset. The following definition explains the principle of this method.

180

Definition

Let Ψ be a set of distribution functions on a nonempty set Ω. Let g be a mapping from Ψ to Ψ, $F \in \Psi$, n be a non-negative integer, $(X_1, X_2, \ldots, X_n)$ be a sample of the CDF F and $\widehat{F}_n$ be the ECDF associated with the sample $(X_1, X_2, \ldots, X_n)$. Then, the quantity $g\left(\widehat{F}_n\right)$ is called the plug-in estimate of the statistical functional g(F).

Glivenko-Cantelli theorem can serve to proof the convergence of $g\left(\widehat{F}_n\right)$ towards $g(F)$ for a large sample which can be expressed using size *n*. Formally, suppose we are interested in the estimation of an unknown quantity Q the image of the CDF *F* by a known mapping g, $Q = g(F)$, as part of an ML model. Then $\widehat{Q}_n = g\left(\widehat{F}_n\right)$ estimates Q. Thus, as we will see in the next section, this method can be used as a basis for prediction in the context of survival analysis.

PREDICTING SURVIVOR AND HAZARD FUNCTIONS FOR UNCENSORED DATA

Survival analysis pays little attention to predicting a single value of the event of interest. The prediction step according to this method mainly concerns the approximation of the survivor and hazard functions. The formation of these estimates in the case of uncensored data will help us to justify the plug-in estimators when we will consider censored data in the next section. Thus, when a sample is completely known, the empirical distribution is often characterized by a distribution function that assigns the same probability to all observations in a sample. To formalize this, let's consider $N_t = n$, under the assumption of selecting that the sample $T_1, T_2, \ldots, T_n$ as a sequence of i.i.d. random variables defined on the probability space $\left(\Omega, \mathcal{A}, \mathrm{Pr}\right)$, with values in $\mathbb{R}_+$ and of CDF denoted *F*. Thus, ECDF $\widehat{F}_n$ of the sample $T_1, T_2, \ldots, T_n$ is defined for all $s \in \mathbb{R}_+$ as

$$\begin{aligned}
\widehat{F}_n(s) &= \frac{1}{n} \sum_{i=1}^{n} \mathbf{1}_{]-\infty, s]}(T_i) \\
&= \frac{1}{n} \sum_{i \neq 0 \mid T_i \leq s} \mathbf{1}_{]-\infty, s]}(T_i)
\end{aligned} \tag{36}$$

So, the SF can be estimated as

$$\hat{S}_n(s) = 1 - \hat{F}_n(s)$$
$$= 1 - \frac{1}{n} \sum_{i \neq 0 | T_i \leq s} \mathbf{1}_{]-\infty, s]}(T_i) \tag{37}$$

Moreover, because the random variables $\mathbf{1}_{]-\infty,s]}(T_i)$, for $i=1,2,\ldots,n$, are distributed according to Bernoulli's distributions with parameter

$$\Pr\left(\mathbf{1}_{]-\infty,s]}(T_i) = 1\right) = \Pr(T_i \leq s)$$
$$= F(s) \tag{38}$$

and in the same way, the complementary of this probability is expressed as

$$\Pr\left(\mathbf{1}_{]-\infty,s]}(T_i) = 0\right) = \Pr(T_i > 0)$$
$$= S(s) \tag{39}$$

In consequence, given the Bernoulli distribution of these variables, we can conclude the mean and the variance as being

$$E\left(\mathbf{1}_{]-\infty,s]}(T_i)\right) = F(s) \text{ and } \mathrm{var}\left(\mathbf{1}_{]-\infty,s]}(T_i)\right) = F(s)S(s) \tag{40}$$

Now, for $i=1,2,\ldots,n$, as the random variables T_i are i.i.d., the random variables $\mathbf{1}_{]-\infty,s]}(T_i)$ are also i.i.d. and then the statistic $n\hat{F}_n(s)$ is a binomial random variable with parameters n and $F(s)$. In fact,

$$E\left(n\hat{F}_n(s)\right) = nF(s) \text{ and } \mathrm{var}\left(n\hat{F}_n(s)\right) = nF(s)S(s) \tag{41}$$

so from the properties of mean and variance, we can write

$$E\left[\hat{F}_n(s)\right] = F(s) \text{ and } \mathrm{var}\left[\hat{F}_n(s)\right] = \frac{F(s)S(s)}{n} \tag{42}$$

Moreover, because the CDF is a step function which presents jumps of height $1/n$ at all the observations $T_i=t_i$ with $i=1,2,\ldots,n$. After ordering the values $t_0=0,t_1,t_2,\ldots,t_n$, we note the ordered distinct values $t_0' = 0 < t_1' < t_2' < \cdots < t_r'$ resulting from this

182

operation. Thus $t'_1, t'_2, \cdots, t'_r$ are the points where the function $\widehat{F}_n$ undergoes jumps with respective heights

$$\widehat{F}_n(t'_k) - \widehat{F}_n(t'_{k-1}) = \frac{\#\{t_i \,|\, (t_i = t'_k) \wedge (i \in [\![1..n]\!])\}}{n} \text{ for } k=1,2,\ldots,r \tag{43}$$

To simplify the notations let us note in the following

$$c_k = \#\{t_i \,|\, (t_i = t'_k) \wedge (i \in [\![1..n]\!])\} \text{ for } k=1,2,\ldots,r$$

Let g be a numerical function, because the ECDF $\widehat{F}_n$ jumps in t'_k for $k=1,2,\ldots$,r, plug-in estimator of $E_F[g(T)]$ with respect to $t'_1, t'_2, \cdots, t'_r$ is written as the expectation of $g(T)$ with respect to ECDF $\widehat{F}_n$, i.e.,

$$\begin{aligned} E_{\widehat{F}_n}\left[g(T)\right] &= \int_{\mathbb{R}} g(t)\, d\widehat{F}_n(t) \\ &= \sum_{k=1}^{r} g(t_k)\left[\widehat{F}_n(t'_k) - \widehat{F}_n(t'_{k-1})\right] \\ &= \frac{1}{n}\sum_{k=1}^{r} c_k\, g(t'_k) \end{aligned} \tag{44}$$

PREDICTING SURVIVOR AND HAZARD FUNCTIONS FOR CENSORED DATA

Note first, as with the Kaplan-Meier and Cox models, the type of models we have developed so far are based on the simplest assumption where there is a fully determined sample of lifetime. In other words, these models only characterize distributions of data in homogeneous populations where the observations of lifetime are i.i.d. In this section, we will give the fundamentals for such the prediction of when the data is censored in intervals. However, in real life, data is censored. To take censoring into account, we will consider as above $N_t=n$, $J_t=j$, $T_1,T_2,\ldots,T_n$ an unknown n-sample and a grid $\{\tau 0_= 0, \tau 1,_\tau 2,\ldots_a j\}$ o$_f$ the interval of observation [0,t] s*uch* as

$$\tau 0 = {}_0 < \tau 1 < \tau_2 < \ldots < {}_a j \le t$$

define the interval-censoring thresholds. Because lifetime observations are not known, the ECDF $\widehat{F}_n$ it cannot be assessed in its form (36), but, it can be rewritten as a step function $\widehat{F}_{n:j}$ undergoing jumps of height $\delta \bullet k/n$ at the end of each censoring interval $]\tau_{k-1}, \tau_k]$, for k=1,2,...,r and we write

$$\widehat{F}_{n:j}(s) = \sum_{k \neq 0 | \tau_k \leq s} \frac{\delta_{\bullet k}}{n} \tag{45}$$

and for the same reasons, the step function

$$\widehat{S}_{n:j}(s) = 1 - \sum_{k \neq 0 | \tau_k \leq s} \frac{\delta_{\bullet k}}{n} \tag{46}$$

evaluates the empirical SF. Moreover, the average of any mapping g of lifetime T can be computed with respect to CDF $\widehat{F}_{n:j}$ as

$$\begin{aligned} E_{\widehat{F}_{n:j}}\left[g(T)\right] &= \int_{\mathbb{R}} g(t) \, d\widehat{F}_{n:j}(t) \\ &= \sum_{k=1}^{j} g(\tau_k)\left[\widehat{F}_{n:j}(\tau_k) - \widehat{F}_{n:j}(\tau_{k-1})\right] \\ &= \frac{1}{n} \sum_{k=1}^{j} \delta_{\bullet k} \, g(\tau_k) \end{aligned} \tag{47}$$

and since we have no information on what is happening outside of the interval $[0, \tau j_j$, $E_{\widehat{F}_{n:j}}\left[g(T)\right]$ can be considered as a plug-in estimate of $E_F[g(T)]$ with respect to the censoring grid $\{\tau 0_{=} 0, \tau 1, {}_\tau 2, \ldots {}_\tau j\}$.

As a consequence of the developments carried out so far, because $\widehat{F}_{n:j}$ is a right continuous step function with jumps at times $\tau 1, \tau_2, \ldots \tau_j$ and because the sequence $\tau 1, \tau 2, \ldots j$ can be considered as j independent random variables, we can define the likelihood of survivors at a given time s∈[0,t] as

$$\begin{aligned} \widehat{f}_{n:j}(s) &= \widehat{F}_{n:j}(s) - \widehat{F}_{n:j}(s^-) \\ &= \widehat{S}_{n:j}(s^-) - \widehat{S}_{n:j}(s) \end{aligned} \tag{48}$$

where

$$\widehat{F}_{n:j}(s^-) = \lim_{t \uparrow s} \widehat{F}_{n:j}(t) \text{ and } \widehat{S}_{n:j}(s^-) = \lim_{t \uparrow s} \widehat{S}_{n:j}(t)$$

are respectively the values of functions $\widehat{F}_{n:j}$ and $\widehat{S}_{n:j}$ just before time s (or left of s). One must pay attention to the understanding of the time "*just before*". This instant

184

must be located in the framework of the dense half-line $\mathbb{R}_+$ and in fact, the notation ts should be interpreted as "*t tends by increasing to s*".

Now, as $\widehat{F}_{n:j}$ changes its values only at times $\tau 1, \tau 2, \ldots \tau j$, then

$$\widehat{F}_{n:j}\left(\tau_k\right) - \widehat{F}_{n:j}\left(\tau_k^-\right) = \frac{\delta_{\bullet k}}{n}$$

and the likelihood of survivors at a given time $s \in [0,t]$ can be calculated as

$$\widehat{f}_{n:j}(s) = \begin{cases} \dfrac{\delta_{\bullet k}}{n} & \text{if } s = \tau_k \text{ for } k \in [\![1..j]\!] \\ 0 & \text{otherwise} \end{cases} \qquad (49)$$

Thus, the likelihood $\widehat{f}_{n:j}\left(\tau_k\right)$ at time τk defines the height of the kth jump of the step function $\widehat{F}_{n:j}$ which can be rewritten with respect to the likelihood function $\widehat{f}_{n:j}$ as

$$\widehat{F}_{n:j}\left(s\right) = \sum_{k \neq 0 | \tau_k \leq s} \widehat{f}_{n:j}\left(\tau_k\right) \qquad (50)$$

Because $\tau 1, \tau 2, \ldots \tau j$ can be a random sequence, the last equation establishes a plug-in estimate of $\widehat{F}_{n:j}\left(s\right)$ calculated on the basis of the grid $\tau 0 = {}_0$, $\tau 1, \tau 2, \ldots \tau j$. More generally, let's consider g a continuous mapping and Φj a step function with jump heights $\alpha 1, \alpha 2, \ldots, \alpha j$ respectively at times $\tau 1, \tau 2, \ldots \tau j$ and such that $\sum_{k=1}^{j} \alpha_k = 1$, then the expected value of the random variable g(T) with respect to Φj can be computed as

$$E_{\Phi_j}\left[g(T)\right] = \int_{\mathbb{R}} g(t)\, d\Phi_j(t)$$
$$= \sum_{k=1}^{j} g\left(\tau_k\right)\left[\Phi_j\left(\tau_k\right) - \Phi_j\left(\tau_{k-1}\right)\right] \quad (51)$$
$$= \sum_{k=1}^{j} \alpha_k\, g\left(\tau_k\right)$$

Now, according to equation (14), we can derive a step estimator of the HF such that for k=1,2,…,*j*, the quantities

$$\hat{\lambda}_k = \frac{\hat{f}_{n:j}(\tau_k)}{\hat{S}^{E}_{n:j}(\tau_k)}$$

$$= \frac{\delta_{\bullet k}}{n - \sum_{i=1}^{k} \delta_{\bullet i}} \qquad (52)$$

are well defined. In addition, because (14), $\hat{\lambda}_k$ defines a plug-in estimate of the HF (or intensity of death) at time τk such that

$$\hat{\lambda}_s = \begin{cases} \dfrac{\delta_{\bullet k}}{n - \sum_{i=1}^{k} \delta_{\bullet i}} & \text{if } s = \tau_k, \text{ for } k \in [\![1..j]\!] \\ 0 & \text{otherwise} \end{cases} \qquad (53)$$

PREDICTING THE CONDITIONAL SURVIVOR FUNCTION

The portion of patients who will survive at least until τk, knowing they survived until τ_{k-1} can be deduced from the equation (29) as

$$\mathbb{S}_k = \Pr\left(T > \tau_k \mid T > \tau_{k-1}\right)$$

$$= \frac{S_T(\tau_k)}{S_T(\tau_{k-1})} \qquad (54)$$

So, using the estimates of $S_T(\tau_{k-1})$ and $S_T(\tau k)$ given by equation (46), the plug-in estimator of the conditional SF over the kth censorship period can be defined as

$$\widehat{\mathbb{S}}_k = \frac{\hat{S}_{n:j}(\tau_k)}{\hat{S}_{n:j}(\tau_{k-1})}$$

$$= \frac{n - \sum_{i=1}^{k} \delta_{\bullet i}}{n - \sum_{i=1}^{k-1} \delta_{\bullet i}} \qquad (55)$$

186

Similarly, the probability of surviving until at least the end of a period s, knowing that the individual survived until period r, with $r, s \in [\![1..j]\!]$ and $r < s$ can be written

$$
\begin{aligned}
\mathbb{S}_{r,s} &= \Pr\left(T > \tau_s \mid T > \tau_r\right) \\
&= \prod_{k=r}^{s-1} \Pr\left(T > \tau_k \mid T > \tau_{k+1}\right) \\
&= \prod_{k=r}^{s-1} \frac{S_T\left(\tau_{k+1}\right)}{S_T\left(\tau_k\right)} \\
&= \frac{S_T\left(\tau_s\right)}{S_T\left(\tau_r\right)}
\end{aligned}
\tag{56}
$$

Given equations (55) and (56), the plug-in estimator of the probability $\mathbb{S}_{r,s}$ is given by

$$
\begin{aligned}
\widehat{\mathbb{S}}_{r,s} &= \frac{\widehat{S}_{n:j}\left(\tau_s\right)}{\widehat{S}_{n:j}\left(\tau_r\right)} \\
&= \frac{n - \sum_{i=1}^{s} \delta_{\bullet i}}{n - \sum_{i=1}^{r} \delta_{\bullet i}}
\end{aligned}
\tag{57}
$$

ANALYSIS OF COVID-19 DATA

COVID-19 emerged in central China's city of Wuhan where an increasing number of pneumonia cases of unknown origin were reported around December 2019. It has been recognized as a global pandemic by the World Health Organization. Health (WHO) in March 2020. This disease has affected millions of people around the world and continues to do so. Many of them died. In this section, we analyze daily censored data of coronavirus deaths reported by WHO (WHO, 2021) for four countries, namely, China (CN), Great Britain (GB), Morocco (MA) and the United States of America (US) for the period between March 1, 2020 and November 12, 2021. The idea here is to consider four countries sufficiently distant from each other in the objective to neglect the risk induced by spread neighborhood facts between countries.

Data Visualization

Data visualization has become an essential technique in ML for exploring data in the early stages of analysis. It consists in visualizing graphically the raw data in order to try to discover information and understand their behavior. When the data comes from large datasets, there may be residual defects that the cleaning phase overlooked still persist in data.

Figure 3. Visualization of censored death data
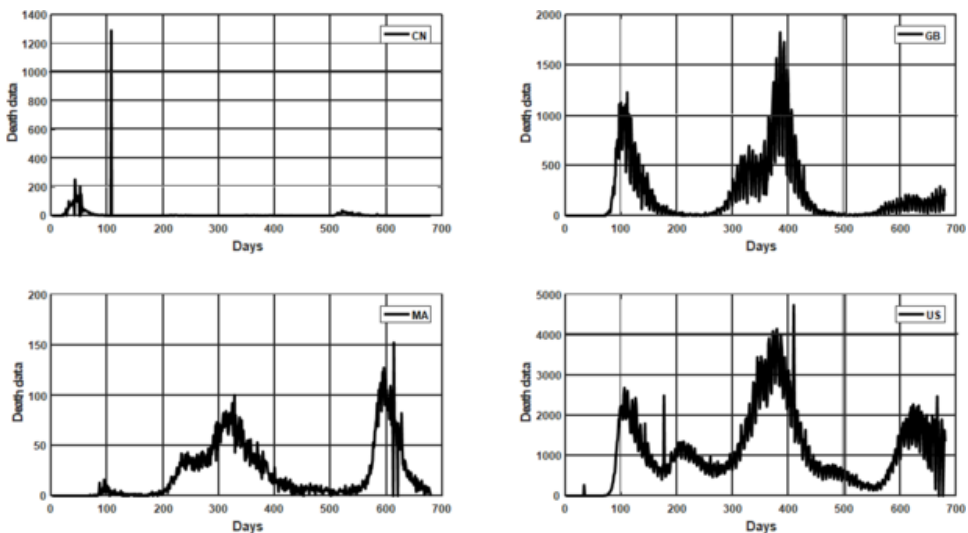
These faults should be identified at this point and purged immediately. In case of interval-censored data, as the raw death data are not directly usable, the visualization procedure rather concerns the process of counting death cases by interval.

We have already explained in section 2.4 how interval-censored data can be segmented into aliquots (here in days) and how their counting can be done using indicators characterizing the interval-censoring procedure. As soon as the data thus processed is visually represented, some on-board information can already be noticed. This process is usually performed using graphic libraries, analysis tools and programming languages dedicated to ML. For our part, we carried out this step using the MATLAB scripting language and its graphic libraries. Figure 3 visualizes COVID-19 death data for the four countries targeted by this study. The order of magnitude of the data differs from one country to another. This is explained by the different sizes of the populations of these countries and the aggressiveness of the

188

pandemic in each of them. Some important information may already be provided at this stage.

Visualizing the dataset CN reveals that China suffered a brutal death toll on the 107th day after observations began. This number can be considered as an accidental (or exceptional) value since, apart from this date, the number of deaths in China remained remarkably under control throughout the other 679 days of the follow-up considered by this study. According to GB data, Britain experienced two major waves during this period. During the second wave, the British beta variant caused the most deaths over a relatively short period of time and with a peak amplitude of around 2000 deaths in a single day. The amplitude of the peak and the importance of the base of the second wave compared to the base of the first wave show the importance of the severity of the delta wave in this country. The return to a period of low mortality values after this wave shows the effectiveness of the measures taken by the entire country's health system during this period: the third dose of the vaccine and the adherence of the population to the barrier measures between others. The trajectory of data GB also shows that this country suffered a third wave of lower severity around August. This latest wave is explained by the relaxation of constraints on popular movements and the gradual return to normal life in this country. Morocco observed a relatively low number of deaths throughout the period of this study with essentially two waves of the pandemic. The dataset MA shows that the base extent of the first wave lasted more than a year despite a low peak during that period of time. This shows that the country's health system was unprepared for the pressure it was subjected to due to the first wave of COVID-19. After a truce which lasted a little over three months, the country was shaken by a second wave of greater amplitude but which lasted less long than the first. This is explained by a better responsiveness of the health system of this country this time. The epicenter of this second wave was around July-August. The causes in question explaining this behavior are the population movements during the summer holidays, the reopening of air borders since June 15 and a certain loss of collective vigilance. The peculiarity of the US data as shown in figure 3 exhibits three waves with important amplitudes and two waves with relatively modest amplitudes. Also, data shows that since the start of the first wave the death toll has never subsided. A priori, this phenomenon is explained by the magnitudes of the three waves in a population which is quite large. The bases of these waves had never exceeded four months and had a tendency to weaken somewhat. This is shown by an aggressive covid-19 testing and the readiness of the American health care system to face such crises.

Survivor Function Visualization

SF is a decreasing function. The value of the SF at time *t* provides the proportion of patients who will survive beyond this time. Drawing its plot for a range of time makes it possible to graphically determine the evolution of the proportion of the population which will survive past the time *t* along this period.

Figure 4. Visualization of the estimated SF
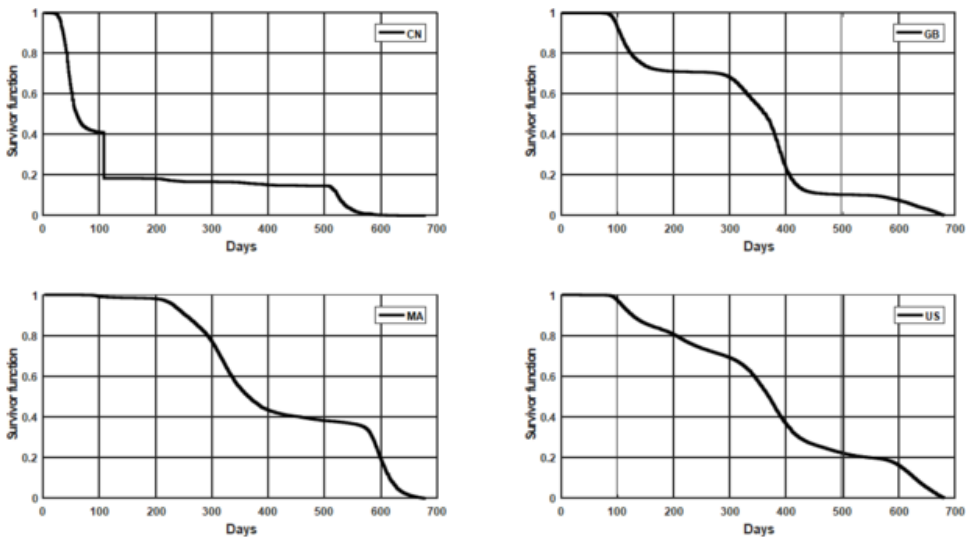
Regardless of the number of deaths caused in each of the four countries, SF plots for the censored death datasets CN, GB, MA and US show that the pandemic has caused death in these countries with dissimilar behaviors (see figure 4). Changes in shape in the plot of an SF have precise meanings as to the beginning or end of waves of the pandemic in the country for which the death data is analyzed. A return to horizontal (or almost horizontal) behavior indicates the end of a wave and a decreasing trend from horizontal behavior marks the beginning of a new wave in this country.

The descent slope of this curve indicates the degree of severity of the associated wave. The steeper the slope marking a wave, the more catastrophic the wave. The constancy of this curve indicates the control of the state of the pandemic and the adequacy of the public health policy. On the other hand, when the SF curve has a downward trend, indicates an insufficiency of the measures taken to combat the pandemic. The country in question must look for to strengthen the health security

190

policy through new measures that would bring the situation under control. Any jump in this function indicates a sudden change in data decoding a brutal increase in the value of the number of deaths. Causes must therefore be sought and eradicated. Thus, we can notice in Chinese dataset CN on the one hand an exceptional value occurs on day 107. It is marked by an enough long jump of SF. On the other hand, we remark a flat region of the SF which reflects a period of time during which the country is in perfect control of the pandemic. The experience of China and other countries has made it clear that aggressive testing, community mobilization, mask-wearing and social distancing measures can lead to lower infection risks and therefore reduce the risk of loss of human lives. The SF associated with GB data shows that the second wave was the deadliest with around 60% of deaths recorded in this country during the entire period of this study, while the second wave in the United States only caused nearly 40% of deaths and nearly 35% in Morocco. On the contrary, in Morocco, the SF on the MA's follow-up data shows that it was the first wave which was the deadliest in this country with nearly 60% of deaths.

Hazard Function Visualization

HF is a function that describes the evolution of death risk over time. The HF plots associated with the four studied death datasets CN, GB, MA and US show a succession of repeating bathtubs (see figure 5).

*Figure 5. Visualization of the estimated HF*
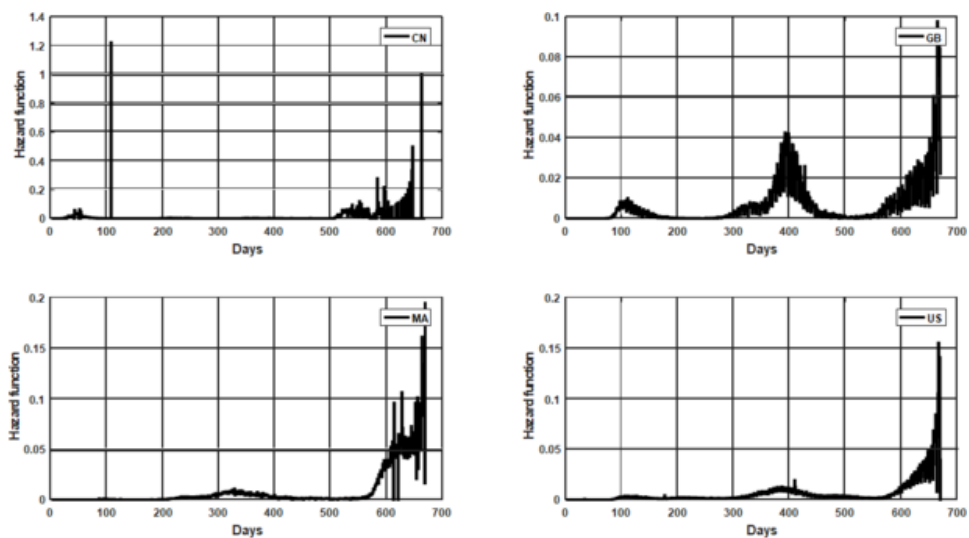
The shape of each of these bathtubs starts by decreasing period (the end of a wave), followed by a period with a flattened trend (period of pandemic control) and an increasing period (start of a new wave). Notice again that the accidental value on the 107th day of the dataset CN produced a very large local fluctuation at this point of the HF plot.

Also note that the fluctuations shown by the plots of the hazard functions confirm that in reality a HF varies randomly and presents periodic waves. Only nonparametric estimation methods are sensitive to the random behavior of the HF. Note that the HF plot associated with the dataset GB shows that Britain experienced two subwaves during the second wave between days 290-500 of this study period. The slope of the SF being steeper during the second subwave shows the severity of the associated COVID-19 variant in this country.

Predictive Quality of the Estimators

Now, recall that the SF estimator can be calculated intrinsically from the distribution function estimator which is calculated on the basis of censored data through equation (46) which then makes it possible to deduce the estimated likelihoods from the equation (49). These two estimators make it possible to deduce a first estimator of the HF through equation (52). Once these calculations have been made, it is possible to recalculate the SF under the perspectives of equation (15). The difference between the results that arise from these two forms of calculating the same function can be evaluated using the algorithmic bias and standard error associated to these two schemes. Algorithmic bias and standard error are two sources of concern in ML. The bias/variance dilemma is a good illustration of the problem of simultaneously minimizing these two sources of error in ML. Indeed, large values of bias and variance prevent learning algorithms from generalizing beyond the learning sample. In the following, we consider the S-S-plot (SF plot versus SF plot) as a visual criterion of the learning quality of the proposed plug-in estimator for SF in survival analysis of censored data (see Figure 6).

Figure 6. Visualization of the S-S-plots of the four countries
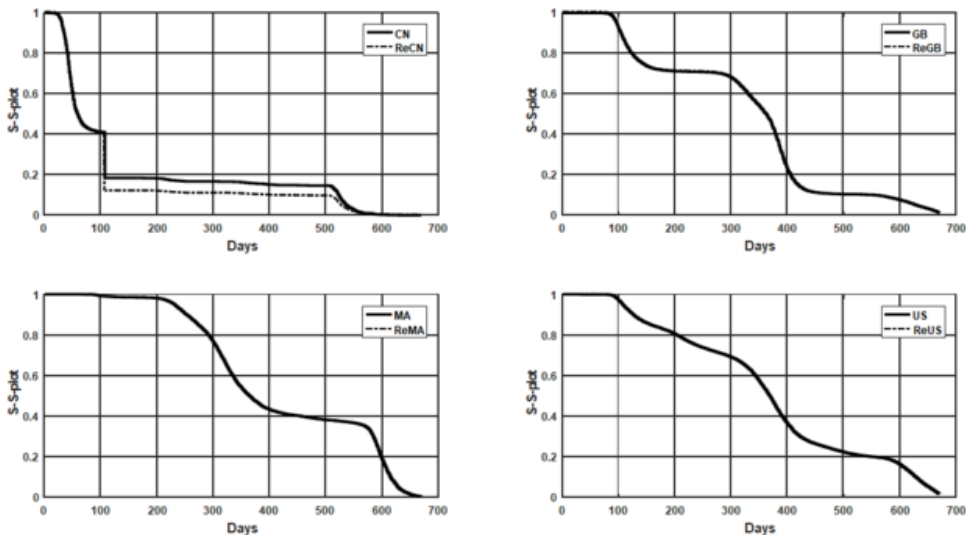
In figure 6, for a dataset called A, we denote by the same name the form of the HF by the algorithm implementing equation (46) and we denote ReA the form of the HF by the algorithm implementing equation (52) followed by equation (15). Thus, the observation of substantial errors between these two adjustments of the SF is interpreted under-learning of the model, whereas negligible errors between these adjustments indicate a good learning of the model. In this sense, the Chinese CN dataset shows a shift in the profile of the S-S-plot at the level of the 107th day. The bias introduced by this aberrant value requires correcting the profile by arbitrating on this value.

So, we propose to transform the data CN into CN' according to the schema

$$\text{CN.data}(i) = \begin{cases} \dfrac{\text{CN.data}(i-1) + \text{CN.data}(i+1)}{2} & \text{if } i = 107 \\ \text{CN.data}(i) & \text{otherwise} \end{cases} \tag{58}$$

which replaces the 107th day's value with a local mean value. This data transform leads to a more stable survival analysis profile (see Figure 7).

Figure 7. Visualization of data and S-S-plot after the transform of the dataset CN into CN'
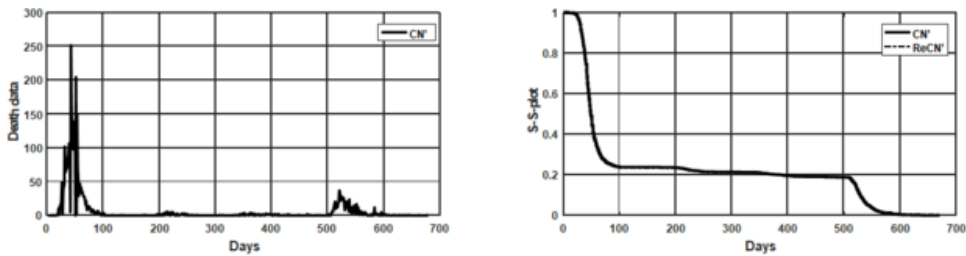
An error of three decimal places on the calculation of probabilities (a smaller error than 0.1%) is generally considered as acceptable. Thus, apart from the dataset CN, all the algorithmic errors made on the recalculation by re-estimation of the SF of the three other countries confirm the comments about figures 6 and 7. Table 1 confirms this graphical analysis by providing the biases and standard errors established from the study of the stability of the S-S-plots for all the analyzed datasets CN, CN', GB, MA and US.

Table 1. Errors induced by the recalculation of the SF

Data	S-S-plot bias	S-S-plot standard error
CN	0.0379	0.0267
CN'	0.0047	0.0025
GB	0.0011	8.0165 e-04
MA	5.9586e-04	6.2461 e-04
US	5.4427e-04	4.2810 e-04

The transformation of the dataset CN into the dataset CN' by replacing the outlier value improves the errors resulting from the re-estimation of the SF and a shows a better match of the S-S-plot (see Figure 7 and Table 1).

STRENGTHENING THE HEALTH SECURITY POLICIES

We want to confect a tool which enables the data-analyst to compare two security policies followed by two different countries over a same period of time. Such a comparison should lead to suggesting the measures and strategies adopted by the

194

reference country to improve the weaknesses of the policy of the targeted country. From the point of view of survival analysis, we will apply the method of signs to the hazard functions that describe the two policies in order to make such a decision. This method can thus be used as a tool to identify weaknesses and suggest the strengthening of policies that have led to higher mortality rates.

Test Design

For this purpose, let's consider a grid of time $\{\tau 0_= 0, \tau 1, _{\tau}2, \ldots _{\tau}j\}$. $_w$e have already discussed above how data can be segmented into aliquots or censorship intervals and how event counting can be done using certain indicators characterizing the interval-censoring survival analysis. Thus, want to analyze what happens for two countries A and B during a period $[\tau r, \tau s]$ wit_h r<s. To $s$how that the policy followed by country B is better and therefore able to be suggested to improve the health security of country A on the period $[\tau r, \tau s]$, $_t$he $_H$F of country B must be lower than that of A a greater number of times during the interval $[\tau r, \tau s]$.

S$_o$, w$_e$ want to test the hypotheses

H0: "The $_p$olicy B do not allow to improve the policy A on $[\tau r, \tau s]$"

v$_e$$rsu_s$
H1: "The $_p$olicy B allow to improve the policy A on $[\tau r, \tau s]$".

$_F$or $_t$he period $[\tau r, \tau s]$, let $\left(\lambda_k^{(A)}, \lambda_k^{(B)} \right)$ b$_e$ the pair of respective estimates of the hazard functions associated with policies A and B over $\left] \tau_{k-1}, \tau_k \right]$ with $k \in [\![r+1 .. s]\!]$ and let's consider the statistic

$$W_{rs} = \sum_{k=r}^{s} \mathbf{1}_{\left\{ \lambda_k^{(B)} < \lambda_k^{(A)} \right\}} \quad (59)$$

From a graphical point of view, the statistic Wrs si_{mp}ly calculates the number of times where the HF plot associated with the policy B falls below the HF plot associated with the policy A, i.e., the observation of a greater number of k su$c$h that $\lambda_k^{(B)} < \lambda_k^{(A)}$, with $k \in [\![r .. s]\!]$.

The only condition required to reject the null hypothesis is that the HF values $\lambda_k^{(B)}$ will fall under of the HF values $\lambda_k^{(A)}$ in more of 50% of cases on $[\tau_{,} \tau s]$. In other words, the test statistic must be as

Wr_s > (s − r +1) / 2

This test examines the sign of the differences $\lambda_k^{(B)} - \lambda_k^{(A)}$ of the s–r pairs $\left(\lambda_k^{(A)}, \lambda_k^{(B)}\right)$ associated with the two health security policies during the period $[\tau r, \tau s]$.

Test Implementation

We want to have an idea if the measures are strategies taken by the United States of America in its fight against COVID-19 can be suggested to improve the Moroccan health security policy and over what periods. These two countries having felt the different waves of COVID-19 practically over the same periods and their hazard functions are roughly similar (see Figure 5) although the importance of the numbers of deaths recorded by each of these two countries are of very different amplitudes (see Figure 3). Thus, four typical time periods are targeted by this analysis, days 57-60, 90-100, 550-555 and 570-605.

Visualization of H-H-plots (hazard plot versus hazard plot) shows that the compared plots associated with these two hazard functions interlace on either side with respect to each other over some of these analysis periods and remain one below the other for other periods (see Figure 8).

Figure 8. Visualization of the H-H-plot of the Moroccan health policy vs. US health policy
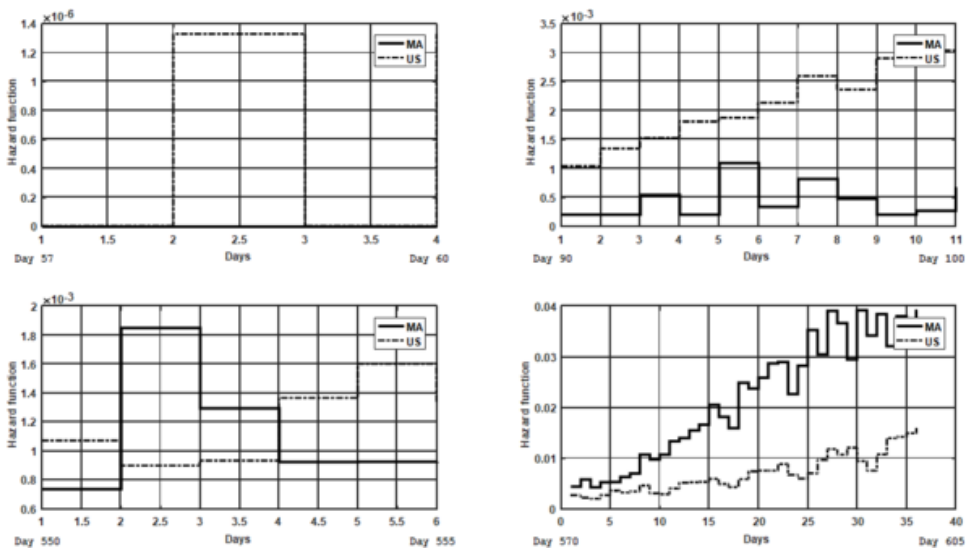
The aliquots where $\lambda_k^{(B)} < \lambda_k^{(A)}$ should be counted and the statistics W_{rs} must be evaluated in order to determine whether or not the null hypothesis should be rejected for the period corresponding to this comparison. When the number of aliquots involved is relatively large, visual counting may be difficult. Thus, it is necessary to automate this procedure. The results of the digitized graphic tests of the H-H-plot corresponding to the periods mentioned above are summarized in Table 2.

Table 2. Some examples testing the Moroccan health policy vs. US health policy

Testing Period			
Starting day	**Ending day**	**Test Statistic**	**Decision**
57	60	$W_{57,60} = 1 < (60-57+1)/2 = 2.0000$	Do not reject H_0
90	100	$W_{90,100} = 0 < (100-90+1)/2 = 5.5000$	Do not reject H_0
550	555	$W_{550,555} = 2 < (555-550+1)/2 = 3.0000$	Do not reject H_0
570	605	$W_{570,605} = 35 > (605-570+1)/2 = 17.5000$	Reject H_0

In summary, we notice that the hypothesis H_0 is rejected by the proposed method only in the last case. This confirms that the American health security policy could be proposed to improve the policy followed by the health system in Morocco over the last period, namely from the 570th to the 605th days, but not over the other three periods of tests.

FUTURE DIRECTIONS AND PESPECTIVES

Both survival analysis methods and sign test we have constructed in this chapter are generic and not specific to death data analysis and the comparison of health security policies. Indeed, this approach can be applied to different types of data for different fields of application and for the appreciation or the denunciation of the strategies that led to a situation compared to other policies that can be tested. As examples, these methods are also applicable in frameworks for monitoring remission of patients, occupation of hospital rooms and medical resources during increased demand, data deriving from development of new drugs and vaccines as well as in frameworks of actuarial science, reliability in engineering and quality assurance in advanced technologies. Indeed, it happens that data is censored in all these areas. Thus, the proposed approach paves the way for their study and interpretation by nonparametric survival analysis methods and the comparison of possible ways to achieve the objectives set by different ways. For these same purposes the proposed

approach is adequate for Monte-Carlo sampling, data resampling and Bootstrap methods in the context of the nonparametric censoring problem. These last viewpoints imply that our methods remain appropriate for the survival analysis of very large datasets (Big Data).

Kernel estimation (respectively wavelet theory) and mean-field theory can also intervene for ML needs in order to determine an efficient estimate of the PDF and thus deduce the estimates of the survivor and hazard functions by the usual formalism described above. The expectation-maximization algorithm (Dempster et al., 1977) can then be used to determine the optimal parameters for the kernel used and allow a significant improvement, particularly in terms of Lévy-Prokhorov distance.

CONCLUSION

As we pointed out on more than one occasion in this chapter, survivor and hazard functions play an important role in the interpretation and understanding of survival data. Indeed, while the shape of the SF tells the analyst how the proportion of deaths changes over time, the shape of the HF provides an active way to analyze how the risk of death changes with time. The functional forms of the fitting estimators of these two functions makes it possible to use them for ML objectives and in particular for prediction. Indeed, once these estimators are established for a set of data, since they are in the form of functions of time, it suffices to evaluate them for any other instant not belonging to the set of the data used for learning.

The methodology presented in this chapter exposes a complete system for the survival analysis of censored and uncensored data as well as the evaluation and the improvement of public health policies. It thus makes it possible to evaluate in nonparametric ways both the survivor and hazard functions in order to follow the evolution of the pandemic and to criticize health security policies against others in view of their effectiveness and with the aim of improving them and reduce mortality from the pandemic. This approach offers an alternative method to the Kaplan-Meier and Cox's regression methods. In addition, all the methods we have proposed in this chapter were adapted for computer implementation making it possible to combine the power of survival analysis to analyze censored data with the performance of processing calculations by the machine and the visualization of analyzes for decision-making. All these factors were in favor of building a digital intelligence capable of achieving the objectives of processing this type of data, understanding it and justifying the decisions made by the machine. For this purpose, we have been led to present diverse statistical methods and detail explanations and examines of practical implications which are not only important for survival analysis, but are also essential to statistical analysis in general.

REFERENCES

Billingsley, P. (1999). Convergence of probability measures (2nd ed.). Wiley-Interscience Publication. doi:10.1002/9780470316962

Bogaerts, K., Komárek, A., & Lesaffre, E. (2018). *Survival analysis with interval-censored data: A practical approach with examples in R, SAS and BUGS*. CRC Press.

Calabuig, J. M., García-Raffi, L. M., García-Valiente, A., & Sánchez-Pérez, E. A. (2021). Kaplan-Meier Type Survival Curves for COVID-19: A Health Data Based Decision-Making Tool. *Frontiers in Public Health*. Advance online publication. doi:10.3389/fpubh.2021.646863

Cox, D. R. (1972). Regression models and life-tables. *Journal of the Rroyal Statistical Society, Series B,* (34), 187-220.

Dempster, A. P., Laird, N. M., & Rubin, D. B. (1977). Maximum Likelihood from Incomplete Data via the EM Algorithm. *Journal of the Royal Statistical Society. Series B. Methodological*, *39*(1), 1–38. doi:10.1111/j.2517-6161.1977.tb01600.x

Dodge, Y. (2008). The Concise Encyclopedia of Statistics. Springer Science + Business Media.

Donsker, M. D. (1952). Justification and extension of Doob's heuristic approach to the Kolmogorov-Smirnov theorems. *Annals of Mathematical Statistics*, *23*, 277-281. DOI: doi:10.1214/aoms/1177729445

Dvoretzky, A., Kiefer, J., & Wolfowitz, J. (1956). Asymptotic minimax character of the sample distribution function and of the classical multinomial estimator. *Annals of Mathematical Statistics*, *27*(3), 642–669. doi:10.1214/aoms/1177728174

Elandt-Johnson, R. C., & Johnson, N. L. (1980). *Survival models and data analysis*. Wiley-Interscience.

Emura, T., & Chen, Y.-H. (2018). Analysis of Survival Data with Dependent Censoring: Copula-Based Approaches. Springer. doi:10.1007/978-981-10-7164-5

Ernesto, P. E., & Lusmeralis, A.-A. (2021). Assessing the impact of vaccination in a COVID-19 compartmental model. *Informatics in Medicine Unlocked*. https://www.sciencedirect.com/science/article/pii/S2352914821002641

Hans, C. van H., & Hein, P. (2012). *Dynamic prediction in clinical survival analysis*. CRC Press.

Jakobsen, L. H., Andersson, T. M.-L., Biccler, J. L., Poulsen, L. Ø., Severinsen, M. T., El-Galaly, T. C., & Bøgsted, M. (2020). On estimating the time to statistical cure. *BMC Medical Research Methodology*, *20*(1), 71. Advance online publication. doi:10.118612874-020-00946-8 PMID:32216765

Jnanendra, P. S., Indrajit, S., Anasua, S., & Ujjwal, M. (2021). Machine learning integrated ensemble of feature selection methods followed by survival analysis for predicting breast cancer subtype specific miRNA biomarkers. *Computers in Biology and Medicine*, *131*. https://www.sciencedirect.com/science/article/pii/S001048252100038X PMID:33550016

Khalik, S. (2020). COVID-19 patients no longer infectious 11 days after getting sick, research shows. *The Straits Times-Singapore*. https://www.straitstimes.com/singapore/health/covid-19-patients-no-longer-infectious-11-days-after-getting-sick-research-shows

Leger, S., Zwanenburg, A., Pilz, K., Lohaus, F., Linge, A., Zöphel, K., Kotzerke, J., Schreiber, A., Tinhofer, I., Budach, V., Sak, A., Stuschke, M., Balermpas, P., Rödel, C., Ganswindt, U., Belka, C., Pigorsch, S., Combs, S., Mönnich, D., ... Richter, C. (2017). A comparative study of machine learning methods for time-to-event survival data for radiomics risk modelling. *Scientific Reports*, *7*(13206), 13206. Advance online publication. doi:10.103841598-017-13448-3 PMID:29038455

Liu, J., Liao, X., Qian, Sh., Yuan, J., Wang, F., Liu, Y., Wang, Z., Wang, F. S., Liu, L., & Zhang, Z. (2020). Community transmission of severe acute respiratory syndrome coronavirus 2, Shenzhen, China, 2020. *Emerging Infectious Diseases*, *26*(6), 1320–1323. doi:10.3201/eid2606.200239 PMID:32125269

Massart, P. (1990). The tight constant in the Dvoretzky–Kiefer–Wolfowitz inequality. *Annals of Probability*, *18*(3), 1269–1283. doi:10.1214/aop/1176990746

Paolella, M. S. (2018). *Fundamental Statistical Inference: A Computational Approach*. Wiley. doi:10.1002/9781119417897

Rezaul, M. K., & Ataharul, M. I. (2019). Reliability and Survival Analysis. Springer.

Ripley, B. D., & Ripley, R. M. (1998). Neural networks as statistical methods in survival analysis. In R. Dybowski & V. Gant (Eds.), *Artificial Neural Networks: Prospects for Medicine*. Landes Biosciences.

Selvin, S. (2008). *Survival analysis for epidemiologic and medical research: A Practical Guide*. Cambridge University Press. doi:10.1017/CBO9780511619809

van den Hout, A. (2017). *Multi-state survival models for interval-censored data*. Chapman and Hall, CRC.

World Health Organization (WHO). (2021). *Coronavirus cases and death data*. https://covid19.who.int/WHO-COVID-19-global-data.csv

Zupan, B., Demšar, J., Kattan, M. W., Beck, J. R., & Bratko, I. (2000). Machine learning for survival analysis: A case study on recurrence of prostate cancer. *Artificial Intelligence in Medicine*, *20*(1), 59–75. doi:10.1016/S0933-3657(00)00053-1 PMID:11185421

Chapter 7
Deep Learning Applied to COVID-19 Detection in X-Ray Images

Harold Brayan Arteaga-Arteaga
Universidad Autónoma de Manizales, Colombia

Melissa delaPava
Universidad Nacional de Colombia, Colombia

Alejandro Mora-Rubio
Universidad Autónoma de Manizales, Colombia

Mario Alejandro Bravo-Ortiz
Universidad Autónoma de Manizales, Colombia

Jesus Alejandro Alzate-Grisales
Universidad Autónoma de Manizales, Colombia

Daniel Arias-Garzón
Universidad Autónoma de Manizales, Colombia

Luis Humberto López-Murillo
Universidad Nacional de Colombia, Colombia

Felipe Buitrago-Carmona
Universidad Autónoma de Manizales, Colombia

Juan Pablo Villa-Pulgarín
https://orcid.org/0000-0003-1263-7618
Universidad Autónoma de Manizales, Colombia

Esteban Mercado-Ruiz
Universidad Autónoma de Manizales, Colombia

Fernanda Martínez Rodríguez
https://orcid.org/0000-0003-0855-2128
Universidad de Guadalajara, Mexico

Maria Jose Palancares Sosa
Instituto Politécnico Nacional, Mexico

Sonia H. Contreras Ortiz
Universidad Tecnológica de Bolívar, Colombia

Simon Orozco-Arias
Universidad Autónoma de Manizales, Colombia

Mahmoud Hassaballah
https://orcid.org/0000-0001-5655-8511
South Valley University, Egypt

María de la Iglesia Vayá
Fundación para el Fomento de la Investigación Sanitario y Biomédica de la Comunidad Valenciana, Spain

Oscar Cardona-Morales
Universidad Autónoma de Manizales, Colombia

Reinel Tabares-Soto
Universidad Autonóma de Manizales, Colombia

INTRODUCTION

In Wuhan 2019, the emerged the coronavirus disease (COVID-19) (Roosa et al., 2020) caused by the virus severe acute respiratory syndrome coronavirus-2 (SARS-CoV-2) (Stoecklin et al., 2020), which is the third highest pathogenic coronavirus detected in humans preceded by the severe acute respiratory syndrome coronavirus (SARS-CoV) and the middle east respiratory syndrome coronavirus (MERS-CoV). On March 11, 2020, the World Health Organization (WHO) declared the COVID-19 outbreak a pandemic (Zhang et al., 2020). An infected person spreads the SARS-CoV-2 virus when coughs or sneezes primarily through droplets of saliva or discharge from the nose (World Health Organization, 2020). Infection can occur within 14 days of exposure but in most cases in no more than 4 to 5 days (Guan et al., 2020). The economical and health consequences of the rapid spread of the virus worldwide forced the adoption of extraordinary social confinement measures to halt its dissemination and to prevent the collapse of the health systems (Martínez Chamorro et al., 2021). It is estimated that between 30–40% of the COVID-19 patients are asymptomatic (Oran & Topol, 2020), others can experience broad symptoms severities. Most of the cases only presented mild or moderate symptoms (Yang et al., 2020), the most common are fever higher than 38°, cough, myalgia, smell and/or taste abnormalities, and headache (Martínez Chamorro et al., 2021). However, a study reports that 15.7% of patients admitted into the hospital developed severe illness (Guan et al., 2020), including severe pneumonia, pulmonary edema, acute respiratory distress syndrome, multiple organ failure, among others (Mo et al., 2020). The early identification and diagnosis are important to mitigate the COVID-19 outbreak (Guan et al., 2020), which as of July 16, 2021, the number of worldwide cases is 188,655,968, including 4,067,517 deaths (World Health Organization, 2021).

A report from the WHO solidarity consultum from February 2021 evaluates multiple drugs and shows that the mortality, initiation of ventilation, and hospitalization duration were not definitely reduced by any trial drug. Until now, no specific drug has been found against COVID-19 (WHO Solidarity Trial Consortium, 2021). Reverse transcription-polymerase chain reaction (RT-PCR) is among the most efficient and reliable methods for the detection of SARS-CoV-2, it is performed using a sample of nasopharyngeal or respiratory secretions. This method has a high specificity and sensitivity that can range from 60–70% to 95–97%, it can vary depending of the time elapsed since exposure to the virus (Martínez Chamorro et al., 2021). However, it takes hours to provide a result and needs specialized equipment and personal. The rapid antigen detection (RAD) tests are used to overcome these limitations since it is fast, easy to perform and interpret (Rathore & Ghosh, 2020).

COVID-19 can cause serious lung complications such as pneumonia. Pneumonia is a lung infection characterized by inflammation and accumulation of fluid in the

alveoli. It may cause breathing problems and in the most severe cases, permanent lung damage. Medical imaging techniques can be used for diagnosing and monitoring this illness (Martínez Chamorro et al., 2021). On the one hand Computed Tomography scan (CT) is an advance technique that allows to generates detailed 3D images of organs and soft tissues (Ohata et al., 2021). On the other hand, chest radiography (X-Ray) is an imaging method that can be portable, is affordable, fast and less harmful than CT (Narin et al., 2020). X-Ray has an important role in the pneumonia diagnosis worldwide (Jaiswal et al., 2019). These images allow doctors to assess different structures, such as the spine, the heart, the lungs, among others, as well as the conditions that affect them (Breiding, 2009). Although X-Ray has a lower sensitivity than PCR and CT, it can be used as a triage method when there is a high prevalence of COVID-19, other resources are limited and it is needed to accelerated patients' admission and treatment (Martínez Chamorro et al., 2021). The COVID-19 diagnosis using X-Ray images can only be done by specialist physicians, which are scare and, in many countries, insufficient. Computer-Aided Diagnosis (CAD) can help to mitigate this panorama by integrating them into the radiologist diagnostic systems, because they can reduce clinicians workload and increases reliability and quantitative analysis (Narin et al., 2021).

Many methods for COVID-19 automatic detection using X-Ray images are proposed in the literature. Many methods are based on using transfer learning along with networks like VGG16, Inception-ResNet v2, MobileNet v2, ResNet50, DenseNet-161, among others (Apostolopoulos & Mpesiana, 2020; De Moura et al., 2020; Zebin & Rezvy, 2021). A two stages model that includes ResNet50 and ResNet101, initially classifies pneumonia and healthy images to later classify COVID-19 examples from the pneumonia cases (Jain et al., 2020); in other work overfitting due to the lack of COVID-19 positive examples is avoided truncating the Inception network at a layer that is chosen experimentally (Das et al., 2020). Other methods use Convolutional Neural Networks (CNNs) as feature extractors and machine learning classifiers like SVM, k-nearest neighbor, decision tree to make the final predictions (Ismael & Sengür, 2021; Mohammed et al., 2021; Ohata et al., 2021). Ensembles of CNNs (Castiglioni et al., 2021; R. K. Singh et al., 2021) and stages and cascade approaches achieve good results (Karar et al., 2020), even when attempting to classify COVID-19 and together with other 14 chest diseases (Albahli & Yar, 2021).

Some new networks base their structure on state-of-the-art CNNs, such as VGG16 (Panwar et al., 2020), AlexNet (Aslan et al., 2021) and Xception (Narayan Das et al., 2020). The CoroNet network is based on the Xception (Khan et al., 2020) and the COVIDiagnosis-Net includes a fine tuning of the SqueezeNet (Ucar & Korkmaz, 2020). Some authors propose their own architectures from scratch, like a 12 layers CNN that includes convolution, max-pooling, batch normalization, dropout, activation, and

204

fully-connected layers (Sarv Ahrabi et al., 2021) and a 22-layer CNN model, trained for multiple classification scenarios, 2 classes, 3 classes, and 4 classes (Hussain et al., 2021). Most of the actual methods perform a binary classification, COVID-19 vs non-COVID-19 cases. However, other attempt to classify COVID-19 along with other diseases like, pneumonia (Toraman et al., 2020; Ucar & Korkmaz, 2020) and tuberculosis (Das et al., 2020; Yoo et al., 2020). An additional approach classifies the severity of COVID-19 illness (Blain et al., 2021).

The most common preprocessing steps applied in the automatic detection methods of COVID-19 include normalization, cropping, and resizing of the images (Sarv Ahrabi et al., 2021). Some authors select only AP or PA views from the images in the databases (Arias-Londono et al., 2020; Panwar et al., 2020). Many works implement data augmentation to mitigate the dataset imbalance, some techniques reported are rotation, horizontal and vertical flip (Khan et al., 2020; Zebin & Rezvy, 2021), shearing, the Fuzzy Color technique (Toğaçar et al., 2020), elastic distortion (Sarv Ahrabi et al., 2021) and histogram equalization (Tartaglione et al., 2020). Data imbalance is also reduced augmenting the images of COVID-19 class using Generative Adversarial Networks (GANs) (Karakanis & Leontidis, 2021; Waheed et al., 2020; Zebin & Rezvy, 2021). Some works perform a segmentation of the lungs over the training images, to try to guarantee that the network identifies COVID-19 features inside them (Arias-Londono et al., 2020; Aslan et al., 2021; Majeed et al., 2020; Rajaraman et al., 2020; Tartaglione et al., 2020).

This Chapter discusses deep learning architectures, machine learning methods and strategies used in state-of-the-art for COVID-19 detection, from which some classification challenges are identified. It also lists datasets available with COVID-19 and other lung diseases examples used to perform lung segmentation, binary and multiclass classification. Then, different preprocessing techniques, and evaluation metrics are described, along with a comparison of different state-of-the art performances on the classification of COVID-19 and other lung diseases. Finally, future research directions and conclusions are addressed.

DEEP LEARNING ARCHITECTURES

Despite the short time since the emergence of COVID-19, several methods for automatic COVID-19 detection using Chest X-Ray images have been proposed. The strategies for COVID-19 detection are transfer learning (TL), the design of a proprietary CNN, and in some cases, the combination with traditional machine learning (ML) algorithms.

Transfer Learning

TL is the most common method for COVID-19 detection. However, most methods implemented for COVID-19 detection use transfer learning for feature extraction and fully connected layers for classification. To implement transfer learning, the researchers replace the trained fully connected layers with new dense and Softmax layers, according to the classification problem. The final activation function generates predictions from the last dense layer, with a specific number of classes. The most commonly used networks are VGG16, VGG19, Inception-ResNet v2, MobileNet v2, EfficientNetB0, Xception, and GoogLeNet (Apostolopoulos & Mpesiana, 2020; Mohammed et al., 2021; Ohata et al., 2021; Zebin & Rezvy, 2021)

- **VGG16**: It is the CNN that won the ILSVR (Imagenet) competition in 2014. It is considered one of the flagship networks for applying transfer learning to date (Krishnaswamy Rangarajan & Purushothaman, 2020). The benefit of using the VGG16 architecture is that it is easy to handle, and also, instead of having a large number of hyperparameters, they focused on having convolution layers of 3 x 3 filters with a stride 1 and always used the same padding and maxpool layer of 2x2 filters of stride 2. It follows this arrangement of convolution and maxpool layers consistently throughout the architecture, as shown in Figure 1. In the end, it has 3 FC (fully connected layers) followed by a softmax for the output. This CNN has a total of 16 layers, namely 13 2D-convolutional layers and three dense layers. It has about 138 million parameters.

- **VGG19**: VGG19 has a total of 19 layers, namely 16 2D-convolutional layers and three dense layers, the architecture is presented in Figure 2. There are other variants of VGG like VGG11 and VGG16. VGG19 has 19.6 billion FLOPs (Dey et al., 2021).

- **Inception-ResNet v2**: It is a convolutional neural architecture based on the Inception family of architectures but incorporates residual connections from the ResNet family of architectures (replacing the filter concatenation stage of the Inception architecture) (Längkvist et al., 2014).
- **MobileNet v2**: It is a CNN that seeks good performance on mobile devices. It is created from an inverted residual structure in which the residual connections are between the bottleneck layers. The intermediate expansion layer uses light convolutions in-depth to filter features as a source of nonlinearity. The

206

Figure 1. General VGG16 architecture
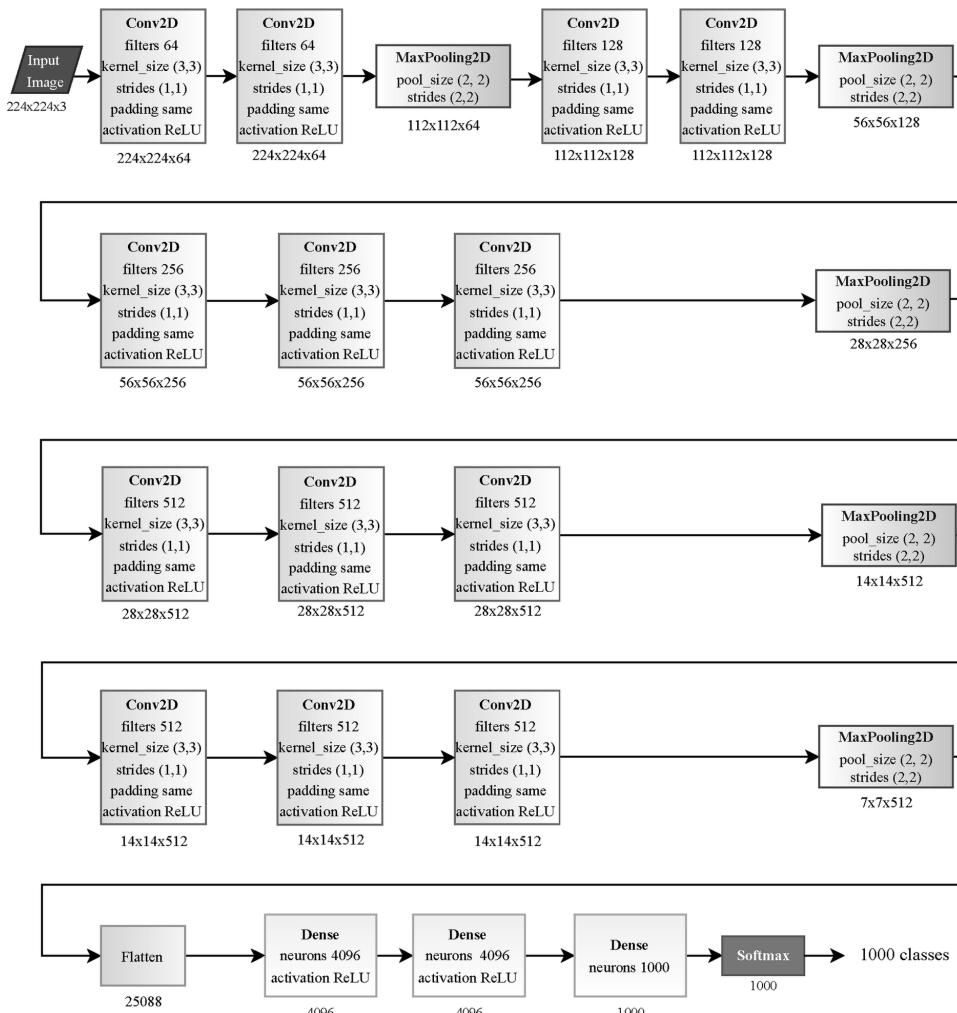
MobileNetV2 architecture comprises an initial complete convolution layer with 32 filters, followed by 19 residual bottleneck layers (Sandler et al., 2018).

- **EfficientNetB0**: It is a CNN with a scaling method that uniformly scales all depth, width, and resolution dimensions using a composite coefficient. Unlike

Figure 2. General VGG19 architecture
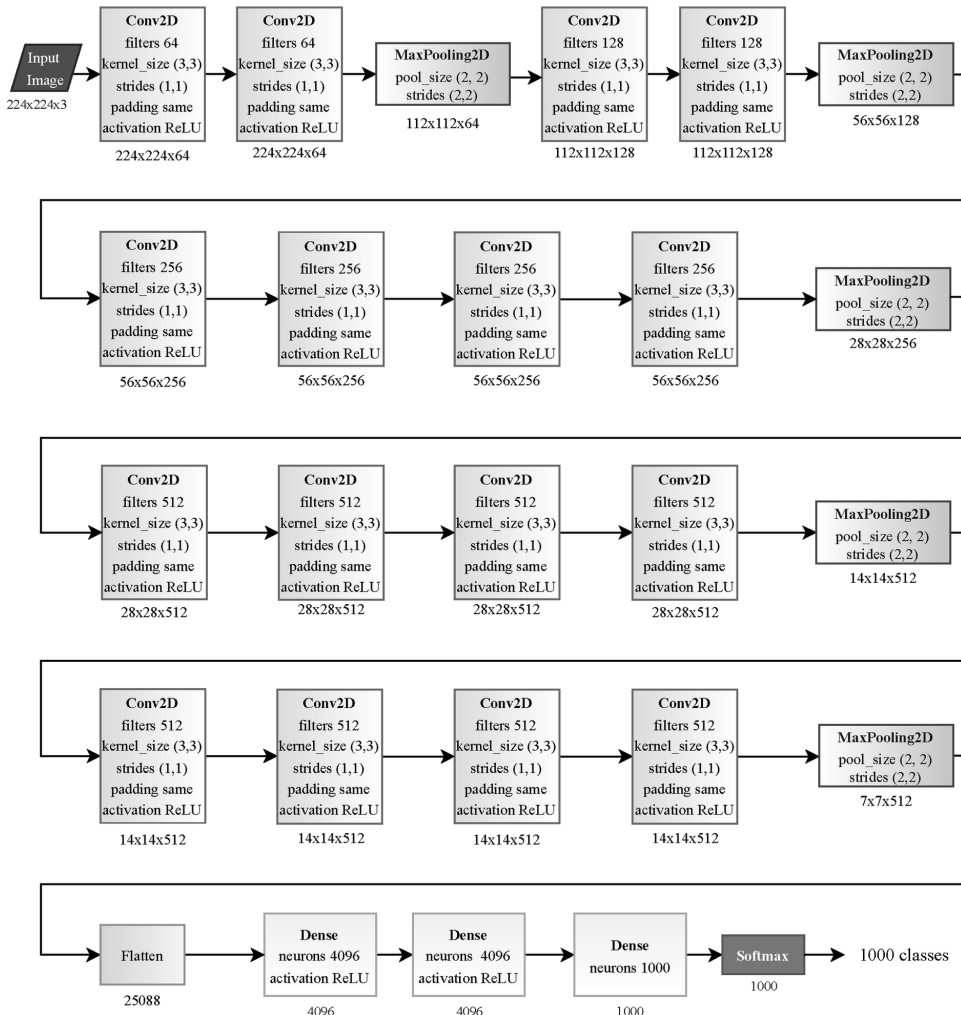
conventional practice that arbitrarily scales these factors, the EfficientNetB0 scaling method uniformly scales the network's width, depth, and resolution with a set of fixed scaling coefficients. The justifies this CNN that if the input image is larger, the network needs more layers to increase the receptive field and more channels to capture more delicate patterns in the larger image. The most basic CNN of the EfficientNets is EfficientNet-B0. EfficientNet-B0 is based on the MobileNetV2 inverted bottleneck residual blocks, plus the squeezing and excitation blocks (Tan & Le, 2019).

- **Xception**: It is a deep CNN with separable convolutions developed by Google. It was presented as an interpretation of the Inception modules of CNNs as an intermediate step between the regular convolution and the separable deep convolution operation (a deep convolution followed by a point convolution). This network is inspired by Inception, in which separable deep convolutions have replaced the Inception module (Chollet, 2017).

- **GoogLeNet**: It is a 22-layer deep convolutional neural network derived from the Inception Network, a Deep Convolutional Neural Network developed by researchers at Google. It utilizes Inception modules, which allow the network to choose between multiple convolutional filter sizes in each block (Szegedy et al., 2015).

- Other state-of-the-art CNNs architectures have also been used in research articles: DenseNet-161 was implemented for the classification of Chest X-Ray images acquired by portable equipment (De Moura et al., 2020); ResNet50 and ResNet101 are used in a cascade-style model where pneumonia and healthy are initially identified, and from the pneumonia cases, images with COVID-19 and viral pneumonia are classified (Jain et al., 2020); ResNet50 obtained the best results from a two-stage model to classify COVID-19, with the results being competitive with those currently reported. Other methods are: an ensemble of CNNs, based on the ResNet50 architecture, and ML models (Castiglioni et al., 2021; A. Singh et al., 2020); pre-trained CNN architectures in a cascade-style classification (Karar et al., 2020); a multi-kernel CNN combined with a pre-trained ResNet-34 model to get around the dataset imbalance problem (Mursalim & Kurniawan, 2021); unsupervised learning, using a technique called Self-Organizing Feature Maps, that can extract features to accurately classify the COVID-19 Chest X-Ray images (King et al., 2020); multimodal learning using clinical and radiographic features, both are compared using the unpaired student's t-test (Blain et al., 2021).

Machine Learning Algorithms

A common approach observed in COVID-19 classification is the use of traditional machine learning methods by replacing fully connected layers, using machine learning methods such as support vector machine (SVM), k-nearest neighbor (KNN), decision tree (DT) in the classification stage, and MobileNets V2, ResNet50, GoogleNet, DarkNet and Xception in the feature extraction stage from transfer learning (Mohammed et al., 2021; Ohata et al., 2021). In (Sahlol et al., 2020) uses Inception for feature extraction and a swarm-based feature selection algorithm to select the most relevant ones, and fuzzy tree transformation is applied to each chest image, then

exemplar splitting. Next, local binary pattern of multiple kernels is used to extract features, the most important ones are selected using the iterative neighborhood component, and finally, conventional classifiers perform the classification. Other implementations of traditional machine learning involve techniques such as late fusion, early fusion, and hierarchical classification to classify not only COVID-19 but also up to 14 other lung diseases (Pereira et al., 2020; Yoo et al., 2020).

Proprietary CNN

Most authors propose their CNNs based on state-of-the-art convolutional neural networks, e.g., CoroNet and COVIDiagnosis-Net. The CoroNet network is created based on Xception architecture pre-trained on the ImageNet dataset, and was fine-tuned using X-Ray images of COVID-19 and other types of pneumonia (Khan et al., 2020). COVIDiagnosis-Net was obtained by fine-tuning the SqueezeNet using a bayesian optimization method and offline augmentation of the COVID-19 class (Ucar & Korkmaz, 2020). Researchers also use neural networks such as VGG16 (Panwar et al., 2020), AlexNet (Aslan et al., 2021), and Xception (Narayan Das et al., 2020) to build their CNNs. For COVID-19 detection, some researchers also propose their architectures from scratch; (Sarv Ahrabi et al., 2021) propose a network with 12 layers, including convolution, max pooling, batch normalization, dropout, activation, and fully connected layers; (Hussain et al., 2021) present a 22-layer CNN model, which a clinician evaluates in multiple classification scenarios of classification, 2-class, 3-class, and 4-class.

COVID-19 DETECTION AND CLASSIFICATION CHALLENGES

Focusing on the possibility of diagnosing COVID-19 from Chest X-Ray images, AI techniques, including ML and DL, have the potential to learn from available data and lay the foundation for automated systems to support professionals in charge of diagnosing various diseases. In general, these techniques are implemented to extract features and find relationships in the data. Therefore, these approaches are well suited for tasks that rely on human expertise (Bravo Ortíz et al., 2021; Orozco-Arias et al., 2019; Tabares-Soto et al., 2019) as is the classification of Chest X-Ray images as positive or negative for COVID-19. For this task, most research works propose a TL approach using models such as VGG19, Inception, and MobileNet (Pham, 2021). A different approach is to develop and implement new CNNs to classify images as positive or negative for COVID-19 (Hussain et al., 2021; Nath et al., 2020).

Data availability is most likely the biggest limitation when developing DL systems to detect COVID-19, even though there are public image databases with very variable

210

image quality, availability, and information, caution must be taken when defining which data will be used to train the DL models as we may face the problem of having to use data from different databases, This can happen if a database does not have the necessary amount of data from patients with positive or negative COVID-19 or even have the presence of other types of diseases such as tuberculosis, lung cancer, among others, which must be filtered before training; this may lead researchers to complement the data with other data distributions to obtain an optimal amount of data to train the DL models adequately. We must also take into account the format with which the data were captured, the noise inherent from the X-Ray equipment, the presence or not of medical devices such as endotracheal tubes present in intubated patients in ICU, electrodes, pacemakers, etc. since these can bias the model to identify patients with these types of devices with positive COVID-19, the variability in the dimensions of the images must be taken into account. The anonymity of the patient whose X-Ray was captured must be guaranteed. These factors can cause biases due to the variability in the information presented, making it difficult for investigators to evaluate their systems under appropriate conditions. In addition, there is no standard benchmark to evaluate and compare the different approaches, which makes the reported results not comparable with each other.

COVID-19 DATASETS

More than two years has passed since SARS-CoV-2 spread and OMS catalog COVID-19 as a pandemic. Therefore, diagnosis of this virus has become an essential key to properly managing the virus's spread. X-Ray data is one of the ways to find pathologies, so to generate models and diagnose COVID-19 on an X-Ray image is necessary to develop public datasets of these images. Figure 3 presents sample Chest X-Ray images from positive and negative diagnoses for COVID-19. Some COVID-19 datasets are going to be exposed, mainly there are three types of datasets, the ones with COVID-19 cases confirmed, COVID-19 negative cases or auxiliary databases used as a control group for experimentation, and finally, some models use some segmentation over the images to limit the information and help models to classify so three groups consist on segmentation datasets. Some datasets have been published, but unfortunately, many issues affect the public dataset; the principal one is image quantity many datasets as COVIDx (L. Wang & Wong, 2020), a compilation from other repositories, so it contains some images from COVID-19 but are fewer than other pathologies or control images. Another problem is the image quantities in general IEEE8023 or Cohen's dataset (Paul Cohen et al., 2020) have more pictures of COVID-19 than another type, but the quantity is considerably less than other datasets. On these parts, there are six primary datasets of study BIMCV-COVID19+

(Vayá et al., 2020), BRIXIA (Signoroni et al., 2021), Cancer Image Archive (Desai et al., 2020), HM Hospitales (Hospitales, 2021), ML Hannover (Winther et al., 2020) and IEEE8023, the last one even though it have many less image was one of the first datasets created. Many researchers use it as a COVID-19 positive dataset or as part of the COVID-19 positive dataset, so it is also meaningful research development.

- **BIMCV-COVID19+:** It is a dataset from the Valencian Region Medical ImageBank (BIMCV) with X-Ray images CXR (CR, DX) and computed tomography (CT) of COVID-19 patients that present a positive result on a Polymerase chain reaction (PCR), Immunoglobulin G (IgG), or Immunoglobulin M(IgM) diagnosis test, it contained 5381 images of 1311 patients in which 3141 are RX images, and 2239 are CT images, all images are in DICOM format. For the acquisition process, images were taken from February 26 to April 18, 2020, from 11 hospitals from the Valencian Region, then Dicom images were anonymized with Clinical Trial Processor (CTP). Additionally, to anonymization process used all radiological reports processed through a natural language algorithm to extract labels to classify the information. These labelings lead to a total of 336 tags. Images were also processed and stored on 16 bits PNG images, so the dataset is available on DICOM raw data or Adjusted to a PNG image. On the overall data, we find 1311

Figure 3. Sample chest X-Ray images with and without COVID-19

212
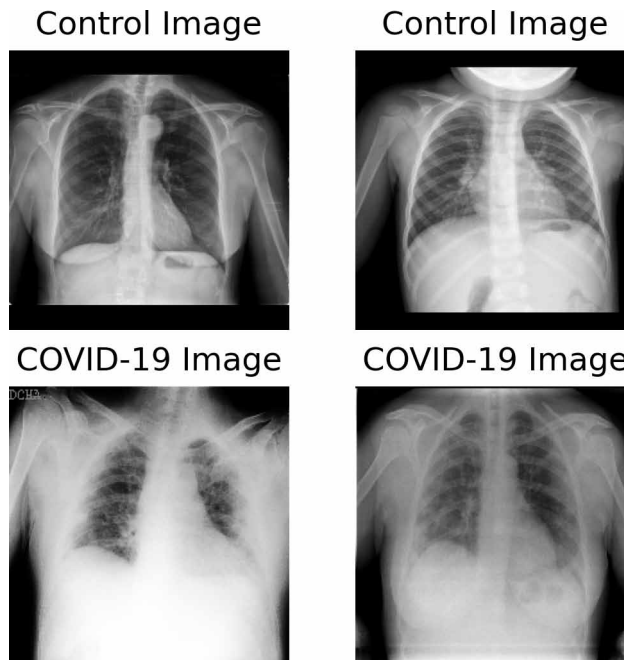
subjects, where 45.92% were female, the mean age is 63.11%, approximately 1.9 images per subject. 1,380 CX, 885 DX and 163 CT studies. 2427 images on monochrome 2 and 751 in monochrome 1. it suggests inverted monochrome one images; images were taken using 20 different devices, there was a total of 2425 PCR applied (1773 positives, 622 negatives, and 30 indeterminates), 29 IgM, 29 IgG and 35 ACT (44 positives, 32 negatives, 17 indeterminates) (Vayá et al., 2020). Finally, these datasets use the ROI system to point out some pathologies marked by radiologists on the images. There were two prominent that are ground-glass opacities and consolidation. This dataset is available on https://bimcv.cipf.es/bimcv-projects/bimcv-COVID19/.

- **BRIXIA**: Was a collected dataset following the Brixia score and have 4703 images from 2351 subjects, taken from hospitals of northern Italy from March to April of 2020, all photos are anteroposterior (AP = 87%) and posteroanterior (PA = 13%) Chest X-Ray images, each image comes with a complete structured report of the patient's medical record, revised by around 30 specialists. Also, it provides a score (Brixia score) that indicates the severity of pneumonia on six zones of the lungs (3 each) from X-Ray images associated with the affectation of different tissues. This punctuation suggests the following: no lung abnormalities (0), interstitial infiltrates (1), interstitial and alveolar infiltrates (2), interstitial dominant, or interstitial and alveolar infiltrates, alveolar dominant (3), the Brixia score is a quantification of 50 radiologists mean report findings (Signoroni et al., 2021). This project also provides a lungs segmentation algorithm that merges three datasets: Montgomery, JSRT, and Shenzen. Then the algorithm was validated over the IEEE8023 dataset. The dataset is available on https://brixia.github.io/.

- **ML Hannover**: Anonymized dataset from 243 COVID-19 X-Ray case images from 71 subjects from the Institute for Diagnostic and Interventional Radiology on Hannover, Germany, contains images and metadata such as patient master data, laboratory results, and if they go to ICU. These datasets have two versions the second one is the one with 243 images; meanwhile, the first version only has 186 (Winther et al., 2020). Datasets are available on https://data.uni-hannover.de/dataset/cov-19-img.

- **Cancer Image Archive**: Image dataset from the United States, with X-Ray images and computed tomography from hospitalized patients with images on the eight days before diagnosis and at least one image after diagnosis, each diagnosis was by a PCR test. There are a total of 256 studies (233 radiographs and 23 CT), studies include on radiograph studies one image in different views (AP, PA, Lateral), and CT studies contain multiple shots (1 to 572 images each). Metadata provided contained a report from a certified radiologist on main image findings. In addition, multiple clinical correlations were developed for

213

these image classifications as comorbidities, ICU admissions, Race, among others. One of the essential contribution correlations used was a Genomic Correlate with a Genbank repository of the SARS-CoV-2 genome (Desai et al., 2020). Image Dataset and Genbank repository are available on https://wiki.cancerimagingarchive.net/pages/viewpage.action?pageId=70226443.

- **COVID Data Save lives:** Anonymized image dataset from hospitals of HM Hospital Group from different locations in Spain has 2310 subjects. Still, only 189 subjects have X-Ray images, so there are in total 419 images. According to its web page, the dataset is actualizing up to the end of the pandemic, so once requested, there might be more images.The clinical dataset contains multiple tables, so they included subject data such as age, sex, and ICU admission. The second table contains all medication applied during the time of the hospital. The third table contains vital signs recorded, the fourth table has lab test results, and the final table includes a codification code according to CIE10 (Hospitales, 2021). Dataset is available for investigation and academic or health institution by request on the following page https://www.hmhospitales.com/coronavirus/COVID-data-save-lives/english-version.

- **IEEE8023:** An image compilation from different public sources that claim to be a type of pneumonia (Especifily COVID-19, SARS, Streptococcus spp, Pneumocystis spp, and ARDS), so not all images contained are from COVID-19 cases, specifically 468 COVID-19 X-Ray images on three different views(AP, PA, and AP Supine) it also comes with a severity score in terms of Pneumonia affectations as a Mean of three experts rates, on two parameters Geographic Extent that is how extent does ground-glass opacity or consolidation is seen for each lung (score from 0 to 8) and opacity that is how advance is the opacities name before (score 0 to 6) (Paul Cohen et al., 2020).The image dataset is available on https://github.com/ieee8023/COVID-chestxray-dataset.

Complementary Datasets

Control or complementary datasets are helpful for make binary or multiclass classification on these datasets. The main goal is to find information that differs from a COVID-19 diagnosis to make the model recognize a COVID-19 image and images with other characteristics. On these parts, we see multiple datasets, even some of the mentioned before have images out of a COVID-19 diagnosis. Images on these datasets are mainly of 3 types: Normal X-Ray images of healthy subjects. These Pneumonia X-Ray images are images of different kinds of pneumonia diagnoses that are not from COVID-19, and finally, images of other pathologies that differ

from a COVID-19 diagnosis. For this part, will be exposed six different datasets as complementary databases for COVID-19 detection in X-Ray images.

- **Padchest:** Pathology Detection in Chest radiographs (Padchest) is a Spain dataset that contains 160,868 images from 67,625 patients, with 193 diagnosis labels, the most common ones are COPD signs, pneumonia, heart insufficiency, and pulmonary edema as differential diagnoses and infiltrates, cardiomegaly, aortic elongation and unchanged as radiographic findings, images where obtained from studies from 2008 to 2017, Dicom images projection are mainly PA(96010) and Lateral (51,124), but other projections are AP, Costal and Pediatric views (Bustos et al., 2020). This dataset can be downloaded from https://bimcv.cipf.es/bimcv-projects/padchest/.This dataset has a variant called BIMCV-COVID-Padchest that combines pneumonia and normal diagnosis on the Padchest image dataset and COVID-19 datasets. It is also available on https://bimcv.cipf.es/bimcv-projects/ bimcv-COVID19/#1590857662078-c30d2790-05dc.
- **BIMCV-COVID-:** Spain dataset from the same time as the positive dataset, also of subjects with a PCR, IgM, or IgG diagnosis test with a negative result for COVID-19. The dataset contained X-Ray Images (CD, DX) and computed tomography. Images quantity is 6540 from 3238 subjects, and it also comes with labeled metadata from finding unified into the Unified Medical Language System (UMLS) terminology (BIMCV, 2020). As BIMCV-COVID19+, negative one has two iterations available on https://bimcv.cipf. es/bimcv-projects/bimcv-COVID19/#1590859488150-148be708-c3f3.
- **CheXpert:** Chest collection dataset from radiographic studies of Standard Hospital from 2002 to 2017 contained 224316 images from 65240 patients classified on 14 observation labels such as No Findings, Cardiomegaly, or Pneumonia. This dataset has two versions, the complete one and a reduced one (Irvin et al., 2019). For acquiring those is necessary to fill a request on the following page https://stanfordmlgroup.github.io/competitions/chexpert/.
- **RSNA:** A Kaggle dataset based on NIH Chest X-Ray Dataset of 14 common chest diagnoses such as Atelectasis or Cardiomegaly has 112120 images from 30805 subjects all in frontal view and using natural language processing each image is classified on one or more of the 14 labels (X. Wang et al., 2017), Kaggle challenge is available on https://www.kaggle.com/c/ rsna-pneumonia-detection-challenge.
- **Chest X-Ray Images (Pneumonia):** A Kaggle dataset that contains 5232 images from children's of which 3883 are labeled on pneumonia (2,538 bacterial and 1,345 viral) and 1,349 have a normal diagnosis there where a total of 5856 patients bus some images were for validation purposes (Kermany

et al., 2018). The Kaggle challenge is available https://www.kaggle.com/paultimothymooney/chest-xray-pneumonia.

Lung Segmentation

There are three datasets performing lung segmentation

- **Montgomery dataset (Jaeger et al., 2020):** This database was obtained from the Department of Health and Human Services, Montgomery County, Maryland, USA, and the Shenzhen No. 3 People's Hospital in China. The two datasets contain normal and abnormal chest radiographs with manifestations of pulmonary tuberculosis and include associated radiologist readings. The number of images in this database is 138.
- **JSTR (Shiraishi et al., 2020):** It is a database composed of 247 chest radiograph images with and without pulmonary nodules. This database aimed to evaluate the solitary pulmonary nodules included in the database. Currently, this database is used for lung segmentation.
- **NIH (Tang et al., 2020):** This database contains 100 chest radiographs with lung masks with posterior-anterior and anteroposterior views for further segmentation and evaluation

PROCESSING APPROACHES

It is often necessary to adjust or modify the available raw data so it is suited for the development of DL models. In this case, the detection of COVID-19 from Chest X-Ray images involves working with data, from different sources and with various acquisition conditions, which creates a problem around inconsistencies in data distribution. This section presents a selection of the most common operations, as reported in the literature, that have been used by researchers to mitigate this problem and improve the overall quality of the data.

Database Manipulation

Chest X-Rays are captured from two projections, a frontal projection that could be posteroanterior (PA) or anteroposterior (AP), and a lateral projection. Given the amount of information and detail available in each projection, it is common to select only the images from PA and AP projections to train and evaluate DL models. Before applying any preprocessing techniques to the images, the operations of cropping and resizing are often applied. Cropping refers to removing unwanted

216

sections of an image or picture, in this case, the region outside the patient's lungs does not contain relevant information to the task at hand. Regarding the resizing operation and recognizing the positive impact of transfer learning, the majority of researchers resize the images down to 224 pixels by 224 pixels (Horry et al., 2020; Ismael & Sengür, 2021; Ohata et al., 2021), which is the most common input size for image classification CNNs, and allows taking advantage of pretrained weights on much larger datasets such as ImageNet.

Normalization

Image normalization is a technique commonly used in the preprocessing stages for classification to improve and accelerate different classical machine learning algorithms or neural networks (Shalabi et al., 2006). This technique can be divided into three different types: Min-max normalization, z-score normalization, and decimal scaling normalization.Min-max normalization is designed to maintain the relationship between the original data and a rescaled version within a predefined range of values (Gopal et al., 2015). The definition of this type of normalization is as follows:

$$Nx = \left(\frac{x - \min(x)}{\max(x) - \min(x)} \right) * (N\max - N\min) + N\min \qquad (1)$$

Where, Nx is the normalized data, x is the original data, min(x) and max(x) are the minimum and maximum values of the data respectively, Nmax is the new maximum, and Nmin is the new minimum of the data.

Similarly, z-score normalization maps original data to a new range of values, but in this case, using the mean and standard deviation of the data (Eesa & Arabo, 2017). The equation that defines this type of normalization is as follows:

$$Nx = \frac{x - mean(x)}{std(x)} \qquad (2)$$

Where, Nx is the normalized data, mean(x) is the mean of the data, and std(x) is the standard deviation of the data. This type of normalization is used to normalize both individual images and the entire dataset. Finally, decimal scaling normalization is based on moving the decimal point of every value in the dataset (Eesa & Arabo, 2017). The equation that represents this type of normalization is

$$Nv = \frac{v}{10^j} \tag{3}$$

Where Nv represents the new value in a sample of the data, v is the original value, and j corresponds to the count of numbers at the maximum absolute value of the sample.

The normalization technique has proven to be successful in addressing the problem of COVID-19 classification (dos Santos et al., 2021), and many researchers have used the technique in order to reduce the data variability presented between datasets from different sources (Arias-Garzón et al., 2021; Narayanan et al., 2020).

Fuzzy Color Technique

Fuzzy Color algorithms define an input-output function which receives 3 input variables corresponding to the color channels (red, green and blue) and outputs a single variable representing the information. This technique is useful for image analysis and allows to separate the original information into different representations, known as windows. After applying the Fuzzy Color technique, it is possible to reconstruct the original image through a weighted sum of the obtained windows (Toğaçar et al., 2020).

Data Augmentation

Training artificial intelligence models requires large amounts of data to generalize well to the task at hand. Conversely, the models tend not to generalize and cause overfitting when the task contains limited data, or when there is a class imbalance within datasets. To overcome this problem, the data augmentation strategy has been proposed, where the principal objective is to increase the amount of data using different methodologies, as traditional geometric transformations and more sophisticated methods based on deep neural networks (Mikołajczyk & Grochowski, 2018). Traditional geometric transformations consist of taking an image of the data and generating a "duplicate" of this image that is rotated, flipped, sheared, or zoomed. Some of the most common transformations used in the COVID-19 classification task are rotation, flip, crop, shear, elastic distortion, brightness variation, and the addition of Gaussian noise (Nayak et al., 2021; Sarv Ahrabi et al., 2021; Zebin & Rezvy, 2021). Among the transformations mentioned above, the addition of Gaussian noise is one of the most outstanding ones, it consists of injecting a matrix of random values with a gaussian distribution, and some made tests have demonstrated that adding noise to images can help the algorithms to learn more robust features (Shorten

& Khoshgoftaar, 2019). Likewise, the methods of deep neural networks are based explicitly on GANs. These are a new DL tool to perform the generation of new images. The idea with GANs is to have two models: a generative model G and a discriminative model D. Model G captures the data distribution. In contrast model D estimates the probability that the sample came from the data rather than being generated by model G. The objective is that model G generated images make the mistake of model D (GoodfellowIan et al., 2020). This type of data augmentation has been widely used to generate new images on COVID-19 classification task, given that the data for this is very limited. Some examples of GANs applied to COVID-19 classification are the Auxiliary Classifier Generative Adversarial Network (ACGAN) (Waheed et al., 2020), CycleGAN (Zebin & Rezvy, 2021), and Conditional Generative Adversarial Networks (cGAN) (Karakanis & Leontidis, 2021).

Segmentation

One of the reported issues of DL models when detecting COVID-19 in Chest X-Ray images, is that the prediction is based on areas outside the Region of Interest (ROI) (Majeed et al., 2020), which in this application corresponds to the patient's lungs. To overcome this situation and force the model to focus on the ROI, some research works have implemented a lung segmentation stage in the preprocessing pipeline (Arias-Londono et al., 2020; Rajaraman et al., 2020; Tartaglione et al., 2020). The task of segmenting the lungs region out of a Chest X-Ray, corresponds to a semantic segmentation performed at a pixel level. The most common DL architecture for this task is the U-Net, which has an encoding, a decoding stage, and uses skip-connections. The U-Net architecture was originally proposed in 2015 for biomedical image segmentation (Ronneberger et al., 2015; Siddique et al., 2021).

Histogram Equalization

Similar to radiologists, DL models take advantage of high-quality images acquired under good conditions, which is not always the case when dealing with real-world data, especially when it comes from different sources. Histogram equalization enhances image quality and detail, by redistributing the pixel intensity values to equalize them in the full range of the histogram, which improves the brightness and contrast of the image (Patel et al., 2020; Salem et al., 2019; Tartaglione et al., 2020). The Contrast Limited Adaptive Histogram Equalization is a widely used histogram equalization technique to enhance details, textures and low contrast in the X-Ray images giving an augmented visibility of edges and curves in the CX-R images (Al-Waisy et al., 2021). This method has the advantage over others of enhancing an image definition and local contrast, giving a more natural appearance with a reduction of saturation

in certain regions compared with the HE and overcoming the amplification of noise in near constant regions (Sejuti Rahman et al., 2021). Its use in the dataset images for COVID-19 classification has shown higher values of accuracy, sensitivity and specificity contrasted to using the original data (Dimas et al., 2021). Based on how the intensities are distributed in the histogram, this method sets a clipping (threshold) value in order to limit the amplification of homogeneous regions, so that the intensities higher than the clip limit take the value of the threshold itself (Maity et al., 2020; Salem et al., 2019). Following the procedure describing (Salem et al., 2019), first the input image has a partition process into corner, border and inner regions. Then the histogram of each region is obtained according to the clipping level to calculate the Cumulative Distribution Functions (CDFs). According to the evaluated pixel and using its intensity value as an index, the four closest neighboring pixels are mapped based on their CDF. Finally, the current pixel's position is mapped using those values. In this way, the output image's intensities will be in the range [min,max), set by the user (Sejuti Rahman et al., 2021).

A solid contrast enhancement improves pattern recognition and the quality of processing digital images (Huang et al., 2013). This type of contrast correction aims to ensure a correct diagnosis of disease (Agarwal & Mahajan, 2018) and has been recently applied as a universal preprocessing step for COVID-19 detection (Oh et al., 2020). Gamma correction is a non-linear operation that enhances image brightness on the input image pixels according to a given gamma value (γ) and based on a logarithmic relationship between luminous intensity and the resultant image density. However, the traditional gamma correction is limited to a manually given γ.

To overcome the time-consuming task of setting an appropriate value, some authors (Huang et al., 2013; Shanto Rahman et al., 2016; Veluchamy & Subramani, 2019) have proposed an adaptive algorithm. The adaptive gamma correction automatically fixes an adequate value upon the statistics of the input image, with a weighted distribution based on the Cumulative Density Function (CDF) and the Probability Distribution Function (PDF) relying on an adjusted alpha (α) parameter (Agarwal & Mahajan, 2018; Dailla et al., 2014; Huang et al., 2013).

The Recursively Separated and Weighted Histogram Equalization method assist to optimize the α value present in the AGCWD technique. Alpha is calculated by the summatory of the probability densities in each sub-histogram previously obtained. This technique employs a mean-based segmentation algorithm in the original histogram at every iteration (Dailla et al., 2014). Some of the characteristics that embrace this method is the preserving of image brightness after its contrast enhancement (Huang et al., 2013), demonstrating low values in the Absolute Mean Brightness Error (AMBE), and its high Peak Signal to Noise Ratio (PSNR) (Kaur & Singh, 2016).

Local Phase-Based Image Enhancement

The Local phase-based image enhancement consists in extracting three phase features from the image, this are local weighted mean phase angle (LwPA), its weighted local phase energy (LPE) and the enhanced local energy attenuation image (ELEA) (Hacihaliloglu, 2018; Meng et al., 2013). The CXR image enhanced by this method comes out as a multi- feature image compounded by the features extracted from it. This enhancement technique brings out characteristics that are not visible in the non-treated X-Ray images and is unalterable to intensity variations. Therefore, it brings a solution for the variation in the images' intensity originated by morphological differences among patients and acquisition machine parameters (Qi, Brown, et al., 2021). Furthermore, it has been demonstrated that the use of a multi-feature dataset improves the classification results for COVID-19 detection using Chest X-Ray images in a semi-supervised learning approach (Qi, Nosher, et al., 2021).

EVALUATION METRICS

An evaluation metric refers to a quantitative method of evaluating the training and performance, of a DL model. The choice of an adequate metric is an important step when designing an image classification system, and points researchers in the right direction to improve the performance of the model. This section describes the most used evaluation metrics in the development of DL models to detect COVID-19 in Chest X-Ray images. As a convention, the metrics will be expressed in terms of True Positive (TP) or the positive instances classified correctly, True Negatives (TN) or the negative instances classified correctly, False Positives (FP) or the negative instances classified incorrectly, and False Negatives (FN) or the positive instances classified incorrectly classified.

Accuracy

Accuracy is probably the most used metric and the easiest one to interpret, it represents the proportion or percentage of correct predictions the model makes (Arteaga-Arteaga et al., 2021; M & M.N, 2015). Accuracy is expressed in the range from 0 to 1, or 0 to 100 as

$$Accuracy = \frac{TP + TN}{TP + TN + FP + FN} \tag{4}$$

221

Precision

Precision indicates the proportion of the samples predicted by the model as positive that are actually positive (Arteaga-Arteaga et al., 2021; M & M.N, 2015). Precision is expressed in the range from 0 to 1, or 0 to 100, where,

$$\text{Precision} = \frac{TP}{TP + FP} \tag{5}$$

Recall

Recall indicates the proportion of the samples labeled as positive that were predicted by the model as positive, it can be seen as a measure of model performance on positive instances (Arteaga-Arteaga et al., 2021; M & M.N, 2015).. Recall is expressed in the range from 0 to 1, or 0 to 100 in the form

$$\text{Recall} = \frac{TP}{TP + FN} \tag{6}$$

F1 Score

In practice, there is a trade-off between precision and recall defined by the classification threshold, by changing this threshold one metric will rise and the other one will drop. The F1 score is a metric that combines precision and recall, making it easier to optimize model performance, it is especially useful in tasks were both high precision and recall are needed (Arteaga-Arteaga et al., 2021; M & M.N, 2015). Mathematically, the F1 score corresponds to the harmonic mean of precision and recall, as expressed by

$$F_1 = 2 \cdot \frac{\text{Precision} \cdot \text{Recall}}{\text{Precision} + \text{Recall}} \tag{7}$$

Specificity

Specificity indicates the proportion of the samples labeled as negative that were predicted by the model as negative, it can be seen as a measure of model performance

on negative instances (M & M.N, 2015). Specificity is expressed in the range from 0 to 1, or 0 to 100.

$$\text{Specificity} = \frac{TN}{TN + FP} \tag{8}$$

Receiver Operator Characteristic (ROC) Curve

A ROC curve is a graphical method of evaluating the performance of a DL model at different classification thresholds. As mentioned before, changing the classification threshold determines the number of positive and negative predictions, in this case measured in terms of True Positive Rate (TPR), or recall, and False Positive Rate (FPR), defined in Equation No. 9

With this in mind, the ROC curve consists of a plot of TPR vs. FPR at different classification thresholds. There is an important metric derived from this curve, it corresponds to the Area Under the Curve (AUC) and gives a measure of model performance independent of the classification threshold (Arteaga-Arteaga et al., 2021; Flach et al., 2003).

$$\text{FPR} = \frac{FP}{FP + TN} \tag{9}$$

Intersection Over Union (IoU)

Intersection over union is a metric that computes similarity between two sets, it is widely used in image segmentation tasks to compare the real and predicted masks. It is defined as the intersection of the ground truth mask and the predicted mask over the union of both regions (Harouni & Baghmaleki, 2021).

$$\text{IoU} = \frac{|A \cap B|}{|A \cup B|} \tag{10}$$

Dice Coefficient

Similar to the IoU metric, the Dice coefficient is used as an evaluation metric in semantic segmentation models, furthermore it can be modified to be used as a loss function to train the algorithms. It is defined as two times the intersection of the ground truth mask and the predicted mask over the sum of the area of each region (Harouni & Baghmaleki, 2021).

$$\text{Dice} = \frac{2 \cdot |A \cap B|}{|A| + |B|} \tag{11}$$

EXPERIMENTAL RESULTS AND COMPARISONS

The interpretability of the CNNs is a problem in comparing CNN performance (A. Singh et al., 2020). For the mentioned reason, some researchers present visualization methods as an alternative to generating credibility. One crucial tool is heat maps. (Ozturk et al., 2020) classifiy COVID-19 and uses heat maps to provide the best interpretability on CNN working. Also, other techniques include t-SNE (Arias-Londono et al., 2020), class activation maps (Ucar & Korkmaz, 2020), and Grad-CAM (Liang et al., 2021; R. K. Singh et al., 2021). Transfer learning is the most common technique to classify images. Some researchers compare different state-of-the-art CNN. It is the case of (Majeed et al., 2020); they use twelve different architectures. For (Majeed et al., 2020) the Xception, InceptionResnetV2, and SqueezeNet networks are the best alternatives to classifying COVID-19 in a binary scenario. Also, they show the time that the CNN needs to learn as an essential parameter. In another case, (Apostolopoulos & Mpesiana, 2020) compare five networks using TL, showing as the best alternative the VGG19 network. (Nayak et al., 2021) tune different hyperparameters on eight CNNs as the trainable layers, epochs, batch size, learning rate, optimizer algorithm, etc. They show the best alternatives to the ResNet architectures.

(Pham, 2021) presents an important work in terms of comparison through comparing different networks to classify COVID-19 like COVIDGAN, CoroNet, DarkCOVIDNet, and state-of-the-art fine-tuned CNNs. Similar setups were used to the original studies in the experimental process. This work shows that the database update does not allow a perfect comparison. Alternately, (Horry et al., 2020) compare results of pre-trained CNNs like VGG16 but using X-Ray images and CT and

Ultrasound chest images to classify the COVID-19, other pneumonia, and healthy persons. In this case, the Ultrasound images provide the best CNN performance.

Table 1 presents a comparison of previous works showing the DL architectures, the classes considered, and the references. The comparison shows that many researchers used models to classify COVID-19 among other classes, such as Normal (without COVID-19), and Pneumonia (bacterial and viral). In addition, some works also try to include in the classification different types like MERS, SARS, Varicella, Edema, Effusion, Tuberculosis, among others. The accuracy, sensitivity, specificity, F1 score, and others metrics validate the achieved experimental results. It is not easy to compare one result with the obtained by other researchers because some databases

Table 1. Comparison of experimental results for COVID-19 classification using deep learning

Paper	DL architectures	Classes to classify	Outstanding results
(Apostolopoulos & Mpesiana, 2020)	• VGG16 • MobileNetV2 • Inception • Xception • Inception-ResNet-v2	• COVID-19 • Pneumonia • Normal	MobileNetV2: • Accuracy, 94.7%; • Sensitivity, 98.7%; • Specificity, 96.5%
(Ucar & Korkmaz, 2020)	COVID Diagnosis-Net (SqueezeNet based CNN)	• COVID-19 • Pneumonia • Normal	• Accuracy, 98.3%; • Sensitivity, 99.1%; • FI, 98.3%
(Ozturk et al., 2020)	Dark COVID-Net (Darknet-19 based CNN)	• COVID-19 & Normal • COVID-19 & Pneumonia & Normal	Binary accuracy, 98.1%
(Toğaçar et al., 2020)	• MobileNetV2 • SqueezeNet • Social Mimic optimization method • SVM	• COVID-19 • Pneumonia • Normal	• Overall accuracy, 98.3% • COVID-19 sensitivity, 99.3% • COVID-19 specificity, 99.4%
(Pereira et al., 2020)	• KNN • SVM • MLP • DT • RF • Hierarchical Clus-HMC	• COVID-19 • Normal • MERS • SARS • Varicella • Streptococcus • Pneumocystis	• COVID-19 F1 Score, 83.3% (multiclass) • COVID-19 F1 Score, 88.8% (hierarchical)
(Apostolopoulos et al., 2020)	MobileNetV2	• COVID-19 • Edema • Effusion • Emphys • Fibrosis • Pneumonia • Normal	Accuracy, 87.7% (all classes)

are constantly updated, and some researchers use data combinations. However,

Table 1. Continued

Paper	DL architectures	Classes to classify	Outstanding results
(Waheed et al., 2020)	● ACGAN ● VGG16	● COVID-19 ● Normal	Using actual data: ● Sensitivity, 69.0%; ● Specificity, 95.0%; ● Accuracy, 85.0% Including synthetic images: ● Sensitivity, 95.0%; ● Specificity, 90.0%; ● Accuracy, 97.0%
(Khan et al., 2020)	CoroNet	● COVID-19 & Normal & Bacterial pneumonia & Viral pneumonia ● COVID-19 & Pneumonia & Normal	● Accuracy, 93.0% (four classes) ● Accuracy, 95.0% (three classes)
(Das et al., 2020)	Truncated Inception Net	● COVID-19 ● Pneumonia ● Tuberculosis ● Normal	● Accuracy, 99.96% (COVID-19 positive cases) ● AUC, 100%
(Toraman et al., 2020)	CapsNet	● COVID-19 & Normal ● COVID-19 & Normal & Pneumonia	● Accuracy, 97.2% (binary class) ● Accuracy, 84.2% (multi class)
(Blain et al., 2021)	● U-Net ● DenseNet121	Lung segmentation	● Accuracy, 78.5% (Diagnosing alveolar opacities) ● Accuracy, 90.7% (Diagnosing interstitial opacities)
(Horry et al., 2020)	VGG19	● COVID-19 ● Pneumonia ● Normal	● Accuracy, 86% (X-Ray) ● Accuracy, 100% (Ultrasound) ● Accuracy, 84% (CT)
(King et al., 2020)	Self-Organizing Feature Map	● COVID-19 ● Normal	Euclidean distance of 1.1 between 1st and 2nd winning neurons
(Karar et al., 2020)	● VGG16 ● ResNet50V2 ● DenseNet169	● COVID-19 ● Normal ● Viral pneumonia ● Bacterial pneumonia	Accuracy, 99.9%
(Ohata et al., 2021)	● MobileNet ● DenseNet121 ● Inception-ResNet-v2 ● Bayes ● RF ● MLP ● KNN ● SVM	● COVID-19 ● Normal	MobileNet+SVM: ● Accuracy, 98.6% ● F1-score, 98.5%

Table 1. Continued

Paper	DL architectures	Classes to classify	Outstanding results
(Shorfuzzaman & Hossain, 2020)	Siamese Network	● COVID-19 ● Pneumonia ● Normal	● Accuracy, 95.6% ● AUC, 98.9%
(De Moura et al., 2020)	DenseNet161	● COVID-19 ● Pathological ● Normal ● Combinations	Accuracy, 90.3% COVID-19 & (Normal+Pathological)
(Nayak et al., 2021)	● AlexNet ● VGG16 ● GoogleNet ● MobileNetV2 ● SqueezeNet ● ResNet34 ● ResNet50 ● InceptionV3	● COVID-19 ● Normal	ResNet34: Accuracy, 98.3%
(Karakanis & Leontidis, 2021)	CNN Designed	● COVID-19 & Normal ● COVID-19 & Normal & Bacterial pneumonia	Binary classification: ● Accuracy, 98.7% ● Sensitivity, 100% ● Specificity, 98.3%
(R. K. Singh et al., 2021)	● VGG19 ● VGG16 ● ResNet50 ● DenseNet161 ● DenseNet169 ● Naïve Bayes	● COVID-19 ● Pneumonia ● Normal	Accuracy, 98.7%
(Sheykhivand et al., 2021)	● GANs ● LSTM Networks	● Normal & COVID-19 ● Normal & Pneumonia (Viral, Bacterial, COVID-19) ● Normal & COVID-19 & (Viral Pneumonia, Bacterial Pneumonia) ● Normal & COVID-19 & Bacterial pneumonia ● Normal & COVID-19 & Viral pneumonia ● COVID-19 & Bacterial pneumonia & Viral pneumonia	Binary accuracy, 99.5%
(Tuncer et al., 2021)	SVM	● COVID-19 ● Pneumonia ● Normal	Accuracy, 97.0%
(Elkorany & Elsharkawy, 2021)	SqueezeNet and ShuffleNet CNN models for deep learned features extraction and multiclass SVM classifier.	● COVID-19 ● Normal ● Viral pneumonia ● Bacterial pneumonia	Accuracy: ● 4 classes, 94.4% ● 3 classes (Normal, COVID-19, Pneumonia), 99.72% ● Binary (COVID/non COVID), 100%

Continued on following page

227

Table 1. Continued

Paper	DL architectures	Classes to classify	Outstanding results
(Jin et al., 2021)	Hybrid ensemble model (AlexNet+RelieF+SVM).	• Normal • Viral pneumonia • COVID-19	• Accuracy rate, 98.642 ± 0.398% • Total time required for total classification in seconds, 5.917 ± 0.001
(Albahli & Yar, 2021)	• NasNetLarge • Xception • InceptionV3 • Inception-ResNet-v2 • ResNet50	• COVID-19 • Normal • 14 other chest diseases	First classifier • Accuracy, 96.3% Second classifier • Accuracy, 87.8%
(Nur-a-alam et al., 2021)	Fusion features (CNN+HOG) + VGG19 pre-train model	COVID-19	Accuracy, 99.49%
(Uçar et al., 2021)	DenseNet121 and EfficientNet B0 (Feature extraction) Bi-LSTM (classifier).	Two-stage classification: 1st: Infected (COVID-19/ pneumonia) and not infected. 2nd: COVID-19 and pneumonia.	Accuracy, 92.49%
(Bekhet et al., 2021)	Light-weight deep CNN model	• ARDS • Chlamydophilia • COVID-19 • E. Coli • Klebsiella • Legionella • No Finding • Pneumocystis • SARS • Streptococcus	• Accuracy X-Ray images, 96% • Accuracy CT images, 92.08%
(Rehman et al., 2021)	ResNet50 for cloud service system.	• COVID-19 • non-COVID	Accuracy, 98%
(Arias-Garzón et al., 2021)	• VGG19 • VGG16 • U-Net	• COVID-19 • Normal & Other chest diseases	• Accuracy, 97% • Dice Coefficient, 96.5%
(Goyal & Singh, 2021)	• F-RNN-LSTM • SVM • ANN • KNN • Ensemble classifier	• Normal • Bacterial pneumonia • Viral pneumonia	• Accuracy, 95.04% • Training and detection time in seconds, 1289

Table 1 provides a reference point about how DL is working in the COVID-19 classification. Deep learning models provide the best alternative to classify Chest X-Ray images. The most used are MobileNet, DenseNet, ResNet, VGG, and Inception families. Also, other works classify using models like CoroNet, CapsNet, or Siamese Network, among others. In some cases, the authors include traditional machine learning algorithms such as SVM, KNN, DT, RF, and other models. Table 2 shows

a comparison between different deep learning architectures using the same data (Cohen) and shows promising results using similar conditions. These results allow comparing between works. However, it is not a typical results comparison due to the differences in databases. However, to obtain the best models is essential to use all data available. Moreover, in many cases is not possible to compare directly with some other works because these old works generally do not use the same available data.

FUTURE RESEARCH DIRECTIONS

As seen throughout this chapter, the efforts to classify COVID-19 in X-Ray images have been considerable, achieving accurate classification results. However, there are still research opportunities in this area. Initially, although there are many models for classification with good results, there is still a lack of studies on the actual application of these models in a clinical setting. Therefore, it is recommended to

Table 2. DL model performance with the same dataset conditions

Deep learning architecture	Accuracy [%]	Precision [%]	Recall [%]	F1 score [%]
U-Net+VGG19 (Arias-Garzón et al., 2021)	99.06	99.07	99.06	99.06
CoroNet (Khan et al., 2020)	99.00	98.30	99.30	98.50
VGG19 (Apostolopoulos & Mpesiana, 2020)	98.75	93.27	92.85	93.06

apply these models in health institutions, where there is access to X-Ray images, following detection protocols with the proposed DL models and evaluating with the already established tests, in order to have information on the feasibility of the studies already carried out in images from different sources.

Additionally, in order to support the health professional and give more robustness to the developed algorithms, it is recommended to highlight the symptoms that are attributed to COVID-19, and that can be observed in the same X-Ray images. Even there are works where strategies like using heatmaps to provide the best interpretability on CNN working (Arias-Garzón et al., 2021; Ozturk et al., 2020), it doesn't mean the models are focusing specifically on the zones where the symptoms are presented. Thus, strategies like lung segmentation (Arias-Londono et al., 2020; Rajaraman et al., 2020; Tartaglione et al., 2020), are an excellent option to analyze only the zones with the visible symptoms. However, it is necessary to make an effort to create this database, with previous segmentation work made for specialized radiologists.

Furthermore, it is recommended to use the medical records from patients who underwent radiographs and had a positive COVID-19 test result. These data can be the time of admission to the hospital, time of discharge, the severity of the disease, symptoms, and whether the patient died or not. This information can be used to improve the performance of the algorithms for classification, and make predictions. For example, to estimate the probability that the patient will present severe symptoms, or the probability of death of a patient. The above examples are just a few possibilities of what could be done with the data; it depends on each researcher's motivation. Likewise, it is a good idea to combine the images with clinical information, of which there are large amounts, and sometimes it is ignored.

DISCUSSION AND CONCLUSION

This chapter focused on a compilation of information about the different methodologies for early detection of COVID-19. Due to the damage that the disease can cause to the lungs and the various deaths caused worldwide, different diagnostic tests have been currently carried out that although their accuracy is high as is the PCR test, with a sensitivity of up to 97%, the time and professionals needed for its interpretation are not, since this process takes hours. So, the Chest X-Ray for the study of the disease is usually used by radiologists to monitor the severity of the disease. Still, in all countries, these professionals with the necessary knowledge to interpret these images are limited. CAD can help mitigate this scenario by integrating a diagnostic model for the disease into the systems. It can reduce the workload of clinics and increase reliability and quantitative analysis. Furthermore, because its output is instantaneous, it would help optimize diagnostic processes.

A current challenge is the presence of medical devices, such as endotracheal tubes presenting in intubated patients in ICU, electrodes, pacemakers, etc., as they can bias the model to identify patients with such devices as positive COVID-19; also, it is necessary to take into account the variability in the dimensions of the images and ensure the anonymity of the patient whose X-Ray was captured. In addition to this, it is almost impossible to compare the results of many researchers due to the variability of the data, size, and device with which each database was taken. The most commonly used databases are BIMCV-COVID19+, BRIXIA, ML Hannover, Cancer Image Archive, COVID Data Save lives, and IEEE8023. Also, there are different complementary databases with more classes including Padchest, BIMCV-COVID, CheXpert, RSNA and Chest X-Ray Images. On the other hand, there are three sets of lung segmentation databases: Montgomery dataset, JSTR, and NIH. These provide the Rx image and its respective mask.

230

As the data are collected in real-time, from different devices and acquisition conditions, pre-processing can help to improve the models. As an initial step, images are resized to 224x224, as they are the most used dimensions in the literature. A normalization of the data can reduce the variability presented among datasets from different sources. In addition, Fuzzy Color algorithms are useful for image analysis and separate the original information into various representations. Usually, COVID-19 datasets present imbalance in their databases, so a well-known solution is data augmentation which consists in taking an image of the data and generate a "duplicate." Some of the most common transformations used are rotation, flipping, cropping, shearing, elastic distortion, brightness variation and the addition of Gaussian noise. On the other hand, Generative Networks are a new DL tool to generate new images using two discriminators to create a new image. After the processing stage, Deep learning models provide the best alternative for classifying Chest X-Ray images. And the most widely used are MobileNet, DenseNet, ResNet, VGG, and Inception families in the feature extraction stage of transfer learning. Most authors propose their CNNs based on state-of-the-art convolutional neural networks, e.g., CoroNet and COVIDiagnosis-Net. In some cases, the authors include traditional machine learning algorithms such as SVM, KNN, DT, RF, and other models.

A contribution and method employed by several researchers for eliminating insignificant data in Rx images is the task of segmenting the lung region of a Chest X-Ray, where the most common DL architecture for this task is U-Net. Another technique to improve image quality and commonly employed for various cases of real-time imaging is Histogram Equalization. Improves image quality and detail, which enhances image brightness and contrast, provides better quality images. Gamma Correction, on the other hand, improves pattern recognition and the quality of digital image processing. Lastly, Local Phase-Based Image Enhancement consists of extracting three-phase features from the image. This technique brings out elements that are not visible in X-Ray images, providing a solution for the variation of the intensity of radiographs caused by morphological differences between patients and acquisition machine parameters.

For efficiency in artificial intelligence algorithms, quantitative methods are used to evaluate training and performance, such as Precision, Recall, F1 Score, Specificity, and the Roc curve are used to assess the performance of a DL model. On the other hand, the IoU metric allows to compare the authentic and predicted masks, which is helpful for lung segmentation processes, and finally the Dice Coefficient which like the IoU metric, the coefficient is used as an evaluation metric in semantic segmentation models, and can be used to evaluate the loss. When interpreting the data obtained, we found a very often used tool, called heat maps, because heat maps illustrate the area of higher concentration in the radiographs of patients with COVID-19 than the area in which the disease is not seen, and other

techniques such as t-SNE, class activation maps, and Grad-CAM are used. Deep learning models provide the best alternative for classifying Chest X-Ray images. And the most widely used are MobileNet, DenseNet, ResNet, VGG, and Inception families in the feature extraction stage of transfer learning. Most authors propose their CNNs based on state-of-the-art convolutional neural networks, e.g., CoroNet and COVIDiagnosis-Net. In some cases, the authors include traditional machine learning algorithms such as SVM, KNN, DT, RF, and other models.

Finally, it can only be said that studies on the actual application of these models in real-time cases are still lacking. So, it is recommended to apply these in health institutions, where there is access to Rx images and evaluate with the different metrics already established, to have information about the feasibility of the studies performed on images from other sources. It should be validated at the same time by the dermatologist to verify its accuracy and recommended to use the data associated with patients who undergo radiographs and have a positive result of COVID-19. This data can be used at the time of admission to the hospital, discharge time, patient severity, presenting symptoms, and whether or not the patient died.

ACKNOWLEDGMENT

REFERENCES

Agarwal, M., & Mahajan, R. (2018). Medical Image Contrast Enhancement using Range Limited Weighted Histogram Equalization. *Procedia Computer Science, 125*(2017), 149–156. doi:10.1016/j.procs.2017.12.021

Al-Waisy, A. S., Mohammed, M. A., Al-Fahdawi, S., Maashi, M. S., Garcia-Zapirain, B., Abdulkareem, K. H., Mostafa, S. A., Kumar, N. M., & Le, D. N. (2021). COVID-DeepNet: Hybrid Multimodal Deep Learning System for Improving COVID-19 Pneumonia Detection in Chest X-ray Images. *Computers*. *Materials and Continua*, *67*(2), 2409–2429. doi:10.32604/cmc.2021.012955

232

Alam, N.-A.-A., Ahsan, M., Based, M. A., Haider, J., & Kowalski, M. (2021). COVID-19 detection from chest X-ray images using feature fusion and deep learning. *Sensors (Basel)*, *21*(4), 1–30. doi:10.339021041480 PMID:33672585

Albahli, S., & Yar, G. N. A. H. (2021). Fast and Accurate Detection of COVID-19 Along With 14 Other Chest Pathologies Using a Multi-Level Classification: Algorithm Development and Validation Study. *Journal of Medical Internet Research*, *23*(2), e23693. doi:10.2196/23693 PMID:33529154

Apostolopoulos, I. D., Aznaouridis, S. I., & Tzani, M. A. (2020). Extracting Possibly Representative COVID-19 Biomarkers from X-ray Images with Deep Learning Approach and Image Data Related to Pulmonary Diseases. *Journal of Medical and Biological Engineering*, *40*(3), 462–469. doi:10.100740846-020-00529-4 PMID:32412551

Apostolopoulos, I. D., & Mpesiana, T. A. (2020). COVID-19: Automatic detection from X-ray images utilizing transfer learning with convolutional neural networks. *Physical and Engineering Sciences in Medicine*, *43*(2), 635–640. doi:10.100713246-020-00865-4 PMID:32524445

Arias-Garzón, D., Alzate-Grisales, J. A., Orozco-Arias, S., Arteaga-Arteaga, H. B., Bravo-Ortiz, M. A., Mora-Rubio, A., Saborit-Torres, J. M., Serrano, J. Á. M., de la Iglesia Vayá, M., Cardona-Morales, O., & Tabares-Soto, R. (2021). COVID-19 detection in X-ray images using convolutional neural networks. *Machine Learning with Applications*, *6*, 100138. doi:10.1016/j.mlwa.2021.100138 PMID:34939042

Arias-Londono, J. D., Gomez-Garcia, J. A., Moro-Velazquez, L., & Godino-Llorente, J. I. (2020). Artificial Intelligence applied to chest X-Ray images for the automatic detection of COVID-19. A thoughtful evaluation approach. *IEEE Access: Practical Innovations, Open Solutions*, *8*, 226811–226827. Advance online publication. doi:10.1109/ACCESS.2020.3044858 PMID:34786299

Arteaga-Arteaga, H. B., Mora-Rubio, A., Florez, F., Murcia-Orjuela, N., Diaz-Ortega, C. E., Orozco-Arias, S., delaPava, M., Bravo-Ortíz, M. A., Robinson, M., Guillen-Rondon, P., & Tabares-Soto, R. (2021). Machine learning applications to predict two-phase flow patterns. *PeerJ. Computer Science*, *7*, e798. doi:10.7717/peerj-cs.798 PMID:34909465

Aslan, M. F., Unlersen, M. F., Sabanci, K., & Durdu, A. (2021). CNN-based transfer learning–BiLSTM network: A novel approach for COVID-19 infection detection. *Applied Soft Computing*, *98*(106912), 106912. Advance online publication. doi:10.1016/j.asoc.2020.106912 PMID:33230395

Bekhet, S., Alkinani, M. H., Tabares-Soto, R., & Hassaballah, M. (2021). An efficient method for COVID-19 detection using light weight convolutional neural network. *Computers. Materials and Continua*, *69*(2), 2475–2491. doi:10.32604/cmc.2021.018514

BIMCV. (2020). BIMCV-COVID19 – BIMCV. *Soon*. https://bimcv.cipf.es/bimcv-projects/bimcv-COVID19/#1590859488150-148be708-c3f3

Blain, M., Kassin, M. T., Varble, N., Wang, X., Xu, Z., Xu, D., Carrafiello, G., Vespro, V., Stellato, E., Ierardi, A. M., Di Meglio, L., Suh, R. D., Walker, S. A., Xu, S., Sanford, T. H., Turkbey, E. B., Harmon, S., Turkbey, B., & Wood, B. J. (2021). Determination of disease severity in COVID-19 patients using deep learning in chest x-ray images. *Diagnostic and Interventional Radiology*, *27*(1), 20–27. doi:10.5152/dir.2020.20205 PMID:32815519

Bravo Ortíz, M. A., Arteaga Arteaga, H. B., Tabares Soto, R., Padilla Buriticá, J. I., & Orozco-Arias, S. (2021). Cervical cancer classification using convolutional neural networks, transfer learning and data augmentation. *Revista EIA*, *18*(35), 1–12. doi:10.24050/reia.v18i35.1462

Breiding, M. J. (2009). Radiation Dose Associated with Common Computed Tomography Examinations and the Associated Lifetime Attributable Risk of Cancer. *Archives of Internal Medicine*, *63*(169(22)), 2078–2086. doi:10.1001/archinternmed.2009.427.Radiation PMID:20008690

Bustos, A., Pertusa, A., Salinas, J. M., & de la Iglesia-Vayá, M. (2020). PadChest: A large chest x-ray image dataset with multi-label annotated reports. *Medical Image Analysis*, *66*, 101797. doi:10.1016/j.media.2020.101797 PMID:32877839

Castiglioni, I., Ippolito, D., Interlenghi, M., Monti, C. B., Salvatore, C., Schiaffino, S., Polidori, A., Gandola, D., Messa, C., & Sardanelli, F. (2021). Machine learning applied on chest x-ray can aid in the diagnosis of COVID-19: A first experience from Lombardy, Italy. *European Radiology Experimental*, *5*(1), 7. Advance online publication. doi:10.118641747-020-00203-z PMID:33527198

Chollet, F. (2017). Xception: Deep learning with depthwise separable convolutions. *Proceedings - 30th IEEE Conference on Computer Vision and Pattern Recognition, CVPR 2017*, 1800–1807. 10.1109/CVPR.2017.195

Dailla, M., Kaur, P., & Dhawan, V. (2014). Adaptive Gamma Correction With Weighted Distribution And Recursively Separated And Weighted Histogram Equalization: A Comparative Study. *International Journal of Engineering Research & Technology (Ahmedabad)*, *3*(8), 129–133.

234

Das, D., Santosh, K. C., & Pal, U. (2020). Truncated inception net: COVID-19 outbreak screening using chest X-rays. *Physical and Engineering Sciences in Medicine*, *43*(3), 915–925. doi:10.100713246-020-00888-x PMID:32588200

De Moura, J., Garcia, L. R., Vidal, P. F. L., Cruz, M., Lopez, L. A., Lopez, E. C., Novo, J., & Ortega, M. (2020). Deep Convolutional Approaches for the Analysis of COVID-19 Using Chest X-Ray Images From Portable Devices. *IEEE Access: Practical Innovations, Open Solutions*, *8*, 195594–195607. doi:10.1109/ ACCESS.2020.3033762 PMID:34786295

Desai, S., Baghal, A., Wongsurawat, T., Jenjaroenpun, P., Powell, T., Al-Shukri, S., Gates, K., Farmer, P., Rutherford, M., Blake, G., Nolan, T., Sexton, K., Bennett, W., Smith, K., Syed, S., & Prior, F. (2020). Chest imaging representing a COVID-19 positive rural U.S. population. *Scientific Data*, *7*(1), 414. doi:10.103841597-020-00741-6 PMID:33235265

Dey, N., Zhang, Y. D., Rajinikanth, V., Pugalenthi, R., & Raja, N. S. M. (2021). Customized VGG19 Architecture for Pneumonia Detection in Chest X-Rays. *Pattern Recognition Letters*, *143*, 67–74. doi:10.1016/j.patrec.2020.12.010

Dimas, S. R. D., Negara, B. S., Sanjaya, S., & Satria, E. (2021). COVID-19 Classification for Chest X-Ray Images using Deep Learning and Resnet-101. *International Congress of Advanced Technology and Engineering, ICOTEN 2021*, 21–24. 10.1109/ICOTEN52080.2021.9493431

dos Santos, C. F. G., Passos, L. A., de Santana, M. C., & Papa, J. P. (2021). Normalizing images is good to improve computer-assisted COVID-19 diagnosis. *Data Science for COVID-19*, 51–62. doi:10.1016/B978-0-12-824536-1.00033-2

Eesa, A. S., & Arabo, W. K. (2017). A Normalization Methods for Backpropagation: A Comparative Study. *Science Journal of University of Zakho*, *5*(4), 319–323. doi:10.25271/2017.5.4.381

Elkorany, A. S., & Elsharkawy, Z. F. (2021). COVIDetection-Net: A tailored COVID-19 detection from chest radiography images using deep learning. *Optik (Stuttgart)*, *231*(January), 1–10. doi:10.1016/j.ijleo.2021.166405 PMID:33551492

Flach, P. A., Lach, P. E. F., & Ac, B. (2003). *The Geometry of ROC Space : Understanding Machine Learning Metrics through ROC Isometrics*. Academic Press.

Goodfellow, I., Pouget-Abadie, J., Mirza, M., Xu, B., Warde-Farley, D., Ozair, S., Courville, A., & Bengio, Y. (2020). Generative adversarial networks. *Communications of the ACM*, *63*(11), 139–144. doi:10.1145/3422622

Gopal, S., Patro, K., & Kumar Sahu, K. (2015). Normalization: A Preprocessing Stage. *International Advanced Research Journal in Science*. *Engineering and Technology*, *2*, 20–22. Advance online publication. doi:10.17148/IARJSET.2015.2305

Goyal, S., & Singh, R. (2021). Detection and classification of lung diseases for pneumonia and COVID-19 using machine and deep learning techniques. *Journal of Ambient Intelligence and Humanized Computing*. Advance online publication. doi:10.100712652-021-03464-7 PMID:34567277

Guan, W., Ni, Z., Hu, Y. W., Liang, C., Ou, J., He, L., Liu, H., Shan, C., Lei, D. S. C., Hui, B., Du, L., Li, G., Zeng, K., Yuen, R., Chen, C., Tang, T., Wang, P., Chen, J., Xiang, S., … Zhong, N. (2020). Clinical Characteristics of Coronavirus Disease 2019 in China. The Journal of Emergency Medicine, 58(4), 711–712. doi:10.1016/j.jemermed.2020.04.004

Hacihaliloglu, I. (2018). Localization of bone surfaces from ultrasound data using local phase information and signal transmission maps. Lecture Notes in Computer Science, 10734, 1–11. doi:10.1007/978-3-319-74113-0_1

Harouni, M., & Baghmaleki, H. Y. (2021). Color Image Segmentation Metrics. Encyclopedia of Image Processing, 121–139. doi:10.1201/9781351032742-16

Horry, M. J., Chakraborty, S., Paul, M., Ulhaq, A., Pradhan, B., Saha, M., & Shukla, N. (2020). COVID-19 Detection Through Transfer Learning Using Multimodal Imaging Data. *IEEE Access: Practical Innovations, Open Solutions*, *8*, 149808–149824. doi:10.1109/ACCESS.2020.3016780 PMID:34931154

Hospitales, H. M. (2021). *COVID Data Save Lives*. https://www.hmhospitales.com/coronavirus/COVID-data-save-lives

Huang, S. C., Cheng, F. C., & Chiu, Y. S. (2013). Efficient contrast enhancement using adaptive gamma correction with weighting distribution. *IEEE Transactions on Image Processing*, *22*(3), 1032–1041. doi:10.1109/TIP.2012.2226047 PMID:23144035

Hussain, E., Hasan, M., Rahman, M. A., Lee, I., Tamanna, T., & Parvez, M. Z. (2021). CoroDet: A deep learning based classification for COVID-19 detection using chest X-ray images. *Chaos, Solitons, and Fractals*, *142*, 110495. doi:10.1016/j.chaos.2020.110495 PMID:33250589

Irvin, J., Rajpurkar, P., Ko, M., Yu, Y., Ciurea-Ilcus, S., Chute, C., Marklund, H., Haghgoo, B., Ball, R., Shpanskaya, K., Seekins, J., Mong, D. A., Halabi, S. S., Sandberg, J. K., Jones, R., Larson, D. B., Langlotz, C. P., Patel, B. N., Lungren, M. P., & Ng, A. Y. (2019). CheXpert: A large chest radiograph dataset with uncertainty labels and expert comparison. *33rd AAAI Conference on Artificial Intelligence, AAAI 2019, 31st Innovative Applications of Artificial Intelligence Conference, IAAI 2019 and the 9th AAAI Symposium on Educational Advances in Artificial Intelligence, EAAI 2019*, 590–597. 10.1609/aaai.v33i01.3301590

Ismael, A. M., & Sengür, A. (2021). Deep learning approaches for COVID-19 detection based on chest X-ray images. *Expert Systems with Applications*, *164*(114054), 114054. Advance online publication. doi:10.1016/j.eswa.2020.114054 PMID:33013005

Jaeger, S., Candemir, S., Antani, S., Wáng, Y.-X. J., Lu, P.-X., & Thoma, G. (2020). Two public chest X-ray datasets for computer-aided screening of pulmonary diseases. *Quantitative Imaging in Medicine and Surgery*, *4*(6), 475–477. doi:10.3978/j.issn.2223-4292.2014.11.20 PMID:25525580

Jain, G., Mittal, D., Thakur, D., & Mittal, M. K. (2020). A deep learning approach to detect COVID-19 coronavirus with X-Ray images. *Biocybernetics and Biomedical Engineering*, *40*(4), 1391–1405. doi:10.1016/j.bbe.2020.08.008 PMID:32921862

Jaiswal, A. K., Tiwari, P., Kumar, S., Gupta, D., Khanna, A., & Rodrigues, J. J. P. C. (2019). Identifying pneumonia in chest X-rays: A deep learning approach. *Measurement*, *145*, 511–518. doi:10.1016/j.measurement.2019.05.076

Jin, W., Dong, S., Dong, C., & Ye, X. (2021). Hybrid ensemble model for differential diagnosis between COVID-19 and common viral pneumonia by chest X-ray radiograph. *Computers in Biology and Medicine*, *131*(January), 104252. doi:10.1016/j.compbiomed.2021.104252 PMID:33610001

Karakanis, S., & Leontidis, G. (2021). Lightweight deep learning models for detecting COVID-19 from chest X-ray images. *Computers in Biology and Medicine*, *130*(104181), 104181. Advance online publication. doi:10.1016/j.compbiomed.2020.104181 PMID:33360271

Karar, M. E., Hemdan, E. E.-D., & Shouman, M. A. (2020). Cascaded deep learning classifiers for computer-aided diagnosis of COVID-19 and pneumonia diseases in X-ray scans. *Complex & Intelligent Systems*, *7*(1), 235–247. doi:10.100740747-020-00199-4 PMID:34777953

Kaur, N., & Singh, E. H. (2016). Enhancement of Medical Images using Histogram Based Hybrid Technique. *International Journal of Advanced Engineering Management Science*, *2*(9). www.ijaems.com

Kermany, D. S., Goldbaum, M., Cai, W., Valentim, C. C. S., Liang, H., Baxter, S. L., McKeown, A., Yang, G., Wu, X., Yan, F., Dong, J., Prasadha, M. K., Pei, J., Ting, M., Zhu, J., Li, C., Hewett, S., Dong, J., Ziyar, I., ... Zhang, K. (2018). Identifying Medical Diagnoses and Treatable Diseases by Image-Based Deep Learning. *Cell*, *172*(5), 1122–1131.e9. doi:10.1016/j.cell.2018.02.010 PMID:29474911

Khan, A. I., Shah, J. L., & Bhat, M. M. (2020). CoroNet: A deep neural network for detection and diagnosis of COVID-19 from chest x-ray images. *Computer Methods and Programs in Biomedicine*, *196*, 105581. Advance online publication. doi:10.1016/j.cmpb.2020.105581 PMID:32534344

King, B., Barve, S., Ford, A., & Jha, R. (2020). Unsupervised Clustering of COVID-19 Chest X-Ray Images with a Self-Organizing Feature Map. *Midwest Symposium on Circuits and Systems,* 395–398. 10.1109/MWSCAS48704.2020.9184493

Krishnaswamy Rangarajan, A., & Purushothaman, R. (2020). Disease Classification in Eggplant Using Pre-trained VGG16 and MSVM. *Scientific Reports*, *10*(1), 1–11. doi:10.103841598-020-59108-x PMID:32047172

Längkvist, M., Karlsson, L., & Loutfi, A. (2014). Inception-v4, Inception-ResNet and the Impact of Residual Connections on Learning. *Pattern Recognition Letters*, *42*(1), 11–24. https://arxiv.org/abs/1512.00567

Liang, S., Liu, H., Gu, Y., Guo, X., Li, H., Li, L., Wu, Z., Liu, M., & Tao, L. (2021). Fast automated detection of COVID-19 from medical images using convolutional neural networks. *Communications Biology*, *4*(1), 35. Advance online publication. doi:10.103842003-020-01535-7 PMID:33398067

M, H., & M.N, S. (2015). A Review on Evaluation Metrics for Data Classification Evaluations. *International Journal of Data Mining & Knowledge Management Process, 5*(2), 1–11. doi:10.5121/ijdkp.2015.5201

Maity, A. R., Nair, T., & Chandra, A. (2020). Image Pre-processing techniques comparison: COVID-19 detection through Chest X-Rays via Deep Learning. *International Journal of Scientific Research in Science and Technology*, *2*, 113–123. doi:10.32628/IJSRST207614

Majeed, T., Rashid, R., Ali, D., & Asaad, A. (2020). Issues associated with deploying CNN transfer learning to detect COVID-19 from chest X-rays. *Physical and Engineering Sciences in Medicine*, *43*(4), 1289–1303. doi:10.100713246-020-00934-8 PMID:33025386

Martínez Chamorro, E., Díez Tascón, A., Ibáñez Sanz, L., Ossaba Vélez, S., & Borruel Nacenta, S. (2021). Radiologic diagnosis of patients with COVID-19. *Radiología (Madrid.)*, *63*(1), 56–73. doi:10.1016/j.rx.2020.11.001 PMID:33339622

Meng, G., Wang, Y., Duan, J., Xiang, S., & Pan, C. (2013). Efficient image dehazing with boundary constraint and contextual regularization. *IEEE International Conference on Computer Vision*, 617–624. 10.1109/ICCV.2013.82

Mikołajczyk, A., & Grochowski, M. (2018). Data augmentation for improving deep learning in image classification problem. *International Interdisciplinary PhD Workshop,* 117–122. 10.1109/IIPHDW.2018.8388338

Mo, P., Xing, Y., Xiao, Y., Deng, L., Zhao, Q., Wang, H., Xiong, Y., Cheng, Z., Gao, S., Liang, K., Luo, M., Chen, T., Song, S., Ma, Z., Chen, X., Zheng, R., Cao, Q., Wang, F., & Zhang, Y. (2020). Clinical characteristics of refractory COVID-19 pneumonia in Wuhan, China. *Clinical Infectious Diseases*, 3–8. doi:10.1093/cid/ciaa270

Mohammed, M. A., Abdulkareem, K. H., Garcia-Zapirain, B., Mostafa, S. A., Maashi, M. S., Al-Waisy, A. S., Subhi, M. A., Mutlag, A. A., & Le, D. N. (2021). A comprehensive investigation of machine learning feature extraction and classification methods for automated diagnosis of COVID-19 based on X-ray images. *Computers. Materials and Continua*, *66*(3), 3289–3310. doi:10.32604/cmc.2021.012874

Mursalim, M. K. N., & Kurniawan, A. (2021). Multi-kernel CNN block-based detection for COVID-19 with imbalance dataset. *Iranian Journal of Electrical and Computer Engineering*, *11*(3), 2467–2476. doi:10.11591/ijece.v11i3.pp2467-2476

Narayan Das, N., Kumar, N., Kaur, M., Kumar, V., & Singh, D. (2020). Automated Deep Transfer Learning-Based Approach for Detection of COVID-19 Infection in Chest X-rays. *IRBM*. Advance online publication. doi:10.1016/j.irbm.2020.07.001 PMID:32837679

Narayanan, B. N., Hardie, R. C., Krishnaraja, V., Karam, C., & Davuluru, V. S. P. (2020). Transfer-to-Transfer Learning Approach for Computer Aided Detection of COVID-19 in Chest Radiographs. *AI 2020, 1*(4), 539–557. doi:10.3390/ai1040032

Narin, A., Kaya, C., & Pamuk, Z. (2020). *Department of Biomedical Engineering, Zonguldak Bulent Ecevit University*. https://arxiv.org/abs/2003.10849

Narin, A., Kaya, C., & Pamuk, Z. (2021). Automatic detection of coronavirus disease (COVID-19) using X-ray images and deep convolutional neural networks. *Pattern Analysis & Applications*, *24*(3), 1207–1220. doi:10.100710044-021-00984-y PMID:33994847

Nath, M. K., Kanhe, A., & Mishra, M. (2020). A Novel Deep Learning Approach for Classification of COVID-19 Images. *IEEE 5th International Conference on Computing Communication and Automation (ICCCA)*, 752–757. 10.1109/ICCCA49541.2020.9250907

Nayak, S. R., Nayak, D. R., Sinha, U., Arora, V., & Pachori, R. B. (2021). Application of deep learning techniques for detection of COVID-19 cases using chest X-ray images: A comprehensive study. *Biomedical Signal Processing and Control*, *64*, 102365. Advance online publication. doi:10.1016/j.bspc.2020.102365 PMID:33230398

Oh, Y., Park, S., & Ye, J. C. (2020). Deep Learning COVID-19 Features on CXR Using Limited Training Data Sets. *IEEE Transactions on Medical Imaging*, *39*(8), 2688–2700. doi:10.1109/TMI.2020.2993291 PMID:32396075

Ohata, E. F., Bezerra, G. M., Chagas, J. V. S. Das, Lira Neto, A. V., Albuquerque, A. B., Albuquerque, V. H. C. D., & Reboucas Filho, P. P. (2021). Automatic detection of COVID-19 infection using chest X-ray images through transfer learning. *IEEE/CAA Journal of Automatica Sinica, 8*(1), 239–248. doi:10.1109/JAS.2020.1003393

Oran, D. P., & Topol, E. J. (2020). Prevalence of Asymptomatic SARS-CoV-2 Infection : A Narrative Review. *Annals of Internal Medicine*, *173*(5), 362–367. doi:10.7326/M20-3012 PMID:32491919

Orozco-Arias, S., Isaza, G., Guyot, R., & Tabares-Soto, R. (2019). A systematic review of the application of machine learning in the detection and classification of transposable elements. *PeerJ*, *7*, e8311. doi:10.7717/peerj.8311 PMID:31976169

Ozturk, T., Talo, M., Yildirim, E. A., Baloglu, U. B., Yildirim, O., & Rajendra Acharya, U. (2020). Automated detection of COVID-19 cases using deep neural networks with X-ray images. *Computers in Biology and Medicine*, *121*(April), 103792. doi:10.1016/j.compbiomed.2020.103792 PMID:32568675

Panwar, H., Gupta, P. K., Siddiqui, M. K., Morales-Menendez, R., & Singh, V. (2020). Application of deep learning for fast detection of COVID-19 in X-Rays using nCOVnet. *Chaos, Solitons, and Fractals*, *138*, 109944. Advance online publication. doi:10.1016/j.chaos.2020.109944 PMID:32536759

Patel, S. P. B. K., & Muthu, R. K. (2020). *Medical Image Enhancement Using Histogram Processing and Feature Extraction for Cancer Classification*. https://arxiv.org/abs/2003.06615v1

Paul Cohen, J., Morrison, P., & Dao, L. (2020). *COVID-19 Image Data Collection*. ArXiv.

Pereira, R. M., Bertolini, D., Teixeira, L. O., Silla, C. N. Jr, & Costa, Y. M. G. (2020). COVID-19 identification in chest X-ray images on flat and hierarchical classification scenarios. *Computer Methods and Programs in Biomedicine*, *194*, 105532. Advance online publication. doi:10.1016/j.cmpb.2020.105532 PMID:32446037

Pham, T. D. (2021). Classification of COVID-19 chest X-rays with deep learning: New models or fine tuning? *Health Information Science and Systems*, *9*(1), 2. Advance online publication. doi:10.100713755-020-00135-3 PMID:33235710

Qi, X., Brown, L. G., Foran, D. J., Nosher, J., & Hacihaliloglu, I. (2021). Chest X-ray image phase features for improved diagnosis of COVID-19 using convolutional neural network. *International Journal of Computer Assisted Radiology and Surgery*, *16*(2), 197–206. doi:10.100711548-020-02305-w PMID:33420641

Qi, X., Nosher, J. L., Foran, D. J., & Hacihaliloglu, I. (2021). *Multi-Feature Semi-Supervised Learning for COVID-19 Diagnosis from Chest X-ray Images.* https://arxiv.org/abs/2104.01617

Rahman, S., Rahman, M. M., Abdullah-Al-Wadud, M., Al-Quaderi, G. D., & Shoyaib, M. (2016). An adaptive gamma correction for image enhancement. *EURASIP Journal on Image and Video Processing*, *2016*(1), 1–13. doi:10.118613640-016-0138-1

Rahman, S., Sarker, S., Miraj, M. A. A., Nihal, R. A., Nadimul Haque, A. K. M., & Noman, A. A. (2021, March 2). Deep Learning–Driven Automated Detection of COVID-19 from Radiography Images: A Comparative Analysis. *Cognitive Computation*. Advance online publication. doi:10.100712559-020-09779-5 PMID:33680209

Rajaraman, S., Siegelman, J., Alderson, P. O., Folio, L. S., Folio, L. R., & Antani, S. K. (2020). Iteratively Pruned Deep Learning Ensembles for COVID-19 Detection in Chest X-Rays. *IEEE Access: Practical Innovations, Open Solutions*, *8*, 115041–115050. doi:10.1109/ACCESS.2020.3003810 PMID:32742893

Rathore, J. S., & Ghosh, C. (2020). Severe acute respiratory syndrome coronavirus-2 (SARS-CoV-2), a newly emerged pathogen: An overview. *Pathogens and Disease*, *78*(6), 1–9. doi:10.1093/femspd/ftaa042 PMID:32840560

Rehman, A., Sadad, T., Saba, T., Hussain, A., & Tariq, U. (2021). Real-Time Diagnosis System of COVID-19 Using X-Ray Images and Deep Learning. *IT Professional*, *23*(4), 57–62. doi:10.1109/MITP.2020.3042379

Ronneberger, O., Fischer, P., & Brox, T. (2015). *U-Net: Convolutional Networks for Biomedical Image Segmentation*. doi:10.1007/978-3-319-24574-4_28

Roosa, K., Lee, Y., Luo, R., Kirpich, A., Rothenberg, R., Hyman, J. M., Yan, P., & Chowell, G. (2020). Real-time forecasts of the COVID-19 epidemic in China from February 5th to February 24th, 2020. *Infectious Disease Modelling*, *5*, 256–263. doi:10.1016/j.idm.2020.02.002 PMID:32110742

Sahlol, A. T., Yousri, D., Ewees, A. A., Al-qaness, M. A. A., Damasevicius, R., & Elaziz, M. A. (2020). COVID-19 image classification using deep features and fractional-order marine predators algorithm. *Scientific Reports*, *10*(1), 1–15. doi:10.103841598-020-71294-2 PMID:32958781

Salem, N., Malik, H., & Shams, A. (2019). Medical image enhancement based on histogram algorithms. *Procedia Computer Science*, *163*, 300–311. doi:10.1016/j. procs.2019.12.112

Sandler, M., Howard, A., Zhu, M., Zhmoginov, A., & Chen, L. C. (2018). MobileNetV2: Inverted Residuals and Linear Bottlenecks. *Proceedings of the IEEE Computer Society Conference on Computer Vision and Pattern Recognition*, 4510–4520. 10.1109/CVPR.2018.00474

Sarv Ahrabi, S., Scarpiniti, M., Baccarelli, E., & Momenzadeh, A. (2021). An accuracy vs. Complexity comparison of deep learning architectures for the detection of COVID-19 disease. *Computation (Basel, Switzerland)*, *9*(1), 1–20. doi:10.3390/ computation9010003

Shalabi, L. A., Shaaban, Z., & Kasasbeh, B. (2006). Data Mining: A Preprocessing Engine. *Journal of Computational Science*, *2*(9), 735–739. doi:10.3844/ jcssp.2006.735.739

Sheykhivand, S., Mousavi, Z., Mojtahedi, S., Yousefi Rezaii, T., Farzamnia, A., Meshgini, S., & Saad, I. (2021). Developing an efficient deep neural network for automatic detection of COVID-19 using chest X-ray images. *Alexandria Engineering Journal*, *60*(3), 2885–2903. doi:10.1016/j.aej.2021.01.011

Shiraishi, J., Katsuragawa, S., Ikezoe, J., Matsumoto, T., Kobayashi, T., Komatsu, K. I., Matsui, M., Fujita, H., Kodera, Y., & Doi, K. (2020). Development of a digital image database for chest radiographs with and without a lung nodule: Receiver operating characteristic analysis of radiologists' detection of pulmonary nodules. *AJR. American Journal of Roentgenology*, *174*(1), 71–74. doi:10.2214/ajr.174.1.1740071 PMID:10628457

Shorfuzzaman, M., & Hossain, M. S. (2020). MetaCOVID: A Siamese neural network framework with contrastive loss for n-shot diagnosis of COVID-19 patients. *Pattern Recognition*, *113*(107700), 107700. Advance online publication. doi:10.1016/j. patcog.2020.107700 PMID:33100403

Shorten, C., & Khoshgoftaar, T. M. (2019). A survey on Image Data Augmentation for Deep Learning. *Journal of Big Data, 6*(1), 1–48. doi:10.1186/s40537-019-0197-0

Siddique, N., Paheding, S., Elkin, C. P., & Devabhaktuni, V. (2021). *U-net and its variants for medical image segmentation: A review of theory and applications.* IEEE. doi:10.1109/ACCESS.2021.3086020

Signoroni, A., Savardi, M., Benini, S., Adami, N., Leonardi, R., Gibellini, P., Vaccher, F., Ravanelli, M., Borghesi, A., Maroldi, R., & Farina, D. (2021). BS-Net: Learning COVID-19 pneumonia severity on a large chest X-ray dataset. *Medical Image Analysis*, *71*, 102046. doi:10.1016/j.media.2021.102046 PMID:33862337

Singh, A., Sengupta, S., & Lakshminarayanan, V. (2020). Explainable deep learning models in medical image analysis. *Journal of Imaging*, *6*(6), 1–19. doi:10.3390/jimaging6060052 PMID:34460598

Singh, R. K., Pandey, R., & Babu, R. N. (2021). COVIDScreen: Explainable deep learning framework for differential diagnosis of COVID-19 using chest X-rays. *Neural Computing & Applications*, *6*(14), 8871–8892. Advance online publication. doi:10.100700521-020-05636-6 PMID:33437132

Stoecklin, B. S., Rolland, P., Silue, Y., Mailles, A., Campese, C., Simondon, A., Mechain, M., Meurice, L., Nguyen, M., Bassi, C., Yamani, E., Behillil, S., Ismael, S., Nguyen, D., Malvy, D., Lescure, F. X., Georges, S., Lazarus, C., Tabaï, A., ... Team, I. (2020). First cases of coronavirus disease 2019 (COVID-19) in France: Surveillance, investigations and control measures, January 2020. *Eurosurveillance*, *25*(6). PMID:32070465

Szegedy, C., Liu, W., Jia, Y., Sermanet, P., Reed, S., Anguelov, D., Erhan, D., Vanhoucke, V., & Rabinovich, A. (2015). Going deeper with convolutions. *2015 IEEE Conference on Computer Vision and Pattern Recognition (CVPR)*, 1–9. 10.1109/CVPR.2015.7298594

Tabares-Soto, R., Raúl, R. P., & Gustavo, I. (2019). Deep learning applied to steganalysis of digital images: A systematic review. *IEEE Access: Practical Innovations, Open Solutions*, *7*, 68970–68990. doi:10.1109/ACCESS.2019.2918086

Tan, M., & Le, Q. V. (2019). EfficientNet: Rethinking model scaling for convolutional neural networks. *36th International Conference on Machine Learning, ICML 2019*, 10691–10700.

Tang, Y. B., Tang, Y. X., Xiao, J., & Summers, R. M. (2020). Xlsor: A robust and accurate lung segmentor on chest x-rays using criss-cross attention and customized radiorealistic abnormalities generation. *ArXiv*, 457–467.

243

Tartaglione, E., Barbano, C. A., Berzovini, C., Calandri, M., & Grangetto, M. (2020). Unveiling COVID-19 from chest x-ray with deep learning: A hurdles race with small data. *International Journal of Environmental Research and Public Health*, *17*(18), 1–17. doi:10.3390/ijerph17186933 PMID:32971995

Toğaçar, M., Ergen, B., & Cömert, Z. (2020). COVID-19 detection using deep learning models to exploit Social Mimic Optimization and structured chest X-ray images using fuzzy color and stacking approaches. *Computers in Biology and Medicine*, *121*(103805). Advance online publication. doi:10.1016/j.compbiomed.2020.103805 PMID:32568679

Toraman, S., Alakus, T. B., & Turkoglu, I. (2020). Convolutional capsnet: A novel artificial neural network approach to detect COVID-19 disease from X-ray images using capsule networks. *Chaos, Solitons, and Fractals*, *140*, 110122. Advance online publication. doi:10.1016/j.chaos.2020.110122 PMID:32834634

Tuncer, T., Ozyurt, F., Dogan, S., & Subasi, A. (2021). A novel COVID-19 and pneumonia classification method based on F-transform. *Chemometrics and Intelligent Laboratory Systems*, *210*(104256), 104256. Advance online publication. doi:10.1016/j.chemolab.2021.104256 PMID:33531722

Uçar, E., Atila, Ü., Uçar, M., & Akyol, K. (2021). Automated detection of COVID-19 disease using deep fused features from chest radiography images. *Biomedical Signal Processing and Control*, *69*(June), 102862. doi:10.1016/j.bspc.2021.102862 PMID:34131433

Ucar, F., & Korkmaz, D. (2020). COVIDiagnosis-Net: Deep Bayes-SqueezeNet based diagnosis of the coronavirus disease 2019 (COVID-19) from X-ray images. *Medical Hypotheses*, *140*(109761), 109761. Advance online publication. doi:10.1016/j.mehy.2020.109761 PMID:32344309

Vayá, M. de la I., Saborit, J. M., Montell, J. A., Pertusa, A., Bustos, A., Cazorla, M., Galant, J., Barber, X., Orozco-Beltrán, D., García-García, F., Caparrós, M., González, G., & Salinas, J. M. (2020). BIMCV COVID-19+: a large annotated dataset of RX and CT images from COVID-19 patients. *ArXiv*, 1–22.

Veluchamy, M., & Subramani, B. (2019). Image contrast and color enhancement using adaptive gamma correction and histogram equalization. *Optik (Stuttgart)*, *183*, 329–337. doi:10.1016/j.ijleo.2019.02.054

Waheed, A., Goyal, M., Gupta, D., Khanna, A., Al-Turjman, F., & Pinheiro, P. R. (2020). COVIDGAN: Data Augmentation Using Auxiliary Classifier GAN for Improved COVID-19 Detection. *IEEE Access: Practical Innovations, Open Solutions*, *8*, 91916–91923. doi:10.1109/ACCESS.2020.2994762 PMID:34192100

244

Wang, L., & Wong, A. (2020). *COVID-Net: A Tailored Deep Convolutional Neural Network Design for Detection of COVID-19 Cases from Chest X-Ray Images*. https://arxiv.org/abs/2003.09871

Wang, X., Peng, Y., Lu, L., Lu, Z., Bagheri, M., & Summers, R. M. (2017). ChestX-ray8: Hospital-scale chest X-ray database and benchmarks on weakly-supervised classification and localization of common thorax diseases. *Proceedings - 30th IEEE Conference on Computer Vision and Pattern Recognition, CVPR 2017,* 3462–3471. 10.1109/CVPR.2017.369

WHO Solidarity Trial Consortium. (2021). Repurposed Antiviral Drugs for COVID-19 — Interim WHO Solidarity Trial Results. New England Journal of Medicine, 384(6), 497–511. doi:10.1056/NEJMoa2023184

Winther, H. B., Hans Gerbel, S., Maschke, S. K., Hinrichs, J. B., Vogel-Claussen, J., Wacker, F. K., Höper, M. M., & Meyer, B. C. (2020). Dataset: COVID-19 Image Repository. doi:10.25835/0090041

World Health Organization. (2020). *Coronavirus*. https://www.who.int/en/health-topics/coronavirus#tab=tab_1

World Health Organization. (2021). *WHO Coronavirus (COVID-19) Dashboard*. https://COVID19.who.int/

Yang, X., Yu, Y., Xu, J., Shu, H., Xia, J., Liu, H., Wu, Y., Zhang, L., Yu, Z., Fang, M., Yu, T., Wang, Y., Pan, S., Zou, X., Yuan, S., & Shang, Y. (2020). Clinical Course and outcomes of critically ill patients with COVID19 in Wuhan China. *The Lancet. Respiratory Medicine*, *8*(5), 475–481. doi:10.1016/S2213-2600(20)30079-5 PMID:32105632

Yoo, S. H., Geng, H., Chiu, T. L., Yu, S. K., Cho, D. C., Heo, J., Choi, M. S., Choi, I. H., Cung Van, C., Nhung, N. V., Min, B. J., & Lee, H. (2020). Deep Learning-Based Decision-Tree Classifier for COVID-19 Diagnosis From Chest X-ray Imaging. *Frontiers in Medicine*, *7*, 427. doi:10.3389/fmed.2020.00427 PMID:32760732

Zebin, T., & Rezvy, S. (2021). COVID-19 detection and disease progression visualization: Deep learning on chest X-rays for classification and coarse localization. *Applied Intelligence*, *51*(2), 1010–1021. doi:10.100710489-020-01867-1 PMID:34764549

Zhang, W., Zhao, Y., Zhang, F., Wang, Q., Li, T., Liu, Z., Wang, J., Qin, Y., Zhang, X., Yan, X., Zeng, X., & Zhang, S. (2020). The use of anti-inflammatory drugs in the treatment of people with severe coronavirus disease 2019 (COVID-19): The Perspectives of clinical immunologists. *Clinical Immunology (Orlando, Fla.)*, *214*(January), 108393. doi:10.1016/j.clim.2020.108393 PMID:32222466

ADDITIONAL READING

Al-Waisy, A. S., Mohammed, M. A., Al-Fahdawi, S., Maashi, M. S., Garcia-Zapirain, B., Abdulkareem, K. H., Mostafa, S. A., Kumar, N. M., & Le, D. N. (2021). COVID-DeepNet: Hybrid Multimodal Deep Learning System for Improving COVID-19 Pneumonia Detection in Chest X-ray Images. Computers. *Materials and Continua*, *67*(2), 2409–2429. doi:10.32604/cmc.2021.012955

Arias-Garzón, D., Alzate-Grisales, J. A., Orozco-Arias, S., Arteaga-Arteaga, H. B., Bravo-Ortiz, M. A., Mora-Rubio, A., Saborit-Torres, J. M., Serrano, J. Á. M., de la Iglesia Vayá, M., Cardona-Morales, O., & Tabares-Soto, R. (2021). COVID-19 detection in X-Ray images using convolutional neural networks. *Machine Learning with Applications*, *6*, 100138. doi:10.1016/j.mlwa.2021.100138 PMID:34939042

Aslan, M. F., Unlersen, M. F., Sabanci, K., & Durdu, A. (2021). CNN-based transfer learning–BiLSTM network: A novel approach for COVID-19 infection detection. *Applied Soft Computing*, *98*(106912), 106912. Advance online publication. doi:10.1016/j.asoc.2020.106912 PMID:33230395

Bekhet, S., Alkinani, M. H., Tabares-Soto, R., & Hassaballah, M. (2021). An efficient method for COVID-19 detection using light weight convolutional neural network. Computers. *Materials and Continua*, *69*(2), 2475–2491. doi:10.32604/cmc.2021.018514

Bekhet, S., Hassaballah, M., Kenk, M. A., & Hameed, M. A. (2020). An artificial intelligence based technique for COVID-19 diagnosis from Chest X-Ray. In *2nd Novel Intelligent and Leading Emerging Sciences Conference (NILES)* (pp. 191-195) 10.1109/NILES50944.2020.9257930

Hassaballah, M., & Awad, A. I. (Eds.). (2020). *Deep learning in computer vision: principles and applications*. CRC Press. doi:10.1201/9781351003827

Ismael, A. M., & Sengür, A. (2021). Deep learning approaches for COVID-19 detection based on chest X-ray images. *Expert Systems with Applications*, *164*(114054). Advance online publication. doi:10.1016/j.eswa.2020.114054 PMID:33013005

Jin, W., Dong, S., Dong, C., & Ye, X. (2021). Hybrid ensemble model for differential diagnosis between COVID-19 and common viral pneumonia by chest X-ray radiograph. *Computers in Biology and Medicine*, *131*(January), 104252. doi:10.1016/j.compbiomed.2021.104252 PMID:33610001

Narin, A., Kaya, C., & Pamuk, Z. (2021). Automatic detection of coronavirus disease (COVID-19) using X-ray images and deep convolutional neural networks. *Pattern Analysis & Applications*, *24*(3), 1207–1220. doi:10.100710044-021-00984-y PMID:33994847

KEY TERMS AND DEFINITIONS

Artificial Intelligence: Artificial Intelligence refers to the set of algorithms or computational methods that aim to give computers the characteristics or abilities of human intelligence.

Chest X-Ray: A Chest X-Ray is an image of the internal structures of the patient's chest that is captured using radiation.

Classification: In the context of Deep Learning applications, a classification task consists of assigning a label to each sample of the input data based on the learned features and relationships. In this chapter, the classification task consists of assigning a Chest X-Ray image the label "Positive for COVID-19" or "Negative for COVID-19".

Convolutional Neural Network (CNN): It is a type of deep learning model commonly used for image-related tasks. It uses the mathematical operation of convolution to extract features from images. In this chapter the models developed are based on CNN.

COVID-19: A respiratory disease, caused by the SARS-CoV-2 virus, that spreads rapidly through saliva droplets or discharge from the nose. The most common symptoms are fever, dry cough, and fatigue.

Deep Learning: Deep Learning corresponds to a subset of Artificial Intelligence techniques that comprises models based on artificial neural networks.

Semantic Segmentation: In the context of Deep Learning applications and image processing, semantic segmentation consists of assigning a label to each pixel in the image, which returns a segmentation mask for each input image. In this chapter, the labels for the semantic segmentation task are "Lung" and "Background".

Chapter 8
Generation of Novel Synthetic Portable Chest X–Ray Images for Automatic COVID–19 Screening

Daniel Iglesias Morís
Grupo VARPA, CITIC, INIBIC, Universidade da Coruña, Spain

Jorge Novo
Grupo VARPA, CITIC, INIBIC, Universidade da Coruña, Spain

Joaquim de Moura
https://orcid.org/0000-0002-2050-3786
Grupo VARPA, CITIC, INIBIC, Universidade da Coruña, Spain

Marcos Ortega
Grupo VARPA, CITIC, INIBIC, Universidade da Coruña, Spain

ABSTRACT

The diagnosis and the study of the evolution of COVID-19 is crucial to tackle the challenge that this disease represents for healthcare services. Chest x-ray imaging allows us to visualize the pulmonary regions, where COVID-19 causes its main affectation. In order to reduce the risk of cross-contamination, a crucial aspect in the pandemic, portable chest x-ray devices are advantageous being easier to decontaminate in comparison with the fixed machinery, despite offering a lower image quality. Furthermore, the recent emergence of COVID-19 implies a data scarcity that must be tackled. In this chapter, the authors present the analysis of a strategy that generates novel synthetic portable chest x-ray images using the CycleGAN, an architecture for image translation that is trained with unpaired data. The novel set of images is then added to the original dataset, improving the performance of the classification model.

INTRODUCTION

The COVID-19 is a pathology that can affect several parts of the body, while its main affectation is located on the respiratory tissues. The pathogen that causes this disease is known as SARS-CoV-2, a type of coronavirus, which is highly contagious, reason why it was rapidly spread worldwide forcing the World Health Organization to declare the COVID-19 as a global pandemic in 12th March 2020 (Ciotti et al., 2020). Currently, more than 242 million confirmed cases alongside more than 4.9 million deaths were reported worldwide (Coronavirus Resource Center, Johns Hopkins, 2020). There are several techniques to diagnose the COVID-19 but the gold-standard is the RT-PCR test (Tahamtan & Ardebili, 2020). However, it could be interesting for clinicians to have more information than the simple diagnostic provided by this technique. The main affectation of the COVID-19 is located in the pulmonary area and, therefore, chest X-ray imaging can be very useful to visualize this region to diagnose the pathology, to study its severity and to understand its evolution (Jacobi et al., 2020), as it has been widely used in the last decades to diagnose other typical pulmonary diseases and detect pathological structures as is the case, for example, of the pneumonia (Fiszman et al., 2000), the tuberculosis (Van Cleeff et al., 2005), the fibrosis (Puderbach et al., 2007) or the lung nodules (Wei et al., 2002). In the context of the COVID-19, this image modality can be used as a complement to the diagnostic result of the RT-PCR. With all these ideas into account, we can conclude that chest X-ray emerges as a powerful approach to visualize the affection of this pulmonary disease. Despite its lower quality in comparison with other advanced methods, as the Computerized Tomography (CT) (Hayden & Wrenn, 2009), the chest X-ray captures are easier and cheaper to perform. On the other hand, as the SARS-CoV-2 is easily spread, it is very important to decontaminate the capture devices. In the same way, many patients are bedridden and, therefore, it is impossible for them to move to the radiology room. To solve these problematics, radiologists are recommended to use portable chest X-ray devices instead of the fixed machinery (Kooraki et al., 2020), as this kind of devices are easier to decontaminate and can be moved to where the patient is placed. However, in some cases, clinicians could decide to use more advanced techniques that provide a more detailed visualization of the pulmonary regions if it is necessary, in order to have a more precise localization of the pathological structures, despite the higher cost and difficulty of the captures. This is the case of the CT, that provide a 3-dimensional visualization of the captured region.

With the aim to reduce the workload of the healthcare services, the development of computer-aided diagnosis systems (CAD) is very relevant (Doi, 2007). To do so, in the last years, the deep learning strategies have emerged as powerful techniques to solve medical imaging problems very effectively (Suzuki, 2017). However, there

249

are some challenges to tackle when dealing with image modalities as CT or chest X-ray. First of all, the inferior level of detail and quality of the chest X-ray images implies that find representative patterns of the pathological affectation is more difficult (aspect that is even more accused in the case of the captures provided by the portable chest X-ray devices). Secondly, in the case of the CT images, despite the higher quality and higher detail of the captures, the methods are inherently more complex to develop. A CT image is a conjunction of different X-ray images that are captured with different angles. Then, this set of different captures can be merged to create a 3-dimensional representation, in this case, of the chest, where each X-ray capture represents a 2-dimensional slice. The difficulty of the analysis process mainly emerges from the fact that only certain slices are useful to perform a study of the affectation of the disease. Therefore, one part of the methodological proposal must be to remove all the slices that are useless for the process. Moreover, both biomedical image modalities are affected by the issue of data scarcity. Deep learning models need datasets with large-scale dimensionality to be trained and provide effective results. However, it is well-known that in many biomedical imaging domains, the data scarcity is a very important problematic to deal with. In the case of the COVID-19, that has emerged very recently in contrast with other common pulmonary diseases, the aspect of data scarcity is even more important.

In this chapter, we explore a methodology developed for the automatic COVID-19 screening using chest X-ray images captured using with portable devices, providing the expert clinicians an automatic tool to reduce their workload in the global pandemic. Due to the recently emergence of this disease, the available data used for training the classification models is scarce. To overcome that data scarcity, the methodology can be splitted in 2 different parts. The first step performs a synthetic image generation with the CycleGAN, an image translation model (*i.e.,* a model that can convert images from a source scenario to another different target scenario) considering 4 different configurations for the generative models: an Unet-128 (Unet with 7 downsampling blocks), Unet-256 (Unet with 8 downsampling blocks), ResNet-6 (ResNet with 6 residual blocks) and ResNet-9 (ResNet with 9 residual blocks). Then, this set of generated images is added to original dataset. For the second step of the methodology, the augmented dataset is used to train the screening model, while the test is performed using only original images. Apart from data scarcity, the screening models must deal with the lower quality and lower level of detail of the images provided by the portable chest X-ray devices, in contrast with the fixed machinery. The methodology proposed on that work provides a reliable and robust method for COVID-19 screening despite the mentioned issues.

This chapter is structured as follows: The Background section talks about the techniques that can be found on the state of the art for COVID-19 screening or related tasks using chest X-ray and chest CT images, as well as some works that develop

methodologies for image generation as data augmentation strategies. The Synthetic Image Generation and COVID-19 Screening with The Augmented Dataset section describes the dataset used for the development of the reference work, the proposed methodology, the experimental validation design and the obtained results with their correspondent discussion. The Solutions and Recommendations section proposes some of the possible solutions to tackle the problematics that appeared during the progress of the developed methodology. The Future Research Directions talks about the possible directions that could be follow in the research line that is related with this chapter, as the applications of synthetic image generation for biomedical imaging analysis. Finally, in Conclusion, we talk about the most important facts extracted from the analyzed topic and the studied methodology.

BACKGROUND

As chest X-ray and CT imaging are useful to diagnose a variety of diseases, many efforts have been done to develop CAD systems able to help clinicians while using this kind of biomedical imaging modalities, using classical computer vision techniques and classical machine learning strategies. As reference, the work from (Kumar et al., 2014) obtains a set of features from Gabor filtering that are then used as input for a classification model, which in this case is a Support Vector Machine (Cortes & Vapnik, 1995), with the aim of distinguishing between normal and pulmonary edema. The contribution of (Novo et al., 2015) proposes the use of the central adaptive medialness (Krissian et al., 2000), which is a method for detecting tubular structures in 3D images, for selecting lung nodule candidates on CT images. In another proposal (Novo et al., 2014), the authors used a dataset of thoracic CT images to perform a reliable lung segmentation using different region growing approaches, including the juxtapleural nodules. The work from (Yan et al., 2012) proposes the development of a methodology for the lung segmentation task using chest X-ray images with the support of landmarks learned from manual annotation. The proposal of (Gonçalves et al., 2017) extracts a set of features from a nodular image region that is used as the input of classical machine learning classifier methods as Support Vector Machines and k Nearest Neighbors (Hwang & Wen, 1998) to compute the malignancy likelihood of a lung nodule. In this case, the authors use the dataset Lung Image Database Consortium (Armato III et al., 2011), that is composed of both CT and chest X-ray images.

With regards to data scarcity, many contributions have addressed the possible approaches to tackle this very relevant problematic. The most conventional data augmentation techniques are based on applying trivial transformations on images as random rotations or translations, among many other possible kinds of transformations

(Wang et al., 2017). However, these data augmentation strategies can be insufficient to represent the notable variability of a specific medical imaging domain. In the last years, many works have proposed the image generation as a powerful data augmentation technique. Particularly, the Generative Adversarial Networks (GANs) are one of the most used network architectures for image generation (Creswell et al., 2018). One specific GAN architecture is the Cycle Consistent Adversarial Network, often denoted as CycleGAN (Zhu et al., 2017). The CycleGAN is an image translation model which is able to convert images from a scenario A to its hypothetical version in a scenario B and vice versa. The motivation of using the CycleGAN in this problem is due to the fact that this model is able to deal with unpaired datasets, in contrast with other translation models that are specifically designed for paired data. In the context of the chest X-ray imaging, GAN models have been used to solve data scarcity problems in some specific cases. As reference, the work from (Zhang et al., 2020) uses a GAN to perform organ segmentation in chest X-ray images in an unsupervised manner. The contribution of (Xu et al., 2020) uses GANs to recover high resolution chest X-ray images from low resolution images in a super-resolution fashion. The work from (Malygina et al., 2019) demonstrates the use of the CycleGAN to improve the pathology prediction in several different scenarios as pneumonia or fibrosis. With regards to the topic of this chapter, the work from (Morís et al., 2021a) demonstrates the suitability of image translation in the context of the COVID-19 screening using images provided by portable chest X-ray devices.

In the case of the automatic screening using chest CT imaging datasets, there are relevant contributions of CAD systems to help clinicians in the diagnostic processes. As reference, the work from (Xie et al., 2019) uses deep learning for lung nodule classification in 2 different classes, benignant and malignant, obtaining an accuracy of 91.60% and an AUC of 95.70%. The contribution of (Shadmi et al., 2018) proposes a deep learning strategy for coronary calcium segmentation, an important biomarker to measure the severity of cardiovascular diseases. The proposal of (Li et al., 2019) is developing a method for a fast pneumotorax detection in chest CT images, obtaining a 100% of sensitivity and an 82.5% of specificity. There are also other works that propose methods for image generation, to improve the performance of the screening systems. As reference, the work from (Han et al., 2019) uses a deep model based on the GAN paradigm to generate synthetic chest CT images with lung nodules. On the other hand, with regards to the main topic of this chapter, there are also many interesting works that proposes methods for COVID-19 detection and image generation working with chest CT images. As reference, the work from (Zheng et al., 2020) uses weakly-supervised deep learning models to detect COVID-19 in chest CT images, obtaining a ROC AUC of 0.959. Furthermore, the work from (Acar et al., 2021) tackles the problem of data scarcity using a GAN architecture to improve the performance of the COVID-19 screening in chest CT images.

252

On the other hand, many contributions have addressed other important tasks directly or indirectly related with COVID-19 screening on chest X-ray datasets. As reference, the work from (Vidal et al., 2021) uses a transfer learning framework to reuse the knowledge extracted from other different and well-known domain with a great number of samples to adapt it to the COVID-19 chest X-ray imaging domain, where data is much more scarce, in order to perform a reliable lung segmentation. The work from (Basu et al., 2020) uses transfer learning to develop a reliable automatic COVID-19 screening method. The contribution of (Misra et al., 2020) uses an ensemble of 3 different ResNet pretrained models to classify in 3 different classes: Normal, Pneumonia and COVID-19. (De Moura, Novo, et al., 2020) developed a methodology to perform an automatic COVID-19 screening using publicly available data of chest X-ray imaging. The work of (De Moura, García, et al., 2020) proposes the use of a classification model for the COVID-19 screening, considering a dataset of chest X-ray images captured with portable devices. Moreover, the work of (Morís et al., 2021b) proves the utility of adding a novel set of synthetic images generated with the method proposed on the above-mentioned work from the same authors, to the original dataset in the context of the COVID-19 screening. A work from the same authors (Morís et al., 2021c) proves the potential of training with a larger amount of portable chest X-ray imaging data.

SYNTHETIC IMAGE GENERATION AND COVID-19 SCREENING WITH THE AUGMENTED DATASET

In order to develop this methodology, the authors used a portable chest X-ray imaging dataset provided by the Radiology Service of the Complexo Hospitalario Universitario de A Coruña (CHUAC). In this line, the authors used a private dataset provided by a local public hospital institution, the Complexo Hospitalario Universitario de A Coruña (CHUAC). This dataset is divided in 3 different classes: Normal, Pathological and COVID-19. The class Normal is composed of patients without signs of pulmonary affectation that, however, can present other kinds of pathologies. The class Pathological is composed of patients that present pulmonary affectation caused by pulmonary pathologies different from COVID-19, but with compatible symptomatology. Lastly, the COVID-19 class refers to all the genuine COVID-19 cases. Examples of these images for each class are depicted in Figure 1. The dataset is balanced as is composed of 240 Normal cases, 240 Pathological cases and 240 COVID-19 cases. The images have variable resolutions that can be 1523 X 1904, 1526 X 1753, 1526 X 1754, 1526 X 1910, 949 X 827, 950 X 827 and 950 X 833 pixels. Those images were provided by 2 different models of portable chest X-ray devices: the Agfa dr100E GE and the Optima Rx200.

Figure 1. Representative examples for each class of the dataset (a) Normal sample (b) Pathological sample (c) COVID-19 sample

       (a)   (b)   (c)
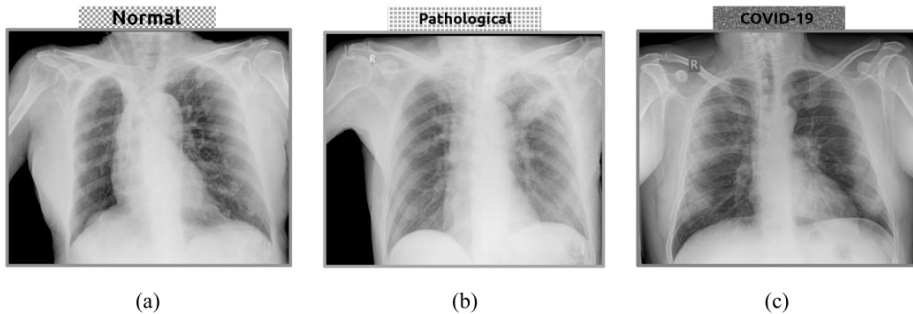
With regards to the proposed methodology itself, that is schematically described in Figure 2, the process is divided in 2 different parts where the first part of the methodology is in charge of the synthetic image generation that is performed using an image translation model (and is described in detail in Subsection Image Generation for Data Augmentation) and where the second part of the methodology uses the novel set of synthetic images to artificially increase the size of the original input dataset (and is described in detail in Subsection Automatic Screening).

Figure 2. Overview of the methodology for data augmentation and COVID-19 screening using portable chest X-ray images; The first part performs the image generation while the second part performs the automatic COVID-19 Screening

254
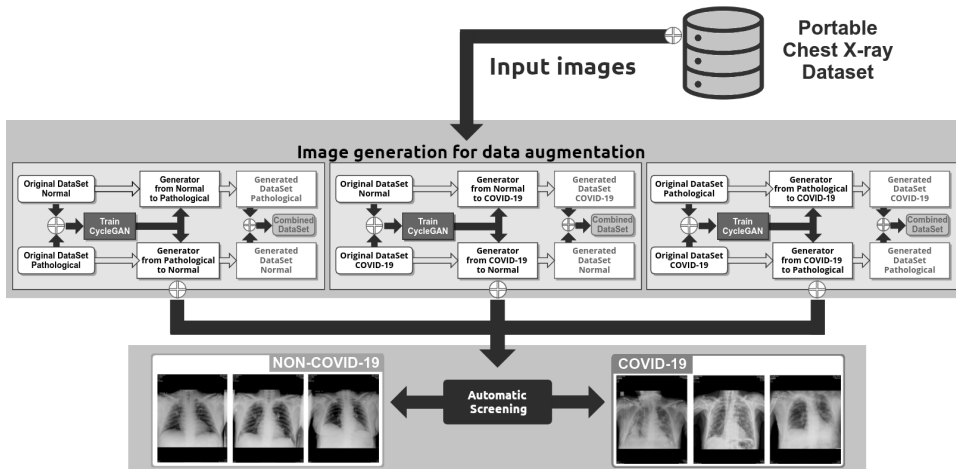
Image Generation for Data Augmentation

The CycleGAN is composed of 2 different generative models (G_{AB} and G_{BA}) and 2 different discriminative models (D_A and D_B). Its schematical representation can be seen in Figure 3. The model G_{AB} is trained to translate images from a domain A to its correspondent representation in domain B. On the other side, the model G_{BA} is trained to translate images from a domain B to a domain A. In addition, the discriminative model D_A is trained to distinguish original images from domain A and fake images generated by G_{BA} while the discriminative model D_B is trained to distinguish original images from domain B and fake images generated by G_{AB}. Therefore, the image translation is performed in 3 different scenarios: the first one converts from Normal to Pathological and vice versa, the second one converts from Normal to COVID-19 and vice versa while the third one converts from Pathological to COVID-19 and vice versa. Moreover, in the case of the considered reference work, authors used 4 different configurations for the generative model: Unet-128, Unet-256, ResNet-6 and ResNet-9 (those that were allowed by the CycleGAN original implementation). With regards to the discriminative models, a 70 X 70 PatchGAN is used as the architecture in both cases. Thanks to the implementation of the CycleGAN, both generative and discriminative models are trained simultaneously for the 2 possible pathways on each case.

Figure 3. Overall description of the CycleGAN architecture for image generation; In this schematic representation, the class Normal is assumed as the domain A and the class COVID-19 is assumed as the class B
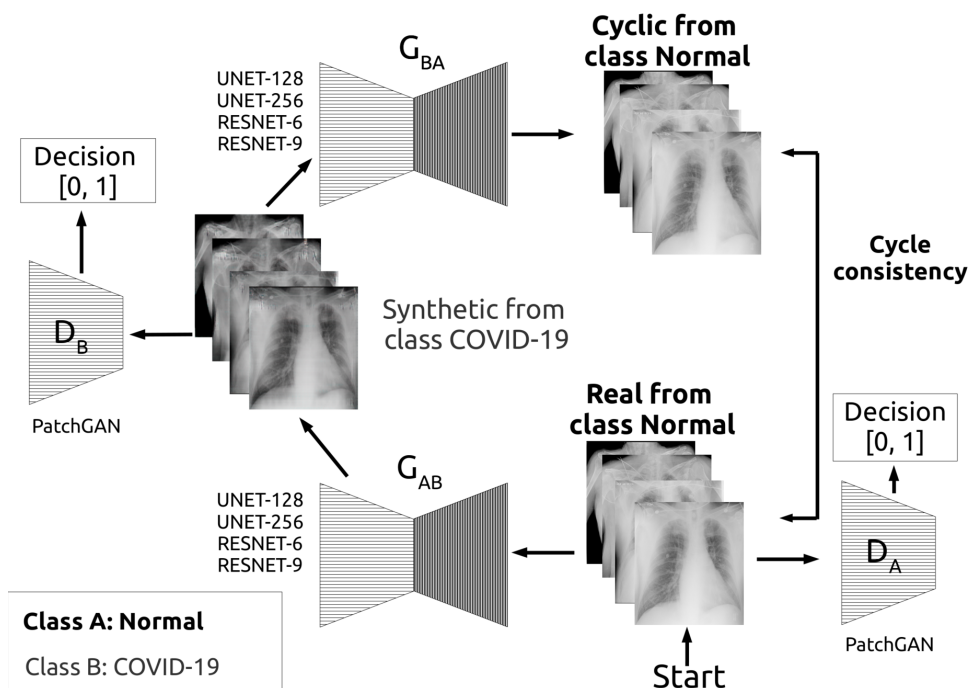
When all models are trained, G_{AB} and G_{BA} can be used to perform the image translations. Therefore, if we consider the class Normal as the domain A and the class Pathological as the domain B, the model G_{AB} is able to convert Normal images to their Pathological version while the model G_{BA} converts the Pathological images to their Normal version. The same idea applies for the other remaining 2 scenarios. The CycleGAN is complex to train, needing the definition of several different types of losses. With regards to this, there are 2 loss definitions: the adversarial loss and the cycle consistency loss. The adversarial loss is computed using the least-square loss to compare the predicted and the expected output. The expression of the adversarial loss is shown in Equation 1:

$$L_{GAN} = \left(G_{AB}, D_B, A, B\right) = E_{a \sim p_{data}(a)}\left[\left(D_B\left(G_{AB}\left(a\right)\right) - 1\right)^2\right] \tag{1}$$

where *a* denotes a particular original image that belongs to domain A and the generative model G_{AB} and the discriminative model D_B are used as reference,

256

In addition, the discriminative models must be trained to minimize the expression stated in Equation 2 taking the case of D_B as reference and considering b as an original image that belongs to domain B:

$$L_{GAN}\left(G_{AB},D_B\right) = \frac{E_{a\sim p_{data}(a)}\left[\left(D_B\left(G_{AB}\right)(a)\right)^2\right] + E_{b\sim p_{data}(b)}\left[\left(D_B\left(b\right)-1\right)^2\right]}{2}$$

(2)

On the other hand, the model defines the cycle consistency loss. This expression adds 2 weight values, λA and λB. The weight value λA re$_f$ers to the path that converts images from domain A to domain B and then to domain A again while the weight λB re$_f$ers to the path that converts images from domain B to domain A and then to domain B again. The expression of the cycle consistency loss is stated in Equation 3:

$$L_{cyc}\left(G_{AB},G_{BA},\lambda_A,\lambda_B\right)$$
$$= \lambda_A \cdot E_{a\sim p_{data}}\left(a\right)\left[\|G_{BA}\left(G_{AB}\left(a\right)\right)-a\|_1\right] + \lambda_B \cdot E_{b\sim p_{data}(b)}\left[\|G_{AB}\left(G_{BA}\left(b\right)\right)-b\|_1\right]$$

(3)

Given an original image a from the domain A the idea of cycle consistency is that, if we convert that image to the domain B using the generative model GA_B and, afterwards, we use that output as the input of the generative model GB_A to convert the synthetic image from the domain B to the domain A, the final output image (denoted as Cycle A) must be the same as the original a. In other words, this means that a must be equal to Cycle A = $GB_{A(}GA_{B(}a)$).

Finally, the used implementation of the CycleGAN also uses another loss expression, which is known as identity loss. This loss value is used to prevent the model to perform undesired transformations on images. Given an image *a* from the domain *A*, the idea of identity loss is that, if we use that image as the input of the generative model G_{BA}, the model should obtain the same exact image (that can be denoted as idt_A). In other words, this means that a must be equal to idt_A = G_{BA}(a). Considering all these aspects, the identity loss is expressed as can be seen in Equation 4.

$$L_{idt}\left(G_{AB},G_{BA},\lambda_A,\lambda_B\right) = E_{a\sim p_{data}(a)}\left[\|G_{BA}\left(a\right)-a\|_1\right]\lambda_A \cdot \lambda_{idt} + E_{b\sim p_{data}(b)}\left[\|G_{AB}\left(b\right)-b\|_1\right]\cdot \lambda_B \cdot \lambda_{idt}$$

(4)

where λi$_{dt}$ gives a weight value to the identity loss in the final objective expression. With all the loss functions defined, the joint expression is shown in Equation 5.

$$L\left(G_{AB}, G_{BA}, D_A, D_B, \lambda_A, \lambda_B, \lambda_{idt}\right) = L_{GAN}\left(G_{AB}, D_B, A, B\right)$$
$$+ L_{GAN}\left(G_{BA}, D_A, B, A\right) + L_{cyc}\left(G_{AB}, G_{BA}, \lambda_A, \lambda_B\right) + L_{idt}\left(G_{AB}, G_{BA}, \lambda_A, \lambda_B, \lambda_{idt}\right)$$

(5)

Therefore, to update the networks weights, the expression defined in Equation 6 must be optimized:

$$G_{AB}{}^*, G_{BA}{}^* = arg \min_{G_{AB}, G_{BA}} \max_{D_A, D_B} L\left(G_{AB}, G_{BA}, D_A, D_B, \lambda_A, \lambda_B, \lambda_{idt}\right)$$

(6)

Other important training detail is that all the input images are resized to 256 X 256 X 3. Moreover, the CycleGAN models are all trained during 250 epochs with the Adam algorithm (Kingma & Ba, 2014) and a mini-batch size of 1. In terms of the optimization algorithm parameters, the authors use a constant value of learning rate of $\alpha = 0.0002$. Finally, an important aspect that must be noted is that all the images of the input dataset were used with the aim of training the CycleGAN models.

Automatic Screening

For the second part of the methodology, the new set of synthetic images is added to the training set of the COVID-19 screening. Therefore, the model is trained with a higher amount of data while the test is performed using only original images, in order to have a fair comparison against previous state of the art methods. The automatic COVID-19 screening is performed to prove 2 different hypotheses. First of all, it is used to measure the separability among the synthetic images generated for the 3 different above-mentioned scenarios (i.*e.*, Normal vs Pathological, Normal vs COVID-19 and Pathological vs COVID-19). The second hypothesis to prove is that using the novel set of synthetic images can improve the performance of the screening model.

In order to develop this COVID-19 screening method, the reference work adapts the training details designed for a previous approach. Particularly, for the classification task, authors use a Densely Connected Convolutional Network (DenseNet) as the network architecture (Huang et al., 2017), more precisely, a DenseNet-161. All screening models were trained during 200 epochs, optimizing with the Stochastic Gradient Descent Algorithm (SGD) (Ketkar, 2017) and a constant learning rate of $\alpha = 0.01$ with a first-order momentum of 0.9. Moreover, a mini-batch size of 4 was used, the input dataset is randomly splitted in 3 different sets, using a 60% of the samples for training, 20% of the samples for validation and the remaining 20% of

the samples for test and the training process is conducted 5 times. To have a global metric representative of the models behavior, given the values of the 5 repetitions, the mean and the standard deviation are obtained. Furthermore, the loss function used to train the screening model was the cross-entropy, which is defined in Equation 7:

$$L = -Y \cdot log\left(\widehat{Y}\right) \tag{7}$$

RESULTS AND DISCUSSION

To validate the methodology, authors made a qualitative analysis of the generated synthetic images and they performed 5 different experiments with the automatic screening method as well as an additional sixth experiment, that are briefly described below:

- **1st experiment:** validates the separability between the class Normal and the class Pathological using only generated images.
- **2nd experiment:** performs the separability validation between the class Normal and the class COVID-19 using only generated images.
- **3rd experiment:** studies the separability between the class Pathological and the class COVID-19 using only generated images.
- **4th experiment:** the screening model is trained with the augmented dataset (composed of both original and generated images) but tested only with original images to separate between the class NON-COVID-19 (that merges the class Normal with the class Pathological) and the class COVID-19.
- **5th experiment:** ablation study to understand the behavior of the screening model given the number of generated images.
- **6th experiment:** qualitative analysis of the synthetic generated images.

To make the experimental validation, authors used metrics that are usually used in the state of the art. Denoting TP as True Positives, TN as True Negatives, FP as False Positives and FN as False Negatives, accuracy is expressed in Equation 8, recall is stated in Equation 9, precision is shown in Equation 10 and F1-Score can be seen in Equation 11.

$$Accuracy = \frac{TP + TN}{TP + FP + TN + FN} \tag{8}$$

$$Recall = \frac{TP}{TP + FN} \tag{9}$$

$$Precision = \frac{TP}{TP + FP} \tag{10}$$

$$F1 - Score = 2 \cdot \frac{Precision \cdot Recall}{Precision + Recall} \tag{11}$$

Moreover, authors complement the experimental validation with the correct classification and the misclassification ratios obtained from confusion matrices representative of each experiment and each generative model configuration.

1st Experiment: Separability Between Normal and Pathological (Only Generated Images)

Considering the test results of the first experiment (that validates the separability between the generated Normal samples and the generated Pathological samples), in terms of accuracy, the screening models obtain a 95.83%, 97.92%, 100.00% and 96.88% for each of the generative models configurations, respectively, Unet-128, Unet-256, ResNet-6 and ResNet-9. On the other hand, precision, recall and F1-Score of this first experiment are depicted in Figure 4. There, it can be seen that all metrics are equal or over 96% and, even in some cases, values are 100%, demonstrating the robustness of the method. Moreover, Figure 5 depicts the confusion matrices for the third experiment, where it can be seen that the correct classification ratios are satisfactory for both Normal class and Pathological class with all the 4 configurations, being higher or equal than 96% in all cases.

260

Figure 4. Metrics values in the case Normal vs Pathological (separability among generated images) (a) Values obtained for the Normal class (b) Values obtained for the Pathological class
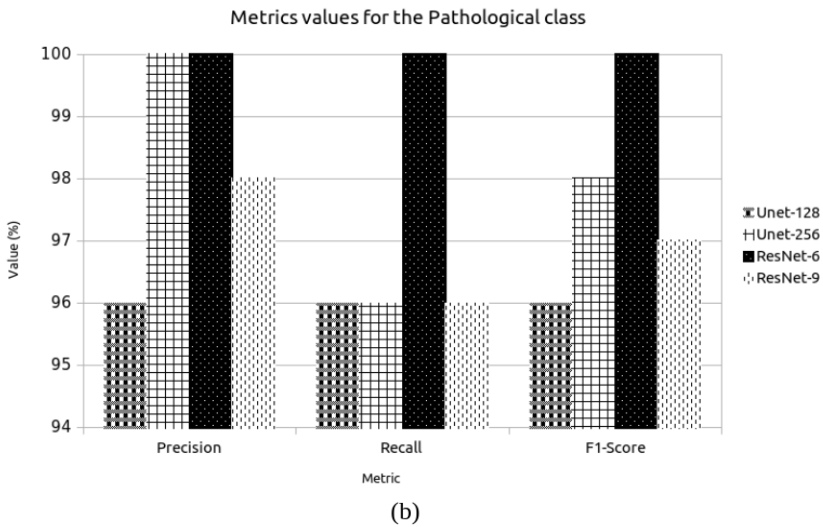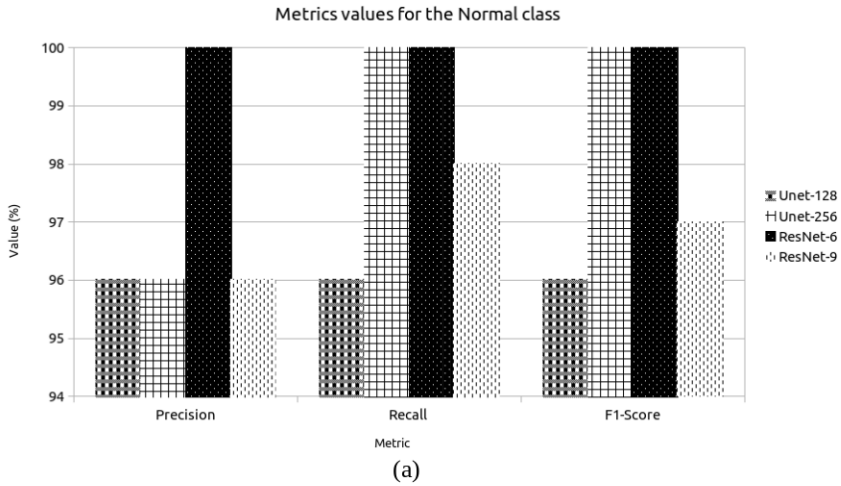

(a)

(b)

Figure 5. Confusion matrices of the 1ˢᵗ experiment given the 4 CycleGAN configurations that were selected (a) Unet-128 (b) Unet-256 (c) ResNet-6 (d) ResNet-9
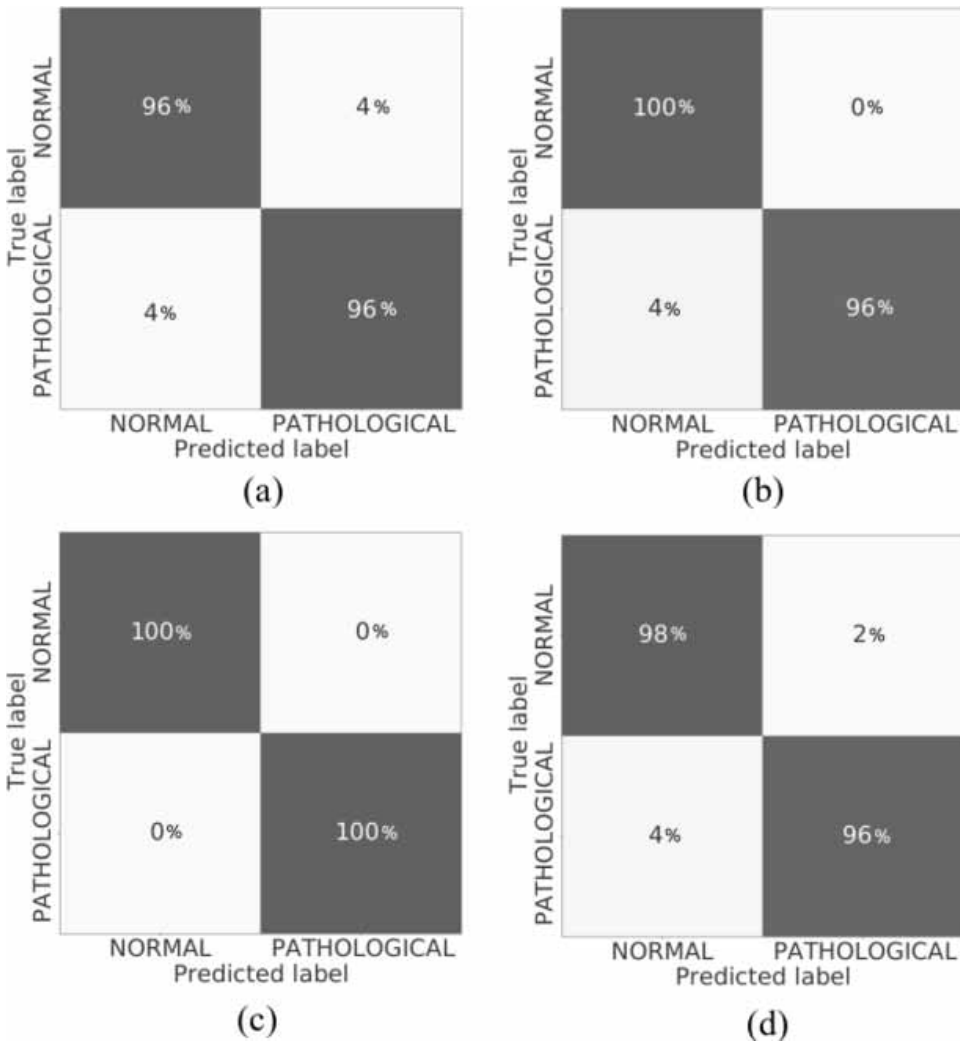
2ⁿᵈ Experiment: Separability Between Normal and COVID-19 (Only Generated Images)

With regards to the test results of the second experiment, the separability between the Normal class and the COVID-19 class is proved, as it can be seen in Figure 6. In particular, once again, all values are close to 100%. The same happens with regards to the accuracy values and, in the same order as in the previous case, the screening models obtained a 94.79%, 100.00%, 96.88% and 96.88%. For this case,

262

the confusion matrices are shown in Figure 7 where it can be seen that the correct classification ratio is always higher or equal than 94% for both classes and with all the configurations.

Figure 6. Metrics values in the case Normal vs COVID-19 (using only generated images) (a) Metrics values obtained for the Normal class (b) Metrics values obtained for the COVID-19 class

Metrics values for the Normal class

(a)

Metrics values for the COVID-19 class

(b)

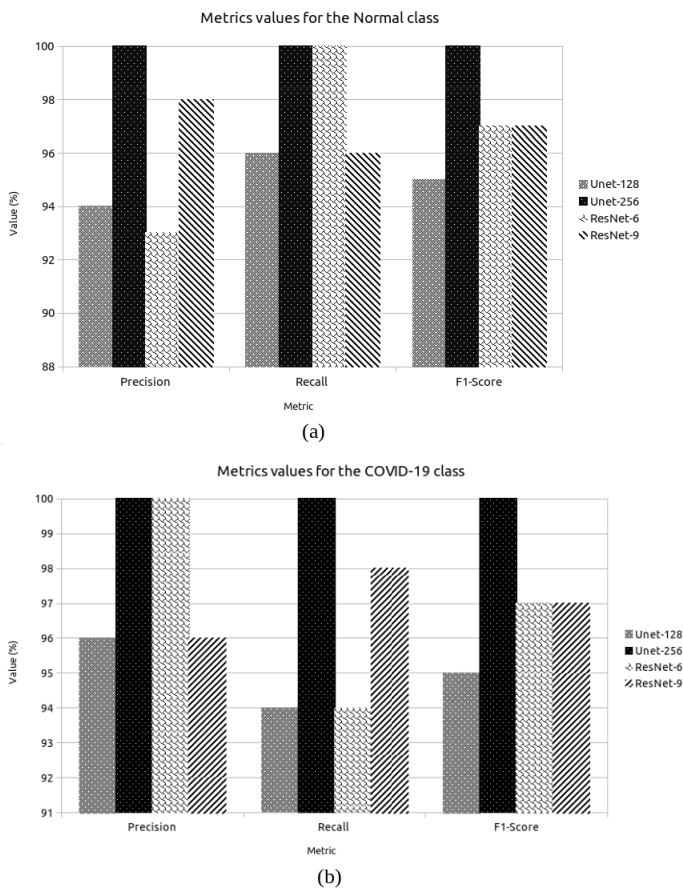*Figure 7. Confusion matrices results achieved during the 2ⁿᵈ experiment showing the 4 CycleGAN configurations that were chosen (a) Unet-128 (b) Unet-256 (c) ResNet-6 (d) ResNet-9*
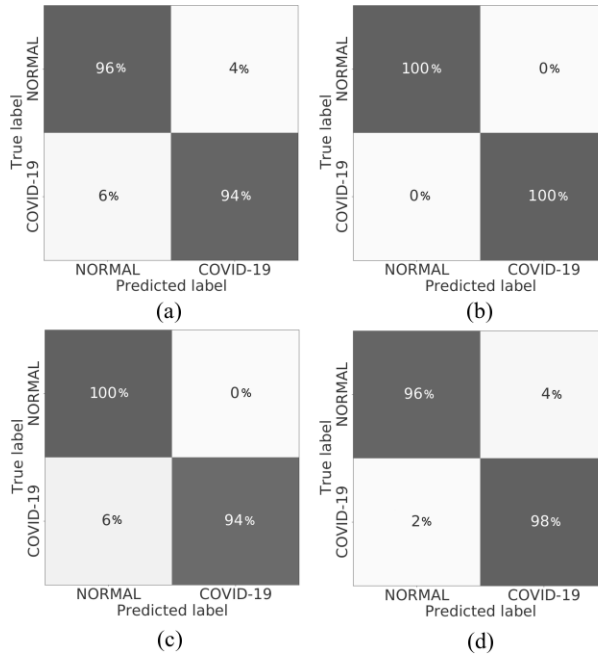
3rd Experiment: Separability Between Pathological and COVID-19 (Only Generated ImAges)

In terms of test results for the third experiment, Figure 8 has the metrics values for this experiment, showing that all cases are significantly close to 100% in a similar way as in the previous cases. Accuracy values have an identical behavior with a 98.96%, 100.00%, 97.92% and 100.00% considering the same order as in the previous cases. The confusion matrices that are shown in Figure 9 depict similar results as those seen in previous experiments. The correct classification ratios are significantly high for both classes and for all the 4 configurations considered for the image generation.

264

Figure 8. Metrics in the case Pathological vs COVID-19 (separability among generated images) (a) Normal class (b) COVID-19 class
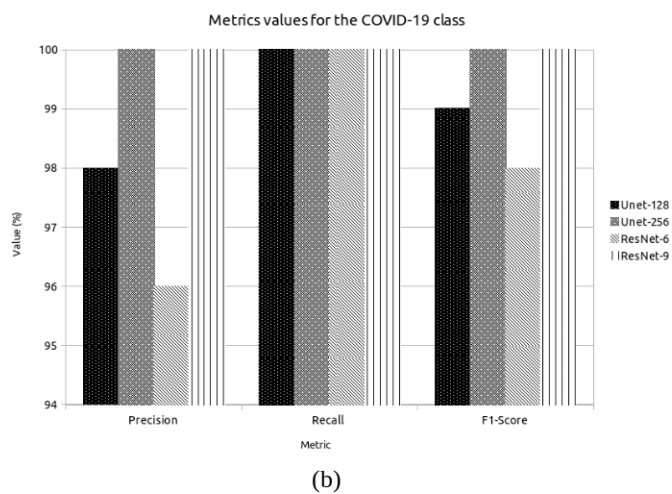

(a)

(b)
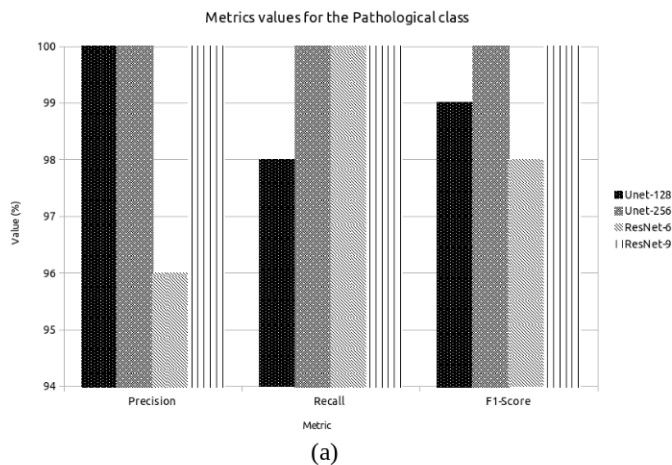
Figure 9. Confusion matrices results for the 3rd experiment with regards to the 4 CycleGAN configurations that were taken into account (a) Unet-128 (b) Unet-256 (c) ResNet-6 (d) ResNet-9
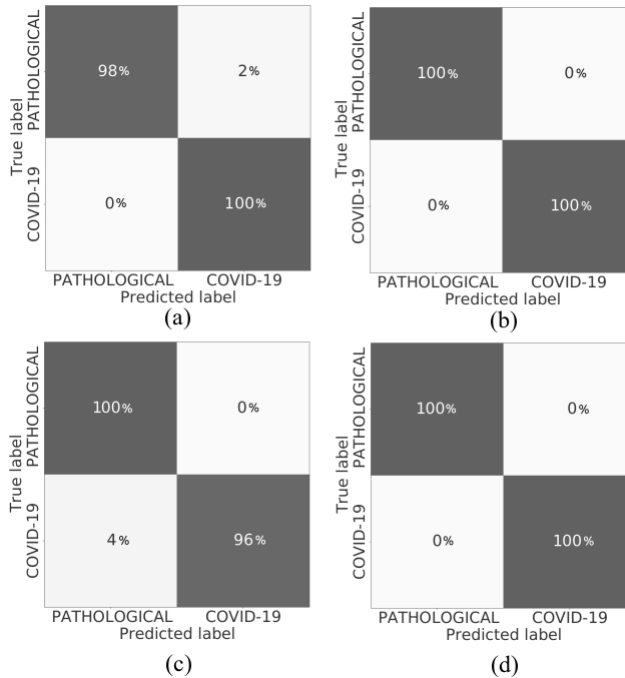
4th Experiment: Separability Between NON-COVID-19 and COVID-19 (Augmented Dataset)

Finally, the fourth experiment is the one that trains with the augmented dataset. In this experiment, the Normal class and the Pathological class are merged together to create a new NON-COVID-19 class, while the original COVID-19 class remains the same. For this last experiment, test results demonstrate that the automatic COVID-19 screening performed using the augmented dataset can obtain considerably acceptable results. The best effectiveness is obtained when generating the novel set of images configuring the generative model with the ResNet-9, obtaining an accuracy of 98.61%. More detailed results are shown in Figure 10, in terms of precision, recall and F1-Score. There it can be seen that, in an identical way as in the previous cases, all metrics are significantly close to 100%. Furthermore, in terms of correct classification ratios, values are higher or equal than 96% in all cases, for both classes and for all the considered configurations for image generation as it is shown in the confusion matrices of the Figure 11.

266

With respect to the previous contribution of (De Moura, García, et al., 2020) that proposes the same architectural and training details but without generating synthetic images, there is a significant improvement from 90.27% to 98.61% in terms of accuracy. More detailed results can be seen in Figure 12 regarding recall, F1-Score and precision. For those results, it is remarkable the improvement in all metrics for both classes, but specially in the case of the COVID-19 class, as they improve from less than 90% to values considerably close to 100%.

Figure 10. Metrics values in the case NON-COVID-19 vs COVID-19 (training with the augmented dataset and testing with only original images) (a) Values achieved in the case of the NON-COVID-19 class (b) Values achieved in the case of the COVID-19 class

(a)

(b)
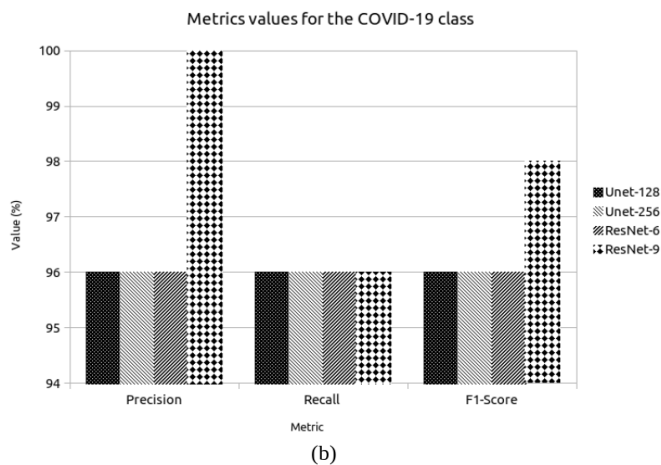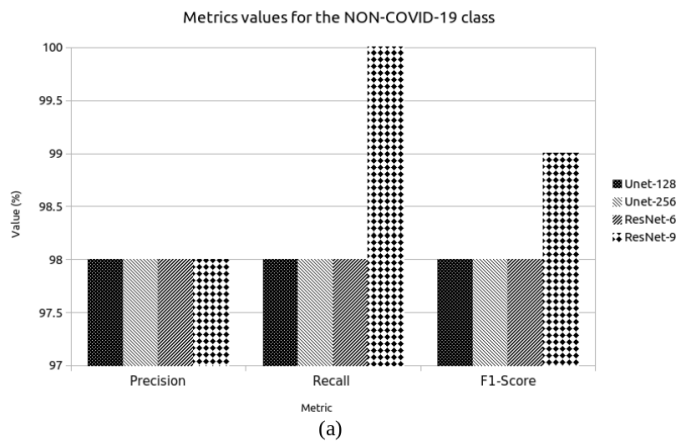
Figure 11. Confusion matrices results obtained during the 4th experiment with respect to the 4 CycleGAN configurations that were chosen for this work (a) Unet-128 (b) Unet-256 (c) ResNet-6 (d) ResNet-9
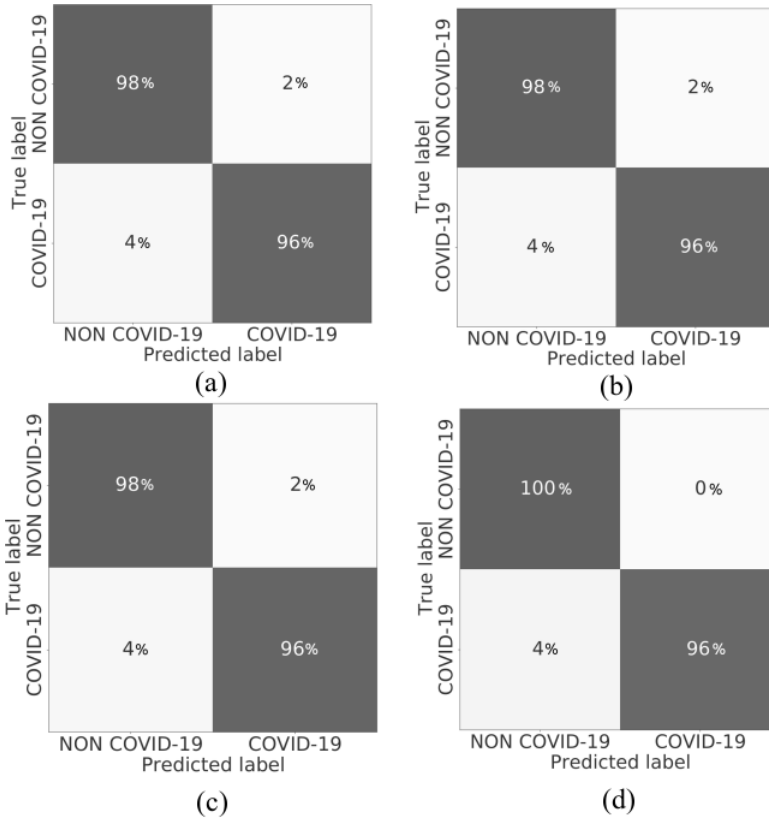
Figure 12. Metrics values comparison between 2 approaches: the screening with data augmentation (Morís et al., 2021b) and the screening without data augmentation (De Moura, García, et al., 2020). (a) Results in the case of the NON-COVID-19 class (b) Results in the case of the COVID-19 class

(a)

(b)
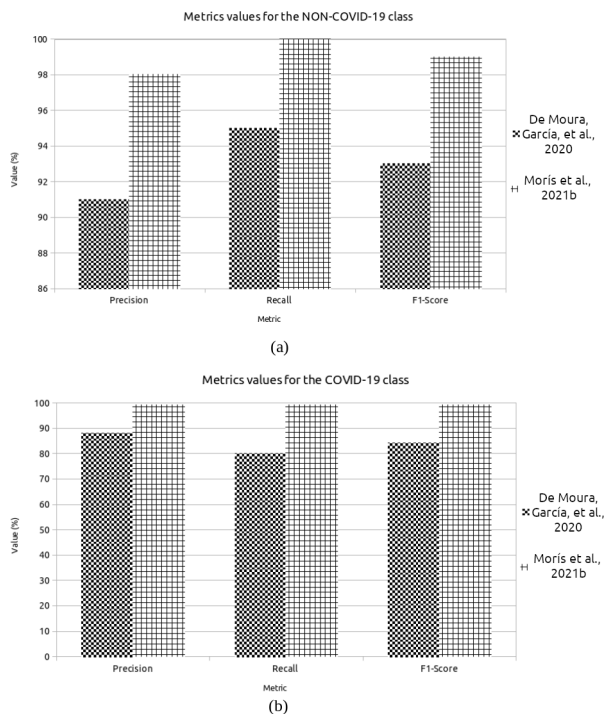
5th Experiment: Impact of the Number of Used Generated Images on the Performance of the Screening Model

Moreover, authors conducted 5 additional experimental tests to prove the impact on the performance of the number of used generated images. In particular, they analyzed the performance while using the 0% of the whole set of generated images, the 20% (288 images), the 40% (576 images), the 60% (864 images), the 80% (1152 images) and the 100% (1440 images). To do this, they only considered 1 configuration for image generation, the ResNet-9, the one that achieved the best performance for the fourth experiment. The results, that can be seen in Figure 13, clearly show that performance increases when the number of synthetic images is higher, while it starts to converge at about the 80%.

269

Figure 13. Impact of the number of synthetic images on the automatic screening effectiveness
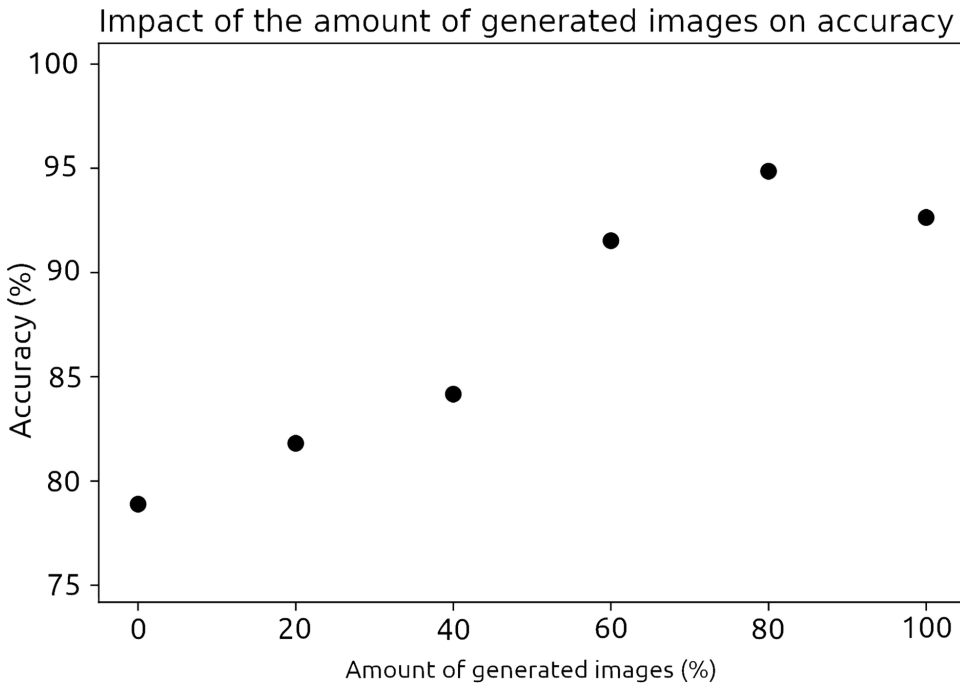
6th Experiment: Qualitative Analysis of the Synthetic Generated Images

With regards to the synthetic image generation, the image translation models are able to generate fully synthesized images with a realistic appearance and with representative patterns of the scenario that want to be modeled, as it can be seen in the examples depicted in Figure 14. The difference images show that the most remarkable differences are noticed in pulmonary regions. Thus, as models are able to recognize the most remarkable patterns of each class, they can compute the differences to have a proper representation of the image in the target domain. Once the novel set of generated images is available, it can be added to a small size dataset, to increase its dimensionality and improve the performance that the deep models could achieve training with that artificially augmented dataset.

Therefore, the method is able to not only generate realistic chest X-ray images, but also to generate useful samples for clinical uses without paired data. Moreover, the great differences in the pulmonary regions, which are the most important areas of the images representative of the disease affectation, demonstrate that the method

is focused on clinical criteria rather than other possible artifacts or irrelevant regions of the images for the diagnostic process.

Figure 14. Examples of generated images and the differences between the generated and the original version for the 3 different scenarios (Normal vs Pathological, Normal vs COVID-19 and Pathological vs COVID-19)
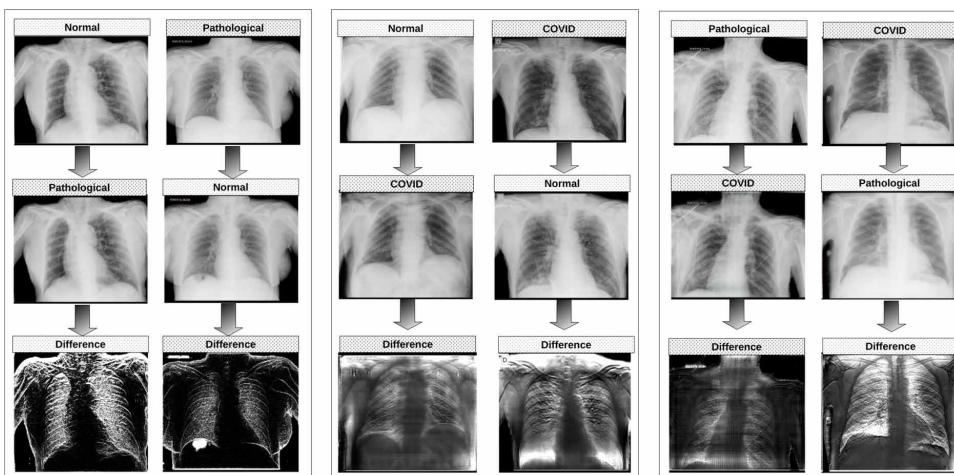
SOLUTIONS AND RECOMMENDATIONS

The proposed methods for image generation have some problems that could be tackled to improve the performance of the screening models. As is stated on the content of this chapter, the portable chest X-ray devices provide images with lower quality, aspect that could be mitigated with several techniques such as the super resolution to resize original images to a higher resolution without losing quality or other classical enhancement strategies. Other interesting approach would be to train an image translation model to convert images from portable devices to their hypothetical version if they were captured with fixed machinery, to improve their quality. On the other hand, to help models to focus on the most important parts of the input images, an interesting approach would be to apply a ROI mask for images to only obtain the pulmonary regions. Furthermore, authors specified that they use a resolution of 256 X 256 X 3, which is considerably small. This makes the development of automatic screening methods more challenging and especially in this case, as the resolution of the chest X-ray images is very important because the pathological affectation must be explored looking at the fine details.

Apart from these challenges, many chest X-ray images from this kind of datasets show artifacts related with elements that are placed on patients to do the captures, elements that are placed on patients due to their condition (like the tubes that most critical patients need for mechanical ventilation), as well as other artifacts such as implants or other foreign objects that can appear on images. An approach to tackle this problem is to remove those elements from images. In the same way, as the important elements related with COVID-19 affectation can be detected on lung regions, bones suppression on images can be very useful.

FUTURE RESEARCH DIRECTIONS

Data scarcity is a challenging and well-known problem in the domain of biomedical imaging, not only for COVID-19 but also for many image modalities and for an important diversity of pathologies, especially when trying to train deep learning models, that need great amounts of data. Many efforts have been done in the direction of overcoming this data scarcity, developing several strategies as the application of traditional data augmentation techniques (such as random translations, rotations and other kind of linear and non-linear transformations), the transfer learning, the multi-task learning, the self-supervised learning or the weak supervised learning, among many others. In the last years, the focus has also been put on synthetic image generation, a powerful technique to artificially augment the size of the datasets, mitigating the data scarcity problem.

The Generative Adversarial Networks (GANs) have been often used for image generation in recent contributions. However, most of the GAN implementations are initially tested on broad domain image datasets. Therefore, their strength dealing with biomedical imaging problems is less frequently proved. Nevertheless, this chapter shows that are some interesting works that deal with this problematic. In particular, for the topic of this chapter, they demonstrate that image generation is a powerful data augmentation to overcome data scarcity in the domain of the COVID-19 when using image modalities as the CT or the chest X-ray, even with low quality images. Thus, the most probable future research directions are focused on developing and proving the strength of image generation methods to overcome data scarcity in specific biomedical imaging domains, different from those described in this chapter and applied to a great variety of diseases.

On the other hand, as it is well-known, in contrast with a broad domain, a particular biomedical imaging domain always represents the similar reality. This means that models can learn better from the reality they are looking at, presumably obtaining greater results. Furthermore, in the context of GANs applied to biomedical imaging,

the image translation models are very relevant, especially those that can be trained without paired and registered data, as this kind of data is usually difficult to retrieve.

CONCLUSION

The COVID-19 disease has represented a great challenge for the whole humanity. Many efforts have been done to develop useful tools to tackle the dramatic situation of the healthcare services. One of the most important parts to mitigate the expansion of the pathogen that causes the COVID-19 is the early diagnose and the assessment of the evolution of the disease. There are several techniques to do so but, as the main affectation provoked by the coronavirus SARS-CoV-2 is located at the pulmonary regions, biomedical image modalities as chest X-ray are very useful to understand the severity of the disease on each moment. Chest X-ray imaging is a cheap and easy to perform diagnosis technique that allows clinicians to visualize the captured regions and, therefore, analyze the patterns that can be representative of different types of diseases. In the case of the COVID-19, considering the importance of cutting the chains of transmission, the decontamination of chest X-ray devices is a critical aspect. In that sense, the portable chest X-ray devices provide an alternative to fixed machinery, as they are easier to decontaminate.

The CAD systems have shown their utility in the last decades and specially in the last years with the raise of novel powerful strategies for biomedical imaging analysis. Particularly, the contributions of machine learning and, more precisely, the contributions of deep learning are remarkable in this field. These models are able to perform complex tasks directly dealing with raw data. During the COVID-19 pandemic, this kind of systems are helpful for the clinicians to alleviate their workload, providing an automatic tool that also mitigates the subjectivity of the human experts. With regards to the chest X-ray image modality, deep models are able to directly deal with images of patients with suspected COVID-19 and extract the patterns that can conclude if that sample presents COVID-19 affectation or not, in a fully automatic way.

In this chapter, we analyzed the proposals of methods for portable chest X-ray image generation to improve the COVID-19 screening. To do so, we have taken into account a representative work from the state of the art. In that work, the methodology is splitted in 2 different modules. The first module generates the synthetic images using a CycleGAN architecture and considering 4 different configurations for the generative models. The CycleGAN architecture is used to do an image translation that can convert images from a source scenario to another target scenario. For the specific case of the reference work, the input dataset has 3 different classes: Normal, Pathological and COVID-19. Therefore, the translations are performed in 3 different

contexts: the context where Normal images are converted to their Pathological version and vice versa, the context where Normal images are converted to their COVID-19 version and vice versa, and the context where Pathological images are converted to their COVID-19 representation and vice versa. This novel set is characterized of having synthetic images very similar to real chest X-ray captures and representative of the variability of the domain. Thus, this means that image generation represents a more powerful strategy in comparison with the classical data augmentation techniques.

For the second part of the methodology, an automatic COVID-19 screening is performed. This part of the methodology is developed using a DenseNet-161 architecture as the classification model. To prove the separability among the generated images, authors performed 3 different experiments, one for each translation scenario. Therefore, the first experiment is performed to validate the separability between the Normal and the Pathological class, the second experiment is performed to validate the separability between the Normal and the COVID-19 class and the third experiment is performed to validate the separability between the Pathological and the COVID-19 class. While these experiments are solely conducted using synthetic images, authors performed a fourth experiment using both original and synthetic images for training. In this case, they merge the Normal and the Pathological class to create a novel NON-COVID-19 class while the original COVID-19 class remains as the new COVID-19 class. To make a fair comparison with previous state of the art methods, they only add the novel set of generated samples in the training set. Therefore, the test is only performed with original images. Results show that there is a satisfactory separability between the generated images for all the considered scenarios. Furthermore, the fourth experiment proves that adding the novel set of synthetic images is useful to improve the automatic COVID-19 screening, obtaining an accuracy of 98.61% in contrast with the previous state of the art approach that only obtained a 90.27%. A fifth experiment was conducted to understand the impact of the number of generated images on the screening performance demonstrating that the effectiveness gets better when the amount of generated images is bigger. Finally, the sixth experiment performs the qualitative analysis of the generated synthetic images.

ACKNOWLEDGMENT

REFERENCES

Acar, E., Şahin, E., & Yılmaz, İ. (2021). Improving effectiveness of different deep learning-based models for detecting COVID-19 from computed tomography (CT) images. *Neural Computing & Applications*, *33*(24), 1–21. doi:10.100700521-021-06344-5 PMID:34345118

Armato, S. G. III, McLennan, G., Bidaut, L., McNitt-Gray, M. F., Meyer, C. R., Reeves, A. P., Zhao, B., Aberle, D. R., Henschke, C. I., Hoffman, E. A., Kazerooni, E. A., MacMahon, H., van Beek, E. J. R., Yankelevitz, D., Biancardi, A. M., Bland, P. H., Brown, M. S., Engelmann, R. M., Laderach, G. E., ... Clarke, L. P. (2011). The Lung Image Database Consortium (LIDC) and Image Database Resource Initiative (IDRI): A Completed Reference Database of Lung Nodules on CT Scans. *Medical Physics*, *38*(2), 915–931. doi:10.1118/1.3528204 PMID:21452728

Basu, S., Mitra, S., & Saha, N. (2020). Deep Learning for Screening COVID-19 using Chest X-Ray Images. *2020 IEEE Symposium Series on Computational Intelligence (SSCI)*, 2521–2527. 10.1109/SSCI47803.2020.9308571

Ciotti, M., Ciccozzi, M., Terrinoni, A., Jiang, W.-C., Wang, C.-B., & Bernardini, S. (2020). The COVID-19 pandemic. *Critical Reviews in Clinical Laboratory Sciences*, *57*(6), 365–388. doi:10.1080/10408363.2020.1783198 PMID:32645276

Coronavirus Resource Center, Johns Hopkins. (2020). COVID-19 Dashboard by the Center for Systems Science and Engineering (CSSE) at John Hopkins University. ArcGIS Dashboards.

Cortes, C., & Vapnik, V. (1995). Support vector machine. *Machine Learning*, *20*(3), 273–297. doi:10.1007/BF00994018

Creswell, A., White, T., Dumoulin, V., Arulkumaran, K., Sengupta, B., & Bharath, A. A. (2018). Generative adversarial networks: An overview. *IEEE Signal Processing Magazine*, *35*(1), 53–65. doi:10.1109/MSP.2017.2765202

275

De Moura, J., García, L. R., Vidal, P. F. L., Cruz, M., López, L. A., Lopez, E. C., Novo, J., & Ortega, M. (2020). Deep Convolutional Approaches for the Analysis of COVID-19 Using Chest X-Ray Images From Portable Devices. *IEEE Access: Practical Innovations, Open Solutions*, *8*, 195594–195607. doi:10.1109/ACCESS.2020.3033762 PMID:34786295

De Moura, J., Novo, J., & Ortega, M. (2020). Fully automatic deep convolutional approaches for the analysis of Covid-19 using chest X-ray images. MedRxiv. doi:10.1101/2020.05.01.20087254

Doi, K. (2007). Computer-aided diagnosis in medical imaging: Historical review, current status and future potential. *Computerized Medical Imaging and Graphics*, *31*(4–5), 198–211. doi:10.1016/j.compmedimag.2007.02.002 PMID:17349778

Fiszman, M., Chapman, W. W., Aronsky, D., Evans, R. S., & Haug, P. J. (2000). Automatic detection of acute bacterial pneumonia from chest X-ray reports. *Journal of the American Medical Informatics Association: JAMIA*, *7*(6), 593–604. doi:10.1136/jamia.2000.0070593 PMID:11062233

Gonçalves, L., Novo, J., Cunha, A., & Campilho, A. (2017). Learning Lung Nodule Malignancy Likelihood from Radiologist Annotations or Diagnosis Data. *Journal of Medical and Biological Engineering*, *38*(3), 424–442. Advance online publication. doi:10.100740846-017-0317-2

Han, C., Kitamura, Y., Kudo, A., Ichinose, A., Rundo, L., Furukawa, Y., Umemoto, K., Li, Y., & Nakayama, H. (2019). Synthesizing Diverse Lung Nodules Wherever Massively: 3D Multi-Conditional GAN-Based CT Image Augmentation for Object Detection. *2019 International Conference on 3D Vision (3DV),* 729–737. 10.1109/3DV.2019.00085

Hayden, G. E., & Wrenn, K. W. (2009). Chest radiograph vs. Computed tomography scan in the evaluation for pneumonia. *The Journal of Emergency Medicine*, *36*(3), 266–270. doi:10.1016/j.jemermed.2007.11.042 PMID:18571356

Huang, G., Liu, Z., & Weinberger, K. Q. (2017). Densely Connected Convolutional Networks. *2017 IEEE Conference on Computer Vision and Pattern Recognition (CVPR)*, 2261–2269. 10.1109/CVPR.2017.243

Hwang, W.-J., & Wen, K.-W. (1998). Fast kNN classification algorithm based on partial distance search. *Electronics Letters*, *34*(21), 2062–2063. doi:10.1049/el:19981427

276

Jacobi, A., Chung, M., Bernheim, A., & Eber, C. (2020). Portable chest X-ray in coronavirus disease-19 (COVID-19): A pictorial review. *Clinical Imaging*, *64*, 35–42. doi:10.1016/j.clinimag.2020.04.001 PMID:32302927

Ketkar, N. (2017). Stochastic Gradient Descent. In Deep Learning with Python: A Hands-on Introduction (pp. 113–132). Apress. doi:10.1007/978-1-4842-2766-4_8

Kingma, D. P., & Ba, J. (2014). *Adam: A method for stochastic optimization*. ArXiv Preprint ArXiv:1412.6980.

Kooraki, S., Hosseiny, M., Myers, L., & Gholamrezanezhad, A. (2020). Coronavirus (COVID-19) Outbreak: What the Department of Radiology Should Know. *Journal of the American College of Radiology*, *17*(4), 447–451. doi:10.1016/j.jacr.2020.02.008 PMID:32092296

Krissian, K., Malandain, G., Ayache, N., Vaillant, R., & Trousset, Y. (2000). Model-Based Detection of Tubular Structures in 3D Images. *Computer Vision and Image Understanding*, *80*(2), 130–171. doi:10.1006/cviu.2000.0866

Kumar, A., Wang, Y.-Y., Liu, K.-C., Tsai, I.-C., Huang, C.-C., & Hung, N. (2014). Distinguishing normal and pulmonary edema chest x-ray using Gabor filter and SVM. *2014 IEEE International Symposium on Bioelectronics and Bioinformatics (IEEE ISBB 2014),* 1–4. 10.1109/ISBB.2014.6820918

Li, X., Thrall, J. H., Digumarthy, S. R., Kalra, M. K., Pandharipande, P. V., Zhang, B., Nitiwarangkul, C., Singh, R., Khera, R. D., & Li, Q. (2019). Deep learning-enabled system for rapid pneumothorax screening on chest CT. *European Journal of Radiology*, *120*, 108692. doi:10.1016/j.ejrad.2019.108692 PMID:31585302

Malygina, T., Ericheva, E., & Drokin, I. (2019). Data Augmentation with GAN: Improving Chest X-Ray Pathologies Prediction on Class-Imbalanced Cases. *International Conference on Analysis of Images, Social Networks and Texts*, 321–334. 10.1007/978-3-030-37334-4_29

Misra, S., Jeon, S., Lee, S., Managuli, R., Jang, I.-S., & Kim, C. (2020). Multi-Channel Transfer Learning of Chest X-ray Images for Screening of COVID-19. *Electronics (Basel)*, *9*(9), 1388. Advance online publication. doi:10.3390/electronics9091388

Morís, D. I., de Moura, J., Novo, J., & Ortega, M. (2021a). Cycle Generative Adversarial Network Approaches to Produce Novel Portable Chest X-Rays Images for Covid-19 Diagnosis. *ICASSP 2021-2021 IEEE International Conference on Acoustics, Speech and Signal Processing (ICASSP),* 1060–1064.

Morís, D. I., de Moura, J., Novo, J., & Ortega, M. (2021c). Comprehensive Analysis of the Screening of COVID-19 Approaches in Chest X-ray Images from Portable Devices. *European Symposium on Artificial Neural Networks (ESANN 2021)*, 165–170.

Morís, D. I., de Moura Ramos, J. J., Buján, J. N., & Hortas, M. O. (2021b). Data augmentation approaches using cycle-consistent adversarial networks for improving COVID-19 screening in portable chest X-ray images. *Expert Systems with Applications*, *185*, 115681. doi:10.1016/j.eswa.2021.115681 PMID:34366577

Novo, J., Gonçalves, L., Mendonça, A. M., & Campilho, A. (2015). 3D lung nodule candidate detection in multiple scales. *2015 14th IAPR International Conference on Machine Vision Applications (MVA),* 61–64. 10.1109/MVA.2015.7153133

Novo, J., Rouco, J., Mendonça, A., & Campilho, A. (2014). Reliable Lung Segmentation Methodology by Including Juxtapleural Nodules. *Reliable Lung Segmentation Methodology by Including Juxtapleural Nodules.*, *8815*, 227–235. doi:10.1007/978-3-319-11755-3_26

Puderbach, M., Eichinger, M., Haeselbarth, J., Ley, S., Kopp-Schneider, A., Tuengerthal, S., Schmaehl, A., Fink, C., Plathow, C., Wiebel, M., & ... (2007). Assessment of morphological MRI for pulmonary changes in cystic fibrosis (CF) patients: Comparison to thin-section CT and chest x-ray. *Investigative Radiology*, *42*(10), 715–724. doi:10.1097/RLI.0b013e318074fd81 PMID:17984769

Shadmi, R., Mazo, V., Bregman-Amitai, O., & Elnekave, E. (2018). Fully-convolutional deep-learning based system for coronary calcium score prediction from non-contrast chest CT. *2018 IEEE 15th International Symposium on Biomedical Imaging (ISBI 2018),* 24–28. 10.1109/ISBI.2018.8363515

Suzuki, K. (2017). Overview of deep learning in medical imaging. *Radiological Physics and Technology*, *10*(3), 257–273. doi:10.100712194-017-0406-5 PMID:28689314

Tahamtan, A., & Ardebili, A. (2020). Real-time RT-PCR in COVID-19 detection: Issues affecting the results. *Expert Review of Molecular Diagnostics*, *20*(5), 453–454. doi:10.1080/14737159.2020.1757437 PMID:32297805

Van Cleeff, M., Kivihya-Ndugga, L., Meme, H., Odhiambo, J., & Klatser, P. (2005). The role and performance of chest X-ray for the diagnosis of tuberculosis: A cost-effectiveness analysis in Nairobi, Kenya. *BMC Infectious Diseases*, *5*(1), 1–9. doi:10.1186/1471-2334-5-111 PMID:16343340

Vidal, P. F., de Moura, J., Novo, J., & Ortega, M. (2021). Multi-stage transfer learning for lung segmentation using portable X-ray devices for patients with COVID-19. *Expert Systems with Applications*, *173*, 114677. doi:10.1016/j.eswa.2021.114677 PMID:33612998

Wang, J., Perez, L., & ... (2017). The effectiveness of data augmentation in image classification using deep learning. *Convolutional Neural Networks Vis. Recognit*, *11*, 1–8.

Wei, J., Hagihara, Y., Shimizu, A., & Kobatake, H. (2002). Optimal image feature set for detecting lung nodules on chest X-ray images. In *CARS 2002 computer assisted radiology and surgery* (pp. 706–711). Springer. doi:10.1007/978-3-642-56168-9_118

Xie, Y., Xia, Y., Zhang, J., Song, Y., Feng, D., Fulham, M., & Cai, W. (2019). Knowledge-based Collaborative Deep Learning for Benign-Malignant Lung Nodule Classification on Chest CT. *IEEE Transactions on Medical Imaging*, *38*(4), 991–1004. doi:10.1109/TMI.2018.2876510 PMID:30334786

Xu, L., Zeng, X., Huang, Z., Li, W., & Zhang, H. (2020). Low-dose chest X-ray image super-resolution using generative adversarial nets with spectral normalization. *Biomedical Signal Processing and Control*, *55*, 101600. doi:10.1016/j.bspc.2019.101600

Yan, Z., Zhang, J., Zhang, S., & Metaxas, D. N. (2012). Automatic rapid segmentation of human lung from 2D chest X-ray images. *Proc. of MICCAI Workshop on Sparsity Techniques in Medical Imaging*.

Zhang, Y., Miao, S., Mansi, T., & Liao, R. (2020). Unsupervised X-ray image segmentation with task driven generative adversarial networks. *Medical Image Analysis*, *62*, 101664. doi:10.1016/j.media.2020.101664 PMID:32120268

Zheng, C., Deng, X., Fu, Q., Zhou, Q., Feng, J., Ma, H., Liu, W., & Wang, X. (2020). Deep learning-based detection for COVID-19 from chest CT using weak label. MedRxiv. doi:10.1101/2020.03.12.20027185

Zhu, J.-Y., Park, T., Isola, P., & Efros, A. A. (2017). Unpaired image-to-image translation using cycle consistent adversarial networks. *Proceedings of the IEEE International Conference on Computer Vision*, 2223–2232. 10.1109/ICCV.2017.244

279

ADDITIONAL READING

Alghamdi, H. S., Amoudi, G., Elhag, S., Saeedi, K., & Nasser, J. (2021). Deep Learning Approaches for Detecting COVID-19 From Chest X-Ray Images: A Survey. *IEEE Access: Practical Innovations, Open Solutions*, *9*, 20235–20254. doi:10.1109/ACCESS.2021.3054484 PMID:34786304

Fatima, S., Ratnani, I., Husain, M., & Surani, S. (2020). Radiological Findings in Patients with COVID-19. *Cureus*, *12*(4), e7651. doi:10.7759/cureus.7651 PMID:32411552

Fusco, R., Grassi, R., Granata, V., Setola, S. V., Grassi, F., Cozzi, D., Pecori, B., Izzo, F., & Petrillo, A. (2021). Artificial Intelligence and COVID-19 Using Chest CT Scan and Chest X-ray Images: Machine Learning and Deep Learning Approaches for Diagnosis and Treatment. *Journal of Personalized Medicine*, *11*(10), 993. Advance online publication. doi:10.3390/jpm11100993 PMID:34683133

Hervella, Á. S., Rouco, J., Novo, J., & Ortega, M. (2020). Self-supervised multimodal reconstruction of retinal images over paired datasets. *Expert Systems with Applications*, *161*, 113674. doi:10.1016/j.eswa.2020.113674

Hervella, Á. S., Rouco, J., Novo, J., & Ortega, M. (2021). Chapter 15 - Multimodal reconstruction of retinal images over unpaired datasets using cyclical generative adversarial networks. In A. Solanki, A. Nayyar, & M. Naved (Reds), Generative Adversarial Networks for Image-to-Image Translation (pp. 347–376). doi:10.1016/B978-0-12-823519-5.00014-2

Huang, S., Yang, J., Fong, S., & Zhao, Q. (2021). Artificial intelligence in the diagnosis of COVID-19: Challenges and perspectives. *International Journal of Biological Sciences*, *17*(6), 1581–1587. doi:10.7150/ijbs.58855 PMID:33907522

Lee, J. G., Jun, S., Cho, Y. W., Lee, H., Kim, G. B., Seo, J. B., & Kim, N. (2017). Deep learning in medical imaging: General overview. *Korean Journal of Radiology*, *18*(4), 570–584. doi:10.3348/kjr.2017.18.4.570 PMID:28670152

Yi, X., Walia, E., & Babyn, P. (2019). Generative adversarial network in medical imaging: A review. *Medical Image Analysis*, *58*, 101552. doi:10.1016/j.media.2019.101552 PMID:31521965

KEY TERMS AND DEFINITIONS

Chest X-Ray: Medical image modality that allows to visualize the inside of the thoracic region of a patient using a low dose of ionic radiation.

Computer-Aided Diagnosis: Systems that are developed to improve the comprehension of medical images and help clinicians to make decisions.

Computerized Tomography: Medical image modality that combines a set of X-ray slices to get a 3-dimensional representation of a particular studied region of the body.

Deep Learning: Type of machine learning strategies that allows to create powerful classification and regression models able to deal directly with raw data.

Image Translation: Algorithmic process that converts an image from a source domain to another different target domain (for example, convert the image of an orange to an image of an apple).

Portable X-Ray Devices: X-ray capturing devices that can moved to where the patients are placed.

Screening: Medical strategy that performs a diagnostic test on people that are considered healthy a priori with the aim to detect a possible disease on its mild stages.

Compilation of References

Abdi, A. H., Luong, C., Tsang, T., Allan, G., Nouranian, S., Jue, J., Hawley, D., Fleming, S., Gin, K., Swift, J., Rohling, R., & Abolmaesumi, P. (2017). Automatic quality assessment of echocardiograms using convolutional neural networks: Feasibility on the apical four-chamber view. *IEEE Transactions on Medical Imaging*, *36*(6), 1221–1230. doi:10.1109/TMI.2017.2690836 PMID:28391191

Abràmoff, M., Lavin, P., Birch, M., Shah, N., & Folk, J. (2018). Pivotal trial of an autonomous AI-based diagnostic system for detection of diabetic retinopathy in primary care offices. *NPJ Digital Medicine*, *1*(1), 39. Advance online publication. doi:10.103841746-018-0040-6 PMID:31304320

Abràmoff, M., Lou, Y., Erginay, A., Clarida, W., Amelon, R., Folk, J., & Niemeijer, M. (2016). Improved Automated Detection of Diabetic Retinopathy on a Publicly Available Dataset Through Integration of Deep Learning. *Investigative Ophthalmology & Visual Science*, *57*(13), 5200. doi:10.1167/iovs.16-19964 PMID:27701631

Abramoff, M., Niemeijer, M., Suttorp-Schulten, M., Viergever, M., Russell, S., & van Ginneken, B. (2007). Evaluation of a System for Automatic Detection of Diabetic Retinopathy From Color Fundus Photographs in a Large Population of Patients With Diabetes. *Diabetes Care*, *31*(2), 193–198. doi:10.2337/dc07-1312 PMID:18024852

Acar, E., Şahin, E., & Yılmaz, İ. (2021). Improving effectiveness of different deep learning-based models for detecting COVID-19 from computed tomography (CT) images. *Neural Computing & Applications*, *33*(24), 1–21. doi:10.100700521-021-06344-5 PMID:34345118

Accenture. (2021). *What Is Artificial Intelligence*. Retrieved 17 November 2021, from https://www.accenture.com/us-en/insights/artificial-intelligence-summary-index

Agarwal, M., & Mahajan, R. (2018). Medical Image Contrast Enhancement using Range Limited Weighted Histogram Equalization. *Procedia Computer Science, 125*(2017), 149–156. doi:10.1016/j.procs.2017.12.021

Agarwal, N., Singh, P., Singh, N., Singh, K. K., & Jain, R. (2021). Machine Learning Applications for IoT Healthcare. In *Machine Learning Approaches for Convergence of IoT and Blockchain* (pp. 129–144). Scrivener Publishing LLC. doi:10.1002/9781119761884.ch6

Compilation of References

Ahmed, N., Natarajan, T., & Rao, K. R. (1974). Discrete cosine transform. *IEEE Transactions on Computers*, *C-23*(1), 90–93. https://doi.org/10.1109/t-c.1974.223784

Alam, N.-A.-A., Ahsan, M., Based, M. A., Haider, J., & Kowalski, M. (2021). COVID-19 detection from chest X-ray images using feature fusion and deep learning. *Sensors (Basel)*, *21*(4), 1–30. doi:10.339021041480 PMID:33672585

Albahli, S., & Yar, G. N. A. H. (2021). Fast and Accurate Detection of COVID-19 Along With 14 Other Chest Pathologies Using a Multi-Level Classification: Algorithm Development and Validation Study. *Journal of Medical Internet Research*, *23*(2), e23693. doi:10.2196/23693 PMID:33529154

Aldahiri, A., Alrashed, B., & Hussain, W. (2021). *Trends in Using IoT with Machine Learning in Health Prediction System*. https://www.mdpi.com/journal/forecasting

Ali, E. S., Hassan, M. B., & Saeed, R. A. (2021). Machine Learning Technologies in Internet of Vehicles. In *Intelligent Technologies for Internet of Vehicles.* Springer. . doi:10.1007/978-3-030-76493-7_7

Alloghani, M., Al-Jumeily, D., Mustafina, J., Hussain, A., & Aljaaf, A. J. (2019). A systematic review on supervised and unsupervised machine learning algorithms for Data Science. *Unsupervised and Semi-Supervised Learning*, 3–21. doi:10.1007/978-3-030-22475-2_1

Almotiri, S. H., Khan, M. A., & Alghamdi, M. A. (2016). Mobile health (m-health) system in the context of IoT. *Proc. IEEE 4th Int. Conf. Future Internet Things Cloud Workshops (FiCloudW)*, 39–42.

Alnazir, A., Mokhtar, R. A., Alhumyani, H., Ali, E. S., Saeed, R. A., & Abdel-Khalek, S. (2021). Quality of Services Based on Intelligent IoT WLAN MAC Protocol Dynamic Real-Time Applications in Smart Cities. *Computational Intelligence and Neuroscience*, *2021*, 1–20. doi:10.1155/2021/2287531 PMID:34754301

Al-Rubeaan, K., Siddiqui, K., Al-Ghonaim, M. A., Youssef, A. M., Al-Sharqawi, A. H., & AlNaqeb, D. (2017). Assessment of the diagnostic valueMarkan, A., Agarwal, A., Arora, A., Bazgain, K., Rana, V., & Gupta, V. (2020). Novel imaging biomarkers in diabetic retinopathy and diabetic macular edema. *Therapeutic Advances in Ophthalmology*, *12*, 251584142095051. doi:10.1177/2515841420950513

Alsheikh, M. A., Lin, S., Niyato, D., & Tan, H.-P. (2016). Rate-distortion balanced data compression for wireless sensor networks. *IEEE Sensors Journal*, *16*(12), 5072–5083. doi:10.1109/JSEN.2016.2550599

Al-Turjman, F., & Baali, I. (2019). *Machine learning for wearable IoT-based applications: A survey*. Wiley. doi:10.1002/ett.3635

Al-Waisy, A. S., Mohammed, M. A., Al-Fahdawi, S., Maashi, M. S., Garcia-Zapirain, B., Abdulkareem, K. H., Mostafa, S. A., Kumar, N. M., & Le, D. N. (2021). COVID-DeepNet: Hybrid Multimodal Deep Learning System for Improving COVID-19 Pneumonia Detection in Chest X-ray Images. *Computers. Materials and Continua*, *67*(2), 2409–2429. doi:10.32604/cmc.2021.012955

An Introduction to Autoencoders: Everything You Need to Know. (n.d.). Retrieved February 16, 2022, from https://www.v7labs.com/blog/autoencoders-guide#autoencoders-intro

Analytics Vidhya. (2020, October 19). *CNN image classification: Image Classification using CNN*. Retrieved February 16, 2022, from https://www.analyticsvidhya.com/blog/2020/02/learn-image-classification-cnn-convolutional-neural-networks-3-datasets/

Analytics Vidhya. (2021, May 27). *Supervised deep learning algorithms*: *Types and applications*. Retrieved November 18, 2021, from https://www.analyticsvidhya.com/blog/2021/05/introduction-to-supervised-deep-learning-algorithms/

Antoine, J.-P. (2003). Wavelet transforms and their applications wavelet transforms and their applications, Lokenath Debnath, Birkhäuser, Boston, 2002. $79.95 (565 pp.). ISBN 0-8176-4204-8. *Physics Today*, *56*(4), 68–68. https://doi.org/10.1063/1.1580056

Anwar, S. M., Gul, M., Majid, M., & Alnowami, M. (2018). Arrhythmia classification of ecg signals using hybrid features. *Computational and Mathematical Methods in Medicine*, *2018*, 1–8. doi:10.1155/2018/1380348 PMID:30538768

Apostolopoulos, I. D., Aznaouridis, S. I., & Tzani, M. A. (2020). Extracting Possibly Representative COVID-19 Biomarkers from X-ray Images with Deep Learning Approach and Image Data Related to Pulmonary Diseases. *Journal of Medical and Biological Engineering*, *40*(3), 462–469. doi:10.100740846-020-00529-4 PMID:32412551

Apostolopoulos, I. D., & Mpesiana, T. A. (2020). COVID-19: Automatic detection from X-ray images utilizing transfer learning with convolutional neural networks. *Physical and Engineering Sciences in Medicine*, *43*(2), 635–640. doi:10.100713246-020-00865-4 PMID:32524445

Arias-Garzón, D., Alzate-Grisales, J. A., Orozco-Arias, S., Arteaga-Arteaga, H. B., Bravo-Ortiz, M. A., Mora-Rubio, A., Saborit-Torres, J. M., Serrano, J. Á. M., de la Iglesia Vayá, M., Cardona-Morales, O., & Tabares-Soto, R. (2021). COVID-19 detection in X-ray images using convolutional neural networks. *Machine Learning with Applications*, *6*, 100138. doi:10.1016/j.mlwa.2021.100138 PMID:34939042

Arias-Londono, J. D., Gomez-Garcia, J. A., Moro-Velazquez, L., & Godino-Llorente, J. I. (2020). Artificial Intelligence applied to chest X-Ray images for the automatic detection of COVID-19. A thoughtful evaluation approach. *IEEE Access: Practical Innovations, Open Solutions*, *8*, 226811–226827. Advance online publication. doi:10.1109/ACCESS.2020.3044858 PMID:34786299

Compilation of References

Armañanzas, R., Bielza, C., Chaudhuri, K. R., Martinez-Martin, P., & Larrañaga, P. (2013). Unveiling relevant non-motor Parkinson's disease severity symptoms using a machine learning approach. *Artificial Intelligence in Medicine*, *58*(3), 195–202. doi:10.1016/j.artmed.2013.04.002 PMID:23711400

Armato, S. G. III, McLennan, G., Bidaut, L., McNitt-Gray, M. F., Meyer, C. R., Reeves, A. P., Zhao, B., Aberle, D. R., Henschke, C. I., Hoffman, E. A., Kazerooni, E. A., MacMahon, H., van Beek, E. J. R., Yankelevitz, D., Biancardi, A. M., Bland, P. H., Brown, M. S., Engelmann, R. M., Laderach, G. E., ... Clarke, L. P. (2011). The Lung Image Database Consortium (LIDC) and Image Database Resource Initiative (IDRI): A Completed Reference Database of Lung Nodules on CT Scans. *Medical Physics*, *38*(2), 915–931. doi:10.1118/1.3528204 PMID:21452728

Arteaga-Arteaga, H. B., Mora-Rubio, A., Florez, F., Murcia-Orjuela, N., Diaz-Ortega, C. E., Orozco-Arias, S., delaPava, M., Bravo-Ortíz, M. A., Robinson, M., Guillen-Rondon, P., & Tabares-Soto, R. (2021). Machine learning applications to predict two-phase flow patterns. *PeerJ. Computer Science*, *7*, e798. doi:10.7717/peerj-cs.798 PMID:34909465

Aslan, M. F., Unlersen, M. F., Sabanci, K., & Durdu, A. (2021). CNN-based transfer learning–BiLSTM network: A novel approach for COVID-19 infection detection. *Applied Soft Computing*, *98*(106912), 106912. Advance online publication. doi:10.1016/j.asoc.2020.106912 PMID:33230395

Assery, N., Xiaohong, Y., Almalki, S., Kaushik, R., & Xiuli, Q. (2019). Comparing learning-based methods for identifying disaster-related tweets. *Proc. 18th IEEE Int. Conf. Mach. Learn. Appl. (ICMLA)*, 1829–1836.

Avendi, M. R., Kheradvar, A., & Jafarkhani, H. (2016). A combined deep-learning and deformable-model approach to fully automatic segmentation of the left ventricle in cardiac MRI. *Medical Image Analysis*, *30*, 108–119. doi:10.1016/j.media.2016.01.005 PMID:26917105

Azad, M., Khaled, F., & Pavel, M. I. (2019). A novel approach to classify and convert 1D signal to 2D grayscale image implementing support vector machine and empirical mode decomposition algorithm. *International Journal of Advanced Research*, *7*(1), 328–335. https://doi.org/10.21474/ijar01/8331

Baamonde, S., de Moura, J., Novo, J., Charlón, P., & Ortega, M. (2019a). Automatic identification and characterization of the epiretinal membrane in OCT images. *Biomedical Optics Express*, *10*(8), 4018. doi:10.1364/BOE.10.004018 PMID:31452992

Baamonde, S., de Moura, J., Novo, J., Charlón, P., & Ortega, M. (2019b). Automatic Identification and Intuitive Map Representation of the Epiretinal Membrane Presence in 3D OCT Volumes. *Sensors (Basel)*, *19*(23), 5269. doi:10.339019235269 PMID:31795480

Baamonde, S., de Moura, J., Novo, J., & Ortega, M. (2017a). Automatic Detection of Epiretinal Membrane in OCT Images by Means of Local Luminosity Patterns. In I. Rojas, G. Joya, & A. Catala (Eds.), *Advances in Computational Intelligence* (pp. 222–235). Springer International Publishing. doi:10.1007/978-3-319-59153-7_20

Baamonde, S., de Moura, J., Novo, J., Rouco, J., & Ortega, M. (2017b). Feature Definition and Selection for Epiretinal Membrane Characterization in Optical Coherence Tomography Images. In *Image Analysis and Processing - ICIAP 2017* (pp. 456–466). Springer International Publishing. doi:10.1007/978-3-319-68548-9_42

Baker, S. B., Xiang, W., & Atkinson, I. (2017). Internet of Things for Smart Healthcare: Technologies, Challenges, and Opportunities. *IEEE Access: Practical Innovations, Open Solutions*, *5*, 26521–26544. doi:10.1109/ACCESS.2017.2775180

Bank, D., Koenigstein, N., & Giryes, R. (2021, April 3). *Autoencoders*. Retrieved November 19, 2021, from https://arxiv.org/abs/2003.05991

Basu, S., Mitra, S., & Saha, N. (2020). Deep Learning for Screening COVID-19 using Chest X-Ray Images. *2020 IEEE Symposium Series on Computational Intelligence (SSCI)*, 2521–2527. 10.1109/SSCI47803.2020.9308571

Bawankar, P., Shanbhag, N., K, S. S., Dhawan, B., Palsule, A., Kumar, D., Chandel, S., & Sood, S. (2017). Sensitivity and specificity of automated analysis of single-field non-mydriatic fundus photographs by Bosch DR Algorithm—Comparison with mydriatic fundus photography (ETDRS) for screening in undiagnosed diabetic retinopathy. *PLoS One*, *12*(12), e0189854. doi:10.1371/journal.pone.0189854 PMID:29281690

Beede, E., Baylor, E., Hersch, F., Iurchenko, A., Wilcox, L., & Ruamviboonsuk, P., & Vardoulakis, L. M. (2020). A human-centered evaluation of a deep learning system deployed in clinics for the detection of diabetic retinopathy. *Proceedings of the 2020 CHI Conference on Human Factors in Computing Systems*. 10.1145/3313831.3376718

Bekhet, S., Alkinani, M. H., Tabares-Soto, R., & Hassaballah, M. (2021). An efficient method for COVID-19 detection using light weight convolutional neural network. *Computers*. *Materials and Continua*, *69*(2), 2475–2491. doi:10.32604/cmc.2021.018514

Berrahal, M., & Azizi, M. (2021). Augmented binary multi-labeled CNN for practical facial attribute classification. *Indonesian Journal of Electrical Engineering and Computer Science*, *23*(2), 973. https://doi.org/10.11591/ijeecs.v23.i2.pp973-979

Bharadwaj, H. K., Agarwal, A., Chamola, V., Lakkaniga, N. R., Hassija, V., Guizani, M., & Sikdar, B. (2021). A Review on the Role of Machine Learning in Enabling IoT Based Healthcare Applications. *IEEE Access: Practical Innovations, Open Solutions*, *9*, 38859–38890. doi:10.1109/ACCESS.2021.3059858

Bhardwaj, R., Nambiar, A. R., & Dutta, D. (2017). *A Study of Machine Learning in Healthcare*. IEEE. doi:10.1109/COMPSAC.2017.164

Bhaskaranand, M., Ramachandra, C., Bhat, S., Cuadros, J., Nittala, M., Sadda, S., & Solanki, K. (2016). Automated Diabetic Retinopathy Screening and Monitoring Using Retinal Fundus Image Analysis. *Journal of Diabetes Science and Technology*, *10*(2), 254–261. doi:10.1177/1932296816628546 PMID:26888972

Compilation of References

Billingsley, P. (1999). Convergence of probability measures (2nd ed.). Wiley-Interscience Publication. doi:10.1002/9780470316962

BIMCV. (2020). BIMCV-COVID19 – BIMCV. *Soon*. https://bimcv.cipf.es/bimcv-projects/bimcv-COVID19/#1590859488150-148be708-c3f3

Blain, M., Kassin, M. T., Varble, N., Wang, X., Xu, Z., Xu, D., Carrafiello, G., Vespro, V., Stellato, E., Ierardi, A. M., Di Meglio, L., Suh, R. D., Walker, S. A., Xu, S., Sanford, T. H., Turkbey, E. B., Harmon, S., Turkbey, B., & Wood, B. J. (2021). Determination of disease severity in COVID-19 patients using deep learning in chest x-ray images. *Diagnostic and Interventional Radiology*, *27*(1), 20–27. doi:10.5152/dir.2020.20205 PMID:32815519

Bogaerts, K., Komárek, A., & Lesaffre, E. (2018). *Survival analysis with interval-censored data: A practical approach with examples in R, SAS and BUGS*. CRC Press.

Borrelli, E., Sarraf, D., Freund, K. B., & Sadda, S. R. (2018, November). OCT angiography and evaluation of the choroid and choroidal vascular disorders. *Progress in Retinal and Eye Research*, *67*, 30–55. doi:10.1016/j.preteyeres.2018.07.002 PMID:30059755

Borthakur, D., Dubey, H., Constant, N., Mahler, L., & Mankodiya, K. (2017). Smart fog: Fog computing framework for unsupervised clustering analytics in wearable internet of things. *2017 IEEE Global Conference on Signal and Information Processing (GlobalSIP)*, 472–476. 10.1109/GlobalSIP.2017.8308687

Bradley, A. P. (1997). The use of the area under the ROC curve in the evaluation of machine learning algorithms. *Pattern Recognition*, *30*(7), 1145–1159. https://doi.org/10.1016/s0031-3203(96)00142-2

Bravo Ortíz, M. A., Arteaga Arteaga, H. B., Tabares Soto, R., Padilla Buriticá, J. I., & Orozco-Arias, S. (2021). Cervical cancer classification using convolutional neural networks, transfer learning and data augmentation. *Revista EIA*, *18*(35), 1–12. doi:10.24050/reia.v18i35.1462

Breiding, M. J. (2009). Radiation Dose Associated with Common Computed Tomography Examinations and the Associated Lifetime Attributable Risk of Cancer. *Archives of Internal Medicine*, *63*(169(22)), 2078–2086. doi:10.1001/archinternmed.2009.427.Radiation PMID:20008690

Brigham, E. O., & Morrow, R. E. (1967). The fast fourier transform. *IEEE Spectrum*, *4*(12), 63–70. https://doi.org/10.1109/mspec.1967.5217220

Browning, D. (2004). Comparison of the clinical diagnosis of diabetic macular edema with diagnosis by optical coherence tomography*1. *Ophthalmology*, *111*(4), 712–715. doi:10.1016/j.ophtha.2003.06.028 PMID:15051203

Brownlee, J. (2019, July 5). *A gentle introduction to pooling layers for Convolutional Neural Networks*. Machine Learning Mastery. Retrieved November 19, 2021, from https://machinelearningmastery.com/pooling-layers-for-convolutional-neural-networks/

287

Brownlee, J. (2020, April 16). *How do convolutional layers work in Deep Learning Neural Networks?* Machine Learning Mastery. Retrieved October 15, 2021, from https://machinelearningmastery.com/convolutional-layers-for-deep-learning-neural-networks/

Burlina, P., Pacheco, K. D., Joshi, N., Freund, D. E., & Bressler, N. M. (2017). Comparing humans and deep learning performance for grading AMD: A study in using universal deep features and transfer learning for automated AMD analysis. *Computers in Biology and Medicine*, *82*, 80–86. doi:10.1016/j.compbiomed.2017.01.018 PMID:28167406

Burton, R. J., Albur, M., Eberl, M., & Cuff, S. M. (2019). Using artificial intelligence to reduce diagnostic workload without compromising detection of urinary tract infections. *BMC Medical Informatics and Decision Making*, *19*(1), 171. Advance online publication. doi:10.118612911-019-0878-9 PMID:31443706

Bustos, A., Pertusa, A., Salinas, J. M., & de la Iglesia-Vayá, M. (2020). PadChest: A large chest x-ray image dataset with multi-label annotated reports. *Medical Image Analysis*, *66*, 101797. doi:10.1016/j.media.2020.101797 PMID:32877839

Calabuig, J. M., García-Raffi, L. M., García-Valiente, A., & Sánchez-Pérez, E. A. (2021). Kaplan-Meier Type Survival Curves for COVID-19: A Health Data Based Decision-Making Tool. *Frontiers in Public Health*. Advance online publication. doi:10.3389/fpubh.2021.646863

Carrio, A., Sampedro, C., Rodriguez-Ramos, A., & Campoy, P. (2017). *A review of deep learning methods and applications for unmanned aerial vehicles*. *Hindawi Journal of Sensors*. doi:10.1155/2017/3296874

Castiglioni, I., Ippolito, D., Interlenghi, M., Monti, C. B., Salvatore, C., Schiaffino, S., Polidori, A., Gandola, D., Messa, C., & Sardanelli, F. (2021). Machine learning applied on chest x-ray can aid in the diagnosis of COVID-19: A first experience from Lombardy, Italy. *European Radiology Experimental*, *5*(1), 7. Advance online publication. doi:10.118641747-020-00203-z PMID:33527198

Chakraborty, C., Banerjee, A., Kolekar, M. H., & Garg, L. (2021). *Internet of Things for Healthcare Technologies*. Springers. doi:10.1007/978-981-15-4112-4

Chen, X. A., Grossman, T., Wigdor, D. J., & Fitzmaurice, G. (2014). Duet: Exploring joint interactions on a smart phone and a smart watch. In The SIGCHI conference on human factors in computing systems (pp. 159–168). ACM.

Cheng, J.-Z., Ni, D., Chou, Y.-H., Qin, J., Tiu, C.-M., Chang, Y.-C., Huang, C.-S., Shen, D., & Chen, C.-M. (2016, April). Computer-Aided Diagnosis with Deep Learning Architecture: Applications to Breast Lesions in US Images and Pulmonary Nodules in CT Scans. *Scientific Reports*, *6*(1), 24454. Advance online publication. doi:10.1038rep24454 PMID:27079888

Chollet, F. (2017). Xception: Deep learning with depthwise separable convolutions. *Proceedings - 30th IEEE Conference on Computer Vision and Pattern Recognition, CVPR 2017*, 1800–1807. 10.1109/CVPR.2017.195

Compilation of References

Ciotti, M., Ciccozzi, M., Terrinoni, A., Jiang, W.-C., Wang, C.-B., & Bernardini, S. (2020). The COVID-19 pandemic. *Critical Reviews in Clinical Laboratory Sciences*, *57*(6), 365–388. doi:1 0.1080/10408363.2020.1783198 PMID:32645276

Commandeur, F., Goeller, M., Betancur, J., Cadet, S., Doris, M., Chen, X., Berman, D. S., Slomka, P. J., Tamarappoo, B. K., & Dey, D. (2018). Deep learning for quantification of epicardial and thoracic adipose tissue from Non-Contrast CT. *IEEE Transactions on Medical Imaging*, *37*(8), 1835–1846. doi:10.1109/TMI.2018.2804799 PMID:29994362

Coronavirus Resource Center, Johns Hopkins. (2020). COVID-19 Dashboard by the Center for Systems Science and Engineering (CSSE) at John Hopkins University. ArcGIS Dashboards.

Cortes, C., & Vapnik, V. (1995). Support vector machine. *Machine Learning*, *20*(3), 273–297. doi:10.1007/BF00994018

Cox, D. R. (1972). Regression models and life-tables. *Journal of the Rroyal Statistical Society, Series B,* (34), 187-220.

Creswell, A., White, T., Dumoulin, V., Arulkumaran, K., Sengupta, B., & Bharath, A. A. (2018). Generative adversarial networks: An overview. *IEEE Signal Processing Magazine*, *35*(1), 53–65. doi:10.1109/MSP.2017.2765202

Culurciello, E. (2018, December 24). *Navigating the unsupervised learning landscape*. Medium. Retrieved November 19, 2021, from https://medium.com/intuitionmachine/navigating-the-unsupervised-learning-landscape-951bd5842df9#:~:text=Unsupervised%20learning%20is%20the%20Holy,be%20trained%20with%20little%20data.&text=Today%20Deep%20Learning%20models%20are,there%20is%20a%20corresponding%20label

Dailla, M., Kaur, P., & Dhawan, V. (2014). Adaptive Gamma Correction With Weighted Distribution And Recursively Separated And Weighted Histogram Equalization: A Comparative Study. *International Journal of Engineering Research & Technology (Ahmedabad)*, *3*(8), 129–133.

Darcy, A. M., Louie, A. K., & Roberts, L. W. (2016). Machine Learning and the Profession of Medicine. *Journal of the American Medical Association*, *315*(6), 551. doi:10.1001/jama.2015.18421 PMID:26864406

Das, D., Santosh, K. C., & Pal, U. (2020). Truncated inception net: COVID-19 outbreak screening using chest X-rays. *Physical and Engineering Sciences in Medicine*, *43*(3), 915–925. doi:10.100713246-020-00888-x PMID:32588200

De Moura, J., Novo, J., & Ortega, M. (2020). Fully automatic deep convolutional approaches for the analysis of Covid-19 using chest X-ray images. MedRxiv. doi:10.1101/2020.05.01.20087254

De Moura, J., Garcia, L. R., Vidal, P. F. L., Cruz, M., Lopez, L. A., Lopez, E. C., Novo, J., & Ortega, M. (2020). Deep Convolutional Approaches for the Analysis of COVID-19 Using Chest X-Ray Images From Portable Devices. *IEEE Access: Practical Innovations, Open Solutions*, *8*, 195594–195607. doi:10.1109/ACCESS.2020.3033762 PMID:34786295

de Moura, J., Novo, J., & Ortega, M. (2019). Deep Feature Analysis in a Transfer Learning-based Approach for the Automatic Identification of Diabetic Macular Edema. In *2019 International Joint Conference on Neural Networks (IJCNN)* (pp. 1-8). Institute of Electrical and Electronics Engineer. 10.1109/IJCNN.2019.8852196

de Moura, J., Novo, J., Ortega, M., & Charlón, P. (2016). 3D retinal vessel tree segmentation and reconstruction with OCT images. In *Image Analysis and Recognition* (pp. 716–726). Lecture Notes in Computer Science. Springer. doi:10.1007/978-3-319-41501-7_80

de Moura, J., Novo, J., Rouco, J., Penedo, M. G., & Ortega, M. (2017). *Automatic detection of blood vessels in retinal OCT images*. International Work-Conference on the Interplay Between Natural and Artificial Computation. doi:10.1007/978-3-319-59773-7_1

de Moura, J., Samagaio, G., Novo, J., Almuina, P., Fernández, M. I., & Ortega, M. (2020, June). Joint Diabetic Macular Edema Segmentation and Characterization in OCT Images. *Journal of Digital Imaging*, *33*(5), 1335–1351. doi:10.100710278-020-00360-y PMID:32562127

de Moura, J., Vidal, P. L., Novo, J., Rouco, J., & Ortega, M. (2017). Feature definition, analysis and selection for cystoid region characterization in Optical Coherence Tomography. In *Knowledge-Based and Intelligent Information & Engineering Systems: Proceedings of the 21st International Conference* (pp. 1369-1377). Elsevier. 10.1016/j.procs.2017.08.043

Dempster, A. P., Laird, N. M., & Rubin, D. B. (1977). Maximum Likelihood from Incomplete Data via the EM Algorithm. *Journal of the Royal Statistical Society. Series B. Methodological*, *39*(1), 1–38. doi:10.1111/j.2517-6161.1977.tb01600.x

Desai, S., Baghal, A., Wongsurawat, T., Jenjaroenpun, P., Powell, T., Al-Shukri, S., Gates, K., Farmer, P., Rutherford, M., Blake, G., Nolan, T., Sexton, K., Bennett, W., Smith, K., Syed, S., & Prior, F. (2020). Chest imaging representing a COVID-19 positive rural U.S. population. *Scientific Data*, *7*(1), 414. doi:10.103841597-020-00741-6 PMID:33235265

Dey, N., Zhang, Y. D., Rajinikanth, V., Pugalenthi, R., & Raja, N. S. M. (2021). Customized VGG19 Architecture for Pneumonia Detection in Chest X-Rays. *Pattern Recognition Letters*, *143*, 67–74. doi:10.1016/j.patrec.2020.12.010

Dhillon & Singh. (2019). *Machine Learning in Healthcare Data Analysis: A Survey*. doi:10.15412/J.JBTW.01070206

Diabetic retinopathy. (2021). Retrieved 17 November 2021, from https://www.aoa.org/healthy-eyes/eye-and-vision-conditions/diabetic-retinopathy?sso=y

Diller, G.-P., Babu-Narayan, S., Li, W., Radojevic, J., Kempny, A., Uebing, A., Dimopoulos, K., Baumgartner, H., Gatzoulis, M. A., & Orwat, S. (2019). Utility of machine learning algorithms in assessing patients with a systemic right ventricle. *European Heart Journal Cardiovascular Imaging*, *20*(8), 925–931. doi:10.1093/ehjci/jey211 PMID:30629127

Compilation of References

Dimas, S. R. D., Negara, B. S., Sanjaya, S., & Satria, E. (2021). COVID-19 Classification for Chest X-Ray Images using Deep Learning and Resnet-101. *International Congress of Advanced Technology and Engineering, ICOTEN 2021*, 21–24. 10.1109/ICOTEN52080.2021.9493431

Dodge, Y. (2008). The Concise Encyclopedia of Statistics. Springer Science + Business Media.

Doi, K. (2007). Computer-aided diagnosis in medical imaging: Historical Review, current status and future potential. *Computerized Medical Imaging and Graphics*, *31*(4-5), 198–211. doi:10.1016/j.compmedimag.2007.02.002 PMID:17349778

Donsker, M. D. (1952). Justification and extension of Doob's heuristic approach to the Kolmogorov-Smirnov theorems. *Annals of Mathematical Statistics*, *23*, 277-281. Doi:10.1214/aoms/1177729445

Dorsemaine, B., Gaulier, J.-P., Wary, J.-P., Kheir, N., & Urien, P. (2015). Internet of Things: a definition & taxonomy. In *9th International Conference on Next Generation Mobile Applications, Services and Technologies*. IEEE.

dos Santos, C. F. G., Passos, L. A., de Santana, M. C., & Papa, J. P. (2021). Normalizing images is good to improve computer-assisted COVID-19 diagnosis. *Data Science for COVID-19*, 51–62. doi:10.1016/B978-0-12-824536-1.00033-2

Dragorad, M. O., & Zoran, B. (2017). *Cloud-based IoT healthcare applications: Requirements and recommendations. International Journal of Internet of Things and Web Services*.

Durga, & Nag, & Daniel. (2019). Survey on Machine Learning and Deep Learning Algorithms used in Internet of Things (IoT) Healthcare. *IEEE Access: Practical Innovations, Open Solutions*.

Du, X., Song, Y., Liu, Y., Zhang, Y., Liu, H., Chen, B., & Li, S. (2020). An integrated deep learning framework for joint segmentation of Blood Pool and myocardium. *Medical Image Analysis*, *62*, 101685. doi:10.1016/j.media.2020.101685 PMID:32272344

Dvoretzky, A., Kiefer, J., & Wolfowitz, J. (1956). Asymptotic minimax character of the sample distribution function and of the classical multinomial estimator. *Annals of Mathematical Statistics*, *27*(3), 642–669. doi:10.1214/aoms/1177728174

Education, I. (2021). *What is Artificial Intelligence (AI)?* Retrieved 17 November 2021, from https://www.ibm.com/cloud/learn/what-is-artificial-intelligence

Eesa, A. S., & Arabo, W. K. (2017). A Normalization Methods for Backpropagation: A Comparative Study. *Science Journal of University of Zakho*, *5*(4), 319–323. doi:10.25271/2017.5.4.381

El Omary, S., Lahrache, S., & El Ouazzani, R. (2021). Detecting heart failure from chest X-ray images using deep learning algorithms. *2021 3rd IEEE Middle East and North Africa COMMunications Conference (MENACOMM)*. 10.1109/MENACOMM50742.2021.9678291

Elandt-Johnson, R. C., & Johnson, N. L. (1980). *Survival models and data analysis*. Wiley-Interscience.

Elfatih, N. M., Hasan, M. K., Kamal, Z., Gupta, D., Saeed, R. A., Ali, E. S., & Hosain, M. S. (2021). Internet of vehicle's resource management in 5G networks using AI technologies: Current status and trends. *IET Communications*, 1–21.

Elkorany, A. S., & Elsharkawy, Z. F. (2021). COVIDetection-Net: A tailored COVID-19 detection from chest radiography images using deep learning. *Optik (Stuttgart)*, *231*(January), 1–10. doi:10.1016/j.ijleo.2021.166405 PMID:33551492

Elmustafa & Ahmed. (2021). Algorithms Optimization for Intelligent IoV Applications. In Handbook of Research on Innovations and Applications of AI, IoT, and Cognitive Technologies. IGI Global. doi:10.4018/978-1-7998-6870-5.ch001

Emad, O., Yassine, I. A., & Fahmy, A. S. (2015). Automatic localization of the left ventricle in cardiac MRI images using Deep Learning. *2015 37th Annual International Conference of the IEEE Engineering in Medicine and Biology Society (EMBC)*. 10.1109/EMBC.2015.7318454

Emura, T., & Chen, Y.-H. (2018). Analysis of Survival Data with Dependent Censoring: Copula-Based Approaches. Springer. doi:10.1007/978-981-10-7164-5

Ernesto, P. E., & Lusmeralis, A.-A. (2021). Assessing the impact of vaccination in a COVID-19 compartmental model. *Informatics in Medicine Unlocked*. https://www.sciencedirect.com/science/article/pii/S2352914821002641

Essa, Y. M., Attiya, G., El-Sayed, A., & ElMahalawy, A. (2018). Data processing platforms for electronic health records. *Health and Technology*, *8*(4), 271–280. doi:10.100712553-018-0219-5

Esteva, A., Chou, K., Yeung, S., Naik, N., Madani, A., Mottaghi, A., Liu, Y., Topol, E., Dean, J., & Socher, R. (2021, January 8). *Deep learning-enabled Medical Computer Vision*. Nature News. Retrieved November 19, 2021, from https://www.nature.com/articles/s41746-020-00376-2

Explorium. (2021, July 11). *Unsupervised learning wiki*. Retrieved November 19, 2021, from https://www.explorium.ai/wiki/unsupervised-learning/

Fang, L., Yang, L., Li, S., Rabbani, H., Liu, Z., Peng, Q., & Chen, X. (2017, June). Automatic detection and recognition of multiple macular lesions in retinal optical coherence tomography images with multi-instance multilabel learning. *Journal of Biomedical Optics*, *22*(6), 066014. doi:10.1117/1.JBO.22.6.066014 PMID:28655052

Fei, C., Liu, R., Li, Z., Wang, T., & Baig, F. N. (2021). *Machine and Deep Learning Algorithms for Wearable Health Monitoring*. Springer. doi:10.1007/978-3-030-68723-6_6

Fernández, A., Ortega, M., de Moura, J., Novo, J., & Penedo, M. G. (2018, June). Detection of reactions to sound via gaze and global eye motion analysis using camera streaming. *Machine Vision and Applications*, *29*(7), 1069–1082. doi:10.100700138-018-0952-9

Ferris, F. L. III, Wilkinson, C. P., Bird, A., Chakravarthy, U., Chew, E., Csaky, K., & Sadda, S. R. (2013). Clinical Classification of Age-related Macular Degeneration. *Ophthalmology*, *120*(4), 844–851. doi:10.1016/j.ophtha.2012.10.036 PMID:23332590

292

Compilation of References

Fiszman, M., Chapman, W. W., Aronsky, D., Evans, R. S., & Haug, P. J. (2000). Automatic detection of acute bacterial pneumonia from chest X-ray reports. *Journal of the American Medical Informatics Association: JAMIA*, *7*(6), 593–604. doi:10.1136/jamia.2000.0070593 PMID:11062233

Flach, P. A., Lach, P. E. F., & Ac, B. (2003). *The Geometry of ROC Space : Understanding Machine Learning Metrics through ROC Isometrics*. Academic Press.

Fong, D., Aiello, L., Ferris, F. III, & Klein, R. (2004). Diabetic Retinopathy. *Diabetes Care*, *27*(10), 2540–2553. doi:10.2337/diacare.27.10.2540 PMID:15451934

Gadkari, S. S. (2018). Diabetic retinopathy screening: Telemedicine, the way to go! *Indian Journal of Ophthalmology*. Retrieved from https://pubmed.ncbi.nlm.nih.gov/29380754/

Gawlik, K., Hausser, F., Paul, F., Brandt, A. U., & Kadas, E. M. (2018, December). Active contour method for ILM segmentation in ONH volume scans in retinal OCT. *Biomedical Optics Express*, *9*(12), 6497–6518. doi:10.1364/BOE.9.006497 PMID:31065445

Gende, M., Moura, J. D., Novo, J., Charlon, P., & Ortega, M. (2021). Automatic Segmentation and Intuitive Visualisation of the Epiretinal Membrane in 3D OCT Images Using Deep Convolutional Approaches. *IEEE Access: Practical Innovations, Open Solutions*, *9*, 75993–76004. doi:10.1109/ACCESS.2021.3082638

Ghassemi, M., Naumann, T., Schulam, P., Beam, A. L., Chen, I. Y., & Ranganath, R. A. (2020). Review of Challenges and Opportunities in Machine Learning for Health. *AMIA Joint Summits on Translational Science Proceedings AMIA Summit on Translational Science*, *2020*, 191–200. PMID:32477638

Ghazi, N. G., Ciralsky, J. B., Shah, S. M., Campochiaro, P. A., & Haller, J. A. (2007). Optical coherence tomography findings in persistent diabetic macular edema: The vitreomacular interface. *American Journal of Ophthalmology*, *144*(5), 747–754. doi:10.1016/j.ajo.2007.07.012 PMID:17869207

Godi, Viswanadham, Muttipati, Samantray, & Gadiraju. (2020). E-Healthcare Monitoring System using IoT with Machine Learning Approaches. *IEEE Xplore.*

Gonçalves, L., Novo, J., Cunha, A., & Campilho, A. (2017). Learning Lung Nodule Malignancy Likelihood from Radiologist Annotations or Diagnosis Data. *Journal of Medical and Biological Engineering*, *38*(3), 424–442. Advance online publication. doi:10.100740846-017-0317-2

Goodfellow, I., Pouget-Abadie, J., Mirza, M., Xu, B., Warde-Farley, D., Ozair, S., Courville, A., & Bengio, Y. (2020). Generative adversarial networks. *Communications of the ACM*, *63*(11), 139–144. doi:10.1145/3422622

Gopal, S., Patro, K., & Kumar Sahu, K. (2015). Normalization: A Preprocessing Stage. *International Advanced Research Journal in Science*. *Engineering and Technology*, *2*, 20–22. Advance online publication. doi:10.17148/IARJSET.2015.2305

293

Gope, P., & Hwang, T. (2015). Bsn-care: A secure IoT-based modern healthcare system using body sensor network. *IEEE Sensors Journal*, *16*(5), 1368–1376. doi:10.1109/JSEN.2015.2502401

Goyal, S., & Singh, R. (2021). Detection and classification of lung diseases for pneumonia and COVID-19 using machine and deep learning techniques. *Journal of Ambient Intelligence and Humanized Computing*. Advance online publication. doi:10.100712652-021-03464-7 PMID:34567277

Graham-Rowe, E., Lorencatto, F., Lawrenson, J. G., Burr, J. M., Grimshaw, J. M., Ivers, N. M., Presseau, J., Vale, L., Peto, T., Bunce, C., & Francis, J. (2018). Barriers to and enablers of diabetic retinopathy screening attendance: A systematic review of published and Grey Literature. *Diabetic Medicine*, *35*(10), 1308–1319. doi:10.1111/dme.13686 PMID:29790594

Green, M., Marom, E. M., Konen, E., Kiryati, N., & Mayer, A. (2018). 3-D neural denoising for low-dose coronary CT angiography (CCTA). *Computerized Medical Imaging and Graphics*, *70*, 185–191. doi:10.1016/j.compmedimag.2018.07.004 PMID:30093171

Grossi, E., & Buscema, M. (2007). Introduction to artificial neural networks. *European Journal of Gastroenterology & Hepatology*, *19*(12), 1046–1054. doi:10.1097/MEG.0b013e3282f198a0 PMID:17998827

Grzybowski, A., Brona, P., Lim, G., Ruamviboonsuk, P., Tan, G., Abramoff, M., & Ting, D. (2019). Artificial intelligence for diabetic retinopathy screening: A review. *Eye (London, England)*, *34*(3), 451–460. doi:10.103841433-019-0566-0 PMID:31488886

Guan, W., Ni, Z., Hu, Y. W., Liang, C., Ou, J., He, L., Liu, H., Shan, C., Lei, D. S. C., Hui, B., Du, L., Li, G., Zeng, K., Yuen, R., Chen, C., Tang, T., Wang, P., Chen, J., Xiang, S., … Zhong, N. (2020). Clinical Characteristics of Coronavirus Disease 2019 in China. The Journal of Emergency Medicine, 58(4), 711–712. doi:10.1016/j.jemermed.2020.04.004

Güler, İ., & Übeylı´, E. D. (2005). ECG beat classifier designed by combined neural network model. *Pattern Recognition*, *38*(2), 199–208. https://doi.org/10.1016/j.patcog.2004.06.009

Gulshan, V., Peng, L., Coram, M., Stumpe, M., Wu, D., Narayanaswamy, A., Venugopalan, S., Widner, K., Madams, T., Cuadros, J., Kim, R., Raman, R., Nelson, P. C., Mega, J. L., & Webster, D. R. (2016). Development and Validation of a Deep Learning Algorithm for Detection of Diabetic Retinopathy in Retinal Fundus Photographs. *Journal of the American Medical Association*, *316*(22), 2402. doi:10.1001/jama.2016.17216 PMID:27898976

Gülsün, M. A., Funka-Lea, G., Sharma, P., Rapaka, S., & Zheng, Y. (2016). Coronary centerline extraction via optimal flow paths and CNN path pruning. *Lecture Notes in Computer Science*, *9902*, 317–325. doi:10.1007/978-3-319-46726-9_37

Hacihaliloglu, I. (2018). Localization of bone surfaces from ultrasound data using local phase information and signal transmission maps. Lecture Notes in Computer Science, 10734, 1–11. doi:10.1007/978-3-319-74113-0_1

294

Compilation of References

Hadjem, M., & Nait-Abdesselam, F. (2015). An ECG T-wave anomalies detection using a lightweight classification model for WIRELESS body sensors. *2015 IEEE International Conference on Communication Workshop (ICCW)*. 10.1109/ICCW.2015.7247191

Hamet, P., & Tremblay, J. (2017). Artificial Intelligence in medicine. *Metabolism: Clinical and Experimental*, *69*, S36–S40. Advance online publication. doi:10.1016/j.metabol.2017.01.011 PMID:28126242

Han, C., Kitamura, Y., Kudo, A., Ichinose, A., Rundo, L., Furukawa, Y., Umemoto, K., Li, Y., & Nakayama, H. (2019). Synthesizing Diverse Lung Nodules Wherever Massively: 3D Multi-Conditional GAN-Based CT Image Augmentation for Object Detection. *2019 International Conference on 3D Vision (3DV),* 729–737. 10.1109/3DV.2019.00085

Hannun, A. Y., Rajpurkar, P., Haghpanahi, M., Tison, G. H., Bourn, C., Turakhia, M. P., & Ng, A. Y. (2019). Cardiologist-level arrhythmia detection and classification in ambulatory electrocardiograms using a deep neural network. *Nature Medicine*, *25*(1), 65–69. doi:10.103841591-018-0268-3 PMID:30617320

Hans, C. van H., & Hein, P. (2012). *Dynamic prediction in clinical survival analysis*. CRC Press.

Hansen, M., Abràmoff, M., Folk, J., Mathenge, W., Bastawrous, A., & Peto, T. (2015). Results of Automated Retinal Image Analysis for Detection of Diabetic Retinopathy from the Nakuru Study, Kenya. *PLoS One*, *10*(10), e0139148. doi:10.1371/journal.pone.0139148 PMID:26425849

Harouni, M., & Baghmaleki, H. Y. (2021). Color Image Segmentation Metrics. Encyclopedia of Image Processing, 121–139. doi:10.1201/9781351032742-16

Hatipoglu, B., Yilmaz, C. M., & Kose, C. (2018). A signal-to-image transformation approach for EEG and Meg Signal Classification. *Signal, Image and Video Processing*, *13*(3), 483–490. https://doi.org/10.1007/s11760-018-1373-y

Hayden, G. E., & Wrenn, K. W. (2009). Chest radiograph vs. Computed tomography scan in the evaluation for pneumonia. *The Journal of Emergency Medicine*, *36*(3), 266–270. doi:10.1016/j.jemermed.2007.11.042 PMID:18571356

Hee, M. R. (1995, August). Quantitative Assessment of Macular Edema With Optical Coherence Tomography. *Archives of Ophthalmology*, *113*(8), 1019. doi:10.1001/archopht.1995.01100080071031 PMID:7639652

He, M., Li, Z., Liu, C., Shi, D., & Tan, Z. (2020). Deployment of artificial intelligence in real-world practice: Opportunity and challenge. *Asia-Pacific Journal of Ophthalmology*, *9*(4), 299–307. doi:10.1097/APO.0000000000000301 PMID:32694344

Hirschauer, T. J., Adeli, H., & Buford, J. A. (2015). Computer-Aided diagnosis of Parkinson's Disease Using Enhanced Probabilistic Neural Network. *Journal of Medical Systems*, *39*(11), 179. doi:10.100710916-015-0353-9 PMID:26420585

Hood, D. C. (2017, March). Improving our understanding, and detection, of glaucomatous damage: An approach based upon optical coherence tomography (OCT). *Progress in Retinal and Eye Research*, *57*, 46–75. doi:10.1016/j.preteyeres.2016.12.002 PMID:28012881

Horry, M. J., Chakraborty, S., Paul, M., Ulhaq, A., Pradhan, B., Saha, M., & Shukla, N. (2020). COVID-19 Detection Through Transfer Learning Using Multimodal Imaging Data. *IEEE Access: Practical Innovations, Open Solutions*, *8*, 149808–149824. doi:10.1109/ACCESS.2020.3016780 PMID:34931154

Hosny, A., Parmar, C., Quackenbush, J., Schwartz, L. H., & Aerts, H. J. (2018, May). Artificial intelligence in radiology. *Nature Reviews. Cancer*, *18*(8), 500–510. doi:10.103841568-018-0016-5 PMID:29777175

Hospitales, H. M. (2021). *COVID Data Save Lives*. https://www.hmhospitales.com/coronavirus/COVID-data-save-lives

Howard, J. (2019). Artificial intelligence: Implications for the future of work. *American Journal of Industrial Medicine*, *62*(11), 917–926. doi:10.1002/ajim.23037 PMID:31436850

Huang, D., Swanson, E. A., Lin, C. P., Schuman, J. S., Stinson, W. G., Chang, W., Hee, M. R., Flotte, T., Gregory, K., Puliafito, C. A., & Fujimoto, J. G. (1991). Optical Coherence Tomography. *Science*, *254*(5035), 1178–1181. doi:10.1126cience.1957169 PMID:1957169

Huang, G., Liu, Z., Van Der Maaten, L., & Weinberger, K. Q. (2017). Densely Connected Convolutional Networks. *2017 IEEE Conference on Computer Vision and Pattern Recognition (CVPR)*, 2261-2269. 10.1109/CVPR.2017.243

Huang, J., Chen, B., Yao, B., & He, W. (2019). ECG arrhythmia classification Using STFT-Based spectrogram and convolutional neural network. *IEEE Access: Practical Innovations, Open Solutions*, *7*, 92871–92880. https://doi.org/10.1109/access.2019.2928017

Huang, S. C., Cheng, F. C., & Chiu, Y. S. (2013). Efficient contrast enhancement using adaptive gamma correction with weighting distribution. *IEEE Transactions on Image Processing*, *22*(3), 1032–1041. doi:10.1109/TIP.2012.2226047 PMID:23144035

Hua, Y., Guo, J., & Zhao, H. (2015). Deep belief networks and Deep Learning. *Proceedings of 2015 International Conference on Intelligent Computing and Internet of Things*. 10.1109/ICAIOT.2015.7111524

Humphreys, M., Warlow, C., & McGowan, J. (2013). Arrhythmias and their management. *Nursing the Cardiac Patient,* 132–155. doi:10.1002/9781118785331.ch10

Hussain, E., Hasan, M., Rahman, M. A., Lee, I., Tamanna, T., & Parvez, M. Z. (2021). CoroDet: A deep learning based classification for COVID-19 detection using chest X-ray images. *Chaos, Solitons, and Fractals*, *142*, 110495. doi:10.1016/j.chaos.2020.110495 PMID:33250589

Hwang, W.-J., & Wen, K.-W. (1998). Fast kNN classification algorithm based on partial distance search. *Electronics Letters*, *34*(21), 2062–2063. doi:10.1049/el:19981427

Compilation of References

Imani, E., Pourreza, H.-R., & Banaee, T. (2015). Fully automated diabetic retinopathy screening using morphological component analysis. *Computerized Medical Imaging and Graphics*, *43*, 78–88. doi:10.1016/j.compmedimag.2015.03.004 PMID:25863517

Introduction to convolutional neural networks. (n.d.). Retrieved November 19, 2021, from https://cs.nju.edu.cn/wujx/paper/CNN.pdf

Irvin, J., Rajpurkar, P., Ko, M., Yu, Y., Ciurea-Ilcus, S., Chute, C., Marklund, H., Haghgoo, B., Ball, R., Shpanskaya, K., Seekins, J., Mong, D. A., Halabi, S. S., Sandberg, J. K., Jones, R., Larson, D. B., Langlotz, C. P., Patel, B. N., Lungren, M. P., & Ng, A. Y. (2019). CheXpert: A large chest radiograph dataset with uncertainty labels and expert comparison. *33rd AAAI Conference on Artificial Intelligence, AAAI 2019, 31st Innovative Applications of Artificial Intelligence Conference, IAAI 2019 and the 9th AAAI Symposium on Educational Advances in Artificial Intelligence, EAAI 2019*, 590–597. 10.1609/aaai.v33i01.3301590

Isin, A., & Ozdalili, S. (2017). Cardiac arrhythmia detection using deep learning. *Procedia Computer Science*, *120*, 268–275. doi:10.1016/j.procs.2017.11.238

Ismael, A. M., & Sengür, A. (2021). Deep learning approaches for COVID-19 detection based on chest X-ray images. *Expert Systems with Applications*, *164*(114054), 114054. Advance online publication. doi:10.1016/j.eswa.2020.114054 PMID:33013005

Jacobi, A., Chung, M., Bernheim, A., & Eber, C. (2020). Portable chest X-ray in coronavirus disease-19 (COVID-19): A pictorial review. *Clinical Imaging*, *64*, 35–42. doi:10.1016/j.clinimag.2020.04.001 PMID:32302927

Jaeger, S., Candemir, S., Antani, S., Wáng, Y.-X. J., Lu, P.-X., & Thoma, G. (2020). Two public chest X-ray datasets for computer-aided screening of pulmonary diseases. *Quantitative Imaging in Medicine and Surgery*, *4*(6), 475–477. doi:10.3978/j.issn.2223-4292.2014.11.20 PMID:25525580

Jaffe, G. J., & Caprioli, J. (2004, January). Optical coherence tomography to detect and manage retinal disease and glaucoma. *American Journal of Ophthalmology*, *137*(1), 156–169. doi:10.1016/S0002-9394(03)00792-X PMID:14700659

Jain, G., Mittal, D., Thakur, D., & Mittal, M. K. (2020). A deep learning approach to detect COVID-19 coronavirus with X-Ray images. *Biocybernetics and Biomedical Engineering*, *40*(4), 1391–1405. doi:10.1016/j.bbe.2020.08.008 PMID:32921862

Jaiswal, A. K., Tiwari, P., Kumar, S., Gupta, D., Khanna, A., & Rodrigues, J. J. P. C. (2019). Identifying pneumonia in chest X-rays: A deep learning approach. *Measurement*, *145*, 511–518. doi:10.1016/j.measurement.2019.05.076

Jakobsen, L. H., Andersson, T. M.-L., Biccler, J. L., Poulsen, L. Ø., Severinsen, M. T., El-Galaly, T. C., & Bøgsted, M. (2020). On estimating the time to statistical cure. *BMC Medical Research Methodology*, *20*(1), 71. Advance online publication. doi:10.118612874-020-00946-8 PMID:32216765

Jen, C.-H., Wang, C.-C., Jiang, B. C., Chu, Y.-H., & Chen, M.-S. (2021). Application of classification techniques on development an early-warning system for chronic illnesses. Expert Syst. Appl., 39(10), 8852–8858.

Jenkins, A., Joglekar, M., Hardikar, A., Keech, A., O'Neal, D., & Januszewski, A. (2015). Biomarkers in Diabetic Retinopathy. *The Review of Diabetic Studies; RDS*, *12*(1-2), 159–195. doi:10.1900/RDS.2015.12.159 PMID:26676667

Jiang, Jiang, Zhi, Dong, Li, Ma, Wang, Dong, Shen, & Wang. (2017). *Artificial intelligence in healthcare: past, present and future*. doi:10.1136/svn-2017-000101

Jiang, L., Wu, Z., Xu, X., Zhan, Y., Jin, X., Wang, L., & Qiu, Y. (2021). Opportunities and challenges of artificial intelligence in the medical field: Current application, emerging problems, and problem-solving strategies. *The Journal of International Medical Research*, *49*(3). Advance online publication. doi:10.1177/03000605211000157 PMID:33771068

Jigsaw Academy. (2021). *Deep Neural Network: An Easy Introduction for 2021*. Retrieved 17 November 2021, from https://www.jigsawacademy.com/blogs/ai-ml/deep-neural-network/

Jin, C., Feng, J., Wang, L., Yu, H., Liu, J., Lu, J., & Zhou, J. (2018). Left atrial appendage segmentation and quantitative assisted diagnosis of atrial fibrillation based on fusion of temporal-spatial information. *Computers in Biology and Medicine*, *96*, 52–68. doi:10.1016/j.compbiomed.2018.03.002 PMID:29547711

Jin, W., Dong, S., Dong, C., & Ye, X. (2021). Hybrid ensemble model for differential diagnosis between COVID-19 and common viral pneumonia by chest X-ray radiograph. *Computers in Biology and Medicine*, *131*(January), 104252. doi:10.1016/j.compbiomed.2021.104252 PMID:33610001

Jnanendra, P. S., Indrajit, S., Anasua, S., & Ujjwal, M. (2021). Machine learning integrated ensemble of feature selection methods followed by survival analysis for predicting breast cancer subtype specific miRNA biomarkers. *Computers in Biology and Medicine*, *131*. https://www.sciencedirect.com/science/article/pii/S001048252100038X PMID:33550016

Johnson, D. (2022, February 12). *Supervised vs unsupervised learning: Key differences*. Guru99. Retrieved February 16, 2022, from https://www.guru99.com/supervised-vs-unsupervised-learning.html

Jothi, Rashid, & Husain. (2015). Data Mining in Healthcare – A Review. Elsevier.

Jun, T., Nguyen, H.M., Kang, D., Kim, D., Kim, D., & Kim, Y. (2018). *ECG arrhythmia classification using a 2-D convolutional neural network*. ArXiv, abs/1804.06812.

Kamnitsas, K., Ledig, C., Newcombe, V. F., Simpson, J. P., Kane, A. D., Menon, D. K., Rueckert, D., & Glocker, B. (2017, February). Efficient multi-scale 3D CNN with fully connected CRF for accurate brain lesion segmentation. *Medical Image Analysis*, *36*, 61–78. doi:10.1016/j.media.2016.10.004 PMID:27865153

Compilation of References

Kandel, I., & Castelli, M. (2020). The effect of batch size on the generalizability of the Convolutional Neural Networks on a histopathology dataset. *ICT Express*, *6*(4), 312–315. doi:10.1016/j.icte.2020.04.010

Kang. (2018). *Recent Patient Health Monitoring Platforms Incorporating Internet of Things-Enabled Smart Devices*. Korean Continence Society.

Kanopoulos, N., Vasanthavada, N., & Baker, R. L. (1988). Design of an image edge detection filter using the Sobel operator. *IEEE Journal of Solid-State Circuits*, *23*(2), 358–367. doi:10.1109/4.996

Karakanis, S., & Leontidis, G. (2021). Lightweight deep learning models for detecting COVID-19 from chest X-ray images. *Computers in Biology and Medicine*, *130*(104181), 104181. Advance online publication. doi:10.1016/j.compbiomed.2020.104181 PMID:33360271

Karar, M. E., Hemdan, E. E.-D., & Shouman, M. A. (2020). Cascaded deep learning classifiers for computer-aided diagnosis of COVID-19 and pneumonia diseases in X-ray scans. *Complex & Intelligent Systems*, *7*(1), 235–247. doi:10.100740747-020-00199-4 PMID:34777953

Kashani, A. H., Chen, C.-L., Gahm, J. K., Zheng, F., Richter, G. M., Rosenfeld, P. J., Shi, Y., & Wang, R. K. (2017, September). Optical coherence tomography angiography: A comprehensive review of current methods and clinical applications. *Progress in Retinal and Eye Research*, *60*, 66–100. doi:10.1016/j.preteyeres.2017.07.002 PMID:28760677

Kass, M., Witkin, A., & Terzopoulos, D. (1988, January). Snakes: Active contour models. *International Journal of Computer Vision*, *1*(4), 321–331. doi:10.1007/BF00133570

Kaur, N., & Singh, E. H. (2016). Enhancement of Medical Images using Histogram Based Hybrid Technique. *International Journal of Advanced Engineering Management Science*, *2*(9). www.ijaems.com

Ke, Q., Liu, J., Bennamoun, M., An, S., Sohel, F., & Boussaid, F. (2018). Computer vision for human–machine interaction. *Computer Vision for Assistive Healthcare*, 127–145. doi:10.1016/B978-0-12-813445-0.00005-8

Kermany, D. S., Goldbaum, M., Cai, W., Valentim, C. C. S., Liang, H., Baxter, S. L., McKeown, A., Yang, G., Wu, X., Yan, F., Dong, J., Prasadha, M. K., Pei, J., Ting, M., Zhu, J., Li, C., Hewett, S., Dong, J., Ziyar, I., ... Zhang, K. (2018). Identifying Medical Diagnoses and Treatable Diseases by Image-Based Deep Learning. *Cell*, *172*(5), 1122–1131.e9. doi:10.1016/j.cell.2018.02.010 PMID:29474911

Ketkar, N. (2017). Stochastic Gradient Descent. In Deep Learning with Python: A Hands-on Introduction (pp. 113–132). Apress. doi:10.1007/978-1-4842-2766-4_8

Khalik, S. (2020). COVID-19 patients no longer infectious 11 days after getting sick, research shows. *The Straits Times-Singapore*. https://www.straitstimes.com/singapore/health/covid-19-patients-no-longer-infectious-11-days-after-getting-sick-research-shows

Khan, F., Rehman, A. U., Jan, M. A., & Rahman, I. U. (2019). efficient resource allocation for real time traffic in cognitive radio internet of things. *International Conference on Internet of Things (iThings),* 1143–1147.

Khan, A. I., Shah, J. L., & Bhat, M. M. (2020). CoroNet: A deep neural network for detection and diagnosis of COVID-19 from chest x-ray images. *Computer Methods and Programs in Biomedicine*, *196*, 105581. Advance online publication. doi:10.1016/j.cmpb.2020.105581 PMID:32534344

Khan, F., Rehman, A. U., Zheng, J., Jan, M. A., & Alam, M. (2019). Mobile crowd sensing: A survey on privacy-preservation, task management, assignment models, and incentives mechanisms. *Future Generation Computer Systems*, *100*, 456–472. doi:10.1016/j.future.2019.02.014

Kherraki, A., Maqbool, M., & El Ouazzani, R. (2021). Traffic scene semantic segmentation by using several deep convolutional neural networks. *2021 3rd IEEE Middle East and North Africa COMMunications Conference (MENACOMM)*. doi:10.1109/menacomm50742.2021.9678270

Kim, J., Hong, J., & Park, H. (2018, June). Prospects of deep learning for medical imaging. *Precision and Future Medicine*, *2*(2), 37–52. doi:10.23838/pfm.2018.00030

Kim, J., Lee, S., Lee, G., Park, Y., & Hong, Y. (2016). Using a method based on a modified K-means clustering and mean shift segmentation to reduce file sizes and detect brain tumors from magnetic resonance (MRI) images. *Wireless Personal Communications*, *89*(3), 993–1008. doi:10.100711277-016-3420-8

King, B., Barve, S., Ford, A., & Jha, R. (2020). Unsupervised Clustering of COVID-19 Chest X-Ray Images with a Self-Organizing Feature Map. *Midwest Symposium on Circuits and Systems,* 395–398. 10.1109/MWSCAS48704.2020.9184493

Kingma, D. P., & Ba, J. (2014). *Adam: A method for stochastic optimization*. ArXiv Preprint ArXiv:1412.6980.

Kingma, D. P., & Ba, J. (2015). Adam: A Method for Stochastic Optimization. In Y. Bengio, & Y. LeCun (Ed.), *3rd International Conference on Learning Representations, ICLR 2015*, *San Diego, CA, USA*, *May 7-9, 2015*, *Conference Track Proceedings*. Retrieved from https://arxiv.org/abs/1412.6980

Kiranyaz, S., Ince, T., & Gabbouj, M. (2016). Real-Time patient-specific ECG classification BY 1-D convolutional neural networks. *IEEE Transactions on Biomedical Engineering*, *63*(3), 664–675. doi:10.1109/TBME.2015.2468589 PMID:26285054

Klein, G. J. (2018). *Strategies for Ecg arrhythmia Diagnosis: Breaking down complexity*. Cardiotext Publishing.

Kooraki, S., Hosseiny, M., Myers, L., & Gholamrezanezhad, A. (2020). Coronavirus (COVID-19) Outbreak: What the Department of Radiology Should Know. *Journal of the American College of Radiology*, *17*(4), 447–451. doi:10.1016/j.jacr.2020.02.008 PMID:32092296

Kopparapu, K. (2021). *16: 2017 WebMD Health Hero, Inventor*. WebMD. Retrieved 17 November 2021, from https://www.webmd.com/healthheroes/2017-inventor-kavya-kopparapu

Compilation of References

Krishnaswamy Rangarajan, A., & Purushothaman, R. (2020). Disease Classification in Eggplant Using Pre-trained VGG16 and MSVM. *Scientific Reports*, *10*(1), 1–11. doi:10.103841598-020-59108-x PMID:32047172

Krissian, K., Malandain, G., Ayache, N., Vaillant, R., & Trousset, Y. (2000). Model-Based Detection of Tubular Structures in 3D Images. *Computer Vision and Image Understanding*, *80*(2), 130–171. doi:10.1006/cviu.2000.0866

Krizhevsky, A., Sutskever, I., & Hinton, G. E. (2017, May). ImageNet classification with deep convolutional neural networks. *Communications of the ACM*, *60*(6), 84–90. doi:10.1145/3065386

Kumar, A., Wang, Y.-Y., Liu, K.-C., Tsai, I.-C., Huang, C.-C., & Hung, N. (2014). Distinguishing normal and pulmonary edema chest x-ray using Gabor filter and SVM. *2014 IEEE International Symposium on Bioelectronics and Bioinformatics (IEEE ISBB 2014)*, 1–4. 10.1109/ISBB.2014.6820918

Kumar, Jain, & Mahalakshmi. (2018). Enhancement of Healthcare Using Naïve Bayes Algorithm and Intelligent Data mining of Social Media. *International Journal of Applied Engineering Research*.

Kumar, A., Padhy, S., Takkar, B., & Chawla, R. (2019). Artificial intelligence in diabetic retinopathy: A natural step to the future. *Indian Journal of Ophthalmology*, *67*(7), 1004. doi:10.4103/ijo.IJO_1989_18 PMID:31238395

Kuwayama, S., Ayatsuka, Y., Yanagisono, D., Uta, T., Usui, H., Kato, A., Takase, N., Ogura, Y., & Yasukawa, T. (2019, April). Automated Detection of Macular Diseases by Optical Coherence Tomography and Artificial Intelligence Machine Learning of Optical Coherence Tomography Images. *Journal of Ophthalmology*, *2019*, 1–7. doi:10.1155/2019/6319581 PMID:31093370

Labs, I. C. (2018, August 8). *Deep belief networks - all you need to know*. Medium. Retrieved November 19, 2021, from https://medium.com/@icecreamlabs/deep-belief-networks-all-you-need-to-know-68aa9a71cc53

Lakhani, P., & Sundaram, B. (2017, August). Deep Learning at Chest Radiography: Automated Classification of Pulmonary Tuberculosis by Using Convolutional Neural Networks. *Radiology*, *284*(2), 574–582. doi:10.1148/radiol.2017162326 PMID:28436741

Längkvist, M., Karlsson, L., & Loutfi, A. (2014). Inception-v4, Inception-ResNet and the Impact of Residual Connections on Learning. *Pattern Recognition Letters*, *42*(1), 11–24. https://arxiv.org/abs/1512.00567

LeCun, Y., Bengio, Y., & Hinton, G. (2015, May). Deep learning. *Nature*, *521*(7553), 436–444. doi:10.1038/nature14539 PMID:26017442

Lecun, Y., Bottou, L., Bengio, Y., & Haffner, P. (1998). Gradient-based learning applied to document recognition. *Proceedings of the IEEE*, *86*(11), 2278–2324. doi:10.1109/5.726791

Lee, A., Taylor, P., Kalpathy-Cramer, J., & Tufail, A. (2017). Machine Learning Has Arrived! *Ophthalmology*, *124*(12), 1726–1728. doi:10.1016/j.ophtha.2017.08.046 PMID:29157423

Lee, J.-H., Kim, Y.-T., Lee, J.-B., & Jeong, S.-N. (2020, November). A Performance Comparison between Automated Deep Learning and Dental Professionals in Classification of Dental Implant Systems from Dental Imaging: A Multi-Center Study. *Diagnostics (Basel)*, *10*(11), 910. doi:10.3390/diagnostics10110910 PMID:33171758

Lee, S.-J., Tseng, C.-H., Lin, G., Yang, Y., Yang, P., Muhammad, K., & Pandey, H. M. (2020). A dimension-reduction based multilayer perception method for supporting the medical decision making. *Pattern Recognition Letters*, *131*, 15–22. doi:10.1016/j.patrec.2019.11.026

Leger, S., Zwanenburg, A., Pilz, K., Lohaus, F., Linge, A., Zöphel, K., Kotzerke, J., Schreiber, A., Tinhofer, I., Budach, V., Sak, A., Stuschke, M., Balermpas, P., Rödel, C., Ganswindt, U., Belka, C., Pigorsch, S., Combs, S., Mönnich, D., ... Richter, C. (2017). A comparative study of machine learning methods for time-to-event survival data for radiomics risk modelling. *Scientific Reports*, *7*(13206), 13206. Advance online publication. doi:10.103841598-017-13448-3 PMID:29038455

Lessmann, N., van Ginneken, B., Zreik, M., de Jong, P. A., de Vos, B. D., Viergever, M. A., & Isgum, I. (2018). Automatic calcium scoring in low-dose chest CT using deep neural networks with dilated convolutions. *IEEE Transactions on Medical Imaging*, *37*(2), 615–625. doi:10.1109/TMI.2017.2769839 PMID:29408789

Li, S., Zhao, R., & Zou, H. (2021). Artificial Intelligence for Diabetic retinopathy. *Chinese Medical Journal*. Publish Ahead of Print. doi:10.1097/CM9.0000000000001816

Liang, S., Liu, H., Gu, Y., Guo, X., Li, H., Li, L., Wu, Z., Liu, M., & Tao, L. (2021). Fast automated detection of COVID-19 from medical images using convolutional neural networks. *Communications Biology*, *4*(1), 35. Advance online publication. doi:10.103842003-020-01535-7 PMID:33398067

Lin, Q., & Zhao, Q. (2021). *IoT Applications in Healthcare. In Internet of Things Cases and Studies*. Springer.

Litjens, G., Kooi, T., Bejnordi, B. E., Setio, A. A., Ciompi, F., Ghafoorian, M., van der Laak, J. A. W. M., van Ginneken, B., & Sánchez, C. I. (2017, December). A survey on deep learning in medical image analysis. *Medical Image Analysis*, *42*, 60–88. doi:10.1016/j.media.2017.07.005 PMID:28778026

Litvin, T., Bresnick, G., Cuadros, J., Selvin, S., Kanai, K., & Ozawa, G. (2017). A Revised Approach for the Detection of Sight-Threatening Diabetic Macular Edema. *JAMA Ophthalmology*, *135*(1), 62. doi:10.1001/jamaophthalmol.2016.4772 PMID:27930756

Liu, J., Liao, X., Qian, Sh., Yuan, J., Wang, F., Liu, Y., Wang, Z., Wang, F. S., Liu, L., & Zhang, Z. (2020). Community transmission of severe acute respiratory syndrome coronavirus 2, Shenzhen, China, 2020. *Emerging Infectious Diseases*, *26*(6), 1320–1323. doi:10.3201/eid2606.200239 PMID:32125269

Compilation of References

Li, X., Thrall, J. H., Digumarthy, S. R., Kalra, M. K., Pandharipande, P. V., Zhang, B., Nitiwarangkul, C., Singh, R., Khera, R. D., & Li, Q. (2019). Deep learning-enabled system for rapid pneumothorax screening on chest CT. *European Journal of Radiology*, *120*, 108692. doi:10.1016/j.ejrad.2019.108692 PMID:31585302

Long, J., Shelhamer, E., & Darrell, T. (2015, June). Fully convolutional networks for semantic segmentation. In *2015 IEEE Conference on Computer Vision and Pattern Recognition*. IEEE. 10.1109/CVPR.2015.7298965

López-Linares, K., Aranjuelo, N., Kabongo, L., Maclair, G., Lete, N., Ceresa, M., García-Familiar, A., Macía, I., & González Ballester, M. A. (2018). Fully automatic detection and segmentation of abdominal aortic thrombus in post-operative CTA images using deep convolutional neural networks. *Medical Image Analysis*, *46*, 202–214. doi:10.1016/j.media.2018.03.010 PMID:29609054

Lossau, T., Nickisch, H., Wissel, T., Bippus, R., Schmitt, H., Morlock, M., & Grass, M. (2019). Motion artifact recognition and quantification in coronary ct angiography using Convolutional Neural Networks. *Medical Image Analysis*, *52*, 68–79. doi:10.1016/j.media.2018.11.003 PMID:30471464

Lo, Y.-C., Lin, K.-H., Bair, H., Sheu, W. H.-H., Chang, C.-S., Shen, Y.-C., & Hung, C.-L. (2020, May). Epiretinal Membrane Detection at the Ophthalmologist Level using Deep Learning of Optical Coherence Tomography. *Scientific Reports*, *10*(1), 8424. Advance online publication. doi:10.103841598-020-65405-2 PMID:32439844

Lu, W., Tong, Y., Yu, Y., Xing, Y., Chen, C., & Shen, Y. (2018, December). Deep Learning-Based Automated Classification of Multi-Categorical Abnormalities From Optical Coherence Tomography Images. *Translational Vision Science & Technology*, *7*(6), 41. doi:10.1167/tvst.7.6.41 PMID:30619661

Lv, Y., Duan, Y., Kang, W., Li, Z., & Wang, F.-Y. (2014). Traffic Flow Prediction With Big Data: A Deep Learning Approach. *IEEE Transactions on Intelligent Transportation Systems*, 1–9. doi:10.1109/TITS.2014.2345663

M, H., & M.N, S. (2015). A Review on Evaluation Metrics for Data Classification Evaluations. *International Journal of Data Mining & Knowledge Management Process, 5*(2), 1–11. doi:10.5121/ijdkp.2015.5201

Machorro-Cano, I., Alor-Herna'ndez, G., Paredes-Valverde, M. A., Ramos-Deonati, U., Sánchez-Cervantes, J. L., & Rodríguez-Mazahua, L. (2019). PISIoT: A machine learning and IoT-based smart health platform for overweight and obesity control. *Applied Sciences (Basel, Switzerland)*, *9*(15), 3037. doi:10.3390/app9153037

Mahmud, R., Koch, F. L., & Buyya, R. (2018). Cloud-Fog Interoperability in IoT-enabled Healthcare Solution. *ICDCN*, *18*(January), 4–7.

Maity, A. R., Nair, T., & Chandra, A. (2020). Image Pre-processing techniques comparison: COVID-19 detection through Chest X-Rays via Deep Learning. *International Journal of Scientific Research in Science and Technology*, *2*, 113–123. doi:10.32628/IJSRST207614

303

Majeed, T., Rashid, R., Ali, D., & Asaad, A. (2020). Issues associated with deploying CNN transfer learning to detect COVID-19 from chest X-rays. *Physical and Engineering Sciences in Medicine*, *43*(4), 1289–1303. doi:10.100713246-020-00934-8 PMID:33025386

Malygina, T., Ericheva, E., & Drokin, I. (2019). Data Augmentation with GAN: Improving Chest X-Ray Pathologies Prediction on Class-Imbalanced Cases. *International Conference on Analysis of Images, Social Networks and Texts*, 321–334. 10.1007/978-3-030-37334-4_29

Man, Na, & Kit. (2015). IoT-based Asset Management System for Healthcare-related Industries. *International Journal of Engineering Business Management, 7*(19). doi:10.5772/61821

Martínez Chamorro, E., Díez Tascón, A., Ibáñez Sanz, L., Ossaba Vélez, S., & Borruel Nacenta, S. (2021). Radiologic diagnosis of patients with COVID-19. *Radiología (Madrid.)*, *63*(1), 56–73. doi:10.1016/j.rx.2020.11.001 PMID:33339622

Massart, P. (1990). The tight constant in the Dvoretzky–Kiefer–Wolfowitz inequality. *Annals of Probability*, *18*(3), 1269–1283. doi:10.1214/aop/1176990746

Massin, P., Allouch, C., Haouchine, B., Metge, F., Paques, M., Tangui, L., Erginay, A., & Gaudric, A. (2000, December). Optical coherence tomography of idiopathic macular epiretinal membranes before and after surgery. *American Journal of Ophthalmology*, *130*(6), 732–739. doi:10.1016/S0002-9394(00)00574-2 PMID:11124291

Matsumoto, C., Arimura, E., Okuyama, S., Takada, S., Hashimoto, S., & Shimomura, Y. (2003, September). Quantification of Metamorphopsia in Patients with Epiretinal Membranes. *Investigative Ophthalmology & Visual Science*, *44*(9), 4012. doi:10.1167/iovs.03-0117 PMID:12939323

Mayo Foundation for Medical Education and Research. (2021, October 1). *Heart arrhythmia*. Mayo Clinic. Retrieved February 15, 2022, from https://www.mayoclinic.org/diseases-conditions/heart-arrhythmia/symptoms-causes/syc-20350668

Meng, G., Wang, Y., Duan, J., Xiang, S., & Pan, C. (2013). Efficient image dehazing with boundary constraint and contextual regularization. *IEEE International Conference on Computer Vision*, 617–624. 10.1109/ICCV.2013.82

Mikołajczyk, A., & Grochowski, M. (2018). Data augmentation for improving deep learning in image classification problem. *International Interdisciplinary PhD Workshop,* 117–122. 10.1109/IIPHDW.2018.8388338

Mintz, Y., & Brodie, R. (2019). Introduction to artificial intelligence in medicine. *Minimally Invasive Therapy & Allied Technologies*, *28*(2), 73–81. doi:10.1080/13645706.2019.1575882 PMID:30810430

Miotto, R., Wang, F., Wang, S., Jiang, X., & Dudley, J. T. (2018). Deep learning for healthcare: Review, opportunities and challenges. *Briefings in Bioinformatics*, *19*(6), 1236–1246. doi:10.1093/bib/bbx044 PMID:28481991

304

Compilation of References

Misra, S., Jeon, S., Lee, S., Managuli, R., Jang, I.-S., & Kim, C. (2020). Multi-Channel Transfer Learning of Chest X-ray Images for Screening of COVID-19. *Electronics (Basel)*, *9*(9), 1388. Advance online publication. doi:10.3390/electronics9091388

Mitchell, P., Liew, G., Gopinath, B., & Wong, T. Y. (2018, September). Age-related macular degeneration. *Lancet*, *392*(10153), 1147–1159. doi:10.1016/S0140-6736(18)31550-2 PMID:30303083

Mo, P., Xing, Y., Xiao, Y., Deng, L., Zhao, Q., Wang, H., Xiong, Y., Cheng, Z., Gao, S., Liang, K., Luo, M., Chen, T., Song, S., Ma, Z., Chen, X., Zheng, R., Cao, Q., Wang, F., & Zhang, Y. (2020). Clinical characteristics of refractory COVID-19 pneumonia in Wuhan, China. *Clinical Infectious Diseases*, 3–8. doi:10.1093/cid/ciaa270

Moeen. (2015). Health Monitoring and Management Using Internet-of-Things (IoT) Sensing with Cloud-based Processing: Opportunities and Challenges. *IEEE International Conference on Services Computing*

Mohammed, M. A., Abdulkareem, K. H., Garcia-Zapirain, B., Mostafa, S. A., Maashi, M. S., Al-Waisy, A. S., Subhi, M. A., Mutlag, A. A., & Le, D. N. (2021). A comprehensive investigation of machine learning feature extraction and classification methods for automated diagnosis of COVID-19 based on X-ray images. *Computers. Materials and Continua*, *66*(3), 3289–3310. doi:10.32604/cmc.2021.012874

Mohan Kumar, S., & Majumder, D. (2018). Healthcare solution based on machine learning applications in IoT and edge computing. *International Journal of Pure and Applied Mathematics*, *119*(16), 1473–1484.

Montufar, G. (2018, June 19). *Restricted Boltzmann machines: Introduction and review*. Retrieved November 19, 2021, from https://arxiv.org/abs/1806.07066

Moody, G., & Mark, R. (2005, February 24). *MIT-BIH arrhythmia database*. MIT-BIH Arrhythmia Database v1.0.0. Retrieved September 26, 2021, from https://physionet.org/content/mitdb/1.0.0/

Mookiah, M. R., Acharya, U. R., Chua, C. K., Lim, C. M., Ng, E. Y., & Laude, A. (2013, December). Computer-aided diagnosis of diabetic retinopathy: A review. *Computers in Biology and Medicine*, *43*(12), 2136–2155. doi:10.1016/j.compbiomed.2013.10.007 PMID:24290931

Moradi, M., Madani, A., Gur, Y., Guo, Y., & Syeda-Mahmood, T. (2018). Bimodal network architectures for automatic generation of image annotation from text. Medical Image Computing and Computer Assisted Intervention, 449–456. doi:10.1007/978-3-030-00928-1_51

Morís, D. I., de Moura, J., Novo, J., & Ortega, M. (2021a). Cycle Generative Adversarial Network Approaches to Produce Novel Portable Chest X-Rays Images for Covid-19 Diagnosis. *ICASSP 2021-2021 IEEE International Conference on Acoustics, Speech and Signal Processing (ICASSP),* 1060–1064.

Morís, D. I., de Moura Ramos, J. J., Buján, J. N., & Hortas, M. O. (2021b). Data augmentation approaches using cycle-consistent adversarial networks for improving COVID-19 screening in portable chest X-ray images. *Expert Systems with Applications*, *185*, 115681. doi:10.1016/j. eswa.2021.115681 PMID:34366577

Morís, D. I., de Moura, J., Novo, J., & Ortega, M. (2021c). Comprehensive Analysis of the Screening of COVID-19 Approaches in Chest X-ray Images from Portable Devices. *European Symposium on Artificial Neural Networks (ESANN 2021)*, 165–170.

Motawi, T., Shehata, N., ElNokeety, M., & El-Emady, Y. (2018). Potential serum biomarkers for early detection of diabetic nephropathy. *Diabetes Research and Clinical Practice*, *136*, 150–158. doi:10.1016/j.diabres.2017.12.007 PMID:29253627

Murchison, A., Hark, L., Pizzi, L., Dai, Y., Mayro, E., Storey, P., Leiby, B. E., & Haller, J. A. (2017). Non-adherence to eye care in people with diabetes. *BMJ Open Diabetes Research & Care*, *5*(1), e000333. doi:10.1136/bmjdrc-2016-000333 PMID:28878930

Murff, H. J., FitzHenry, F., Matheny, M. E., Gentry, N., Kotter, K. L., Crimin, K., Dittus, R. S., Rosen, A. K., Elkin, P. L., Brown, S. H., & Speroff, T. (2011). Automated Identification of Postoperative Complications Within an Electronic Medical Record Using Natural Language Processing. *Journal of the American Medical Association*, *306*(8). Advance online publication. doi:10.1001/jama.2011.1204 PMID:21862746

Mursalim, M. K. N., & Kurniawan, A. (2021). Multi-kernel CNN block-based detection for COVID-19 with imbalance dataset. *Iranian Journal of Electrical and Computer Engineering*, *11*(3), 2467–2476. doi:10.11591/ijece.v11i3.pp2467-2476

Mustaqeem, A., Anwar, S. M., Khan, A. R., & Majid, M. (2017). A statistical analysis based recommender model for heart disease patients. *International Journal of Medical Informatics*, *108*, 134–145. doi:10.1016/j.ijmedinf.2017.10.008 PMID:29132619

Namara, K. M., Alzubaidi, H., & Jackson, J. K. (2019). Review of Cardiovascular disease as a leading cause of death: How are pharmacists getting involved? *Integrated Pharmacy Research & Practice*.

Namperumalsamy, P., Nirmalan, P., & Ramasamy, K. (2003). Developing a Screening Program to Detect Sight-Threatening Diabetic Retinopathy in South India. *Diabetes Care*, *26*(6), 1831–1835. doi:10.2337/diacare.26.6.1831 PMID:12766118

Narayan Das, N., Kumar, N., Kaur, M., Kumar, V., & Singh, D. (2020). Automated Deep Transfer Learning-Based Approach for Detection of COVID-19 Infection in Chest X-rays. *IRBM*. Advance online publication. doi:10.1016/j.irbm.2020.07.001 PMID:32837679

Narayanan, B. N., Hardie, R. C., Krishnaraja, V., Karam, C., & Davuluru, V. S. P. (2020). Transfer-to-Transfer Learning Approach for Computer Aided Detection of COVID-19 in Chest Radiographs. *AI 2020, 1*(4), 539–557. doi:10.3390/ai1040032

Compilation of References

Narin, A., Kaya, C., & Pamuk, Z. (2020). *Department of Biomedical Engineering, Zonguldak Bulent Ecevit University*. https://arxiv.org/abs/2003.10849

Narin, A., Kaya, C., & Pamuk, Z. (2021). Automatic detection of coronavirus disease (COVID-19) using X-ray images and deep convolutional neural networks. *Pattern Analysis & Applications*, *24*(3), 1207–1220. doi:10.100710044-021-00984-y PMID:33994847

Natarajan, S., Jain, A., Krishnan, R., Rogye, A., & Sivaprasad, S. (2019). Diagnostic accuracy of community-based diabetic retinopathy screening with an offline artificial intelligence system on a smartphone. *JAMA Ophthalmology*, *137*(10), 1182. doi:10.1001/jamaophthalmol.2019.2923 PMID:31393538

Nath, M. K., Kanhe, A., & Mishra, M. (2020). A Novel Deep Learning Approach for Classification of COVID-19 Images. *IEEE 5th International Conference on Computing Communication and Automation (ICCCA)*, 752–757. 10.1109/ICCCA49541.2020.9250907

Nayak, S. R., Nayak, D. R., Sinha, U., Arora, V., & Pachori, R. B. (2021). Application of deep learning techniques for detection of COVID-19 cases using chest X-ray images: A comprehensive study. *Biomedical Signal Processing and Control*, *64*, 102365. Advance online publication. doi:10.1016/j.bspc.2020.102365 PMID:33230398

Nguyen, K. (2021, October 12). *Detecting heart abnormalities using 1D CNN on data you cannot see*. Medium. Retrieved November 19, 2021, from https://towardsdatascience.com/detecting-heart-abnormalities-using-1d-cnn-on-data-you-cannot-see-with-pysyft-735481a952d8

NHS. (n.d.). *NHS choices*. Retrieved February 16, 2022, from https://www.nhs.uk/conditions/electrocardiogram/

Noriega, A., Meizner, D., Camacho, D., Enciso, J., Quiroz-Mercado, H., Morales-Canton, V., & ... . (2020). Screening Diabetic Retinopathy Using an Automated Retinal Image Analysis System in Mexico: Independent and Assistive use Cases (Preprint). *JMIR Formative Research*. Advance online publication. doi:10.2196/25290 PMID:34435963

Novo, J., Gonçalves, L., Mendonça, A. M., & Campilho, A. (2015). 3D lung nodule candidate detection in multiple scales. *2015 14th IAPR International Conference on Machine Vision Applications (MVA),* 61–64. 10.1109/MVA.2015.7153133

Novo, J., Rouco, J., Mendonça, A., & Campilho, A. (2014). Reliable Lung Segmentation Methodology by Including Juxtapleural Nodules. *Reliable Lung Segmentation Methodology by Including Juxtapleural Nodules.*, *8815*, 227–235. doi:10.1007/978-3-319-11755-3_26

Office of the Commissioner. (2019). *FDA permits marketing of artificial intelligence-based device to detect certain diabetes-related eye problems*. U.S. Food and Drug Administration. https://www.fda.gov/news-events/press-announcements/fda-permits-marketing-artificial-intelligence-based-device-detect-certain-diabetes-related-eye

Ohata, E. F., Bezerra, G. M., Chagas, J. V. S. Das, Lira Neto, A. V., Albuquerque, A. B., Albuquerque, V. H. C. D., & Reboucas Filho, P. P. (2021). Automatic detection of COVID-19 infection using chest X-ray images through transfer learning. *IEEE/CAA Journal of Automatica Sinica, 8*(1), 239–248. doi:10.1109/JAS.2020.1003393

Oh, Y., Park, S., & Ye, J. C. (2020). Deep Learning COVID-19 Features on CXR Using Limited Training Data Sets. *IEEE Transactions on Medical Imaging*, *39*(8), 2688–2700. doi:10.1109/TMI.2020.2993291 PMID:32396075

Onasanya, A., & Elshakankiri, M. (2018). Secured Cancer Care and Cloud Services in IoT/WSN Based Medical Systems. *Second EAI International Conference, SGIoT*.

Open Data Science. (2020, November 5). *The A − Z of supervised learning, use cases, and disadvantages*. Retrieved November 19, 2021, from https://opendatascience.com/the-a-z-of-supervised-learning-use-cases-and-disadvantages/

Oran, D. P., & Topol, E. J. (2020). Prevalence of Asymptomatic SARS-CoV-2 Infection : A Narrative Review. *Annals of Internal Medicine*, *173*(5), 362–367. doi:10.7326/M20-3012 PMID:32491919

Orozco-Arias, S., Isaza, G., Guyot, R., & Tabares-Soto, R. (2019). A systematic review of the application of machine learning in the detection and classification of transposable elements. *PeerJ*, *7*, e8311. doi:10.7717/peerj.8311 PMID:31976169

Østvik, A., Smistad, E., Aase, S. A., Haugen, B. O., & Lovstakken, L. (2019). Real-time standard view classification in transthoracic echocardiography using Convolutional Neural Networks. *Ultrasound in Medicine & Biology*, *45*(2), 374–384. doi:10.1016/j.ultrasmedbio.2018.07.024 PMID:30470606

Ozturk, T., Talo, M., Yildirim, E. A., Baloglu, U. B., Yildirim, O., & Rajendra Acharya, U. (2020). Automated detection of COVID-19 cases using deep neural networks with X-ray images. *Computers in Biology and Medicine*, *121*(April), 103792. doi:10.1016/j.compbiomed.2020.103792 PMID:32568675

Padmavathi & Ran. (2016). Implementation of IOT Based Health Care Solution Based on Cloud Computing. *International Journal of Engineering and Computer Science, 5*(9), 17931-17937.

Panwar, H., Gupta, P. K., Siddiqui, M. K., Morales-Menendez, R., & Singh, V. (2020). Application of deep learning for fast detection of COVID-19 in X-Rays using nCOVnet. *Chaos, Solitons, and Fractals*, *138*, 109944. Advance online publication. doi:10.1016/j.chaos.2020.109944 PMID:32536759

Paolella, M. S. (2018). *Fundamental Statistical Inference: A Computational Approach*. Wiley. doi:10.1002/9781119417897

Papadokostaki, K., Mastorakis, G., Panagiotakis, S., & Mavromoustakis, C. X. (2016). Handling big data in the era of Internet of things (IoT). *Advances in Mobile Cloud Computing and Big Data in the 5G Era.*

Compilation of References

Park, J., Lee, K., & Kang, K. (2013). Arrhythmia detection from heartbeat using k-nearest neighbor classifier. *2013 IEEE International Conference on Bioinformatics and Biomedicine*. doi:10.1109/bibm.2013.6732594

Parra-Mora, E., Cazañas-Gordon, A., Proença, R., & da Silva Cruz, L. A. (2021). Epiretinal Membrane Detection in Optical Coherence Tomography Retinal Images Using Deep Learning. *IEEE Access: Practical Innovations, Open Solutions*, *9*, 99201–99219. doi:10.1109/ACCESS.2021.3095655

Patel, S. P. B. K., & Muthu, R. K. (2020). *Medical Image Enhancement Using Histogram Processing and Feature Extraction for Cancer Classification*. https://arxiv.org/abs/2003.06615v1

Paul Cohen, J., Morrison, P., & Dao, L. (2020). *COVID-19 Image Data Collection*. ArXiv.

Pereira, R. M., Bertolini, D., Teixeira, L. O., Silla, C. N. Jr, & Costa, Y. M. G. (2020). COVID-19 identification in chest X-ray images on flat and hierarchical classification scenarios. *Computer Methods and Programs in Biomedicine*, *194*, 105532. Advance online publication. doi:10.1016/j.cmpb.2020.105532 PMID:32446037

Pham, T. D. (2021). Classification of COVID-19 chest X-rays with deep learning: New models or fine tuning? *Health Information Science and Systems*, *9*(1), 2. Advance online publication. doi:10.100713755-020-00135-3 PMID:33235710

Prabhu. (2019, November 21). *Understanding of convolutional neural network (CNN) - Deep learning*. Medium. Retrieved November 21, 2021, from https://medium.com/@RaghavPrabhu/understanding-of-convolutional-neural-network-cnn-deep-learning-99760835f148

Pratt, H., Coenen, F., Broadbent, D., Harding, S., & Zheng, Y. (2016). Convolutional Neural Networks for Diabetic Retinopathy. *Procedia Computer Science*, *90*, 200–205. doi:10.1016/j.procs.2016.07.014

Pros and cons of using an AI-based diagnosis for diabetic retinopathy. (n.d.). *Optometry Times*. Retrieved November 19, 2021, from https://www.optometrytimes.com/view/pros-and-cons-using-ai-based-diagnosis-diabetic-retinopathy

Puderbach, M., Eichinger, M., Haeselbarth, J., Ley, S., Kopp-Schneider, A., Tuengerthal, S., Schmaehl, A., Fink, C., Plathow, C., Wiebel, M., & ... (2007). Assessment of morphological MRI for pulmonary changes in cystic fibrosis (CF) patients: Comparison to thin-section CT and chest x-ray. *Investigative Radiology*, *42*(10), 715–724. doi:10.1097/RLI.0b013e318074fd81 PMID:17984769

Qayyum, Qadir, Bilal, & Al-Fuqaha. (2020). *Secure and Robust Machine Learning for Healthcare: A Survey*. doi:10.1109/RBME.2020.3013489

Qi, X., Nosher, J. L., Foran, D. J., & Hacihaliloglu, I. (2021). *Multi-Feature Semi-Supervised Learning for COVID-19 Diagnosis from Chest X-ray Images*. https://arxiv.org/abs/2104.01617

Qi, X., Brown, L. G., Foran, D. J., Nosher, J., & Hacihaliloglu, I. (2021). Chest X-ray image phase features for improved diagnosis of COVID-19 using convolutional neural network. *International Journal of Computer Assisted Radiology and Surgery*, *16*(2), 197–206. doi:10.100711548-020-02305-w PMID:33420641

Quinn, N., Brazionis, L., Zhu, B., Ryan, C., D'Aloisio, R., Lilian Tang, H., Peto, T., & Jenkins, A. (2021). Facilitating diabetic retinopathy screening using automated retinal image analysis in underresourced settings. *Diabetic Medicine*, *38*(9). Advance online publication. doi:10.1111/dme.14582 PMID:33825229

Raeesi Vanani, I., & Amirhosseini, M. (2021). IoT-Based Diseases Prediction and Diagnosis System for Healthcare. In *Internet of Things for Healthcare Technologies. Studies in Big Data* (Vol. 73). Springer. doi:10.1007/978-981-15-4112-4_2

Rahhal, M. M. A., Bazi, Y., AlHichri, H., Alajlan, N., Melgani, F., & Yager, R. R. (2016). Deep learning approach for active classification of electrocardiogram signals. *Information Sciences*, *345*, 340–354. doi:10.1016/j.ins.2016.01.082

Rahman, R., & Stephenson, J. (2014, January). Early surgery for epiretinal membrane preserves more vision for patients. *Eye (London, England)*, *28*(4), 410–414. doi:10.1038/eye.2013.305 PMID:24406414

Rahman, S., Rahman, M. M., Abdullah-Al-Wadud, M., Al-Quaderi, G. D., & Shoyaib, M. (2016). An adaptive gamma correction for image enhancement. *EURASIP Journal on Image and Video Processing*, *2016*(1), 1–13. doi:10.118613640-016-0138-1

Rahman, S., Sarker, S., Miraj, M. A. A., Nihal, R. A., Nadimul Haque, A. K. M., & Noman, A. A. (2021, March 2). Deep Learning–Driven Automated Detection of COVID-19 from Radiography Images: A Comparative Analysis. *Cognitive Computation*. Advance online publication. doi:10.100712559-020-09779-5 PMID:33680209

Rajalakshmi, R. (2019). The impact of artificial intelligence in screening for diabetic retinopathy in India. *Eye (London, England)*, *34*(3), 420–421. doi:10.103841433-019-0626-5 PMID:31827270

Rajalakshmi, R., Amutha, A., Ranjani, H., Ali, M., Unnikrishnan, R., Anjana, R., Narayan, K. M. V., & Mohan, V. (2014). Prevalence and risk factors for diabetic retinopathy in Asian Indians with young onset Type 1 and Type 2 Diabetes. *Journal of Diabetes and Its Complications*, *28*(3), 291–297. doi:10.1016/j.jdiacomp.2013.12.008 PMID:24512748

Rajalakshmi, R., Arulmalar, S., Usha, M., Prathiba, V., Kareemuddin, K. S., Anjana, R. M., & Mohan, V. (2015). Validation of smartphone based retinal photography for diabetic retinopathy screening. *PLoS One*, *10*(9), e0138285. Advance online publication. doi:10.1371/journal.pone.0138285 PMID:26401839

Rajalakshmi, R., Subashini, R., Anjana, R., & Mohan, V. (2018). Automated diabetic retinopathy detection in smartphone-based fundus photography using artificial intelligence. *Eye (London, England)*, *32*(6), 1138–1144. doi:10.103841433-018-0064-9 PMID:29520050

310

Compilation of References

Rajaraman, S., Siegelman, J., Alderson, P. O., Folio, L. S., Folio, L. R., & Antani, S. K. (2020). Iteratively Pruned Deep Learning Ensembles for COVID-19 Detection in Chest X-Rays. *IEEE Access: Practical Innovations, Open Solutions*, *8*, 115041–115050. doi:10.1109/ACCESS.2020.3003810 PMID:32742893

Raman, R., Srinivasan, S., Virmani, S., Sivaprasad, S., Rao, C., & Rajalakshmi, R. (2018). Fundus photograph-based deep learning algorithms in detecting diabetic retinopathy. *Eye (London, England)*, *33*(1), 97–109. doi:10.103841433-018-0269-y PMID:30401899

Rameswari, R., & Divya, N. (2018). Smart Health Care Monitoring System Using Android Application: A Review. *International Journal of Recent Technology and Engineering*.

Rathore, J. S., & Ghosh, C. (2020). Severe acute respiratory syndrome coronavirus-2 (SARS-CoV-2), a newly emerged pathogen: An overview. *Pathogens and Disease*, *78*(6), 1–9. doi:10.1093/femspd/ftaa042 PMID:32840560

Rehman, A., Sadad, T., Saba, T., Hussain, A., & Tariq, U. (2021). Real-Time Diagnosis System of COVID-19 Using X-Ray Images and Deep Learning. *IT Professional*, *23*(4), 57–62. doi:10.1109/MITP.2020.3042379

Researchers Reveal New Biomarkers for Early Detection of Diabetic Vision Loss. (2021). *Chinese Academy of Sciences*. Retrieved 19 November 2021, from https://english.cas.cn/newsroom/cas_media/202010/t20201019_244966.shtml

Rezaul, M. K., & Ataharul, M. I. (2019). Reliability and Survival Analysis. Springer.

Rim, B., Sung, N.-J., Min, S., & Hong, M. (2020). Deep learning in Physiological Signal Data: A survey. *Sensors (Basel)*, *20*(4), 969. https://doi.org/10.3390/s20040969

Ripley, B. D., & Ripley, R. M. (1998). Neural networks as statistical methods in survival analysis. In R. Dybowski & V. Gant (Eds.), *Artificial Neural Networks: Prospects for Medicine*. Landes Biosciences.

Romeny, B. M., Zuiderveld, K. J., Waes, P. F., Walsum, T. V., Weijden, R. V., Weickert, J., ... Viergever, M. A. (1998, October). Advances in three-dimensional diagnostic radiology. *Journal of Anatomy*, *193*(3), 363–371. doi:10.1046/j.1469-7580.1998.19330363.x PMID:9877291

Rong, G., Mendez, A., Bou Assi, E., Zhao, B., & Sawan, M. (2021). *Artificial Intelligence in Healthcare: Review and Prediction Case Studies*. Academic Press.

Ronneberger, O., Fischer, P., & Brox, T. (2015). *U-Net: Convolutional Networks for Biomedical Image Segmentation*. doi:10.1007/978-3-319-24574-4_28

Roosa, K., Lee, Y., Luo, R., Kirpich, A., Rothenberg, R., Hyman, J. M., Yan, P., & Chowell, G. (2020). Real-time forecasts of the COVID-19 epidemic in China from February 5th to February 24th, 2020. *Infectious Disease Modelling*, *5*, 256–263. doi:10.1016/j.idm.2020.02.002 PMID:32110742

Rosenberg, J. B., & Tsui, I. (2017). Screening for Diabetic Retinopathy. *The New England Journal of Medicine*, *376*(16), 1587–1588. doi:10.1056/NEJMe1701820 PMID:28423293

Ruamviboonsuk, P., Krause, J., Chotcomwongse, P., Sayres, R., Raman, R., Widner, K., Campana, B. J. L., Phene, S., Hemarat, K., Tadarati, M., Silpa-Archa, S., Limwattanayingyong, J., Rao, C., Kuruvilla, O., Jung, J., Tan, J., Orprayoon, S., Kangwanwongpaisan, C., Sukumalpaiboon, R., ... Webster, D. R. (2019). Deep learning versus human graders for classifying diabetic retinopathy severity in a nationwide screening program. *NPJ Digital Medicine*, *2*(1), 25. Advance online publication. doi:10.103841746-019-0099-8 PMID:31341955

Ryan, M., Rajalakshmi, R., Prathiba, V., Anjana, R., Ranjani, H., Narayan, K., Olsen, T., Mohan, V., Ward, L., Lynn, M., & Hendrick, A. (2015). Comparison Among Methods of Retinopathy Assessment (CAMRA) Study. *Ophthalmology*, *122*(10), 2038–2043. doi:10.1016/j.ophtha.2015.06.011 PMID:26189190

Sadhukhan, B. Das, & Sangaiah. (2018). Producing better disaster management plan in post-disaster situation using social media mining. In Computational Intelligence for Multimedia Big Data on the Cloud With Engineering Applications. Academic.

Sahlol, A. T., Yousri, D., Ewees, A. A., Al-qaness, M. A. A., Damasevicius, R., & Elaziz, M. A. (2020). COVID-19 image classification using deep features and fractional-order marine predators algorithm. *Scientific Reports*, *10*(1), 1–15. doi:10.103841598-020-71294-2 PMID:32958781

Sahoo, J. P. (2011). Analysis of ECG signal for Detection of Cardiac Arrhythmias. National Institute of Technology, Rourkela.

Salem, M., Taheri, S., & Yuan, J.-S. (2018). ECG arrhythmia classification using transfer learning From 2- DIMENSIONAL Deep CNN Features. *2018 IEEE Biomedical Circuits and Systems Conference (BioCAS)*. 10.1109/BIOCAS.2018.8584808

Salem, N., Malik, H., & Shams, A. (2019). Medical image enhancement based on histogram algorithms. *Procedia Computer Science*, *163*, 300–311. doi:10.1016/j.procs.2019.12.112

Salih Ahmed, R., Sayed Ali Ahmed, E., & Saeed, R. A. (2021). Machine Learning in Cyber-Physical Systems in Industry 4.0. In A. Luhach & A. Elçi (Eds.), *Artificial Intelligence Paradigms for Smart Cyber-Physical Systems* (pp. 20–41). IGI Global. doi:10.4018/978-1-7998-5101-1.ch002

Samagaio, G., de Moura, J., Novo, J., & Ortega, M. (2017). Optical Coherence Tomography Denoising by Means of a Fourier Butterworth Filter-based Approach. In *Image Analysis and Processing - ICIAP 2017* (pp. 422–432). Lecture Notes in Computer Science. Springer. doi:10.1007/978-3-319-68548-9_39

Sandler, M., Howard, A., Zhu, M., Zhmoginov, A., & Chen, L. C. (2018). MobileNetV2: Inverted Residuals and Linear Bottlenecks. *Proceedings of the IEEE Computer Society Conference on Computer Vision and Pattern Recognition*, 4510–4520. 10.1109/CVPR.2018.00474

Sarv Ahrabi, S., Scarpiniti, M., Baccarelli, E., & Momenzadeh, A. (2021). An accuracy vs. Complexity comparison of deep learning architectures for the detection of COVID-19 disease. *Computation (Basel, Switzerland)*, *9*(1), 1–20. doi:10.3390/computation9010003

Compilation of References

Scanlon, P., Aldington, S., & Stratton, I. (2013). Epidemiological issues in diabetic retinopathy. *Middle East African Journal of Ophthalmology*, *20*(4), 293. doi:10.4103/0974-9233.120007 PMID:24339678

Secinaro, S., Calandra, D., Secinaro, A., Muthurangu, V., & Biancone, P. (2021). The role of artificial intelligence in healthcare: A structured literature review. *BMC Medical Informatics and Decision Making*, *21*(1), 125. Advance online publication. doi:10.118612911-021-01488-9 PMID:33836752

Selvin, S. (2008). *Survival analysis for epidemiologic and medical research: A Practical Guide*. Cambridge University Press. doi:10.1017/CBO9780511619809

Sethi, P., & Sarangi, S. R. (2017). Internet of things: Architectures, protocols, and applications. *Journal of Electrical and Computer Engineering*, 25. doi:10.1155/2017/9324035

Setio, A. A., Ciompi, F., Litjens, G., Gerke, P., Jacobs, C., van Riel, S. J., Wille, M. M. W., Naqibullah, M., Sanchez, C. I., & van Ginneken, B. (2016, May). Pulmonary Nodule Detection in CT Images: False Positive Reduction Using Multi-View Convolutional Networks. *IEEE Transactions on Medical Imaging*, *35*(5), 1160–1169. doi:10.1109/TMI.2016.2536809 PMID:26955024

Shadmi, R., Mazo, V., Bregman-Amitai, O., & Elnekave, E. (2018). Fully-convolutional deep-learning based system for coronary calcium score prediction from non-contrast chest CT. *2018 IEEE 15th International Symposium on Biomedical Imaging (ISBI 2018),* 24–28. 10.1109/ISBI.2018.8363515

Shalabi, L. A., Shaaban, Z., & Kasasbeh, B. (2006). Data Mining: A Preprocessing Engine. *Journal of Computational Science*, *2*(9), 735–739. doi:10.3844/jcssp.2006.735.739

Shen, D., Wu, G., & Suk, H.-I. (2017, June). Deep Learning in Medical Image Analysis. *Annual Review of Biomedical Engineering*, *19*(1), 221–248. doi:10.1146/annurev-bioeng-071516-044442 PMID:28301734

Sherstinsky, A. (2020). Fundamentals of Recurrent Neural Network (RNN) and long short-term memory (LSTM) network. *Physica D. Nonlinear Phenomena*, *404*, 132306. doi:10.1016/j.physd.2019.132306

Sheykhivand, S., Mousavi, Z., Mojtahedi, S., Yousefi Rezaii, T., Farzamnia, A., Meshgini, S., & Saad, I. (2021). Developing an efficient deep neural network for automatic detection of COVID-19 using chest X-ray images. *Alexandria Engineering Journal*, *60*(3), 2885–2903. doi:10.1016/j.aej.2021.01.011

Shi, L., Wu, H., Dong, J., Jiang, K., Lu, X., & Shi, J. (2015). Telemedicine for detecting diabetic retinopathy: a systematic review and meta-analysis. *British Journal of Ophthalmology, 99*(6), 823-831. doi:10.1136/bjophthalmol-2014-305631

Shiraishi, J., Katsuragawa, S., Ikezoe, J., Matsumoto, T., Kobayashi, T., Komatsu, K. I., Matsui, M., Fujita, H., Kodera, Y., & Doi, K. (2020). Development of a digital image database for chest radiographs with and without a lung nodule: Receiver operating characteristic analysis of radiologists' detection of pulmonary nodules. *AJR. American Journal of Roentgenology*, *174*(1), 71–74. doi:10.2214/ajr.174.1.1740071 PMID:10628457

Shorfuzzaman, M., & Hossain, M. S. (2020). MetaCOVID: A Siamese neural network framework with contrastive loss for n-shot diagnosis of COVID-19 patients. *Pattern Recognition*, *113*(107700), 107700. Advance online publication. doi:10.1016/j.patcog.2020.107700 PMID:33100403

Shorten, C., & Khoshgoftaar, T. M. (2019). A survey on Image Data Augmentation for Deep Learning. *Journal of Big Data, 6*(1), 1–48. doi:10.1186/s40537-019-0197-0

Siddique, N., Paheding, S., Elkin, C. P., & Devabhaktuni, V. (2021). *U-net and its variants for medical image segmentation: A review of theory and applications*. IEEE. doi:10.1109/ACCESS.2021.3086020

Sidey-Gibbons, J. A., & Sidey-Gibbons, C. J. (2019). Machine learning in medicine: A practical introduction. *BMC Medical Research Methodology*, *19*(1), 64. Advance online publication. doi:10.118612874-019-0681-4 PMID:30890124

Signal Processing: A mathematical approach, second. (n.d.). Retrieved November 19, 2021, from https://library.oapen.org/bitstream/id/3eb04f39-67d7-4b4d-8569-3185fbefd944/1005624.pdf

Signoroni, A., Savardi, M., Benini, S., Adami, N., Leonardi, R., Gibellini, P., Vaccher, F., Ravanelli, M., Borghesi, A., Maroldi, R., & Farina, D. (2021). BS-Net: Learning COVID-19 pneumonia severity on a large chest X-ray dataset. *Medical Image Analysis*, *71*, 102046. doi:10.1016/j.media.2021.102046 PMID:33862337

Singh, A., Sengupta, S., & Lakshminarayanan, V. (2020). Explainable deep learning models in medical image analysis. *Journal of Imaging*, *6*(6), 1–19. doi:10.3390/jimaging6060052 PMID:34460598

Singh, R. K., Pandey, R., & Babu, R. N. (2021). COVIDScreen: Explainable deep learning framework for differential diagnosis of COVID-19 using chest X-rays. *Neural Computing & Applications*, *6*(14), 8871–8892. Advance online publication. doi:10.100700521-020-05636-6 PMID:33437132

Singh, R., & Rajesh, E. (2019). Prediction of heart disease by clustering and classification techniques Prediction of Heart Disease by Clustering and Classification Techniques. *International Journal on Computer Science and Engineering*, *7*(5), 861–866.

Solutions, E. (2016, November 11). *Accuracy, precision, recall & f1 score: Interpretation of performance measures.* Exsilio Blog. https://blog.exsilio.com/all/accuracy-precision-recall-f1-score-interpretation-of-performance-measures/

314

Compilation of References

Song, Y. E., Liu, Y., Fang, S., & Zhang, S. (2015). Research on applications of the internet of things in the smart grid. *7th International Conference on Intelligent Human-Machine Systems and Cybernetics (IHMSC)*, 2, 178–181. 10.1109/IHMSC.2015.131

Sonobe, T., Tabuchi, H., Ohsugi, H., Masumoto, H., Ishitobi, N., Morita, S., Enno, H., & Nagasato, D. (2018, September). Comparison between support vector machine and deep learning, machine-learning technologies for detecting epiretinal membrane using 3D-OCT. *International Ophthalmology*, *39*(8), 1871–1877. doi:10.100710792-018-1016-x PMID:30218173

Sood, S. K., & Mahajan, I. (2017). Wearable IoT sensor based healthcare system for identifying and controlling chikungunya virus. *Computers in Industry*, *91*, 33–44. doi:10.1016/j.compind.2017.05.006 PMID:32287550

Sosale, B., Aravind, S., Murthy, H., Narayana, S., Sharma, U., Gowda, S., & Naveenam, M. (2020). Simple, Mobile-based Artificial Intelligence Algorithm in the detection of Diabetic Retinopathy (SMART) study. *BMJ Open Diabetes Research & Care*, *8*(1), e000892. Advance online publication. doi:10.1136/bmjdrc-2019-000892 PMID:32049632

Sosale, B., Sosale, A. R., Murthy, H., Sengupta, S., & Naveenam, M. (2020). Medios– an offline, smartphone-based artificial intelligence algorithm for the diagnosis of diabetic retinopathy. *Indian Journal of Ophthalmology*, *68*(2), 391. doi:10.4103/ijo.IJO_1203_19 PMID:31957735

Spaide, R. F., Fujimoto, J. G., Waheed, N. K., Sadda, S. R., & Staurenghi, G. (2018, May). Optical coherence tomography angiography. *Progress in Retinal and Eye Research*, *64*, 1–55. doi:10.1016/j.preteyeres.2017.11.003 PMID:29229445

Staudemeyer, R. C., & Morris, E. R. (2019, September 12). *Understanding LSTM — a tutorial into long short-term memory recurrent neural networks*. Retrieved February 16, 2022, from https://arxiv.org/abs/1909.09586

Stoecklin, B. S., Rolland, P., Silue, Y., Mailles, A., Campese, C., Simondon, A., Mechain, M., Meurice, L., Nguyen, M., Bassi, C., Yamani, E., Behillil, S., Ismael, S., Nguyen, D., Malvy, D., Lescure, F. X., Georges, S., Lazarus, C., Tabaï, A., ... Team, I. (2020). First cases of coronavirus disease 2019 (COVID-19) in France: Surveillance, investigations and control measures, January 2020. *Eurosurveillance*, *25*(6). PMID:32070465

Suh, M. H., Seo, J. M., Park, K. H., & Yu, H. G. (2009, March). Associations Between Macular Findings by Optical Coherence Tomography and Visual Outcomes After Epiretinal Membrane Removal. *American Journal of Ophthalmology*, *147*(3), 473–480.e3. doi:10.1016/j.ajo.2008.09.020 PMID:19054492

Sun, Y., Chan, K. L., & Krishnan, S. M. (2005). Characteristic wave detection In ECG signal using Morphological transform. *BMC Cardiovascular Disorders*, *5*(1), 28. Advance online publication. doi:10.1186/1471-2261-5-28 PMID:16171531

SuperDataScience. (n.d.). Retrieved November 19, 2021, from https://www.superdatascience.com/blogs/recurrent-neural-networks-rnn-the-vanishing-gradient-problem

315

Suzuki, K. (2017). Overview of deep learning in medical imaging. *Radiological Physics and Technology*, *10*(3), 257–273. doi:10.100712194-017-0406-5 PMID:28689314

Szegedy, C., Liu, W., Jia, Y., Sermanet, P., Reed, S., Anguelov, D., Erhan, D., Vanhoucke, V., & Rabinovich, A. (2015). Going deeper with convolutions. *2015 IEEE Conference on Computer Vision and Pattern Recognition (CVPR)*, 1–9. 10.1109/CVPR.2015.7298594

Tabares-Soto, R., Raúl, R. P., & Gustavo, I. (2019). Deep learning applied to steganalysis of digital images: A systematic review. *IEEE Access: Practical Innovations, Open Solutions*, *7*, 68970–68990. doi:10.1109/ACCESS.2019.2918086

Tahamtan, A., & Ardebili, A. (2020). Real-time RT-PCR in COVID-19 detection: Issues affecting the results. *Expert Review of Molecular Diagnostics*, *20*(5), 453–454. doi:10.1080/14737159.2 020.1757437 PMID:32297805

Taheri Dezaki, F., Liao, Z., Luong, C., Girgis, H., Dhungel, N., Abdi, A. H., Behnami, D., Gin, K., Rohling, R., Abolmaesumi, P., & Tsang, T. (2019). Cardiac phase detection in echocardiograms with densely gated recurrent neural networks and global extrema loss. *IEEE Transactions on Medical Imaging*, *38*(8), 1821–1832. doi:10.1109/TMI.2018.2888807 PMID:30582532

Takalo-Mattila, J., Kiljander, J., & Soininen, J. P. (2018). Inter-patient ECG classification using deep convolutional neural networks. In N. Konofaos, M. Novotny, & A. Skavhaug (Eds.), *2018 21st Euromicro Conference on Digital System Design* (pp. 421-425). IEEE Institute of Electrical and Electronic Engineers. doi:10.1109/DSD.2018.00077

Tang, Y. B., Tang, Y. X., Xiao, J., & Summers, R. M. (2020). Xlsor: A robust and accurate lung segmentor on chest x-rays using criss-cross attention and customized radiorealistic abnormalities generation. *ArXiv*, 457–467.

Tan, M., & Le, Q. V. (2019). EfficientNet: Rethinking model scaling for convolutional neural networks. *36th International Conference on Machine Learning, ICML 2019,* 10691–10700.

Tan, O., Chopra, V., Lu, A. T.-H., Schuman, J. S., Ishikawa, H., Wollstein, G., Varma, R., & Huang, D. (2009, December). Detection of Macular Ganglion Cell Loss in Glaucoma by Fourier-Domain Optical Coherence Tomography. *Ophthalmology*, *116*(12), 2305–2314.e2. doi:10.1016/j. ophtha.2009.05.025 PMID:19744726

Tartaglione, E., Barbano, C. A., Berzovini, C., Calandri, M., & Grangetto, M. (2020). Unveiling COVID-19 from chest x-ray with deep learning: A hurdles race with small data. *International Journal of Environmental Research and Public Health*, *17*(18), 1–17. doi:10.3390/ijerph17186933 PMID:32971995

Taylor, C., Merin, L., Salunga, A., Hepworth, J., Crutcher, T., O'Day, D., & Pilon, B. (2007). Improving Diabetic Retinopathy Screening Ratios Using Telemedicine-Based Digital Retinal Imaging Technology: The Vine Hill Study. *Diabetes Care*, *30*(3), 574–578. doi:10.2337/dc06-1509 PMID:17327323

Compilation of References

Teshome, A. K. (2018). A Review of Implant Communication Technology in WBAN: Progresses and Challenges. *IEEE Access: Practical Innovations, Open Solutions*.

Ting, D. S. W., Cheung, C. Y.-L., Lim, G., Tan, G. S. W., Quang, N. D., Gan, A., Hamzah, H., Garcia-Franco, R., San Yeo, I. Y., Lee, S. Y., Wong, E. Y. M., Sabanayagam, C., Baskaran, M., Ibrahim, F., Tan, N. C., Finkelstein, E. A., Lamoureux, E. L., Wong, I. Y., Bressler, N. M., & Sivaprasad, S. (2017). Development and Validation of a Deep Learning System for Diabetic Retinopathy and Related Eye Diseases Using Retinal Images From Multiethnic Populations With Diabetes. *Journal of the American Medical Association*, *318*(22), 2211. doi:10.1001/jama.2017.18152

Toğaçar, M., Ergen, B., & Cömert, Z. (2020). COVID-19 detection using deep learning models to exploit Social Mimic Optimization and structured chest X-ray images using fuzzy color and stacking approaches. *Computers in Biology and Medicine*, *121*(103805). Advance online publication. doi:10.1016/j.compbiomed.2020.103805 PMID:32568679

Toh, C., & Brody, J. (2021). Applications of machine learning in Healthcare. *Smart Manufacturing - When Artificial Intelligence Meets the Internet of Things*. doi:10.5772/intechopen.92297

Tong, Y., Lu, W., Yu, Y., & Shen, Y. (2020). Application of machine learning in ophthalmic imaging modalities. *Eye and Vision*, *7*(1). Advance online publication. doi:10.118640662-020-00183-6

Toraman, S., Alakus, T. B., & Turkoglu, I. (2020). Convolutional capsnet: A novel artificial neural network approach to detect COVID-19 disease from X-ray images using capsule networks. *Chaos, Solitons, and Fractals*, *140*, 110122. Advance online publication. doi:10.1016/j.chaos.2020.110122 PMID:32834634

Tuncer, T., Ozyurt, F., Dogan, S., & Subasi, A. (2021). A novel COVID-19 and pneumonia classification method based on F-transform. *Chemometrics and Intelligent Laboratory Systems*, *210*(104256), 104256. Advance online publication. doi:10.1016/j.chemolab.2021.104256 PMID:33531722

Übeyli, E. D. (2009). Combining recurrent neural networks WITH eigenvector methods for classification of ECG beats. *Digital Signal Processing*, *19*(2), 320–329. https://doi.org/10.1016/j.dsp.2008.09.002

Uçar, E., Atila, Ü., Uçar, M., & Akyol, K. (2021). Automated detection of COVID-19 disease using deep fused features from chest radiography images. *Biomedical Signal Processing and Control*, *69*(June), 102862. doi:10.1016/j.bspc.2021.102862 PMID:34131433

Ucar, F., & Korkmaz, D. (2020). COVIDiagnosis-Net: Deep Bayes-SqueezeNet based diagnosis of the coronavirus disease 2019 (COVID-19) from X-ray images. *Medical Hypotheses*, *140*(109761), 109761. Advance online publication. doi:10.1016/j.mehy.2020.109761 PMID:32344309

Ullah, W., Siddique, I., Zulqarnain, R. M., Alam, M. M., Ahmad, I., & Raza, U. A. (2021). Classification of arrhythmia in Heartbeat detection using deep learning. *Computational Intelligence and Neuroscience*, *2021*, 1–13. doi:10.1155/2021/2195922 PMID:34712316

Van Cleeff, M., Kivihya-Ndugga, L., Meme, H., Odhiambo, J., & Klatser, P. (2005). The role and performance of chest X-ray for the diagnosis of tuberculosis: A cost-effectiveness analysis in Nairobi, Kenya. *BMC Infectious Diseases*, *5*(1), 1–9. doi:10.1186/1471-2334-5-111 PMID:16343340

van den Hout, A. (2017). *Multi-state survival models for interval-censored data*. Chapman and Hall, CRC.

Van der Heijden, A., Abramoff, M., Verbraak, F., van Hecke, M., Liem, A., & Nijpels, G. (2017). Validation of automated screening for referable diabetic retinopathy with the IDx-DR device in the Hoorn Diabetes Care System. *Acta Ophthalmologica*, *96*(1), 63–68. doi:10.1111/aos.13613 PMID:29178249

Vashist, P., Gupta, N., Singh, S., & Saxena, R. (2011). Role of early screening for diabetic retinopathy in patients with diabetes mellitus: An overview. *Indian Journal of Community Medicine*, *36*(4), 247. doi:10.4103/0970-0218.91324 PMID:22279252

Vayá, M. de la I., Saborit, J. M., Montell, J. A., Pertusa, A., Bustos, A., Cazorla, M., Galant, J., Barber, X., Orozco-Beltrán, D., García-García, F., Caparrós, M., González, G., & Salinas, J. M. (2020). BIMCV COVID-19+: a large annotated dataset of RX and CT images from COVID-19 patients. *ArXiv*, 1–22.

Veluchamy, M., & Subramani, B. (2019). Image contrast and color enhancement using adaptive gamma correction and histogram equalization. *Optik (Stuttgart)*, *183*, 329–337. doi:10.1016/j.ijleo.2019.02.054

Vidal, P. F., de Moura, J., Novo, J., & Ortega, M. (2021). Multi-stage transfer learning for lung segmentation using portable X-ray devices for patients with COVID-19. *Expert Systems with Applications*, *173*, 114677. doi:10.1016/j.eswa.2021.114677 PMID:33612998

Vidal, P. L., de Moura, J., Novo, J., Penedo, M. G., & Ortega, M. (2018, September). Intraretinal fluid identification via enhanced maps using optical coherence tomography images. *Biomedical Optics Express*, *9*(10), 4730. doi:10.1364/BOE.9.004730 PMID:30319899

Vincent, J. (2018, August 13). DeepMind's AI can detect over 50 eye diseases as accurately as a doctor. *The Verge*. https://www.theverge.com/2018/8/13/17670156/deepmind-ai-eye-disease-doctor-moorfields

Virgili, G., Menchini, F., Casazza, G., Hogg, R., Das, R., Wang, X., & Michelessi, M. (2015). Optical coherence tomography (OCT) for detection of macular oedema in patients with diabetic retinopathy. *Cochrane Database of Systematic Reviews*. Advance online publication. doi:10.1002/14651858.CD008081.pub3 PMID:25564068

Waheed, A., Goyal, M., Gupta, D., Khanna, A., Al-Turjman, F., & Pinheiro, P. R. (2020). COVIDGAN: Data Augmentation Using Auxiliary Classifier GAN for Improved COVID-19 Detection. *IEEE Access: Practical Innovations, Open Solutions*, *8*, 91916–91923. doi:10.1109/ACCESS.2020.2994762 PMID:34192100

318

Compilation of References

Walton, O. IV, Garoon, R., Weng, C., Gross, J., Young, A., Camero, K., Jin, H., Carvounis, P. E., Coffee, R. E., & Chu, Y. I. (2016). Evaluation of Automated Teleretinal Screening Program for Diabetic Retinopathy. *JAMA Ophthalmology*, *134*(2), 204. doi:10.1001/jamaophthalmol.2015.5083 PMID:26720694

Wang, L., & Wong, A. (2020). *COVID-Net: A Tailored Deep Convolutional Neural Network Design for Detection of COVID-19 Cases from Chest X-Ray Images*. https://arxiv.org/abs/2003.09871

Wang, X., Peng, Y., Lu, L., Lu, Z., Bagheri, M., & Summers, R. M. (2017). ChestX-ray8: Hospital-scale chest X-ray database and benchmarks on weakly-supervised classification and localization of common thorax diseases. *Proceedings - 30th IEEE Conference on Computer Vision and Pattern Recognition, CVPR 2017*, 3462–3471. 10.1109/CVPR.2017.369

Wang, H., Kadry, S. N., & Raj, E. D. (2020). *Continuous Health Monitoring of Sportsperson using IoT devices based Wearable Technology*. Elsevier.

Wang, J., Perez, L., & ... (2017). The effectiveness of data augmentation in image classification using deep learning. *Convolutional Neural Networks Vis. Recognit*, *11*, 1–8.

Wei, J., Hagihara, Y., Shimizu, A., & Kobatake, H. (2002). Optimal image feature set for detecting lung nodules on chest X-ray images. In *CARS 2002 computer assisted radiology and surgery* (pp. 706–711). Springer. doi:10.1007/978-3-642-56168-9_118

WHO Solidarity Trial Consortium. (2021). Repurposed Antiviral Drugs for COVID-19 — Interim WHO Solidarity Trial Results. New England Journal of Medicine, 384(6), 497–511. doi:10.1056/NEJMoa2023184

Wilkins, J. R., Puliafito, C. A., Hee, M. R., Duker, J. S., Reichel, E., Coker, J. G., Schuman, J. S., Swanson, E. A., & Fujimoto, J. G. (1996, December). Characterization of Epiretinal Membranes Using Optical Coherence Tomography. *Ophthalmology*, *103*(12), 2142–2151. doi:10.1016/S0161-6420(96)30377-1 PMID:9003350

Wilson, D. R., & Martinez, T. R. (2020). The need for small learning rates on large problems. IJCNN'01. *International Joint Conference on Neural Networks. Proceedings*. doi:10.1109/ijcnn.2001.939002

Winther, H. B., Hans Gerbel, S., Maschke, S. K., Hinrichs, J. B., Vogel-Claussen, J., Wacker, F. K., Höper, M. M., & Meyer, B. C. (2020). Dataset: COVID-19 Image Repository. doi:10.25835/0090041

Wood, C. S., Thomas, M. R., Budd, J., Mashamba-Thompson, T. P., Herbst, K., Pillay, D., Peeling, R. W., Johnson, A. M., McKendry, R. A., & Stevens, M. M. (2019). Taking connected mobile-health diagnostics of infectious diseases to the field. *Nature*, *566*(7745), 467–474. doi:10.103841586-019-0956-2 PMID:30814711

World Health Organization (WHO). (2021). *Coronavirus cases and death data*. https://covid19.who.int/WHO-COVID-19-global-data.csv

World Health Organization. (2020). *Coronavirus*. https://www.who.int/en/health-topics/coronavirus#tab=tab_1

World Health Organization. (2021). *WHO Coronavirus (COVID-19) Dashboard*. https://COVID19.who.int/

World Health Organization. (n.d.). *Cardiovascular diseases*. World Health Organization. Retrieved February 16, 2022, from https://www.who.int/health-topics/cardiovascular-diseases#tab=tab_1

Xie, T., Li, R., Zhang, X., Zhou, B., & Wang, Z. (2019). Research on heartbeat classification algorithm based on CART decision tree. *Proc. 8th Int. Symp. Next Gener. Electron. (ISNE)*, 1–3.

Xie, Y., Xia, Y., Zhang, J., Song, Y., Feng, D., Fulham, M., & Cai, W. (2019). Knowledge-based Collaborative Deep Learning for Benign-Malignant Lung Nodule Classification on Chest CT. *IEEE Transactions on Medical Imaging*, *38*(4), 991–1004. doi:10.1109/TMI.2018.2876510 PMID:30334786

Xu, L., Zeng, X., Huang, Z., Li, W., & Zhang, H. (2020). Low-dose chest X-ray image super-resolution using generative adversarial nets with spectral normalization. *Biomedical Signal Processing and Control*, *55*, 101600. doi:10.1016/j.bspc.2019.101600

Yadav, S., & Jadhav, S. (2019). Deep convolutional neural network based medical image classification for disease diagnosis. *Journal of Big Data*, *6*(1), 113. Advance online publication. doi:10.118640537-019-0276-2

Yamada, M. (2006). Wavelets: Applications. *Encyclopedia of Mathematical Physics*, 420–426. doi:10.1016/b0-12-512666-2/00242-x

Yamamoto, T., Akabane, N., & Takeuchi, S. (2001). Vitrectomy for diabetic macular edema: The role of posterior vitreous detachment and epimacular membrane. *American Journal of Ophthalmology*, *132*(3), 369–377. doi:10.1016/S0002-9394(01)01050-9 PMID:11530050

Yang, X., Wang, Y., Byrne, R., Schneider, G., & Yang, S. (2019). Concepts of Artificial Intelligence for computer-assisted drug discovery. *Chemical Reviews*, *119*(18), 10520–10594. doi:10.1021/acs.chemrev.8b00728 PMID:31294972

Yang, X., Yu, Y., Xu, J., Shu, H., Xia, J., Liu, H., Wu, Y., Zhang, L., Yu, Z., Fang, M., Yu, T., Wang, Y., Pan, S., Zou, X., Yuan, S., & Shang, Y. (2020). Clinical Course and outcomes of critically ill patients with COVID19 in Wuhan China. *The Lancet. Respiratory Medicine*, *8*(5), 475–481. doi:10.1016/S2213-2600(20)30079-5 PMID:32105632

Yan, Z., Zhang, J., Zhang, S., & Metaxas, D. N. (2012). Automatic rapid segmentation of human lung from 2D chest X-ray images. *Proc. of MICCAI Workshop on Sparsity Techniques in Medical Imaging*.

Yao, Q., Wang, R., Fan, X., Liu, J., & Li, Y. (2020). Multi-class arrhythmia detection from 12-lead varied-length ECG using Attention-based time-incremental convolutional neural network. *Information Fusion*, *53*, 174–182. doi:10.1016/j.inffus.2019.06.024

Ye, C., Coimbra, M. T., & Vijaya Kumar, B. V. (2010). Arrhythmia detection and classification using morphological and dynamic features of ECG signals. *2010 Annual International Conference of the IEEE Engineering in Medicine and Biology*. 10.1109/IEMBS.2010.5627645

Compilation of References

Yi, H., Sun, S., Duan, X., & Chen, Z. (2016). A study on Deep Neural Networks Framework. *2016 IEEE Advanced Information Management, Communicates*, *Electronic and Automation Control Conference (IMCEC)*. 10.1109/IMCEC.2016.7867471

Yildirim, Ö. (2018). A novel wavelet sequence based on deep bidirectional LSTM network model for ECG signal classification. *Computers in Biology and Medicine*, *96*, 189–202. doi:10.1016/j.compbiomed.2018.03.016 PMID:29614430

Yıldırım, Ö., Pławiak, P., Tan, R.-S., & Acharya, U. R. (2018). Arrhythmia detection using deep convolutional neural network with long duration ECG signals. *Computers in Biology and Medicine*, *102*, 411–420. doi:10.1016/j.compbiomed.2018.09.009 PMID:30245122

Yoo, S. H., Geng, H., Chiu, T. L., Yu, S. K., Cho, D. C., Heo, J., Choi, M. S., Choi, I. H., Cung Van, C., Nhung, N. V., Min, B. J., & Lee, H. (2020). Deep Learning-Based Decision-Tree Classifier for COVID-19 Diagnosis From Chest X-ray Imaging. *Frontiers in Medicine*, *7*, 427. doi:10.3389/fmed.2020.00427 PMID:32760732

Zebin, T., & Rezvy, S. (2021). COVID-19 detection and disease progression visualization: Deep learning on chest X-rays for classification and coarse localization. *Applied Intelligence*, *51*(2), 1010–1021. doi:10.100710489-020-01867-1 PMID:34764549

Zech, J., Pain, M., Titano, J., Badgeley, M., Schefflein, J., Su, A., Costa, A., Bederson, J., Lehar, J., & Oermann, E. K. (2018). Natural language–based machine learning models for the annotation of clinical radiology reports. *Radiology*, *287*(2), 570–580. doi:10.1148/radiol.2018171093 PMID:29381109

Zeinab, K. A. M., & Elmustafa, S. A. A. (2017). Internet of Things Applications, Challenges and Related Future Technologies. *World Scientific News*, *67*(2), 126–148.

Zhang, D., Ye, S., & Pan, T. (2019). The role of serum and urinary biomarkers in the diagnosis of early diabetic nephropathy in patients with type 2 diabetes. *PeerJ*, *7*, e7079. Advance online publication. doi:10.7717/peerj.7079 PMID:31218128

Zhang, W., Zhao, Y., Zhang, F., Wang, Q., Li, T., Liu, Z., Wang, J., Qin, Y., Zhang, X., Yan, X., Zeng, X., & Zhang, S. (2020). The use of anti-inflammatory drugs in the treatment of people with severe coronavirus disease 2019 (COVID-19): The Perspectives of clinical immunologists. *Clinical Immunology (Orlando, Fla.)*, *214*(January), 108393. doi:10.1016/j.clim.2020.108393 PMID:32222466

Zhang, Y., Miao, S., Mansi, T., & Liao, R. (2020). Unsupervised X-ray image segmentation with task driven generative adversarial networks. *Medical Image Analysis*, *62*, 101664. doi:10.1016/j.media.2020.101664 PMID:32120268

Zheng, C., Deng, X., Fu, Q., Zhou, Q., Feng, J., Ma, H., Liu, W., & Wang, X. (2020). Deep learning-based detection for COVID-19 from chest CT using weak label. MedRxiv. doi:10.1101/2020.03.12.20027185

Zheng, T., Xie, W., Xu, L., He, X., Zhang, Y., You, M., Yang, G., & Chen, Y. (2017). A machine learning-based framework to identify type 2 diabetes through electronic health records. *International Journal of Medical Informatics*, *97*, 120–127. doi:10.1016/j.ijmedinf.2016.09.014 PMID:27919371

Zheng, Y., Lamoureux, E., Lavanya, R., Wu, R., Ikram, M., Wang, J., Mitchell, P., Cheung, N., Aung, T., Saw, S.-M., & Wong, T. Y. (2012). Prevalence and Risk Factors of Diabetic Retinopathy in Migrant Indians in an Urbanized Society in Asia. *Ophthalmology*, *119*(10), 2119–2124. doi:10.1016/j.ophtha.2012.04.027 PMID:22709419

Zhu, J.-Y., Park, T., Isola, P., & Efros, A. A. (2017). Unpaired image-to-image translation using cycle consistent adversarial networks. *Proceedings of the IEEE International Conference on Computer Vision*, 2223–2232. 10.1109/ICCV.2017.244

Zupan, B., Demšar, J., Kattan, M. W., Beck, J. R., & Bratko, I. (2000). Machine learning for survival analysis: A case study on recurrence of prostate cancer. *Artificial Intelligence in Medicine*, *20*(1), 59–75. doi:10.1016/S0933-3657(00)00053-1 PMID:11185421

About the Contributors

Rajae El Ouazzani received her PhD in Image and Video Processing from the High National School of Computer Science and Systems Analysis (ENSIAS-Morocco) in 2010 and the Master's degree in Computer Science and Telecommunication from the Mohammed V University of Rabat (FSR-Morocco) in 2006. From 2011, she is a Professor in the School of Technology of Meknes, Moulay Ismail University in Morocco. Since 2007, she is the author of several papers in international conferences and journals. Her domains of interest include AI, multimedia processing, and NLP.

Mohammed Fattah received his Ph.D. degree in Telecommunication Engineering from the University of Sidi Mohamed Ben Abdellah (USMBA) Fez, Morocco, 2011. He is currently working as Professor in the Electrical Engineering Department at the school of technology of Moulay Ismail University (UMI), Meknes, Morocco. He is a responsible of the research team 'Intelligent Systems, Networks and Telecommunications', IMAGE laboratory of UMI. His current research interests include cloud computing, machine learning, radio mobile networks, body sensor networks, medical of things and IoT, mm-wave and THz communication systems. He has authored or coauthored more than 40 papers in different peer-reviewed journals and conferences. He is Guest Editor of Mathematical Problems in Engineering Journal, and Big Data Mining and Analytics Journal. He is a reviewer for peer-reviewed research journals.

Nabil Benamar is a Full Professor of Computer Sciences at the School of Technology, Moulay Ismail University of Meknes. He holds a Ph.D. in Sciences from Faculty of Sciences-Meknes (2004), a Master degree in Physics (2001) and a Master degree in Computer Networks (INPT 2003). His main research topics are IPv6, IoT, Intelligent Transport Systems, Autonomous Driving, and Next Generation Networks. He is the author of several journal papers in highly ranked journals as well as IETF Standard documents. He is currently serving as an Associate Editor of the "IEEE Access" and the "Wireless Communications and Mobile computing" journals, and reviewer for several IEEE, Elsevier, Wiley and Springer journals. Dr. Benamar is a TPC member of different IEEE Flagship conferences (Globecom, ICC,

PIMRC, WCNC, etc..), and a member of the Organizing Committee of WCNC' 2019. Furthermore, He is an IPv6 expert (he.net certified) and IPv6 trainer with many international organizations (RIPE/MENOG, AFRINIC, and Agence Universitaire de Francophonie). He became an expert in Internet Governance after completion of ISOC Next generation e-learning programme. He has been selected as an ISOC Ambassador to IGF(2012 and 2013), Google panelist in the first Arab-IGF, ISOC fellow to IETF'89&92&95&99&103 and ICANN'50&54 fellow. Among his commitments, he is chairing the Task Force for Arabic IDNs which is a part of Global Stakeholder Engagement (GSE) of ICANN a team of people working on making the DNS speaks Arabic and enabling Email address Internationalization. He is the chair of the UASG measurement WG, an ICANN initiative for ensuring Universal Acceptance.

* * *

Syed Ishtiaque Ahmed is an Assistant Professor of Computer Science at the University of Toronto, and the Director of the 'Third Space'' research group. His research focuses on the design challenges around strengthening the 'voices' or marginalized communities around the world. He conducted ethnography and built technologies with many underprivileged communities in Bangladesh, India, Pakistan, Iran, Iraq, Turkey, China, Canada, and the US. Ishtiaque received his PhD and Masters from Cornell University in the USA, and his Bachelor from BUET in Bangladesh. He received the International Fulbright Science and Technology Fellowship, Fulbright Centennial Fellowship, and Schwartz Reisman Institute Fellowship among others. His research has been funded by all three branches of Canadian tri-council research (NSERC, CIHR, SSHRC), NSF, NIH, Google, Microsoft, Facebook, Intel, Samsung, the World Bank, UNICEF, and UNDP, among others.

Hamlili Ali is Full Professor (Grade C) of Computer Sciences since 1994 at IT Engineering school ENSIAS (Ecole Nationale Supérieure d'Informatique et d'Analyse des Systèmes) of Mohamed V- Souissi University in Rabat, Morocco and former Director of SI2M (Multimedia and Mobile Information Systems) Laboratory at ENSIAS. He received his Ph.D. degree in computer science from the Ecole Nationale des Ponts et Chaussées of Paris (France) in 1993 and a Doctorate degree in Applied Sciences from Mohamed V-Agdal University of Rabat (Morocco) in 1999. Previously, he was Assistant-Professor at Paris-XII University, in Créteil, France and Orléans University in Bourges, France between 1992 and 1994. Through his career, he worked on Robotics, Artificial Intelligence, Reliability Growth of Software Versions, Wireless Mobile Networks Modeling and Simulation, Wireless TCP/IP Networks, Network Performance Evaluation, Distributed Systems Perform-

ability, Vehicular Networks & Survival Analysis. Ali Hamlili is author of several per-reviewed scientific papers and chapter books. In addition, he is the President of the ICST-Alliance (Information and Communication Sciences and Technologies Alliance), General Chairman of MICS-10 (Models of Information and Communication Systems) International Conference held in Rabat-Morocco (November 2-4, 2010) and the founder of the Moroccan Chapter of the IEEE-Intelligent Transportation Systems Society (November 2010). Ali Hamlili is certified on: Kaizen method of continuous quality improvement, EST (Ecole Supérieure de Technologie), Montréal, Canada; Big Data Analytics, Institute for Analytics and Data Science, University of Essex, Colchester-UK; Artificial Intelligence and Analytics (Explorer and Mastery Awards), IBM Skills Academy.

Harold Brayan Arteaga-Arteaga is currently pursuing the degree in Electronic Engineering with the Universidad Autónoma de Manizales. He has been a member of the research group on Bioinformatics and Artificial Intelligence since 2018. His current research interests include the application of convolutional neural networks to steganalysis, machine learning applications to predict two-phase flow patterns, detecting cancer through deep learning, and detecting respiratory system diseases from chest X-Ray imaging. He has received the highest honor roll and top-class distinctions and was valedictorian in 2016. He is a young researcher by Minciencias, Colombia.

Alka Bali is Professor of Pharmaceutical Chemistry at University Institute of Pharmaceutical Sciences (UIPS), Panjab University, Chandigarh. She did her B. Pharm., M. Pharm. (Pharmaceutical Chemistry) and Ph. D. from the same institute. She has an academic and research experience spanning 27 years of undergraduate and postgraduate teaching. She has expertise in the fields of pharmaceutical analysis and medicinal chemistry. Her research areas of interest include pharmaceutical analysis with focus on method development and validation, spectroscopic characterization of impurities in drugs and drug products, synthetic medicinal chemistry encompassing computer-aided drug designing (CADD), QSAR, synthesis and pharmacological evaluation of new chemical entities in the area of antipsychotics, anti-inflammatory agents and angiotensin II antagonists. She has three books, five book chapters, 40 research articles in reputed international and national journals and 60 conference papers to her credit. She is on reviewer panel of several reputed international journals including European Journal of Medicinal Chemistry, Bioorganic and Medicinal Chemistry Letters, Medicinal Chemistry Research, and several others.

Nishu Bali is Associate Professor at Department of Computer Sciences, Chitkara University Campus, Punjab Campus, Rajpura, Distt Patiala, India. She has got

325

a teaching experience of more than 15 years in various programming languages like JAVA, Python and she has taught subjects like data structures and computer graphics. Her expert area is Machine learning and Deep learning. She has to her credit publications in journals of high repute. She has been an active participant at international and national conferences. Required Actions

Mario Alejandro Bravo-Ortíz received the degree in biomedical and electronical engineering from the Universidad Autónoma de Manizales. He has been a member of the research group on Bioinformatics and Artificial Intelligence since 2018. He has coauthored chapter 12 of the book Digital Media Steganography (Mahmoud Hassaballah, 2020). His current research interests include the application of convolutional neural networks to steganalysis and the detection of cancer through deep learning. He has participated as a Speaker in research meetings with RREDSI network and the first Congress of Biomedical Engineering and Bioengineering in 2019.

Oscar Cardona-Morales is an electronic engineer with, MSc in Industrial Automation and Ph.D. in Automatic Engineering from Universidad Nacional de Colombia at Manizales. Researcher and entrepreneur with experience in R+D+I process related to the internet of things, remote sensing, machine learning, and image/signal processing. Associated professor and head of automatic research group at Universidad Autonoma de Manizales.

Sonia H. Contreras-Ortiz received BS and MSc degrees in Electronic Engineering from Universidad Industrial de Santander in Bucaramanga, Colombia, and a Ph.D. degree in Biomedical Engineering from the University of Connecticut, Storrs, CT, USA, in 2011. Currently, she is the Director of the Biomedical Engineering program at Universidad Tecnológica de Bolívar, in Cartagena de Indias, Colombia. She is a member of IEEE, SPIE, OWSD, and Catedra Matilda. Her research interests include biosignal and medical image processing and analysis, machine learning, and STEM education.

Joaquim de Moura received his M.Sc. degree in Computer Science in 2016 and his Ph.D. degree in 2019 in a collaborative project between ophthalmology centers in Galicia and the University of A Coruña. He is currently a Postdoctoral Researcher (Xunta de Galicia fellow) at the Varpa group affiliated to the Centre for Information and Communications Technology Research (CITIC). He has worked as a visiting researcher at the Centre for Biomedical Engineering Research (C-BER) affiliated to the Institute for Systems and Computer Engineering, Technology and Science (INESC-TEC). He has published more than 65 peer-reviewed publications, including Computer Methods and Programs in Biomedicine, Expert Systems with

326

Applications, IEEE Access, Biomedical Optics Express, Machine Vision and Applications, Medical & Biological Engineering & Computing, Sensors, Engineering Applications of Artificial Intelligence, among others. His main research interests lie in the fields of computer vision, image processing, machine learning, pattern recognition and biomedical image analysis.

Melissa delaPava received a B.S. degree in chemical engineering from Universidad Nacional de Colombia, Manizales. She is currently pursuing an M.S. degree in Computer Science at Universidad Nacional de Colombia, Bogotá, where she has been a member of the MindLab group since 2018. She is also a member of the research group on Bioinformatics and Artificial Intelligence from Universidad Autónoma de Manizales. Her current research interest includes deep learning and machine learning applied to medical imaging.

Sara El Omary received a B.Sc degree in Computer Science from the Higher School of Technology of Oujda, Morroco in 2016, then an M.Sc. degree in Data Science from the Faculty of Science Semlalia of Marrakech, Morocco in 2020. She is currently a Ph.D. candidate at the Moulay Ismail University of Meknes (Morocco). Her main areas of interest include Machine Learning, Deep Learning, Image Preprocessing, and Computer Vision.

Mateo Gende was born in Spain, in 1995. He received the degree in computer engineering from the University of A Coruña, Spain, in 2018, where he is currently pursuing the Ph.D. degree in computer science and artificial intelligence. Since 2018, he has been working as a Research Assistant with the Centre for Research in Information and Communication Technologies (CITIC), Spain. His research interests include computer vision, medical image analysis, pattern recognition, and machine learning.

Lana Ibrahem Saeed Hamad received her M.Sc. degree in communication and networking engineering from Yildiz Technical University, Turkey in 2021, and B.Sc. in communication engineering from Red Sea University in 2015. Her research interest in IoT, Wireless Sensors Networks, WSNs Routing protocols and communication networking.

Anik Iqbal, Ph.D., is a visiting assistant professor of computer science at Marquette University. In this role, he teaches several computer science and data science courses that are frequently taken by undergrad and grad students in different programs related to public health informatics and digital health data analytics, including data mining, data structures, business intelligence and business analytics. He is involved

in multiple research projects involving development experience in healthcare with mobile computing. He is experienced in patient monitoring, building assistive technologies and activity monitoring for smart phones. His research and development experience in mobile platforms will help him in supervising the software system for this project. His PhD research was in physics where his research work concentrated on the underlying theoretical framework of spintronic devices. He is serving as the registration chair of IEEE COMPSAC 2021 conference.

Luis Humberto López-Murillo received the degree in chemical engineering from the Universidad Nacional de Colombia in 2018 and made three semesters of deepening line in the food field. He is actually finishing a master of science study in chemical engineering at Universidad Nacional de Colombia. He belongs to two research groups: (1) Grupo de Investigación en Aplicación de Nuevas Tecnologías GIANT from Universidad Nacional de colombia and (2) Automática from Universidad Autónoma de Manizales.

Fernanda Martínez Rodríguez is a biomedical engineering student at Universidad de Guadalajara. Her current scientific research focuses on fields such as medical imaging and bio signal processing, evidence-based prosthetic design, and programming. She is interested in the application of artificial intelligence in medical devices in order to improve disease diagnosis and low-invasive treatments as well as in encouraging women and girls in STEM careers.

Esteban Mercado-Ruiz received the degree of biomedical from the Universidad Autónoma de Manizales in the first semester of 2021. He is a member of the Bioinformatics and Artificial Intelligence research group since 2019. His current research interests include the application of convolutional neural networks to different artificial vision application problems such as cancer detection through deep learning, classification of coffee ripening states using convolutional neural networks. He has participated as a speaker in research meetings with the RREDSI network.

Alejandro Mora-Rubio is currently pursuing the degree in biomedical and electronical engineering with the Universidad Autónoma de Manizales. He has been a member of research group on Bioinformatics and Artificial Intelligence since 2018. He has worked on projects involving electrophysiological signals classification using machine learning. He has supported projects involving the application of deep learning techniques to digital media steganalysis and detecting respiratory system diseases from chest X-ray imaging.

Daniel Morís was born in Spain, in 1997. He received the degree in computer engineering from the University of A Coruña, Spain, in 2019, where he is currently pursuing the Ph.D. degree in computer science and artificial intelligence. Since 2021, he has been working as a Research Assistant with the Centre for Research in Information and Communication Technologies (CITIC), Spain. His research interests include computer vision, medical image analysis, pattern recognition, and machine learning.

Jorge Novo was born in Spain, in 1983. He received the M.Sc. and Ph.D. degrees (cum laude) in computer science from the University of A Coruña, in 2007 and 2012, respectively. He worked as a Visiting Researcher with CMR images in the detection of landmark points at Imperial College London, and a Postdoctoral Research Fellow with INEB and INESC-TEC research institutes in the development of CAD systems for lung cancer diagnosis with chest CT images. He is currently an Assistant Professor with the Department of Computer Science and Information Technologies, University of A Coruña. His research interests include computer vision, pattern recognition, and biomedical image processing.

Marcos Ortega received the degree in computer science, in 2004, and the doctor's degree in computer science, in 2009. He currently serves as an Associate Professor for the University of A Coruña, teaching mainly in the Faculty of Computer Science, also serving as his Secretary. He is also a Researcher with the Research Centre in Information and Communication Technologies (CITIC), and a member of its scientific committee and its representative in the ECHAlliance. He is also a member of the Institute of Biomedical Research of A Coruña (INIBIC) with the rank of Principal Investigator. His research interests include computer vision, medical image processing, and medical informatics.

Maria Jose Palancares-Sosa is currently studying the biomedical engineering program at the Instituto Politécnico Nacional in Mexico. One of her biggest interests in the medical field belongs to medical imaging where she aspires to specialize. She has participated in nanotechnology research lines and currently image processing with researchers from the Universidad Autónoma de Manizales in Colombia.

Masud Rabbani is currently working as a research assistant under the ubicomp lab of Marquette University. His research interest on Mobile Health (mHealth) system development. At present, he is pursuing his Ph.D. from the Department of Computer Science at Marquette University, USA. He completed his undergrad with the "Gold Medal" award from Khulna University Of Engineering & Technology, Bangladesh. He also worked as a faculty member for five years of the Department

of Computer Science, Daffodil International University, Bangladesh. Mr. Rabbani has publications in his research area in different renowned conferences and journals.

Rashid A. Saeed received his Ph.D. in Communications Network Engineering, Universiti Putra Malaysia (UPM). Currently, he is a professor in Computer Engineering Department, Taif University. He is also working in the Electronics Department, Sudan University of Science and Technology (SUST). He was a senior researcher in Telekom Malaysia™ Research and Development (TMRND) and MIMOS. Rashid published more than 200 research papers, books, and book chapters on wireless communications and networking in peer-reviewed academic venues. His areas of research interest are around wireless communication network. He is successfully awarded 3 U.S patents in these areas. He supervised more than 50 MSc/Ph.D. students. Rashid is a Senior member of IEEE, a Member in IEM (I.E.M), SigmaXi, and SEC. Rashid co-founder and Technical Committee Chair (TPC) of International Conference on Computing, Electrical and Electronics Engineering (ICCEEE) in Sudan. ·He is an editorial board member in journal of advances in computer sciences, and editor in Scientific African (SCIAF) journal. He is a guest editor in many journals.

Elmustafa Sayed Ali received his MSc in Electronics & Communication Engineering, Sudan University of Science & technology in 2012 and B.Sc in 2008. Worked (former) as a senior engineer in Sudan Sea Port Corporation (5 years) as a team leader of new projects in wireless networks includes (Tetra system, Wi-Fi, Wi-Max, and CCTV). Currently he is a head of marine systems department in Sudan marine industries. He is also working in Electrical and Electronics Engineering Department in the Red Sea University as a senior lecturer. Elmustafa published more than 25 papers, and 12 book chapters in wireless communications, and networking in peer reviewed academic international journals. His areas of research interest include, routing protocols, computer and wireless networks, LPWAN and IoT. He is a member of IEEE Communication Society (ComSoc), International Association of Engineers (IAENG), Six Sigma Yellow Belt (SSYB), and Scrum Fundamentals certified (SFC), and Sudanese Engineering Council (SEC).

Md Ishrak Islam Zarif is currently working as a research assistant under the ubicomp lab of Marquette University as well as the Biorobotics Lab of the University of Wisconsin-Milwaukee. His research interest on telerehabilitation system development. At present, he is pursuing his Ph.D. from the Department of Computer Science at Marquette University, USA. He has a background working in data science, machine learning, IoT, and system development. He completed his undergrad at Khulna University of Engineering & Technology, Bangladesh, in 2018. Mr. Zarif has publications in his research area in different renowned conferences and journals.

Index

332